

**Abstract**

The repair of complex bone defects remains a surgical challenge and it is hoped that tissue-engineering may offer an unlimited source of bone tissue and circumvent many of the drawbacks associated with current clinical approaches. Currently, the majority of bone tissue-engineering research has been focused on the differentiation of mesenchymal stem cells (MSCs) into osteoblasts. Tissue-engineering via the endochondral ossification pathway to prepare a hypertrophic cartilage graft, however, may be a more advantageous approach. This tissue is able to survive the relatively low oxygen tensions found in defects and it may provide growth factors that promote angiogenesis and bone tissue regeneration. Surprisingly little research has been directed at hypertrophic cartilage engineering. The aim of this project was therefore to investigate the ability of nasal chondrocytes to form a hypertrophic cartilage graft capable of regenerating bone tissue *in vivo*.

The methodology used in this study was based on the typical tissue-engineering approach and encompassed scaffold fabrication, tissue characterisation and *in vivo* studies. Rat nasal chondrocytes consistently differentiated to form hypertrophic cartilage grafts on both PGA and PLLA/calcium phosphate scaffold materials. These grafts expressed collagen type X and alkaline phosphatase, co-located with large chondrocytes, in a tissue that had morphological features in common with hypertrophic cartilage. Gene and protein expression studies demonstrated a decrease in hyaline cartilage markers and an increase in markers for hypertrophic chondrocytes as differentiation proceeded. Vital and decellularised grafts cultured on the PGA scaffold material significantly increased bone regeneration *in vivo* when compared to empty defects (4mm) in the rat cranium. Decellularised grafts that were reseeded with MSCs also promoted significant bone tissue regeneration after 12 weeks. This regeneration, however, occurred at a slower rate compared to the other grafts evaluated. Foetal calf serum (FCS) was shown to have a significant effect on the differentiation of the rat nasal chondrocytes. A defined, serum-free medium was therefore developed which was able to support the hypertrophic differentiation of the chondrocytes. Finally proof of concept studies demonstrated the ability of a Quasi-vivo<sup>®</sup> bioreactor to support hypertrophic differentiation of nasal chondrocytes under flow conditions. It was concluded that nasal chondrocytes could be seeded onto scaffold materials and cultured under defined conditions to prepare a hypertrophic cartilage graft capable of stimulating bone tissue regeneration *in vivo*. The use of a decellularised hypertrophic cartilage demonstrated substantial clinical potential for use as a new regenerative graft material.

## **Contents**

Acknowledgements.....	i
Abbreviations.....	iii
List of Figures.....	v
List of Tables.....	xiii
Presentations, Awards and Publications.....	xvi
1 Introduction .....	1
2 Literature Review.....	3
2.1 Basic Bone Biology.....	3
2.1.1 Function and Basic Structure .....	3
2.1.2 Ossification.....	5
2.1.3 Intramembranous Ossification .....	5
2.1.4 Endochondral Ossification .....	6
2.2 Bone Repair and Remodelling .....	11
2.3 Clinical Bone Defect Repair .....	12
2.3.1 Current Approaches for Bone Grafts .....	12
2.4 Current Tissue-Engineering Approaches to Bone Transplants.....	17
2.5 Tissue-Engineering Bone using the Endochondral Ossification Pathway .....	20
2.5.1 Cells for Bone Tissue-Engineering.....	22
2.5.2 Scaffolds for Bone Tissue-Engineering.....	24
2.5.3 Decellularised Extracellular Matrix as a Scaffold for Bone Tissue-Engineering .....	29
2.5.4 Culture Conditions for Bone Tissue-Engineering .....	32

2.5.5	Development of Serum-Free Culture Conditions for Bone Tissue-Engineering .....	34
3	Aims and Objectives .....	36
4	Materials and Methods .....	38
4.1	Materials.....	38
4.2	Methods .....	38
4.2.1	Scaffold Fabrication and Analysis.....	38
4.2.2	Cell Culture .....	40
4.2.3	3D Cell Culture .....	43
4.2.4	Histological and Biochemical Analysis .....	47
4.2.5	Gene Expression.....	50
4.2.6	Construct Decellularisation.....	54
4.2.7	In Vivo Experiments .....	56
4.2.8	Statistical Analysis.....	59
5	Results.....	60
5.1	Scaffold Fabrication .....	60
5.2	The Effect of Serum on Chondrocyte Hypertrophy.....	64
5.3	Hypertrophic Differentiation of Rat Nasal Chondrocytes .....	69
5.4	Protein and Gene Expression during Chondrocyte Hypertrophic Differentiation on PGA and PLLA/Calcium Phosphate Scaffold Materials.....	76
5.4.1	The Effect of 3D Culture on Gene Expression.....	76
5.4.2	Extracellular Matrix Gene and Protein Expression on PGA and PLLA/calcium phosphate composite scaffolds .....	78
5.4.3	Transcription Factor and Signalling Molecule Gene Expression.....	90
5.5	Cranial Implantation of Hypertrophic Constructs Cultured on PGA .....	97

---

5.5.1	Construct Decellularisation .....	97
5.5.2	Constructs Pre-Implantation .....	99
5.5.3	Repair of Cranial Defects 4 Weeks after Implantation .....	103
5.5.4	Repair of Cranial Defects 8 Weeks after Implantation .....	108
5.5.5	Repair of Cranial Defects 12 Weeks after Implantation .....	113
5.5.6	Healing Over a 12 Week Period .....	117
5.6	The Effect of Bioreactor Culture on Hypertrophic Differentiation .....	119
5.7	Serum-Free media .....	125
6	Discussion .....	133
6.1	Scaffold Fabrication .....	134
6.2	The Effect of FCS on Chondrocyte Hypertrophy .....	136
6.3	Hypertrophic Differentiation of Chondrocytes .....	138
6.4	Protein and Gene Expression .....	140
6.4.1	The Effect of Three Dimensional Culture on Gene Expression .....	141
6.4.2	Extracellular Matrix Gene Expression .....	143
6.4.3	Transcription Factor and Signalling Molecule Gene Expression .....	146
6.5	In Vivo Experiments .....	149
6.6	Bioreactor Culture .....	153
6.7	Serum-Free Media .....	155
7	Conclusions .....	160
8	Future Work .....	162
9	References .....	165

## ***Acknowledgements***

I would like to thank my supervisors Aileen Crawford, Paul Hatton and Ian Brook for all their help, support and advice over the last three years, without which I would not have been able to complete this thesis. Aileen requires a special mention for her helpful scientific knowledge and vision for this project, which enabled this thesis to be as successful as it is. Paul, thank you for your help with writing techniques and presentation skills without which I would not have been able to develop as a researcher. Finally thank you to Ian Brook, for helping to organise and bank rolling the *in vivo* work.

I would also like to thank several members of the School of Clinical Dentistry for their help and advice in specific areas of my PhD: Christine Freeman who carried out all the *in vivo* work, without which this my thesis would not be complete; Brenka McCabe who helped to orientate me in the molecular biology lab and answered all my silly questions; Dave Thompson for taking the time to show me how to process my *in vivo* samples and taught me wax embedding and microtome cutting of my samples and Rebecca Goodchild, a former student, who initially helped me with my cell isolations and orientated me around the cell culture laboratory.

I would also like to thank members of The University of Sheffield outside our group who helped me: Nik Reeves-McLaren (X-ray diffraction); Les Coulton (MicroCT) and Chris Hill (scanning electron microscopy).

I would also like to thank my office, especially Eleanor Ashworth, Richard Senior, Caroline Wilcock and Harriet Drouin, for helping to keep me sane with endless amounts of office fun. I have especially enjoyed learning about the origin of chad and that 20:20 vision is not the best vision you can have! Thank you also for the fun we have had on Fridays during after work drinks, some of which have been well needed! A special thank you to Richard Senior my fellow final year student, for keeping me going and for looking after my cells when I needed a holiday!

I would like to thank my friends (there are too many of you to mention individually) for all their support, especially the dinners, nights out, the Women's Ginstitute and the holidays in the snow! A special thank you to Brendon for his support over the last year and helping me take my mind off work when things got stressful.

On a personal note I would like to thank my family for their endless support throughout my life, not only during this PhD. Mum and Dad your support, both emotional and financial, has been invaluable and I love you both, you are the best parents anyone could wish for. Matthew you can stop mocking me now I am actually going to have to get a real job, my endless student life has come to an end! I am proud and thankful to have you as a brother.

## Abbreviations

APES	– (3-aminpropyl) triethoxysilane
ASC	– Adipose stem cells
bFGF	– Basic fibroblast growth factor
BM-MSCs	– Bone marrow mesenchymal stem cells
BSA	– Bovine serum albumin
Ca <sup>2+</sup>	– Calcium ions
cDNA	– Chromosomal deoxyribose nucleic acid
CO <sub>2</sub>	– Carbon dioxide
DAB	– 3,3'-diaminobenzidine
DCM	– Dichloromethane
DMB	– Dimethylethylene blue
DMEM	– Dulbeccos modified eagle medium
dNTP	– Dioxynucleotide triphosphate
ECM	– Extra-cellular matrix
EDTA	– Ethylenediaminetetraacetic acid
FCS	– Foetal calf serum
FDA	– Food and Drug Administration
FGF	– Fibroblast growth factor
GAG	– Glycosaminoglycans
GAPDH	– Glyceraldehyde 3-phosphate dehydrogenase
Glu	– L-glutamine
IBMX	– 3-isobutyl-1-methylxanthine
IGF	– Insulin growth factor
Ihh	– Indian hedgehog
ITS	– Insulin, transferrin and selenium
MEM	– Minimum essential media
Mg <sup>3+</sup>	– Magnesium ions
MicroCT	– Microcomputer tomography
mRNA	– Messenger ribonucleic acid
MSCs	– Mesenchymal stem cells
NEAA	– MEM non-essential amino acids
OCT	– Optimal cutting temperature tissue mounting medium
PBS	– Phosphate buffered saline
PCR	– Polymerase chain reaction
PFA	– Paraformaldehyde
PGA	– Polyglycolic acid

PLLA	– Poly-L-lactic acid
PS	– Penicillin and streptomycin
RNA	– Ribonucleic acid
Rpm	– Revolutions per minute
Runx2	– Runt-related transcription factor 2
SEM	– Scanning electron microscopy
Sox9	– SRY (sex determining region Y)-box 9
TGF- $\beta$	– Transforming growth factor-beta
VEGF	– Vascular endothelial growth factor
XRD	– X-ray diffraction



## List of Figures

Figure 2-1	The structure of a long bone, showing the positioning of the cortical and cancellous bone as well as the positioning of the periosteum (Adapted from Rho et al (Rho et al., 1998))	4
Figure 2-2	Images of the growth plate of the rat, showing the different states of chondrocyte differentiation seen during endochondral ossification. (A) Haematoxylin and eosin staining to show the general cell morphology in the growth plate; (B) collagen type II localisation; (C) collagen type X localisation and (D) alkaline phosphatase localisation. (Images used with permission from Kwarciak (Kwarciak, 2009))	7
Figure 2-3	Gene expression in the growth plate and their role in regulation of hypertrophic differentiation.	9
Figure 4-1	Diagrammatic of a goniometer showing the water droplet, the scaffold surface and the contact angle, $\theta$	35
Figure 4-2	Bioreactor set up showing the peristaltic pump, media reservoir and culture chamber. (A) photograph of the bioreactor set up in a laminar flow hood; (B) a schematic diagram of the flow through the bioreactor system	45
Figure 4-3	Schematic diagram showing the experimental plan and the time points at which the gene expression of the chondrocytes will be assessed	51
Figure 4-4	Schematic of operation showing the positioning of the two 4 mm defects in the skull and the filling of one defect with a construct.	57
Figure 5-1	Weight of the PLLA scaffolds both pre-treatment and post-treatment by the alternative soaking technique to form a PLLA/calcium phosphate composite scaffold. (***) = $p < 0.001$ . n= 6 separate experiments)	61
Figure 5-2	Randomly oriented electrospun PLLA polymer fibres, (A, B) before alternative soaking; (C, D) after alternative soaking. The scale bars in images A, B and D=20 $\mu\text{m}$ and in image C=50 $\mu\text{m}$	61
Figure 5-3	Scanning electron microscopy image of the non-woven needle punched PGA scaffold purchased from Cellon. (scale bar = 50 $\mu\text{m}$ )	63
Figure 5-4	Representative XRD analysis of the precipitate on and within the PLLA fibres. This shows the presence of two phases of calcium phosphate, hydroxyapatite (grey) and brushite ( red) in the precipitate (n=3 )	63

Figure 5-5	Immunohistochemical analysis of rat nasal chondrocyte constructs after 42 days culture. (A) haematoxylin and eosin Stain; (B) toluidine blue; (C) alcian blue; (D) alkaline phosphatase; (E) collagen type II; (F) collagen type X. (Insert micrographs show non-specific staining). Arrows indicate areas of hypertrophy as shown by chondrocytes exhibiting a large morphology co located with high GAG concentrations and collagen type X expression.	65
Figure 5-6	DMB assay showing the GAG concentration present in the PGA pellets 21 days after culture in the 5 different sera (* p <0.05, **p <0.01, n=5).	68
Figure 5-7	Representative analysis of constructs cultured in FCS 1-5, showing the degree of hypertrophic differentiation seen after three weeks of culture. Haematoxylin and eosin staining showed the increase in cellular volume co-located with expression of the hypertrophic marker collagen type X (magnification x10, scale bars = 200 $\mu$ m, insert micrographs show negative controls, n=5)	69
Figure 5-8	Chondrocyte attachment to PGA, PLLA and PLLA/calcium phosphate scaffold materials after 72 hours on a shaker plate. (** p< 0.001, n=6)	69
Figure 5-9	Histological and immunohistochemical analysis of constructs formed by culturing chondrocytes on PGA, PLLA and PLLA/calcium phosphate scaffold materials for 42 days. The images show haematoxylin and eosin; toluidine blue and alcian blue staining. (n=10). Scale bars = 100 $\mu$ m	74
Figure 5-10	Histological and immunohistochemical analysis of constructs formed by culturing chondrocytes on PGA, PLLA and PLLA/calcium phosphate scaffold materials for 42 days. The images show collagen type II; collagen type X and alkaline phosphatase staining. Insert micrographs show non-specific staining (n=10). Scale bars = 100 $\mu$ m.	73
Figure 5-11	GAG content of chondrocyte constructs (expressed as a percentage of the dry weight of the ECM) after 42 days of culture on PGA, PLLA and PLLA/calcium phosphate scaffolds. (**p<0.01, n=6)	74
Figure 5-12	A comparison of the GAG content in the extracellular matrix of constructs produced by chondrocytes cultured on PGA and PLLA/calcium phosphate scaffold materials after 14, 28 and 42 days of culture. (* p<0.05, *** p<0.001. n = 6)	74

Figure 5-13	Mineralisation present within the constructs after 42 days of culture under semi-static conditions. Images show staining for calcium using alizarin red on the PGA scaffold material (A) and the PLLA/calcium phosphate composite scaffold material (B). (C) Shows alizarin red staining of the PLLA/calcium phosphate scaffold at day 0 of culture. Scale bars = 100 $\mu$ m.	77
Figure 5-14	The effect of 3D culture of chondrocytes on the PGA scaffold material after 72 hours in expansion culture media on gene expression. The data is normalised to the gene expression observed at passage 2 on tissue culture plastic (2D culture) (* $p < 0.05$ , **** $p < 0.0001$ , $n = 6$ )	76
Figure 5-15	The effect of 3D culture of chondrocytes on PLLA/calcium phosphate scaffold material on cell gene expression after 72 hours in expansion media. The data is normalised to the gene expression observed at passage 2 on tissue culture plastic (2D culture). (* $p < 0.05$ , ** $p < 0.01$ , $n = 6$ )	77
Figure 5-16	Collagen type II mRNA expression during hypertrophic differentiation on PGA scaffold material relative to its expression level seen after 72 hours of culture in expansion media (day 0 of 3D chondrocyte differentiation). (***) $p < 0.001$ . $n = 8$	80
Figure 5-17	Collagen type II mRNA expression during hypertrophic differentiation on PLLA/calcium phosphate scaffold material relative to the mRNA expression levels seen after 72 hours of culture in expansion media (day 0 of 3D chondrocyte differentiation). (* $p < 0.05$ , $n = 8$ ).	81
Figure 5-18	Collagen type II mRNA expression in the chondrocytes during hypertrophic differentiation culture on PLLA/calcium phosphate scaffold material compared to expression seen on the PGA scaffold material. The data is normalised to the gene expression observed at passage 2 on tissue culture plastic (2D culture). (** $p < 0.01$ and * $p < 0.05$ , $n = 8$ )	81
Figure 5-19	Collagen type X mRNA expression during hypertrophic differentiation on PGA scaffold material relative to mRNA expression levels seen after 72 hours of culture in expansion media (day 0 of 3D chondrocyte differentiation). (** $p < 0.01$ , $n = 8$ )	81
Figure 5-20	Collagen type X mRNA expression during hypertrophic differentiation on PLLA/calcium phosphate scaffold material relative to mRNA expression levels seen after 72 hours of culture in expansion media (day 0 of 3D chondrocyte differentiation). (* $p < 0.05$ , $n = 8$ )	83

Figure 5-21	Collagen type X mRNA expression during hypertrophic differentiation of chondrocytes cultured on PLLA/calcium phosphate scaffolds compared to the expression observed on the PGA. The data is normalised to the gene expression observed at passage 2 on tissue culture plastic (2D culture). (*p< 0.05. n = 8)	84
Figure 5-22	Alkaline phosphatase mRNA expression during hypertrophic differentiation of PGA constructs relative to mRNA expression levels seen after 72 hours of culture in expansion media (day 0 of 3D chondrocyte differentiation). (*p< 0.05. n = 8).	83
Figure 5-23	Alkaline phosphatase mRNA expression during hypertrophic differentiation of PLLA/calcium phosphate constructs relative to mRNA expression levels seen after 72 hours of culture in expansion media (day 0 of 3D chondrocyte differentiation). (*p< 0.05. n = 8)	84
Figure 5-24	Alkaline phosphatase mRNA expression of chondrocytes during hypertrophic differentiation of PLLA/calcium phosphate constructs compared to the alkaline phosphatase expression seen in the PGA constructs. The data is normalised to the gene expression observed at passage 2 on tissue culture plastic (2D culture). (*p< 0.05. n = 8)	84
Figure 5-25	Representative histological analysis of chondrocytes grown on PGA scaffolds after 14, 28 and 42 days of culture, showing the localisation of extracellular proteins and within the ECM of the construct. Inset micrographs show negative controls, scale bars=100 $\mu$ m (n=3 separate experiments).	86
Figure 5-26	Representative immunohistological analysis of chondrocytes grown on PGA scaffolds after 14, 28 and 42 days of culture, showing the localisation of extracellular proteins and within the ECM of the construct. Inset micrographs show negative controls, scale bars=100 $\mu$ m (n=3 separate experiments).	87
Figure 5-27	Representative histological analysis of chondrocytes grown on PLLA/calcium phosphate scaffolds after 14, 28 and 42 days of culture, showing the localisation of extracellular proteins within the ECM of the constructs. Inset micrographs show negative controls, scale bars=100 $\mu$ m (n=3 separate experiments).	88
Figure 5-28	Representative immunohistological analysis of chondrocytes grown on PLLA/calcium phosphate scaffolds after 14, 28 and 42 days of culture, showing the localisation of extracellular proteins within the ECM of the constructs. Inset micrographs show negative controls, scale bars=100 $\mu$ m (n=3 separate experiments).	89

Figure 5-29	Sox9 mRNA expression during hypertrophic differentiation of chondrocytes on PGA scaffolds relative to mRNA expression levels seen after 72 hours of culture in expansion media (day 0 of 3D chondrocyte differentiation). (* $p < 0.05$ . n = 8).	91
Figure 5-30	Sox9 mRNA expression during hypertrophic differentiation of chondrocytes on PLLA/calcium phosphate scaffolds relative to mRNA expression levels seen after 72 hours of culture in expansion media (day 0 of 3D chondrocyte differentiation). (***) $p < 0.001$ . n = 8).	94
Figure 5-31	Sox9 mRNA expression in chondrocytes during hypertrophic differentiation on PLLA/calcium phosphate scaffolds relative to sox9 expression seen in chondrocytes cultured on the PGA scaffold. The data is normalised to the gene expression observed at passage 2 on tissue culture plastic (2D culture). (* $p < 0.05$ . n = 8)	92
Figure 5-32	Ihh mRNA expression in the chondrocytes during hypertrophic differentiation culture on PGA relative to mRNA expression levels seen after 72 hours of culture in expansion media (day 0 of 3D chondrocyte differentiation). (* $p < 0.05$ . n = 8).	93
Figure 5-33	Ihh mRNA expression during chondrocyte hypertrophic differentiation on PLLA/calcium phosphate scaffolds relative to mRNA expression levels seen after 72 hours of culture in expansion media (day 0 of 3D chondrocyte differentiation). (* $p < 0.05$ . n = 8).	96
Figure 5-34	Ihh mRNA expression in the chondrocytes during hypertrophic differentiation culture on PLLA/calcium phosphate scaffolds material compared to Ihh expression seen in the PGA constructs. The data is normalised to the gene expression observed at passage 2 on tissue culture plastic (2D culture). (* $p < 0.05$ . n = 8)	9497
Figure 5-35	Runx2 mRNA expression during chondrocyte hypertrophic differentiation on PGA scaffolds relative to mRNA expression levels seen after 72 hours of culture in expansion media (day 0 of 3D chondrocyte differentiation). (***) $p < 0.001$ . n = 8).	95
Figure 5-36	Runx2 mRNA expression during chondrocyte hypertrophic differentiation on PLLA/calcium phosphate scaffolds, relative to the runx2 mRNA expression level seen after 72 hours of culture in expansion media (day 0 of 3D chondrocyte differentiation). (* $p < 0.05$ . n = 8)	98

Figure 5-37	Runx2 mRNA expression in the chondrocytes during hypertrophic differentiation culture on PLLA/calcium phosphate scaffolds compared to expression seen on the PGA scaffold material. The data is normalised to the gene expression observed at passage 2 on tissue culture plastic (2D culture). (n = 8)	96
Figure 5-38	The percentage DNA removal after cycles of washing the constructs cultured on PGA with SDS and ionic buffers (* p<0.05, n=3)	97
Figure 5-39	DAPI staining illustrating the removal of genetic material from hypertrophic constructs cultured on PGA after (B) 1 cycle, (C) 2 cycles and (D) 3 cycles of the decellularisation protocol compared (A) cellularised grafts (magnification x5	98
Figure 5-40	The percentage loss of GAG from the constructs cultured on PGA after cycles of washing the constructs with SDS and ionic buffers (* p<0.05, n=3).	98
Figure 5-41	Immunohistochemical and histological staining of the PGA constructs before implantation into the cranial defect model. (A) haematoxylin and eosin stain; (B) toluidine blue; (C) alcian blue; (D) alkaline phosphatase; (E) collagen type X; (F) alizarin red. Insert micrographs show non-specific staining. Scale bars = 100µm.	99
Figure 5-42	DAPI staining illustrating the decellularisation of the PGA constructs before implantation into the cranial defect. (A) Construct before decellularisation; (B) construct post decellularisation (magnification x5).	100
Figure 5-43	Immunohistochemical and histological staining of decellularised PGA constructs before implantation into the cranial defect. (A) haematoxylin and eosin stain; (B) toluidine blue; (C) alcian blue; (D) alkaline phosphatase; (E) collagen type X; (F) alizarin red. Insert micrographs show non-specific staining. Scale bars = 100 µm.	101
Figure 5-44	Staining to show the differentiation capacities of rat BM-MSCs. (B) Alcian blue staining to show proteoglycan-rich extracellular matrix of micromass cultures of MSCs cultured under conditions to induce chondrogenic differentiation (control (A)); (D) Alizarin red staining to show mineralisation in MSCs cultured under conditions to induce osteogenesis (control (C)); (F) oil red O staining of lipid vesicles in MSCs cultured under conditions to induce adipogenic differentiation (control (E)).	102
Figure 5-45	DAPI staining showing the attachment and penetration of BM-MSCs into the decellularised PGA constructs.(A) brightfield image of the decellularised construct, (B) DAPI image showing the penetration of the BM-MSC into the construct	103

Figure 5-46	MicroCT analysis of the cranial bone defects 4 weeks after implantation of either 'living', decellularised and BM-MSc recellularised PGA constructs compared to the control 'empty' defects. (n=3 animals/construct group)	104
Figure 5-47	Percentage bone volume in the empty defect compared to the repair seen using 'living', decellularised and MSC recellularised PGA constructs 4 weeks after implantation (n=3 animals/construct group).	105
Figure 5-48	Haematoxylin and eosin staining of cranial defects 4 weeks after implantation with either a 'living' PGA construct, decellularised PGA construct, decellularised PGA construct re-seeded with BM-MSCs or left unfilled. The arrow highlights the initial bone formation in the decellularised PGA construct. Magnifications are x4 (upper 4 images), x10 (middle 4 images) and x20 (bottom 4 images). Scale bars = 500 $\mu$ m (upper 4 images), 200 $\mu$ m (middle 4 images) and 100 $\mu$ m (bottom 4 images). (n=3 animals/construct group)	106
Figure 5-49	Alcian blue staining of cranial defects to show localisation of the glycosaminoglycans in the defects. 4 weeks after implantation with either a 'living' PGA construct, decellularised PGA construct, decellularised PGA construct re-seeded with BM-MSCs or left unfilled. Magnifications are x4 (upper 4 images), x10 (middle 4 images) and x20 (bottom 4 images). Scale bars = 500 $\mu$ m (upper 4 images), 200 $\mu$ m (middle 4 images) and 100 $\mu$ m (bottom 4 images). (n=3 animals/construct group)	107
Figure 5-50	MicroCT analysis of cranial defects after 8 weeks of implantation of either 'living', decellularised or BM-MSc recellularised hypertrophic constructs cultured on PGA compared to the empty (control) defects. (n=3 animals/construct group)	109
Figure 5-51	Percentage bone volume in the empty defect compared to the repair seen using 'living', decellularised and BM-MSc recellularised hypertrophic constructs cultured on PGA 8 weeks after implantation. (* p<0.05, ** p<0.01. n=3 animals/construct group)	110
Figure 5-52	Haematoxylin and eosin staining of defects 8 weeks after implantation with either a 'living' PGA construct, decellularised PGA construct, decellularised PGA construct re-seeded with BM-MSCs or left unfilled. Magnifications are x4 (upper 4 images), x10 (middle 4 images) and x20 (bottom 4 images). Scale bars = 500 $\mu$ m (upper 4 images), 200 $\mu$ m (middle 4 images) and 100 $\mu$ m (bottom 4 images). (n=3 animals/construct group)	111

Figure 5-53	Alcian blue staining of cranial defects to show localisation of the glycosaminoglycans 8 weeks after implantation with either a 'living' PGA construct, decellularised PGA construct, decellularised PGA construct re-seeded with BM-MSCs or left unfilled. Magnifications are x4 (upper 4 images), x10 (middle 4 images) and x20 (bottom 4 images). Scale bars = 500 $\mu$ m (upper 4 images), 200 $\mu$ m (middle 4 images) and 100 $\mu$ m (bottom 4 images). (n=3 animals/construct group)	112
Figure 5-54	MicroCT images of the cranial defects after 12 weeks of implantation of either 'living', decellularised or BM-MSC recellularised hypertrophic constructs cultured on PGA compared to the empty (control) defects. (n=3 animals/construct group)	113
Figure 5-55	Percentage bone volume in the empty defect compared to the repair seen using 'living', decellularised and MSC recellularised hypertrophic constructs cultured on PGA after 12 weeks after implantation. (** p<0.01. n=3 animals/construct group)	114
Figure 5-56	Haematoxylin and eosin staining of cranial defects 12 weeks after implantation with either a 'living' PGA construct, decellularised PGA construct, decellularised PGA construct re-seeded with BM-MSCs or left unfilled. Magnifications are x4 (upper 4 images), x10 (middle 4 images) and x20 (bottom 4 images). Scale bars = 500 $\mu$ m (upper 4 images), 200 $\mu$ m (middle 4 images) and 100 $\mu$ m (bottom 4 images). (n=3 animals/construct group)	115
Figure 5-57	Alcian blue staining of cranial defects 12 weeks after implantation to show localisation of the glycosaminoglycans 12 weeks after implantation with either a 'living' PGA construct, decellularised PGA construct, decellularised PGA construct re-seeded with BM-MSCs or left unfilled. Magnifications are x4 (upper 4 images), x10 (middle 4 images) and x20 (bottom 4 images). Scale bars = 500 $\mu$ m (upper 4 images), 200 $\mu$ m (middle 4 images) and 100 $\mu$ m (bottom 4 images). (n=3 animals/construct group)	116
Figure 5-58	Increase in the percentage bone volume in cranial defects implanted with a 'living' hypertrophic construct cultured on PGA over a 12 week period following implantation (p**<0.01. n=3 animals/time point)	117
Figure 5-59	Increase in the percentage bone volume in cranial defects implanted with a decellularised hypertrophic construct cultured on PGA over a 12 week period following implantation (p *<0.05. n=3 animals/time point)	118



Figure 5-60	Increase in the percentage bone volume increase in cranial defects implanted with BM-MSC recellularised hypertrophic construct cultured on PGA over a 12 week period following implantation ( n=3 animals/time point)	118
Figure 5-61	Percentage GAG accumulation within the ECM of hypertrophic constructs cultured on the PLLA/calcium phosphate scaffold material at day 14, 28 and 42 under static, semi-static and bioreactor culture conditions. (* p<0.05. n=6)	120
Figure 5-62	Histological analysis of PLLA/calcium phosphate constructs cultured under static, semi-static and bioreactor culture conditions. Insert micrographs show non-specific staining. Scale bars = 100µm. (representative images n=6)	1261
Figure 5-63	Immunohistochemical analysis of PLLA/calcium phosphate constructs cultured under static, semi-static and bioreactor culture conditions. Insert micrographs show non-specific staining. Scale bars = 100µm. (representative images n=6)	122
Figure 5-64	Comparison of the effect of static, semi-static and bioreactor culture conditions on collagen type II mRNA expression during a 42 day incubation period. The data is normalised to the gene expression observed after 72 hours on culture in expansion media on the PLLA/calcium phosphate scaffold materials (D0 of 3D chondrocyte differentaiation. (n=6).	123
Figure 5-65	Comparison of the effect of static, semi-static and bioreactor culture conditions on collagen type X mRNA expression during a 42 day incubation. The data is normalised to the gene expression observed after 72 hours on culture in expansion media on the PLLA/calcium phosphate scaffold materials (D0 of 3D chondrocyte differentaiation. (* p<0.05. n = 6)	123
Figure 5-66	Comparison of the effect of static, semi-static and bioreactor culture conditions on alkaline phosphatase mRNA expression during a 42 day differentiation period. The data is normalised to the gene expression observed after 72 hours on culture in expansion media on the PLLA/calcium phosphate scaffold materials (D0 of 3D chondrocyte differentaiation.(* p<0.05, *** p<0.005. n=6).	124
Figure 5-67	The percentage GAG concentration present in the PGA constructs cultured in three serum-free media compared to the serum-containing media. (* p<0.05, ** p<0.01. n=9)	126
Figure 5-68	Representative histological and immunohistochemical analysis of rat nasal chondrocyte constructs after 42 days culture on PGA in serum-free media 1. (A) Haematoxylin and Eosin Stain; (B) Toluidine Blue; (C) Alcian Blue; (D) Alkaline Phosphatase; (E) Collagen II; (F) Collagen X. Insert micrographs show non-specific staining. Scale bars =100 µm. (Representative images n=9)	127

Figure 5-69	Representative histological and immunohistochemical analysis of rat nasal chondrocyte constructs after 42 days culture on PGA in serum-free media 2. (A) Haematoxylin and Eosin Stain; (B) Toluidine Blue; (C) Alcian Blue; (D) Alkaline Phosphatase; (E) Collagen II; (F) Collagen X. Insert micrographs show non-specific staining. Scale bars =100 $\mu$ m. (representative images n=9)	128
Figure 5-70	Representative histological and immunohistochemical analysis of rat nasal chondrocyte constructs after 42 days culture on PGA in serum-free media 3. (A) Haematoxylin and Eosin Stain; (B) Toluidine Blue; (C) Alcian Blue; (D) Alkaline Phosphatase; (E) Collagen II; (F) Collagen X. Insert micrographs show non-specific staining. Scale bars =100 $\mu$ m. (Representative images n=9)	129
Figure 5-71	Collagen type II mRNA expression of the chondrocytes throughout the 42 day culture period on PGA. Showing the effect of serum-free media 2 and serum-free media 3 compared to serum media on the expression of collagen type II within the grafts. The data is normalised to the gene expression observed after 72 hours on culture in expansion media on the PLLA/calcium phosphate scaffold materials (D0 of 3D chondrocyte differentaiaition. (* p<0.05, n=6)	130
Figure 5-72	Collagen type X mRNA expression of chondrocytes throughout the 42 day culture period on PGA. Showing the effect of serum-free media 2 and serum-free media 3 compared to serum media on the expression of collagen type II within the grafts. The data is normalised to the gene expression observed after 72 hours on culture in expansion media on the PLLA/calcium phosphate scaffold materials (D0 of 3D chondrocyte differentaiaition.( * p<0.05 and ** p<0.01, n=6)	131
Figure 5-73	Alkaline phosphatase mRNA expression of chondrocytes throughout the 42 day culture period on PGA. Showing the effect of serum-free media 2 and serum-free media 3 compared to serum-containing media on the expression of collagen type II within the grafts. The data is normalised to the gene expression observed after 72 hours on culture in expansion media on the PLLA/calcium phosphate scaffold materials (D0 of 3D chondrocyte differentaiaition. (* p<0.05 and *** p<0.005, n=6)	132
Figure 6-1	Thyroid hormone activation of the Wnt signalling pathway leading to the production of runx2 and the terminal differentiation of chondrocytes.	159

## ***List of Tables***

Table 2-1	The mechanical strengths of cortical and cancellous bone (Hutmacher et al., 2007)	4
Table 2-2	The different properties of current bone graft techniques, showing their structural strength and osteoconductive and osteoinductive nature (adapted from Brydone et al. (Brydone et al., 2010)).	13
Table 2-3	Current biomaterials approved for clinical use for the repair of large or complex bone tissue defects.	15
Table 2-4	Examples of current bone tissue-engineering approaches for <i>in vivo</i> bone healing	19
Table 2-5	Examples of in human clinical studies looking at the regeneration of bone in a variety of defects	20
Table 4-1	Composition of reagents per cDNA synthesis reaction	52
Table 4-2	Composition of reagents per real time PCR reaction	53
Table 4-3	Taqman primer and probe identification numbers of assays used during q-PCR	54
Table 5-1	Measurement of the contact angle of water on the surface of the scaffold material. Analysis was performed on 3 individual specimen per scaffold group, The results are expressed as the means +/- standard deviations	64
Table 5-2	Manufacturer and batch number of the five FCS batches tested for chondrocyte growth and hypertrophic differentiation	66
Table 5-3	Composition of the three serum-free media tested for chondrocyte survival, growth and hypertrophic differentiation.	125

## ***Presentations, Awards and Publications***

### ***Poster Presentations***

#### **Termis 2011**

Kwarciak A, Bardsley K\*, Freeman C, Brook I, Hatton P, Crawford A. Tissue-engineered hypertrophic cartilage undergoes angiogenesis and osteogenesis in cranial defects. *Histology and Histopathology*, 2011 26(supplement 1): p50

#### **BiTEG 2012**

Bardsley K, Brook I, Hatton P.V, Crawford A. Effect of Scaffolds on Hypertrophy of Cultured Nasal Chondrocytes.

#### **Mellanby Bone Conference 2012**

Bardsley K, Brook I, Hatton P.V, Crawford A. The Effect of PLLA/Calcium Phosphate Composite Scaffolds on the Formation of Hypertrophic Cartilage Constructs for Bone Tissue Engineering.

#### **Termis 2012**

Bardsley K, Brook I, Hatton P.V, Crawford A, The effect of composite Scaffolds on the hypertrophy of nasal chondrocytes. *Journal of Tissue Engineering and regenerative Medicine*, 2012. 6(supplement 1): p31

### ***Oral Presentations***

#### **Clinical School of Dentistry, University of Sheffield 2011**

Bardsley K, Kwarciak A, Freeman C, Brook I, Hatton P, Crawford A. Tissue Engineering Hypertrophic Cartilage.

#### **IADR 2012**

Bardsley K, Hatton P.V, Brook I, Crawford A. Effect of calcium phosphate/poly-L-lactic acid scaffolds on chondrocyte hypertrophy.

#### **Clinical School of Dentistry, University of Sheffield 2013**

Bardsley K, Freeman C, Brook I, Hatton P, Crawford A Tissue-Engineered Hypertrophic Cartilage for Bone Graft Applications

**BSODR 2013 – Senior Colgate Oral Presentation Awards**

Bardsley K, Hatton P.V, Brook I, Crawford A. Mimicking natural bone development to produce tissue for bone grafts.

***Awards***

**September 2012** IADR Travel Bursary, Helsinki

**September 2012** TERMIS Travel Bursary, Vienna

**September 2012** TERMIS International Congress Poster Finalist, Vienna

**September 2013** BSODR Travel Bursary, Bath

**September 2013** Commendation in Senior Colgate Oral Presentation Awards

***Proposed Publications***

Bardsley K, Kwarciak A, Brook I, Hatton P, Crawford A. Characterisation of Tissue Engineered Hypertrophic Cartilage

Bardsley K, Freeman C, Brook I, Hatton P, Crawford A. Repair of Rat Cranial Defects using Tissue Engineered hypertrophic Constructs

Bardsley K, Kwarciak A, Brook I, Hatton P, Crawford A. Novel Calcium Phosphate/Poly-L-Lactic Acid Composite Scaffold for the Fabrication of Tissue-Engineered Hypertrophic Constructs

Bardsley K, Kwarciak A, Brook I, Hatton P, Crawford A. The Development of a Serum-Free Media for Hypertrophic Cartilage Tissue Engineering

***Patents Pending***

Bardsley K, Freeman C, Brook I, Hatton P, Crawford A. The use of Decellularised of Hypertrophic Cartilage for the Repair of Bone Defects

## **1 Introduction**

There is a high demand for graft materials to repair and regenerate bone tissue in a wide variety of conditions including fracture non-unions, congenital defects and trauma. Bone is the second most transplanted tissue, with around 2.2 million grafts being performed every year. Currently the 'gold standard' for the repair of bone tissue is an autograft, where bone is taken from a site within the patient and re-implanted into a defect. While generally giving the best clinical results, this method has drawbacks including as long-term post-operative pain and/or donor site morbidity. There is also a limit to the volume of bone which can be taken by autograft.

Other methods have been used clinically including allografts and xenografts as well as osteoconductive biomaterials. Allografts and xenografts require a high degree of processing before they can be used, which decreases their osteoinductive potential and they have the added risk of disease transmission. Alloplastic biomaterials such as calcium phosphates are widely utilised, but they lack the osteogenic potential of autograft and the observed host response is not consistent. Therefore the repair of bone defects remains a challenge for surgeons and it is hoped that tissue-engineering will provide a new source of bone graft tissue for transplantation.

The majority of bone tissue-engineering research has centred on the differentiation of adult stem cells into osteoblasts to form new tissue through the process of intramembranous ossification. The endochondral ossification pathway which involves the initial formation of a hypertrophic cartilage template, which is then remodelled into bone *in vivo* has until recently been neglected. Use of the endochondral pathway may, however, prove to be the tissue-engineering strategy of choice for bone regeneration. Development of most bones in the body and fracture repair commonly occurs via this pathway. The use of cartilage as a graft material is advantageous as it has the ability to survive in the relatively low oxygen concentrations typically found at

the graft site. Hypertrophic cartilage has also been reported to produce the biological molecules, such as vascular endothelial growth factor (VEGF) that could enable graft integration, blood vessel formation and the subsequent remodelling into bone. For these reasons, the use of a hypertrophic cartilage graft has the potential to become an alternative approach for the regeneration of bone.

Previous research in this area has highlighted the potential of both MSCs and nasal chondrocytes to be a cell source for the production of hypertrophic chondrocyte grafts. Nasal chondrocytes, however, are an advantageous source due to their ease of isolation and high proliferation independent of patient age. Despite the compelling arguments that suggest that hypertrophic cartilage has a significant potential for the regeneration of bone in complex defects, surprisingly little research in this field has been reported to date. Therefore the aim of this research is to further investigate the ability of nasal chondrocytes to produce hypertrophic chondrocyte grafts and to assess their potential for the regeneration of bone *in vivo*. The specific objectives of this research can be found in section 3.

## **2     *Literature Review***

### **2.1    *Basic Bone Biology***

#### **2.1.1    *Function and Basic Structure***

Bone tissue constitutes the major load-bearing part of the endoskeleton of vertebrates and has a variety of functions within the body. It is essential not only for maintaining body structure and allowing for movement, but also for the physical protection of the internal organs and tissues. Bone is also able to store minerals, fat and growth factors which, if required, can be released (Clarke, 2008). The marrow found within the medullary cavities of the long bone and interstices of the cancellous bones is essential for haematopoiesis (blood cell production), as well as being a source for stem cell regeneration (Taichman, 2005).

Bone structures consist of two major macrostructures, cancellous (trabecular) and cortical (compact) bone (Figure 2-1) (Rho et al., 1998). Cancellous bone is composed of trabecular struts, which leads to a honeycomb structure containing pores filled with bone marrow (Rho et al., 1998). This cancellous structure is found in the centre of the bone and the orientation of the trabecular struts allows it to withstand the stresses. Cancellous bone is also more metabolically-active than cortical bone and is remodelled by the osteoblasts, osteocytes and osteoclasts (Rho et al., 1998). Cortical bone has a more compact structure with a more defined architecture and is not as regularly remodelled.



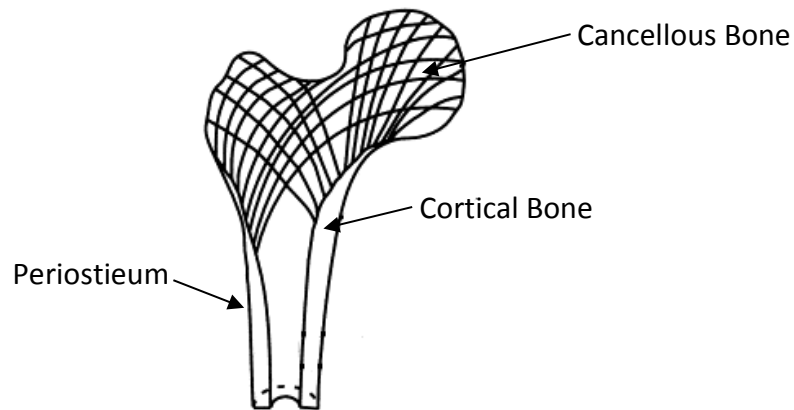


**Figure 2-1:** The structure of a long bone, showing the positioning of the cortical and cancellous bone as well as the positioning of the periosteum (Adapted from Rho et al (Rho et al., 1998)).

The primary tissue of bone, osseous tissue, is hard but lightweight and mainly composed of the mineral, hydroxyapatite, and proteins of which collagen type I is the major component (Clarke, 2008). Bone has a high compressive strength, but poor tensile and shear stress strength (Table 2-1). These properties makes bone relatively brittle, however, it does possess some elasticity due to the high collagen content within the osseous tissue (Hutmacher et al., 2007).

**Table 2-1:** The mechanical strengths of cortical and cancellous bone (Hutmacher et al., 2007)

	<b>Cortical Bone</b>	<b>Cancellous Bone</b>
<b>Compressive Strength (MPa)</b>	100-230	2-12
<b>Tensile Strength (MPa)</b>	50-150	10-20
<b>Fracture Toughness (MPam<sup>1/2</sup>)</b>	2-12	-
<b>Young's Modulus (GPa)</b>	7-30	0.5-0.05

The main cells found within bone tissue are osteoblasts, osteocytes and osteoclasts which are responsible for bone formation, maintenance and resorption respectively. Osteoblasts are mononucleated bone-forming cells, which are found on the active surfaces of bone and are derived from osteoprogenitors. They produce an osteoid (pre-bone) extracellular matrix (ECM) which is mineralised to form new bone (Clarke, 2008). Once osteoblasts are entrapped within the mineralised matrix they then further differentiate into osteocytes. Osteocytes (mature bone cells) are found within lacunae in the bone and maintain the bone through ECM maintenance and calcium homeostasis (Bonewald, 1999). Finally osteoclasts are large multinucleated cells equipped with phagocyte-like mechanisms similar to macrophages. They are found in Howships lacunae on actively resorbing bone surfaces and slowly resorb bone (Boyle et al., 2003).

### **2.1.2 Ossification**

Ossification is the process of bone formation during embryogenesis and skeletal development. It occurs via two pathways, intramembranous ossification and endochondral ossification. Intramembranous ossification is required for the formation of the 'flat' bones, such as the cranium (Ornitz and Marie, 2002), whereas endochondral ossification produces the long bones, such as the tibia.

### **2.1.3 Intramembranous Ossification**

Intramembranous ossification revolves around the direct differentiation of mesenchymal stem cells (MSCs) into osteoblasts, forming the 'flat' bones of the skull. Initially MSCs condense to form compact nodules, producing an osteoid ECM as they differentiate into osteoblasts (Gilbert, 2000). Osteoblasts deposit a calcium-proteoglycan ECM, which has the ability to bind calcium salts allowing for the initiation of calcification (Gawlitza et al., 2010). Calcification of the ECM proceeds in the form of bony spicules radiating from the osteoblasts. Once the osteoblasts are isolated within

the calcified ECM they further differentiate into osteocytes. When calcification is complete MSCs once again compact around the edges of the bone and differentiate to form the periosteum, depositing ECM parallel to the bone (Gilbert, 2000).

Intramembranous ossification relies on the temporal expression of several growth factors and transcription factors. Bone morphogenic proteins (BMP), in particular BMP2, BMP4 and BMP7, are essential in ensuring the direct differentiation of neural crest-derived MSCs into osteoblasts (Gilbert, 2000). Transcription factor, runx2, is also important as it upregulates the expression of genes associated with ECM mineralisation, such as osteopontin and osteocalcin. Runx2 also has an effect on vascular endothelial growth factor (VEGF) expression, a key growth factor for attracting endothelial cells into the ECM enabling the formation of capillaries and the subsequent vascularisation of the bone (Carlevaro et al., 2000). This vascularisation of the bone is essential in intramembranous ossification as osteoblast require a high rate of nutrient exchange in order to survive (Hing, 2004).

#### ***2.1.4 Endochondral Ossification***

The majority of the skeleton, including the axial and appendicular skeleton, is formed during embryogenesis through endochondral ossification (Wuelling and Vortkamp, 2010). This method of ossification involves the formation of a hypertrophic cartilage template which calcifies and is remodelled into bone. Endochondral ossification and the chondrocyte differentiation pathway can be seen the growth plate of young children and adolescents (Figure 2-2). Proliferative columnar chondrocytes, which produce a complex hyaline-cartilage ECM, in which the predominant protein is collagen type II, These cells then undergo terminal differentiation into hypertrophic chondrocytes, which produce a mainly collagen type X ECM (Scotti et al., 2010, Gawlitta et al., 2010).

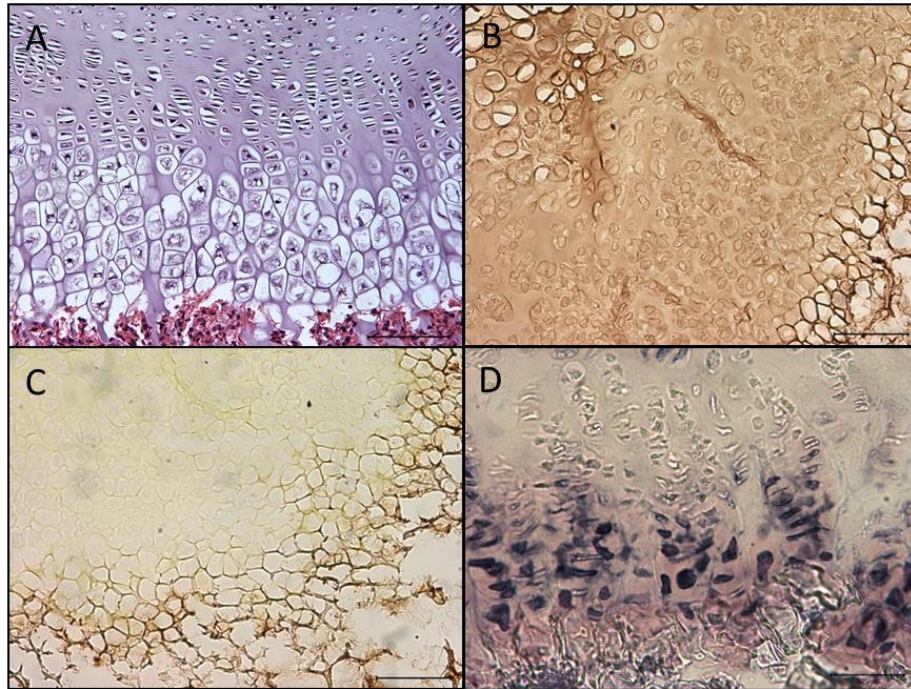


**Figure 2-2:** Images of the growth plate of the rat, showing the different states of chondrocyte differentiation seen during endochondral ossification. (A) Haematoxylin and eosin staining to show the general cell morphology in the growth plate; (B) collagen type II localisation; (C) collagen type X localisation and (D) alkaline phosphatase localisation. (Images used with permission from Kwarciak (Kwarciak, 2009)).

During embryonic endochondral ossification MSCs condense in the area of bone formation and differentiate into two populations of chondrocytes, distal and columnar (Wuelling and Vortkamp, 2010). Distal chondrocytes proliferate at a low rate and form the articular cartilage which is found covering the ends of bones in the joints (Wuelling and Vortkamp, 2010). Columnar chondrocytes are responsible for bone formation and subsequent tissue growth within the growth plate. These columnar chondrocytes are transient, highly proliferative cells, which are organised into columns and can be found towards the centre of the bone (Wuelling and Vortkamp, 2010).

Columnar chondrocytes have a specific morphology and produce a complex hyaline-cartilage ECM, consisting of type II collagen, type IX collagen, type XI collagen,

aggrecan, chondronmodulin-1 and matrilin-3. Columnar chondrocytes also characteristically express the transcription factor SRY (sex determining region Y)-box 9 (sox9), which works through the parathyroid hormone receptor pathway (PTHrP) to keep the chondrocytes in this proliferative state (Deschaseaux et al., 2009).

Hypertrophy is the final differentiation state in chondrocyte differentiation. Hypertrophic chondrocytes are larger than the proliferative chondrocytes and produce a characteristic hypertrophic ECM, which includes collagen type X and alkaline phosphatase (Scotti et al., 2010, Gawlitta et al., 2010). Both of these ECM proteins have specific roles in the endochondral ossification process. Collagen type X plays an essential role in the entrapment and binding of matrix vesicles within the ECM as well as implementing an influx of calcium ions into the vesicles (Kirsch and Wuthier, 1994). A complete deletion of collagen type X in mice resulted in abnormal trabecular development and the under development of bones (Kwan et al., 1997, Chung et al., 1997). Alkaline phosphatase has been shown to be expressed on the membranes of hypertrophic chondrocytes within the growth plate, with a complete deletion in mice resulting in the hypomineralisation of bones (Anderson et al., 2004). Alkaline phosphatase is known to hydrolyse inorganic pyrophosphate (PPi), producing orthophosphate for mineral incorporation and reducing the inhibitory effect of PPi at the mineralisation site (Robison, 1926), (Fleisch et al., 1966).

Endochondral ossification is tightly regulated by the several signalling molecules, growth factors and transcription factors. This regulation can be seen in Figure 2-3 and illustrates the importance of the temporal changes in the expression of these molecules in the differentiation of columnar chondrocytes into hypertrophic. Errors in this gene expression through gene mutations, can lead to developmental problems, such as dwarfism.

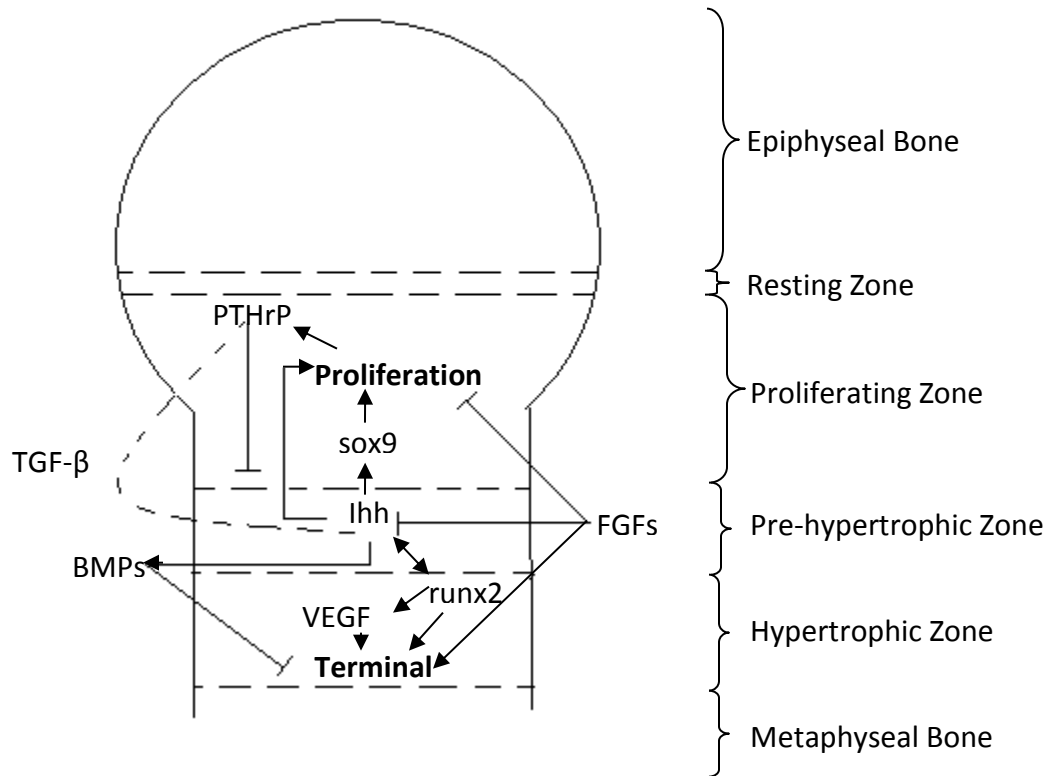


**Figure 2-3:** Gene expression in the growth plate and their role in regulation of hypertrophic differentiation.

Sox9, transforming growth factor-beta (TGF- $\beta$ ) and Indian hedgehog (lhh) all work through the PTHrP pathway in order to keep the chondrocytes in a proliferative, columnar phenotype (Deschaseaux et al., 2009, Pateder et al., 2000, Mak et al., 2008). This expression of PTHrP keeps the chondrocytes in a proliferative state and is essential in the growth plate in order to maintain the width of the proliferative zone of the growth plate. Overexpression of PTHrP in mice leads to chondrodysplasia characterised by a delay in endochondral ossification and mice being born with cartilaginous endochondral skeleton (Weir et al., 1996). As mentioned above sox9 is highly expressed by proliferative chondrocytes within the growth plate, with a heterozygous deletion results in campomelic dysplasia, a severe form of dwarfism affecting all cartilage and endochondral structures (Hattori et al., 2010). TGF- $\beta$  is often employed in

articular cartilage tissue-engineering as it is well known to inhibit hypertrophic differentiation and downregulates collagen type X and alkaline phosphatase expression in cultured chondrocytes (Ferguson et al., 2000, Okeefe et al., 1988). As the chondrocytes start to differentiate, they take on a pre-hypertrophic phenotype, expressing signalling molecule *Ihh*. *Ihh* is essential at regulating the width of the growth plate in developing long bones as it is able to inhibit the further differentiation of proliferative chondrocytes in a dose dependant manor (Mak et al., 2008).

Expression of transcription factor *runx2* is essential to induce proliferative chondrocytes to exit the cell cycle and differentiate into hypertrophic chondrocytes (Deschaseaux et al., 2009). *Runx2* is an essential transcription factor for several other key molecules required for mineralisation, including osteopontin, VEGF and specific matrix metalloproteinases (MMPs). MMPs are required for the breakdown of matrix proteins in order for mineralisation and remodelling into bone to occur (Vu et al., 1998). MMP-13 is especially important during endochondral ossification as it breaks down the collagen type II initially laid down by the proliferative chondrocytes (Inada et al., 2004). Osteopontin is a non-collagenous bone matrix protein, which allows for osteoclast attachment to mineralised matrix, therefore allowing for matrix remodelling (Reinholt et al., 1990). VEGF is essential for attracting endothelial cells and allowing for the ingrowth of blood vessels into the cartilage. Vascularisation of the tissue is essential for nutrient exchange within the tissue as well as delivering osteoblasts, osteoclasts and haematopoietic precursors (Scotti et al., 2010).

The fate of the hypertrophic chondrocytes after terminal differentiation is highly debated (Shapiro et al., 2005). It is believed that some hypertrophic chondrocytes undergo apoptosis, characterised by DNA fragmentation and ultra-structural changes, leaving behind the ECM as a scaffold within which vascularisation and bone formation can occur (Zenmyo et al., 1996). It is also thought that some hypertrophic chondrocytes undergo “transdifferentiation” into bone-forming cells (Shapiro et al., 2005). However, definitive evidence of this process occurring in the growth plate is lacking with most

reports being circumstantial and based on microscopy examination of the chondro-osseous junction (Shapiro et al., 2005).

## **2.2 *Bone Repair and Remodelling***

Unlike soft tissue injuries, which repair through the formation of fibrous scar tissue, bone defects heal through the formation of new bone which is indistinguishable from the uninjured tissue (Glowacki, 1998). The repair of the damaged bone resembles that of ossification during organogenesis and is comprised of a combination of both intramembranous and endochondral ossification (Dimitriou et al., 2005). When bones are fractured a complex cascade of events is required in order to restore the integrity of the bone. These events are essential in ensuring that the required cells (MSCs and osteoclasts) and soluble molecules (growth factors, cytokines, hormones and vitamins) are delivered to the injury site (Barnes et al., 1999, Bolander, 1992).

The initial damage causes the disruption of blood vessels around the fracture, the coagulation of the subsequent internal bleeding leads to the formation of a haematoma enclosing the injury site and initiating angiogenic activity. Inflammatory cells, fibroblasts and stem cells are then recruited to the injury site and new blood vessels are formed from the expansion of the pre-existing vessels. Soluble molecules, such as growth factors and cytokines, are released at this stage in order to encourage and regulate the re-growth of the bone (Carano and Filvaroff, 2003).

Granulation tissue eventually forms at the end of the fractured bone and is gradually replaced by fibrocartilage. The internal callus of this fibrocartilage proceeds through the process of endochondral ossification and becomes mineralised by calcium phosphate, in the form of hydroxyapatite crystals, to form a woven bone callus, while the external callus undergoes intramembranous ossification to form a periosteum. This repair gives rise to a large callus which needs to be remodelled. The callus is reduced in size as the woven bone undergoes remodelling and is replaced with secondary lamellar



bone. The vascular supply also is remodelled to be appropriate for the final bone tissue (Trueta, 1963, Carano and Filvaroff, 2003).

This process of natural bone repair can only occur within a bone defect or fracture which is less than 2-2.5 times the diameter of the bone (critical sized for bone repair), where the fractured surfaces are close together (Reichert et al., 2009, Gugala et al., 2007). Critical size defects in the bone are defects which will not repair within the animal's lifetime and become scarred rather than being regenerated leading to non-union (Petite et al., 2000), which seriously affects the quality of life of the patients due to the associated loss of function (Drosse et al., 2008). It is therefore necessary to investigate the use of a bone graft material in order to allow or aid the healing of these defects.

### **2.3 Clinical Bone Defect Repair**

Healing complex bone defects, which will not heal naturally, can be achieved either through bone transplants or by the insertion of a tissue-engineered graft. Any material used to fill these defects should ideally be osteoconductive and osteoinductive. Osteoconductive materials provide a scaffold which promotes the growth of bone on the graft material, whereas osteoinductive materials stimulate bone precursor cells to progress down the bone-forming cell lineage (Albrektsson and Johansson, 2001).

#### **2.3.1 Current Approaches for Bone Grafts**

The most commonly used method in repairing critical bone defects is by transplanting a bone graft into the defect. Bone grafts are required to fill a void and support and enhance biological regeneration and are classified as: 1) autologous, where the bone is harvested from the patient with the defect; 2) allogeneic, where bone is harvested from another person or cadaver or 3) xenogeneic, where bone is harvested from an animal source (Parikh, 2002). A more recent approach is to use a biomaterial to fill the defect and encourage bone growth. The type of graft material used is dependent on

several factors including: the clinical application; defect size and the volume of bone required; the desired bioactivity and resorption rates; side effects and the availability and cost of the graft (Brydone et al., 2010). All current clinical methods have different activities and strengths (Table 2-2), which affect their ability to aid bone tissue regeneration *in vivo*.

**Table 2-2:** The different properties of current bone graft techniques, showing their structural strength and osteoconductive and osteoinductive nature (adapted from Brydone et al. (Brydone et al., 2010)).

Graft Type	Strength	Osteoconductivity	Osteoinductivity
<b>Autografts</b>			
Cancellous	+	++	+
Cortical	++	+	+/-
<b>Allografts</b>			
Cancellous	+	++	+
Cortical	++	+/-	+/-
Demineralised bone matrix	-	++	+++
<b>Bone Substitutes</b>			
Calcium phosphates	-	+	-
Bioactive Composites	+	+	-

Autologous transplantation (autograft) is seen as the gold standard for bone repair. Bone tissue is harvested from the patient, usually from the iliac crest or tibia, resulting in a living, osteoconductive and osteoinductive graft. Autografts have been proven to allow for efficient repair within the defect *in vivo* (Frohlich et al., 2008). One advantage of autologous grafts is that there is no immune rejection of the graft (Chang et al., 2009). It is also possible to harvest bone with its vascularisation intact, which can be reattached at the site of injury to reduce the chance of tissue necrosis after implantation into a low nutrient wound bed. Autografts, however, do have disadvantages. There is a risk of donor site morbidity and prolonged post-operative

pain, which affects around 10-30 % of patients (Meijer et al., 2007, Goulet et al., 1997). The volume of bone which can be harvested from the patient is also limited, especially in younger patients, and therefore autografts are not suitable when large or multiple defects are present without causing instability of the donor bone (Hing, 2004).

Allografts and xenografts, where bone is taken from a cadaver or animal source respectively, have been used to circumvent the issues seen when using autografts. There is no donor site morbidity or associated post-operative pain. Allografts also allow for higher volumes of bone to be harvested and therefore are useful when looking at large or multi-defect repair. Bone allografts, however, are less osteoconductive and osteoinductive than autologous bone grafts due to the high degree of processing required to reduce immunogenicity and ensure sterility of the allografts. This leads to slower rates of revascularisation and a higher rate of graft re-absorption (Frohlich et al., 2008). Allografts also have the potential disadvantage to cause immunogenic responses and possible viral transmission between patients (Damien and Parsons, 1991, Chang et al., 2009). One study using allografts for bone regeneration after bone tumour resection showed a 19 % chance of fracture, 14 % non-union and a 10% chance of infection (Mankin et al., 1992).

The use of biomaterials to repair defects is a relatively new field and some of the bone substitutes used for clinical applications are shown in

Table 2-3. Calcium phosphates are commonly used as biomaterials for bone repair due to their osteogenic potential and biocompatibility and have been researched for their ability to repair bone defects since the 1920s (Albee, 1920, Ogoose et al., 2005). While hydroxyapatite is the main component in bone and has a high compressive strength, it is a brittle material which has low rates of resorption (Stevens, 2008). A biomaterial should in general degrade *in vivo* at the same rate at which cells within the body deposit new ECM. Tri-calcium phosphate, therefore, is often used as an alternative to hydroxyapatite, as although it is not as strong it has faster resorption rates which are more comparable with the rate of ECM deposition (Ogoose et al., 2005). The use of a

biphasic calcium phosphate (usually a mixture of hydroxyapatite and tri-calcium phosphate), is seen to be advantageous, as this biomaterial is a balance between strength, from the hydroxyapatite, and higher resorption rates, from tri-calcium phosphate. Biphasic calcium phosphates are used in many of the biomaterials used for bone regeneration. The use of calcium phosphates, however, do have drawbacks as these materials can be prone to fatigue, fracture, toxicity and wear (Chang et al., 2009).

Bioactive composites, where there is a combination of polymer and calcium phosphate, have also been used in the repair of defects. The majority of these biomaterials utilise collagen as the polymer, as this is one of the main ECM components within bone itself and is a haemostatic agent as well as aiding bone regeneration (Lawson and Czernuszka, 1998). The advantage of these composite scaffolds is that they may be able to better simulate the mechanical characteristics of natural bone (compressive and tensile strength) (Lickorish et al., 2007).

Bioactive glass (bioglass) are also used for the repair of defects and are composed of  $\text{SiO}_2$ ,  $\text{Na}_2\text{O}$ ,  $\text{CaO}$  and  $\text{P}_2\text{O}_5$  in different proportions. Bioactive glasses have been shown to bond with bone more rapidly than other bioactive ceramics (Oonishi et al., 1997, Oonishi et al., 2000) as well as stimulating osteoblasts. This stimulation has been attributed to the release of soluble silica and calcium ions from bioglasses after implantation. (Xynos et al., 2000). Bioglass 45S5 is the most commonly used formulation of bioglass, developed by Hench et al in the late 1960s, and contains 45 wt %  $\text{SiO}_2$  and a 5:1 ratio of  $\text{CaO}$  to  $\text{P}_2\text{O}_5$ . Bioglass has been shown to be highly reactive in aqueous media and is extremely bioactive, however, it does have disadvantages including mechanical weakness, which makes it unable to be used in load-bearing applications (Jones, 2013).

Other methods include the direct injection of growth factors into the site of the defect in order to promote new bone regeneration. BMP-2 is the most common growth factors used for bone tissue engineering and is approved for use in the treatment of bone defects by the FDA. BMP-2 is a member of the transforming growth factor b

super family and has been shown to promote the osteogenesis of MSCs and result in bone formation both *in vitro* and *in vivo* (Zhang et al., 2014). While this method has been shown to be clinically effective it needs to be implanted with a carrier, such as collagen sponges, to prevent immediate diffusion from the injury site due to its short half-life (7-15 minutes) (Friess et al., 1999). This short half-life means that supraphysical concentrations of BMP-2 are required, which can cause complications and side effects, such as osteolysis, ectopic bone formation and radiculitis (Carragee et al., 2011).

**Table 2-3:** Current biomaterials approved for clinical use for the repair of large or complex bone tissue defects.

<b>Product Name</b>	<b>Company</b>	<b>Composition</b>	<b>Form</b>
<b>Norian®SRS®</b>	DePuy Synthes	Calcium phosphate	<ul style="list-style-type: none"> <li>• Paste</li> <li>• Putty</li> </ul>
<b>Conduit® TCP</b>	DePuy Synthes	$\beta$ -tricalcium phosphate	<ul style="list-style-type: none"> <li>• Granules</li> </ul>
<b>ChronOS®</b>	DePuy Synthes	$\beta$ -tricalcium phosphate	<ul style="list-style-type: none"> <li>• Granules</li> <li>• Preform shapes</li> </ul>
<b>OpteMx®</b>	Exactech	Biphasic calcium phosphate	<ul style="list-style-type: none"> <li>• Granules</li> <li>• Preform shapes</li> </ul>
<b>MasterGraft® Granules</b>	Medtronic Spinal and Biologics	Biphasic calcium phosphate	<ul style="list-style-type: none"> <li>• Granules</li> </ul>
<b>MasterGraft® Matrix</b>	Medtronic Spinal and Biologics	Biphasic calcium phosphate and collagen	<ul style="list-style-type: none"> <li>• Compression resistant blocks</li> </ul>
<b>Vitoss®</b>	Stryker Biotech	$\beta$ -tricalcium phosphate and collagen	<ul style="list-style-type: none"> <li>• Putty</li> <li>• preform shapes</li> </ul>
<b>NovaBone</b>	NovaBone	45S5 Bioglass	<ul style="list-style-type: none"> <li>• Particles (90-710<math>\mu</math>m)</li> </ul>
<b>BioGran®</b>	Biomet3i	45S5 Bioglass	<ul style="list-style-type: none"> <li>• Particles (300-380<math>\mu</math>m)</li> </ul>
<b>INFUSE</b>	Medtronic	12mg recombinant BMP-2 in collagen carrier sponge	<ul style="list-style-type: none"> <li>• Collagen sponge</li> </ul>

## **2.4 Current Tissue-Engineering Approaches to Bone Transplants**

The clinical approaches to bone regeneration discussed in section 2.3.1, have the ability to repair bone defects, however, they all have their disadvantages. Regenerative medicine and in particular tissue-engineering of a bone graft, therefore, would be advantageous as it allows a natural tissue to be produced that will enable complete bone healing which has fewer side-effects to the patient, as well as overcoming problems with material quality and abundance.

Regenerative medicine can be defined as a method which “replaces or regenerates human cells, tissues or organs, to restore or establish normal functions.” (Mason and Dunnill, 2008) Tissue-engineering is found within this field and is an “interdisciplinary field that applies the principles of engineering and life sciences toward the development of biological substitutes that restore maintain, or improve tissue function or a whole organ.” (Langer and Vacanti, 1993). The work presented within this thesis aims to tissue engineer a hypertrophic cartilage which can be used to regenerate bone within complex defects. The area of tissue engineering is quickly evolving to include more novel approaches using a combination of scaffolds, cells and growth factors (Tuan et al., 2003), to allow for tailor-made bone grafts which will enable the repair of the damaged bone. Table 2-4 shows examples of *in vivo* experiments using tissue-engineering approaches using either growth factors, cells or both and a scaffold to induce bone repair in critical defects.

The most common approach in tissue-engineering is to utilise a scaffold to support cells *in vitro* while they create an extracellular matrix, which will provide a foundation for the formation of a new native tissue (Howard et al., 2008). This approach has been utilised for bone tissue-engineering as shown in Table 2-4. The majority of this work revolves around using adult stem cells, MSCs and growing these cells on scaffolds including porous ceramics, such as hydroxyapatite (Bruder et al., 1998), and polymers, such as PGLA (El-Amin et al., 2002), to produce bone through induction of osteoblastic differentiation followed by ECM formation. The bulk of this research has focussed on

following the pathway of intramembranous ossification to produce a bone tissue; however this method of tissue-engineering has drawbacks as bone requires a high nutrient exchange and high vascularisation which is not present within the wound bed (Hing, 2004).

There are several clinical studies utilising regenerative medicine for the regeneration of bone in non-union defects. The majority of these studies utilise MSC derived from the patient and a calcium phosphate scaffold material (Table 2-5). The advantages of these materials is that the use of both MSC and calcium phosphates have been approved for use individually (Chatterjea et al., 2010). The majority of clinical studies have focused on the addition of undifferentiated MSC directly on to the scaffold before direct implantation into the defect without in vitro differentiation. This thesis differs from the current in human clinical studies and aims to fabricate a fully engineered tissue which is both osteoconductive and osteoinductive, which will give equivalent or better surgical outcomes than the current 'gold standard' of autologous bone.

**Table 2-4:** Examples of current bone tissue-engineering approaches for *in vivo* bone healing

Cell Source	Scaffold material	Species	Details	Reference
None	rhTGF- $\beta$ and rhBMP-2 calcium phosphate	Rabbit	<ul style="list-style-type: none"> <li>• Orthopic bone formed in cranial defects compared to implants not loaded with growth factors</li> </ul>	(Jansen et al., 2005)
Human BMCs	VEGF encapsulated PLLA	Nude Mice	<ul style="list-style-type: none"> <li>• Compared to scaffold without VEGF</li> <li>• After 4 weeks enhanced bone formation seen</li> </ul>	(Kanczler et al., 2008)
Human Adipose-derived Stem Cells	PLGA	Nude Mice	<ul style="list-style-type: none"> <li>• Critical size defects (4mm)</li> <li>• Defects engrafted with undifferentiated adipose-derived stem cells showed bone regeneration throughout</li> </ul>	(Levi et al., 2010)
MSCs	Triphasic ceramic coated HA	Goat	<ul style="list-style-type: none"> <li>• 20mm bone defect</li> <li>• After 4 months complete repair seen</li> </ul>	(Nair et al., 2008)
Non-cellular and MSCs	Cross-linked Collagen	Rat	<ul style="list-style-type: none"> <li>• 7mm cranial defects in Wistar rats</li> <li>• Both cell-free and MSC grafts showed excellent healing compared to the empty defect.</li> </ul>	(Lyons et al., 2010)
MSCs	PLGA	Rabbit	<ul style="list-style-type: none"> <li>• <i>in vitro</i> bone formation before implantation into mandibular</li> <li>• After 12 weeks polymer had degraded and defect was filled with bone</li> </ul>	(Ren et al., 2005)
Osteogenic cells derived from ESC	PLGA/hydroxyapatite	Nude Mice	<ul style="list-style-type: none"> <li>• Placed subcutaneously in nude mice</li> <li>• 8weeks post <i>in vivo</i> implantation new bone had formed on the composite scaffold</li> </ul>	(Kim et al., 2008)



**Table 2-5:** Examples of in human clinical studies looking for the regeneration of bone in a variety of defects

Cell Source	Scaffold	Number of patients	Outcomes	Reference
Bone marrow	Hydroxyapatite	3 (long bone defects)	<ul style="list-style-type: none"> <li>• First clinical trial in humans using hMSCs</li> <li>• Good clinical recovery with bone regeneration and integration of the host bone with no side effects after 6-7 years follow up</li> </ul>	(Quarto et al., 2001)
Bone Marrow	Hydroxyapatite	6 (intraoral osseous defects)	<ul style="list-style-type: none"> <li>• 5 patients had no new bone formation and highlighted the variation of bone marrow aspirates</li> </ul>	(Meijer et al., 2008)
Adipose tissue	$\beta$ -tricalcium phosphate	1 (maxiofacial reconstruction)	<ul style="list-style-type: none"> <li>• First clinical study to use autologous MSCs derived from adipose tissue and expanded.</li> <li>• Use of rhBMP-2</li> <li>• Use of a microvascular flap</li> <li>• 8-month follow up indicated presence of mature bone.</li> </ul>	(Mesimaki et al., 2009)

### ***2.5 Tissue-Engineering Bone using the Endochondral Ossification Pathway***

Most bone tissue-engineering research, as discussed in previous sections, has centred on the direct differentiation of stem cells into osteoblasts to produce bone tissue and therefore mimics the intramembranous ossification pathway. This differentiation technique, however, has several drawbacks for clinical applications. Osteoblasts and bone tissue require high nutrient exchange rates and oxygen levels within the tissue and because of these requirements, cannot withstand the hypoxic conditions usually found in a wound bed (Malda et al., 2003). It is therefore, more difficult for these

grafts to survive once implanted into a defect unless a functionally adequate blood supply can be immediately established to the tissue. This need for high nutrient exchange also limits the size of graft that can survive during *in vitro* culture as well as after *in vivo* implantation.

Therefore tissue-engineering a bone graft material following the endochondral ossification pathway maybe an advantageous method to circumvent the problems seen when using the intramembranous pathway. The production of a hypertrophic cartilage template which can be implanted into a defect and be remodelled into bone maybe advantageous as cartilage is an avascular tissue that is better able to survive the low oxygen tensions found within the wound bed. Early work demonstrated the ability of immortalised articular chondrocytes to become hypertrophic and mineralise in pellet culture (Oyajobi et al., 1998). There are, however, significant concerns associated with the use of genetically modified cells for a clinical application. Scotti *et al* have also demonstrated that MSCs can be directed down a hypertrophic lineage producing cell pellets *in vitro* which express a low level of collagen type X, and after extended culture in the absence of TGF- $\beta$  exhibit a mineralised outer collar. After *in vivo* subcutaneous implantation these grafts were able to be remodelled with the cartilage template being reabsorbed and replaced with bone ossicles (Scotti et al., 2010).

Work carried out previously in our laboratory demonstrated that chondrocytes isolated from the nasal septum and the sternum had the ability to progress down a hypertrophic differentiation pathway (Kwarciak, 2009). This was achieved through the addition of ascorbic acid (vitamin C) and insulin into the culture medium. Ascorbic acid has been shown to be a critical factor in the process of endochondral ossification with ascorbic deficiency causing scurvy and an ascorbic acid deficiency in the growth plate causes a decreased chondrocyte proliferation, ECM deposition and osteoblast cell number (Kipp et al., 1996). *In vitro*, addition of ascorbic acid has been shown to significantly increase alkaline phosphatase activity and collagen type X mRNA levels in

chondrocytes (Leboy et al., 1997, Leboy et al., 1989). Insulin is used as an alternative to insulin growth factor (IGF) as it has the ability to bind to both insulin receptors and IGF-1 receptors (Ballock and Reddi, 1994). Insulin causes the morphological increase in the cellular volume of the chondrocytes as well as being mitogenic to chondrocytes (Bohme et al., 1992a). The use of these nasal and sternum chondrocytes resulted in hypertrophic tissue-engineered grafts, which not only had a large cellular morphology but also expressed high levels of alkaline phosphatase and collagen type X. No mineralization of these grafts was detected *in vitro* using the conditions above (Kwarciak, 2009).

Previous research has shown that undifferentiated hyaline chondrocytes will not form new bone when placed into a bone defect (Vacanti, 1995). However, initial work illustrated that tissue engineered hyaline chondrocyte constructs, differentiated down a hypertrophic cartilage phenotype, can produce a mineralised cartilage matrix after *in vivo* subcutaneous implantation (Kwarciak, 2009). Stringer et al also demonstrated that cells derived from 8-9 week human embryonic femurs produced osteoinductive signals for the regeneration of vascularised bone *in vivo* (Stringer et al., 2007). Therefore, the potential of hypertrophic cartilage grafts to be remodelled into bone tissue once placed within a bone defect needs to be further investigated.

### **2.5.1 Cells for Bone Tissue-Engineering**

The advantage of using live and metabolically active cells for tissue-engineering bone is that they can provide the appropriate tissue ECM required to initiate repair. The cell source used for tissue-engineering should be available in high enough numbers, not cause immune-rejection of the graft nor have tumourgenetic potential. It is important for bone tissue-engineering that the chosen cell source has osteogenic potential, and/or is capable of producing a matrix with osteogenic potential.

The majority of previous work in bone tissue-engineering research is currently centred on the use of stem cells and their differentiation down an osteogenic pathway to

recapitulate intramembranous ossification. Adult stem cells have previously been used in bone tissue-engineering as they are isolated from mature tissues and enable the harvesting of an autologous stem cell source while circumventing both the ethical objections and potential immune responses seen with embryonic stem cells (ESC). Adult stem cells however, unlike ESC are multipotent rather than pluripotent in their differentiation capacity and therefore, the appropriate stem cell source is required to ensure that the isolated cells have sufficient capacity to fully differentiate down an osteogenic lineage. Commonly used adult stem cells are bone marrow-derived mesenchymal stem cells (BM-MSCs) and adipose-derived mesenchymal stem cells (ASC).

ASC were first derived by Zuk *et al.* in 2001 and have been shown to have osteogenic and chondrogenic potential (Zuk et al., 2002). In published data, however, there is variation in the consistency of ASC to differentiate down particular pathways, while De Ugarte *et al* and Hattori *et al* showed no difference between the osteogenic and chondrogenic differentiation of ASC and BM-MSCs, Im *et al* and Mehlhorn *et al* observed a lower osteogenic and chondrogenic potential of ASC (De Ugarte et al., 2003, Im et al., 2005, Hattori et al., 2004, Mehlhorn et al., 2006).

BM-MSCs are the most commonly sourced adult stem cells for bone tissue-engineering due to their known ability to directly differentiate into bone precursors, osteoblasts. These cells are available in fewer numbers and their isolation is more invasive than ASC, however their differentiation protocol is well established and bone marrow aspirates have been approved for medical use. BM-MSCs have also previously been shown by Scotti *et al* to differentiate to produce the markers of hypertrophic differentiation.

However, the use of adult stem cells still has drawbacks. BM-MSCs are commonly isolated from a bone marrow biopsy from the iliac crest. This procedure is invasive and can cause post-operative pain for up to 2 years after the bone marrow has been harvested. Also, adult stem cells have not produced high levels of ECM on

differentiation when cultured in a three-dimensional (3D) environment. This restraint, limits the size of a tissue graft which can be produced *in vitro* for implantation into a defect site.

An alternative to adult stem cells is to find a cell source which is able to undergo hypertrophic differentiation and produce a high level of appropriate ECM. Two such cell sources have been identified by previous work by A Kwarciak, the nasal septum cartilage and rib cartilage (Kwarciak, 2009). Both of these cartilage sources have been shown to differentiate down a hypertrophic lineage, producing cells with a large cellular morphology and expressing the hypertrophic markers collagen type X and alkaline phosphatase. The use of chondrocytes harvested from the nasal septum cartilage is advantageous as these cells are easily accessible for harvesting clinically and therefore, the donor site is less likely to be subject to tissue morbidity or pain. Nasal chondrocytes are also highly proliferative and this proliferation capacity is not related to the patient's age. This high proliferation potential should permit the biopsy size to be kept relatively small. Therefore the use of nasal septum chondrocytes is potentially more advantageous than the use of BM-MSCs, due to the high amount of ECM produced, the ease of isolation and the ability to differentiate down a hypertrophic cartilage phenotype.

### **2.5.2 Scaffolds for Bone Tissue-Engineering**

While the majority of research in this area uses pellet cultures as a 3-dimensional (3D) environment for the cells, it is necessary to look at the use of scaffolds in order to produce larger grafts to create a fully functional graft tissue and for repair of critically sized defects. A major function of a scaffold is that of a 3D supporting structure in appropriate shape/templates for cell proliferation, ECM deposition and tissue regeneration. Ideally a scaffold for tissue regeneration should be:- (a) biocompatible, promoting cell adhesion and proliferation; (b) biodegradable (ideally with the rate of scaffold degradation occurring at the same rate as that of new tissue formation); (c)

representative of the physical and mechanical properties of the target tissue (Rahaman et al., 2011). While the physical properties of the scaffold are important when directly implanting into load-bearing sites the method used in this thesis is to use the scaffold to produce a hypertrophic tissue in vitro before implantation into a defect site, therefore the physical and mechanical properties of the scaffold are not as vital in this research, as it is hoped that the new tissue will take on the required properties. Previous research in bone tissue-engineering has utilised ceramics, polymers and ceramic/polymer composites as scaffolds to repair bone defects (Refer Table 2-4); however as we are looking to create a hypertrophic cartilage it is also important to look at scaffolds used for cartilage tissue engineering.

Cell attachment to scaffolds is affected by the adsorption of proteins on to biomaterials. These proteins contain integrins such as RGD (Arg-Gly-Asp), which are essential structures recognised by the transmembrane integrin receptors of the cells. These receptors then form localised focal adhesions which adhere the cells to the biomaterials. This integrin binding can then activate a signalling cascade, which will alter gene and protein expression of the cells (Stevens and George, 2005). Therefore the ability for proteins to adsorb on to biomaterials is essential in cell attachment, survival and differentiation. When biomaterials come into contact with serum based media spontaneous, non-specific adsorption of soluble ECM proteins occurs. ECM proteins adsorb with a wide range of orientations and 3D conformations dependent on the characteristics of the biomaterial, including topography, chemical composition and hydrophobicity (Wang et al., 2012). For example highly hydrophobic biomaterials thermodynamically bind proteins which may cause denaturation and a decrease in bioactivity, however, highly hydrophilic biomaterials expel proteins from the surrounding area and inhibit adsorption (Wilson et al., 2005). It is therefore essential that any biomaterial used for tissue-engineering is able to support the adsorption of proteins and consequently cell attachment.

Calcium phosphate-based ceramics, such as hydroxyapatite, have been used as bone substitutes for around 40 years and most research using scaffolds for bone tissue-engineering has centred on the use of these substrates. This interest is because the inorganic component of natural bone is 85-90 % calcium phosphate, with the mineral present as hydroxyapatite crystals (HA) (Lichte et al., 2011). Calcium phosphates are also known to be biocompatible (Hutmacher et al., 2007) and while they are not osteoinductive, the release of  $\text{Ca}^{2+}$  and  $\text{PO}_4^{3-}$  ions from these materials permits them to bind to bone and allow new tissue formation (Lichte et al., 2011). Calcium phosphates have also been shown to allow for protein absorption and subsequent cell attachment, migration and differentiation (Wang et al., 2012). The optimum pore size for osteogenic differentiation has been shown to be around 300-500  $\mu\text{m}$  (Kuhne et al., 1994). However while this pore size allows good nutrient exchange, as the porosity of the ceramic increases the material become more brittle (Stevens, 2008). Therefore, while calcium phosphate ceramics may have a similar compressive strength and composition to natural bone, their brittleness and low tensile strength seen at the required porosity for bone tissue regeneration makes these ceramics difficult to use in a clinical application due to their potential predisposition to fracture. The use of synthetic hydroxyapatite is common as it has a chemical composition which is similar to bone, as well as being non-toxic and not causing an immune response (Silva et al., 2005). Other calcium phosphates such as brushite are used in bone cements and have been found to be non-toxic and able to bind well to natural bone. Brushite also has the advantage of being remodelled into hydroxyapatite *in vivo*. While calcium phosphates are often used for bone tissue engineering they are not used for cartilage tissue engineering. Calcium phosphates are however often incorporated into the osteochondral constructs where two scaffold layers are utilised, calcium phosphate for the subchondral bone and a polymer based scaffold for the cartilage element of the tissue engineered construct (Martin et al., 2007).

Polymeric scaffolds have also been used for both bone and cartilage tissue-engineering, and both naturally occurring and synthetic polymers have been used.

However, due to their low elastic modulus, loading of these materials leads to plastic deformation and a reduction in scaffold porosity therefore, they are not ideal for load bearing sites (Lichte et al., 2011, Gorna and Gogolewski, 2006).

Naturally occurring polymers such as collagen, gelatin and fibrin, been utilised for bone and cartilage tissue engineering. These protein-based polymers are found in the extracellular matrix of tissues and have the advantage that they have the potential to direct cellular migration, growth and organisation during the process of tissue regeneration. Naturally occurring polymers may cause immunogenic responses and there is less control over mechanical and biodegradable properties. There is also an issue with batch to batch variation and a limited supply leads to them being costly. (Lui et al., 2003). Synthetic polymers are advantageous as they can be fabricated to be biocompatible, degradable and easy to process, making them good candidates for scaffold fabrication for 3D cell culture. There may, however, be issues with cell attachment and growth when using this polymers. Polyesters, such as polyglycolic acid (PGA) and poly(co-lactic) acid (PLLA), have been well researched for tissue-engineering as they have Food and Drug Administration (FDA) approval for other medical uses (Ueda and Tabata, 2003). Although the rates of degradation of these polyesters can be controlled, during their "bulk" degradation they do release lactic and glycolic acid by-products which can cause inflammation and necrosis of nearby tissues (Shoichet, 2010). These polyesters have been used successfully for the formation of both tissue-engineered bone and cartilage grafts (Table 2-4). Cell attachment on to polymeric biomaterials is variable and dependent on the polymer used. Natural polymers have the advantage of being composed of proteins which contain integrins for cell attachment and therefore it is not dependent on protein adsorption. Synthetic polymers, however, do not have proteins and integrins on their surface and therefore cell adhesion to the scaffold is reliant on protein adsorption to the surface of the biomaterial. Polyesters, PGA and PLLA, have both been shown to allow for protein adsorption and subsequent cell attachment without the need for surface modification (Atthoff and Hilborn, 2007).



To overcome the lack of mechanical stability seen with polymers and the brittle nature of ceramics at the required porosity, composite scaffolds have been investigated. The rationale for utilising a composite scaffold of polymer and ceramic is that alone, neither of the materials above mimics the physio-chemical properties of natural trabecular bone. It is therefore hoped that by fabricating composites of polymers and ceramics will allow for the advantages of both materials to be harnessed (Lickorish et al., 2007). For example, the ceramic component will increase the mechanical strength and osteoconductive nature of the scaffold whereas the polymer component enables the fabrication of a porous non-brittle scaffold which can be biodegradable. Most work in the area of composite scaffolds has revolved around the incorporation of hydroxyapatite within the polymer, through electrospinning (Kim et al., 2006, Deng et al., 2007). Therefore the cells will not experience the hydroxyapatite until the polymer degrades and exposes the mineral. Therefore, a method of surface precipitation and modification of a scaffold material may have more of an impact on the cells cultured in it and highlight the osteoconductive nature of the hydroxyapatite.

In this research we are looking to create a hypertrophic cartilage, which will mineralise into bone. It is therefore, essential that the scaffold material is able to support both cartilage and bone. Due to this synthetic polymer scaffolds were chosen as a basis for this research as they have been used for the tissue-engineering of both tissues. Synthetic polymer scaffolds can be fabricated in several different ways, including textile methods, particulate leaching, melt moulding, electrospinning and 3D printing. All of these fabrication methods produce scaffolds with different structures and surface topography (Liu and Ma, 2004). When tissue-engineering it is important that the scaffolds are porous and allow for nutrient exchange and the build-up of extracellular matrix. Particulate leaching, 3D printing and melt moulding produce micropore structures, whereas textile methods and electrospinning produce fibrous scaffolds, with either micro or nanofibers (Stevens and George, 2005). In this thesis we will focus on fibrous scaffolds produce using textile methods and electrospinning. The PGA scaffold material is a non-woven needle-punched PGA scaffold purchased from

Cellon. This method produces a highly porous microfiber scaffold material with a high surface area. Electrospinning will also produce a fibrous scaffold with a more mat like structure. Electrospinning was first used in the 1930s for industrial applications and has recently evolved to process polymers with both micro- and nano- fibers for tissue engineering applications. Electrospun scaffolds are produced by forcing a polymer/solvent solution through a capillary under a high voltage onto a grounded collection target. As the jet travels through the air the solvent evaporates depositing a non woven polymer fabric on the collection target (Ma. 2004).

The scaffolds produced by Cellon have a micrometer fibre diameter, however, different fibre diameters have been shown to have different effects on cell attachment, migration and differentiation. When looking at the ECM the fibrous structures of collagen and other ECM proteins have a nanoscale topography, it has therefore been suggested that a nanofiber diameter maybe best suited for mimicking the natural environment of the cells *in vitro* (Stevens and George, 2005). In this thesis, however, we have decided to utilise microfiber scaffolds as hypertrophic chondrocytes have a large micrometer morphology and therefore should respond to the microfiber topography of the scaffolds.

### ***2.5.3 Decellularised Extracellular Matrix as a Scaffold for Bone Tissue-Engineering***

The ECM is unique and specific to the cell type and function of the tissue. The presence and composition of the ECM is also important for tissue and cell survival and for cell-growth factor and cell-matrix. The ECM is composed of a complex mixture of proteins which have both structural roles (e.g. collagens), and functional roles, (such as growth factors), in the tissue (Badylak et al., 2009). ECM provides the ideal topographic signals for tissue regeneration and it also acts as a store of bioactive factors such as growth factors. In addition, the ECM can modulate the interaction of various growth factors with the cell surface. Therefore, the interaction between the cells and the ECM is important in both the maintenance of the tissues and the migration and differentiation

of cells within the tissue (Badylak, 2002). For these reasons, the use of an ECM scaffold material has some advantages over the use of manufactured, synthetic graft materials. The 3D environment has been shown to have a large effect on cell behaviour, attachment and migration as well as allowing for constructive remodelling, producing a high quality tissue with optimal functionality (Benders et al., 2013).

Currently, decellularised matrices are being investigated for the regeneration of several tissues including heart valves (Kasimir et al., 2003, Rieder et al., 2004), trachea (Remlinger et al., 2010), muscle (Borschel et al., 2004) and abdominal tissues such as bladder and small intestine (Chen et al., 1999). The use of a decellularised ECM as a scaffold material is currently employed in the clinic in the form of a bone allograft. For these bone graft materials, in which the bone is either taken from a cadaver or xenogeneic source. However, before *in vivo* use, allograft bone grafts require a high level of tissue processing to ensure effective removal of all cellular material to prevent an immune reaction to the graft material. However, many of the bioactive factors stored in the bone are removed during the tissue processing. Therefore, the capacity of allogeneic bone grafts to regenerate bone is reduced compared to that of an autologous bone graft.

When developing a decellularised graft it is important that the cellular content is removed in order to modulate the macrophage mediated immune response *in vivo*. However, there are currently no set guidelines for the amount of cellular material which must be removed from the tissue to prevent an immune reaction. It is also important that the architecture and topography of the ECM is minimally altered and that ECM proteins are not removed from the tissue during the decellularisation process as these are essential in enabling cellular migration, invasion and stimulating tissue formation. The biomechanical properties of a tissue should also not be altered by the decellularising process of the tissue as these properties also have a large effect on the cell differentiation and migration within the tissue (Benders et al., 2013).

While the use of decellularised ECM of organs and tissues isolated from the human body are advantageous as they have a better microstructure and biomechanical properties, the availability of tissues for harvest is low (Hoshiba et al., 2010). This is especially the case when looking for hypertrophic tissue which is only present in the growth plate of the young and adolescent. Therefore, approaches for culturing cells in an appropriate 3D environment to produce an ECM *in vitro* which can then be decellularised has been utilised since the 1970s where ECM from fibroblasts was successfully decellularised by both Chen *et al* and Hedman *et al* (Chen et al., 1978, Hedman et al., 1979).

Therefore, it is suggested that a decellularised hypertrophic cartilage may be able to act as a bone graft substitute to stimulate bone formation *in vivo*, as it will contain all the cues required for angiogenesis and bone remodelling. As discussed in Section 2.1.4 hypertrophic chondrocytes undergo apoptosis once terminally differentiated. Hence, these cells may have a limited direct role in the subsequent bone formation, once the ECM of the hypertrophic cartilage contains the appropriate bioactive factors to initiate angiogenesis and to attract osteoclast and osteoblast progenitors to initiate the cartilage remodelling into bone. Therefore, it is therefore that if a decellularised hypertrophic cartilage were used as a bone graft substitute, the ECM is not disrupted and that the growth factors are not removed from the graft during the decellularisation process.

When looking at current decellularisation methods it is essential that a method is chosen which removes the majority of the cellular material without disrupting the ECM. Physical methods, such as repeated freeze-thawing of the tissue, are effective at cell lysis and cause little disruption in ultra-structure or the mechanical properties of the tissue. Hypotonic solutions can also be used as they lyse cells through simple osmotic effects without affecting the ECM. The use of detergents, such as sodium dodecyl sulphate (SDS), can have deleterious effects on the ECM which increase with exposure time to the detergent. However, detergents can be excellent decellularising

agents as they dissolve cell membranes and dissociate cellular DNA from the histone proteins. Therefore detergents should be used at low concentrations for short periods of time in order to minimise ECM disruption. Chelating agents, such as ethylenediaminetetraacetic acid (EDTA), are important for dissociating the cells from the ECM proteins, but can cause subtle protein-protein interaction disruptions. Peracetic acid is often used as a disinfecting agent and to remove residual nucleic acid from the tissue with a minimal effect to the ECM. It is therefore essential to pick the correct decellularisation protocol to optimise the removal of cellular content while minimising ECM disruption (Gilbert et al., 2006).

#### **2.5.4 Culture Conditions for Bone Tissue-Engineering**

The culture conditions used when culturing tissue engineered tissues are important for appropriate cell differentiation, ECM production and tissue survival.

Static cultures are typically used to culture cells as cell pellet. However, mass transport of oxygen and soluble nutrients and exchange of waste products can become a problem if the cell pellets become too large. Cell pellets larger than 1 mm in diameter can exhibit a necrotic core caused by hypoxia and a lack of nutrient exchange (Sutherland et al., 1986). Static culture conditions have also been shown to have a detrimental effect of the production of glycosaminoglycans (GAG) within the ECM of chondrocyte pellet cultures as well as those cultured on PGA (Martin et al., 1999). Hirao *et al* showed that hypoxia inhibits terminal (hypertrophic) differentiation through the activation of the smad pathway keeping the chondrocytes in a hyaline phenotype (Hirao et al., 2006). Therefore when investigating hypertrophic differentiation it is important that the chondrocytes do not experience hypoxia *in vitro* as this will inhibit the hypertrophic differentiation of the chondrocytes.

The mass transport issue can be resolved by adding a dimension of flow of culture medium into the culture system; thereby simulating the transport of nutrients to the centre of the 3D cultured tissue. This mass transfer becomes more essential as the

chondrocytes produce ECM which blocks the pores of the scaffold. Fluid flow has also been shown to have a positive effect on the amount of GAG deposited within the ECM as it increases intracellular signalling which in turn increases cellular proliferation and ECM production (Yellowley et al., 1997). Mild shear stress accelerates endochondral ossification by leading to an increase in collagen type X and runx2 expression (Gawlitta et al., 2010, Wong et al., 2003) during hypertrophic differentiation. Therefore, it is important that both flow and mild shear stress are present within the culture system not only to aid nutrient transfer but also to support the differentiation and ECM production by the chondrocytes. The fluid flow, however, should not result in high shear within the culture system as this will result in cellular damage and may affect chondrocyte attachment on to the scaffold material.

Fluid flow can be added to a tissue culture system by simply placing the culture vessel containing the 3D constructs onto an orbital shaker plate set at low speed. This culture conditions are referred to as “semi-static conditions”. However, the fluid flow in these systems is difficult to model and therefore, the amount of shear and eddies present in this system is unknown. Bioreactors are designed to produce fluid flow in a tissue culture system. Therefore, bioreactors have the ability to produce controllable flow dynamics allowing for external mass transport and shear stress within the system.

Several bioreactor types have previously been utilised for the 3D culture of chondrocytes, such as wavy-walled bioreactors (Bueno et al., 2005), rotating wall vessels (RWV) (Vunjak-Novakovic et al., 1999) and perfusion bioreactors (Davisson et al., 2002). All of these bioreactors produce low shear and enable high chondrocyte proliferation and GAG accumulation within the ECM. However while these reactors have been used for the production of articular cartilage, little research exists using bioreactors for the production of a hypertrophic chondrocyte graft.

Bioreactors are advantageous for the production of tissue *in vitro* for both research and clinical applications of tissue-engineered tissues. The use of bioreactors enables the standardisation of cultures and limit operator variability during the *in vitro* culture

periods resulting in more reproducible tissue production. This will be essential when looking for regulatory approval for future tissue-engineered therapies. Another hindrance to the success of tissue-engineering for clinical applications is the cost of the production of tissue grafts. The use of a bioreactor and the automation of the *in vitro* production may lead to a decrease in costs of production of tissue grafts.

### ***2.5.5 Development of Serum-Free Culture Conditions for Bone Tissue-Engineering***

Foetal calf serum (FCS) has become a key addition to *in vitro* cell culture media as it supplies a cocktail of serum proteins, including growth factors, hormones, enzymes, vitamins and trace elements, which are essential for cell attachment, function and survival (Brunner et al., 2010). However the addition of FCS does have drawbacks when producing a product for clinical use. FCS is derived from animals and therefore, there is a risk of viral transmission through the cultures and into the tissue grafts. FCS is also highly variable between batches as different animals produce different levels of growth factors and hormones. This variability could have a detrimental effect on cell proliferation and differentiation. Culture systems which use FCS will also encounter problems when trying to obtain regulatory approval for use within the clinic due to its highly variable and undefined nature. Therefore, when considering the production of a hypertrophic cellular graft it is vital that a defined media is used with the ability to reproducibly yield the same amount of cellular proliferation and differentiation pattern of the cells.

Hypertrophic chondrocytes have previously been cultured and maintained in serum-free media, where additions of specific bioactive factors have been made to compensate for the lack of FCS. It is important that FCS proteins which are required for cell attachment, proliferation and differentiation are substituted into the serum-free media so as not to affect cell cultures, while making the media more defined.

Bohme *et al* showed that insulin or insulin-like growth factor (IGF) is required for the proliferation of chondrocytes (Bohme et al., 1992a). In 1982 Burch and Lebovitz observed that the addition of thyroxine induced both the growth and maturation of embryonic chick cartilage *in vitro* (Burch and Lebovitz, 1983). More recently both thyroxine and triiodothyronine have been shown to be a strong initiators of chondrocyte hypertrophy when present at a concentration similar to that found in plasma and can create linearly organised chondrocytes while increasing the production of collagen type X and alkaline phosphatase in serum-free conditions (Bohme et al., 1992b, Ballock and Reddi, 1994, Robson et al., 2000, Okubo and Reddi, 2003, Bohme et al., 1992a).



### **3 Aims and Objectives**

As discussed in Section 2, the healing of non-union fractures and large bone defects remains a significant, clinical challenge. Current practices based on the use of autologous bone grafts are the most clinically effective, but suffer from well-known limitations as described in Section 2.3. Therefore the application of tissue-engineering remains an attractive field of research for the regeneration of bone. Bone tissue-engineering to date has often centred on the direct differentiation of MSCs into osteoblasts to form bone following the intramembranous ossification pathway. Surprisingly, limited research has been performed on the potential of the endochondral ossification pathway and hypertrophic cartilage grafts to overcome the limitations of other repair strategies and regenerate bone tissue through the differentiation of chondrocytes. The aim of this PhD thesis, therefore, was to investigate the feasibility of using the endochondral ossification pathway to form hypertrophic cartilage tissue for use as graft materials to repair bone defects. Specific objectives were:

- To investigate the use of electrospinning to produce scaffolds for hypertrophic cartilage tissue-engineering and to consider the modification of these scaffolds with calcium phosphate in order to produce a composite scaffold with enhanced osteogenic potential.
- To investigate the effect of different batches of foetal calf serum on the ability of nasal septum chondrocytes to differentiate down a hypertrophic lineage and produce proteoglycans within the extracellular matrix.
- To reproducibly differentiate chondrocytes down a hypertrophic lineage using a range of experimental and commercial scaffold materials, and to examine this differentiation using both gene and protein expression.

- To investigate the ability of hypertrophic chondrocyte grafts to heal bone defects in an *in vivo* rat model and to compare these results with the use of a decellularised graft and a decellularised graft re-seeded with MSCs.
- To carry out preliminary research into the use of a Quasi-vivo® flow bioreactor for the production of hypertrophic chondrocyte grafts.
- To develop a serum-free media in order to aid with culture standardisation and the possible regulatory approval of hypertrophic chondrocyte grafts.

On completion, this research will add substantially to knowledge of hypertrophic chondrocyte differentiation and the potential clinical application of hypertrophic chondrocyte tissue-engineered grafts as a material or template for bone tissue regeneration.

## **4 Materials and Methods**

### **4.1 Materials**

General tissue culture materials were supplied by Sigma-Aldrich, Poole, UK. Materials for RNA work were supplied by life Technologies, UK and immunohistochemical analysis materials were supplied by Vector Laboratories, UK. Suppliers of other materials are stated within the methods section.

### **4.2 Methods**

#### **4.2.1 Scaffold Fabrication and Analysis**

##### **4.2.1.1 Electrospinning**

PLLA (molecular weight 45-69 kDa) was dissolved in 8 % (w/w) in dichloromethane to produce a polymer spinning solution. Polymer solution (3 mL) was electrospun at a voltage of 16 kV at a rate 3 mL/hour across a distance of 45 cm. Random fibre scaffolds were spun onto a stationary flat metal plate.

##### **4.2.1.2 Alternate Soaking Protocol**

Electrospun PLLA was treated using an alternative soaking protocol based on the method described by Taguchi *et al* (Taguchi et al., 1999). Scaffolds were soaked in 200 mM calcium chloride in 1 M Tris-HCl pH 7.4 containing 10 % (v/v) ethanol (Fisher Scientific, UK) for 30 seconds, washed in 25 % (v/v) ethanol in distilled water for 30 seconds, soaked in 120 mM sodium hydrogen phosphate containing 10 % (v/v) ethanol for 30 seconds and washed in 25 % (v/v) ethanol for 30 seconds. This protocol was repeated for 5 and 10 cycles with the intention of depositing calcium phosphate on and between the scaffold fibres.

#### 4.2.1.3 Scanning Electron Microscopy

Scaffolds were attached to scanning electron microscopy (SEM) specimen stubs using carbon tabs. Samples were then sputter gold coated using an Edwards Sputter coater S150B. Samples were then imaged using Phillips XL20 under a 20 kV beam.

#### 4.2.1.4 X-Ray Diffraction

Scaffolds were mounted on glass slides using micropore tape and analysed using the Phillips PW1830 set at 40 kV and 30 mA. Scans were performed between 5 ° and 80 ° at a rate of 1 °.minute<sup>-1</sup> with a step size of 0.05.

#### 4.2.1.5 Hydrophilic Analysis

A goniometer was used to analyse the hydrophilicity of the scaffolds by using the contact angle method. Scaffolds were placed on the stage and 0.2 mL droplet of distilled water was placed on the surface of the scaffold the contact angle between the water and the surface of the scaffold was then measured. Figure 4-1 illustrates a schematic of a goniometer, showing the contact angle,  $\theta$ , between the water droplet and the surface of the scaffold. Higher contact angle values represent a more hydrophobic surface.

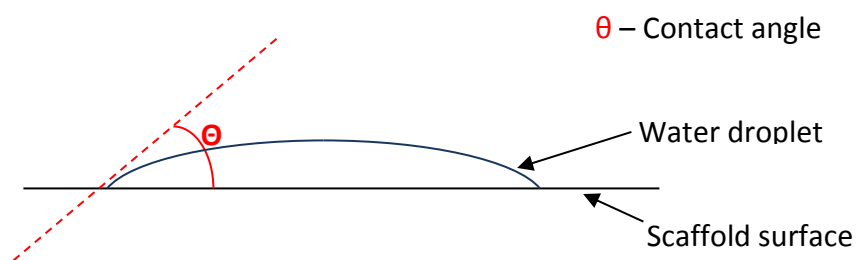


**Figure 4-1:** Diagrammatic of a goniometer showing the water droplet, the scaffold surface and the contact angle,  $\theta$

## **4.2.2 Cell Culture**

### **4.2.2.1 Nasal Chondrocyte Isolation**

Nasal cartilage was harvested from the nasal septum of 6 week-old Wistar rats within 2 hours of slaughter. The cartilage was washed in sterile  $\text{Ca}^{2+}/\text{Mg}^{2+}$ -free phosphate buffered saline (PBS) and cut into small sections before being incubated in 2.5 % (w/v) trypsin solution for 30 minutes on a shaker plate at 37 °C in a humidified atmosphere to remove any remaining endothelial cells from the cartilage tissue. Cartilage tissue was then washed in PBS to remove the trypsin and digested for 15 hours in bacterial collagenase (3  $\text{mg}\cdot\text{mL}^{-1}$ , filter sterilised) with 10 % (v/v) FCS (Biosera, UK) in basic media: Dulbecco's modified eagle media (DMEM) supplemented with 100  $\text{units}\cdot\text{mL}^{-1}$  penicillin and 100  $\mu\text{g}\cdot\text{mL}^{-1}$  streptomycin (PS), 10 mM pH 7.4 Hepes Buffer (Hepes), 1 % (v/v) 100x MEM non-essential amino acids (NEAA) and 2 mM L-alanyl-L-glutamine (Glu) at 37 °C in a humidified atmosphere. Digested tissue was then passed through a 0.2  $\mu\text{m}$  cell strainer (BD Biosciences, Erembodegem, Belgium) to remove any undigested cartilage. The isolated chondrocytes were washed in PBS and centrifuged at 1000 rpm for 5 minutes to remove the collagenase.

Chondrocytes were re-suspended in basic media and a cell count was performed using a haemocytometer. Chondrocytes were plated out at  $2\times 10^6$  cells per 90 cm cell culture dish in 15 mL of expansion media: basic media supplemented with 10 % (v/v) FCS and 10  $\text{ng}\cdot\text{mL}^{-1}$  basic fibroblast growth factor (FGF). Culture dishes were placed in incubator, at 37 °C humidified atmosphere of 5 %  $\text{CO}_2$ /95 % air.

### **4.2.2.2 Mesenchymal Stem Cell Isolation**

Rat MSCs were isolated from the bone marrow of the femur within 2 hours of the animal being slaughtered. Rats were sprayed down with 70 % (v/v) ethanol and Trigene® (Scientific Laboratory Supplies, Nottingham, UK) and the femurs removed from the hind legs. All soft tissue was removed from the femurs before the ends of the bone were removed and 10 mL of expansion media was flushed through the bone

cavity and a syringe and syringe needle was used to harvest the bone marrow. The bone marrow from each femur was placed in a T25 culture flask and transferred to an incubator at 37 °C with a humidified atmosphere of 5 % CO<sub>2</sub>/95 % air. BM-MSCs were allowed to attach to the surface of the culture flask for 24 hours. After 24 hours the attached cells were washed with PBS and the BM-MSCs were cultured in expansion media.

#### **4.2.2.3 Cell Expansion**

When cell cultures had reached 80 % confluence, the culture media was removed from the cells and the cell monolayers washed twice using sterile PBS. 3 mL of trypsin/EDTA (0.05 % (w/v) porcine trypsin and 0.02 % (w/v) EDTA in Ca<sup>2+</sup>/Mg<sup>2+</sup>-free Hanks balanced salt solution) was added to each culture plate and the cultures were incubated for 3-5 minutes at 37 °C until the cells had detached from the culture plastic. The detached cells were transferred to centrifuge tubes, FCS was added (5 % (v/v) final concentration) to inhibit the trypsin and the cell suspension was centrifuged at 1000 rpm for 5 minutes to pellet the cells. Cell pellets were re-suspended in expansion media and a cell count was performed using a haemocytometer. Chondrocytes were plated out at 1x10<sup>6</sup> cells per 9 cm diameter culture dish and MSC were plated out at 2x10<sup>6</sup> cells per T75 culture flask. Cells were placed back into the incubator at 37 °C humidified atmosphere of 5 % CO<sub>2</sub>/95 % air. This process was repeated until a sufficient number of cells were present the maximum number of passages which cells were subject to was 2.

#### **4.2.2.4 Mesenchymal Stem Cell Lineage Testing**

##### **MSC Adipogenesis**

BM-MSCs were plated out in 6 well plates at a density of 1x10<sup>6</sup> cells per well and cultured until 70 % confluent. The BM-MSCs were cultured in adipogenic induction media: basic media supplemented with 1 mg.mL<sup>-1</sup> BSA, 10 µg.mL<sup>-1</sup> insulin, 1 µM

dexamethasone, 100  $\mu\text{M}$  indomethacin and 0.5 mM 3-isobutyl-1 methyl xanthine (IBMX) for 72 hours and then cultured for 5 days in basic medium supplemented with 1  $\text{mg}\cdot\text{mL}^{-1}$  BSA and 10  $\mu\text{g}\cdot\text{mL}^{-1}$  insulin. Once differentiated, cells were washed with sterile PBS and fixed with 2 % (v/v) glutaraldehyde for 30 minutes at room temperature. Fixed cells were then washed twice with sterile PBS and adipogenic differentiation detected by incubation of the cells with Oil Red O [3 parts stock solution (0.5 g Oil red O in 100 mL Isopropanol (Fisher Scientific, UK)) to 2 parts distilled water, filtered] for 2 minutes at room temperature. The stain was removed and cells washed five times with distilled water before imaging.

### **MSC Osteogenesis**

BM-MSCS were plated out in 6 well plate at a density of  $1\times 10^6$  cells per well in basic medium supplemented with 1  $\text{mg}\cdot\text{mL}^{-1}$  BSA and 10 nM dexamethasone for 24 hours. The BM-MSC cultures were then differentiated in osteogenic media: basic media supplemented with 1  $\text{mg}\cdot\text{mL}^{-1}$  BSA, 10 nM dexamethasone, 50  $\mu\text{g}\cdot\text{mL}^{-1}$  ascorbic acid and 10 mM  $\beta$ -glycerophosphate for 14 days. After differentiation, the cells were washed with sterile PBS and fixed in 70 % (v/v) methanol at  $-20\text{ }^\circ\text{C}$  for 30 minutes. The fixed cells were washed twice with distilled water and osteogenic differentiation detected by incubation of the cells for 10 minutes at room temperature with 40 mM alizarin red (pH'd to 4.1 with ammonium hydroxide). Stain was removed and cells washed five times with distilled water before imaging.

### **MSC Chondrogenesis**

BM-MSCs were placed in micromass culture:  $5\times 10^5$  cells in 50  $\mu\text{L}$  of basic media with 10 % (v/v) FCS were pipetted as a droplet in a 12 well plate and left to attach for 24 hours. The culture medium was gently removed and the cell micromasses were cultured for 14 days in chondrogenic media: basic media supplemented with 1  $\text{mg}\cdot\text{mL}^{-1}$  BSA, 100 nM dexamethasone, insulin transferrin and selenium (ITS), 50  $\mu\text{g}\cdot\text{mL}^{-1}$  ascorbic acid and 10  $\text{ng}\cdot\text{mL}^{-1}$  transforming growth factor ( $\text{TGF}\beta$ ). After differentiation, the micromasses

were washed with sterile PBS and fixed in 70 % (v/v) methanol at -20 °C for 30 minutes. Fixed cells were then washed twice with distilled water and chondrogenic differentiation detected by incubation of the cells with 3 % (v/v) acetic acid for 1 minute followed by 1 % (v/v) alcian blue (1 g alcian blue in 100 mL acetic acid, pH 2.5, filtered) for 18 hours at room temperature. The micromasses were then counterstained with 0.05 % (w/v) neutral red (0.5 g neutral red in 100 mL distilled water). The stain was removed and cells washed five times with distilled water before imaging.

### **4.2.3 3D Cell Culture**

#### **4.2.3.1 Pellet Culture**

Cells were expanded until passage 2 and trypsinised as previously described in Section 4.2.2.3. A cell count was performed using a haemocytometer and  $5 \times 10^5$  cells were suspended in 0.5 mL of basic media in a 20 mL tube. The cells were then centrifuged at 1000 rpm for 5 minutes to form a cell pellet. The pellet was allowed to form for 24 hours in a humidified atmosphere of 5% CO<sub>2</sub>/95% air at 37 °C. The basic media was then carefully removed as not to disrupt the pellet and replaced with 2 mL of differentiation media. The pellets were then cultured for 21 days in differentiation media.

#### **4.2.3.2 Scaffold Preparation**

Biofelt® PGA scaffolds (Cellon, Luxemburg) and electrospun PLLA were both cut to a diameter of 6 mm using a cork borer. Scaffolds were then sterilised for 15 minutes in isopropanol. Once sterile, the scaffolds were washed three times in sterile PBS and conditioned in Basic media with 10 % (v/v) FCS for a further 15 minutes.



#### **4.2.3.3 Scaffold Seeding and Culture**

Cells were expanded until passage 2 cells and trypsinised as previously described in section 4.2.2.3. A cell count was performed using a haemocytometer and  $2 \times 10^6$  cells were suspended in expansion medium and then seeded on the scaffolds as follows. Scaffolds were placed in sterile, non-tissue culture treated sterile 9 cm dishes (2 scaffolds per dish), the appropriate number of cells ( $4 \times 10^6$  cells/2 scaffolds) was added and cells allowed to attach for 72 hours at 37 °C in a humidified atmosphere of 5 % CO<sub>2</sub>/95 % air on an orbital shaker set at 35 rpm.

After 72 hours a cell count of the unattached cells present in the culture media was performed to assess the level of cell attachment which had occurred. The cell-seeded scaffolds (constructs) were placed into a 6 well plate (1 construct per well) and cultured in differentiation media for 42 days at 37 °C in a humidified atmosphere of 5 % CO<sub>2</sub>/95 % air on an orbital shaker set at 30 rpm. The Differentiation media was changed every 3 days.

#### **4.2.3.4 Bioreactor Culture**

The Quasi-vivo® bioreactor chamber (Kirkstall Ltd, UK), media reservoir and tubing was sterilised at 121 °C for 15 minutes and washed with sterile PBS. After seeding in sterile, non-tissue culture treated 9 cm dishes; the resulting constructs were placed within the culture chambers (Figure 4-2) and cultured in differentiation media for 42 days at 37 °C in a humidified atmosphere of 5 % CO<sub>2</sub>/95 % air under a flow rate of  $110 \mu\text{L} \cdot \text{minute}^{-1}$  of culture medium.

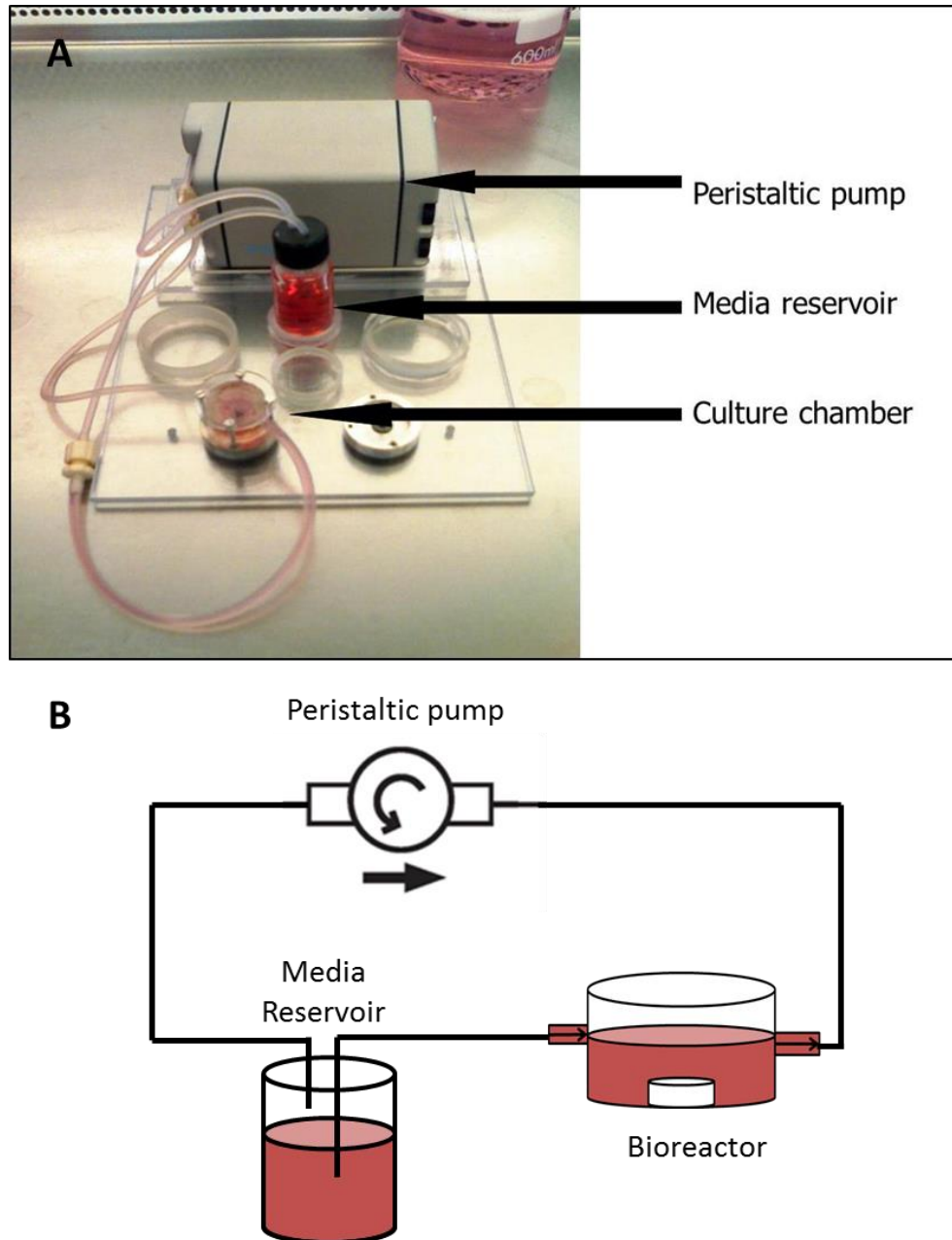


**Figure 4-2:** Bioreactor set up showing the peristaltic pump, media reservoir and culture chamber. (A) photograph of the bioreactor set up in a laminar flow hood; (B) a schematic diagram of the flow through the bioreactor system.

#### **4.2.3.5 Differentiation Media**

##### **Chondrocyte Hypertrophic Differentiation Media**

Chondrocytes were differentiated using basic media supplemented with 10 % (v/v) FCS, 1  $\mu\text{g.mL}^{-1}$  insulin and 50  $\mu\text{g.mL}^{-1}$  ascorbic acid as described by Kwarciak et al (Kwarciak, 2009).

##### **MSC Hypertrophic Differentiation Media**

BM-MSCs were seeded in basic media supplemented with 5 % (v/v) FCS, 1 mg/ml BSA and 100 nM dexamethasone. Chondrogenic media was then used for 14 days: basic media supplemented with 1  $\text{mg.mL}^{-1}$  BSA, 10  $\mu\text{l.mL}^{-1}$ , 100  $\mu\text{l.mL}^{-1}$  10X ITS (1.0  $\text{mg.mL}^{-1}$  recombinant human insulin, 0.55  $\text{mg.mL}^{-1}$  human transferrin (substantially iron-free), 0.5  $\mu\text{g.mL}^{-1}$  sodium selenite, 470  $\mu\text{g.mL}^{-1}$  linoleic acid, 470  $\mu\text{g.mL}^{-1}$  oleic acid and 50  $\text{mg.mL}^{-1}$  bovine FCS albumin), 100 nM dexamethasone, 50  $\mu\text{g.mL}^{-1}$  ascorbic acid and 10  $\text{ng.mL}^{-1}$  TGF $\beta_1$ . The culture medium was then changed to a hypertrophic differentiation media: basic media supplemented with 1  $\text{mg.mL}^{-1}$  BSA, 100  $\mu\text{l.mL}^{-1}$  10X ITS, 100 nM dexamethasone, 50  $\mu\text{g.mL}^{-1}$  ascorbic acid and 1 nM thyroxine for the remaining 14 days of the culture period.

##### **Serum-free Chondrocyte Hypertrophic Differentiation Media**

Serum-free differentiation was carried out without the use of FCS. Three media were tested:

**Media 1:** basic media supplemented with 1  $\text{mg.mL}^{-1}$  BSA, 1  $\mu\text{g.mL}^{-1}$  insulin and 50  $\mu\text{g.mL}^{-1}$  ascorbic acid.

**Media 2:** basic media supplemented with 1  $\text{mg.mL}^{-1}$  BSA, 100  $\mu\text{l.mL}^{-1}$  10X ITS and 50  $\mu\text{g.mL}^{-1}$  ascorbic acid.

**Media 3:** basic media supplemented with 1 mg.mL<sup>-1</sup> BSA, 100 µL.mL<sup>-1</sup> 10X ITS and 50 µg.mL<sup>-1</sup> ascorbic acid and 1 nM thyroxine.

#### **4.2.4 Histological and Biochemical Analysis**

##### **4.2.4.1 Cryopreservation and Weighing of Grafts**

After 42 days of culture the constructs were removed and washed in PBS, gently blotted with tissue to remove excess liquid and each construct cut into two equal-sized pieces with a scalpel. For each construct, half the construct was weighed and placed in a 2 mL conical centrifugation tube, which was stored at -20 °C until required for a GAG assay. The other half of the scaffold was embedded in optimum cutting temperature tissue mounting medium (OCT) (cut side facing upwards) on a cork disc, in a beaker of isopentane (Fisher Scientific, Loughborough, UK) held in liquid nitrogen, wrapped in Parafilm and stored at -20 °C until required for histological and immunohistochemical analysis.

##### **4.2.4.2 Histology and Immunohistochemistry**

OCT embedded constructs were sectioned at a thickness of 8 µm using a cryostat and mounted on to 3-aminopropyltriethoxysilane (APES) coated slides and allowed to dry overnight.

##### **Haematoxylin and Eosin Staining**

Sections on APES slides were fixed in 4 % (w/v) paraformaldehyde (PFA) (pH 7.2-7.4) for 30 minutes at 4 °C. The sections were then washed in PBS and dried overnight. Haematoxylin and Eosin staining was carried out using an automatic staining machine (Shandon, Runcorn, UK). The slides were first placed in haematoxylin washed in 1 % acid alcohol, Scotts tap water and tap water before being stained with eosin. The stained sections were washed again in water, dehydrated through alcohols, cleared in xylene and mounted in DPX (Fisher Scientific, Loughborough, UK).

***Alcian Blue***

Sections on APES slides were fixed in 4 % (w/v) PFA (pH 7.2-7.4) for 30 minutes at 4 °C. The sections were then washed in PBS and dried overnight. Tissue sections were rinsed in 3 % (v/v) acetic acid and stained with 1 % (w/v) alcian blue in acetic acid (pH 2.5) for 18 hours before being counterstained with 0.5 % (w/v) aqueous neutral red in distilled water for 1 minute. The stained sections washed in distilled water, cleared in xylene and mounted in DPX.

***Toluidine Blue***

Sections on APES slides were fixed in 4 % (w/v) PFA (pH 7.2-7.4) for 30 minutes at 4 °C followed by washing in PBS and then dried overnight. The fixed sections were stained with 1 % (w/v) toluidine blue in 0.5 % (w/v) sodium borate for 10 seconds, washed in distilled water, cleared in xylene, air dried overnight and mounted in DPX.

***Alkaline Phosphatase***

Sections on APES slides were fixed in 70 % (v/v) ice cold methanol (Fisher Scientific, Loughborough, UK) at -20 °C for 30 minutes. The tissue sections were then washed in PBS and dried overnight. A SIGMAFAST™ BCIP®/NBT (5-bromo-4-chloro-3-indoyl phosphate/ Nitro blue tetrazolium) tablet was dissolved in 10 mL of distilled water. The tissue sections were then incubated with the SIGMAFAST™ BCIP®/NBT solution for 15 minutes at room temperature (alkaline phosphatase was detected as a blue/black colour change) and washed in distilled water and mounted in DPX.

***Alizarin Red Staining***

Sections were fixed in 70 % (v/v) ice cold methanol at -20 °C for 30 minutes. The tissue sections were then washed in PBS and dried overnight. Sections were stained with alizarin red solution (342 mg of alizarin red in 25 mL of distilled water and pH adjusted to 4.1 with 10 % (v/v) ammonium hydroxide) for 10 minutes, washed in distilled water and mounted using aqueous mount.

## Immunolocalisation of Collagens

Sections on APES slides were fixed in 4 % (w/v) paraformaldehyde (pH 7.2-7.4) (PFA) for 30 minutes at 4 °C. The tissue sections were then washed in PBS and dried overnight.

Fixed sections were pre-treated with 10 mg.mL<sup>-1</sup> bovine testicular hyaluronidase in PBS and 2 mg.mL<sup>-1</sup> pronase from *Streptomyces Griseus* in PBS for 30 minutes at 37 °C in a humidified atmosphere and washed for 10 minutes in PBS. Endogenous peroxide activity was quenched with 3 % (v/v) hydrogen peroxide (30 wt % solution) in 50 % (v/v) methanol for 5 minutes. The sections were then washed for 10 minutes in PBS before being incubated with 3 % (w/v) BSA and 10 % (v/v) horse serum blocking solution for 1 hour to avoid non-specific staining. The sections were incubated for 15 hours at 4 °C with the appropriate primary antibodies: goat anti-collagen type II (0.4 mg.mL<sup>-1</sup>, dilution 1:20) (Cambridge Bioscience, Cambridge, UK); Mouse anti-collagen type X, (0.4 mg.mL<sup>-1</sup>, dilution 1:100) (Quartett, Berlin, Germany); rabbit anti-collagen type X, (0.4 mg.mL<sup>-1</sup>, dilution 1:50) (AbCam, UK) and blocking solution controls. The tissue sections were washed three times for 10 minutes with PBS and incubated with the appropriate biotinylated secondary antibodies: biotinylated rabbit anti-goat IgG (dilution 1:100) (Vector Laboratories, UK); biotinylated rabbit anti-goat IgG (dilution 1:100) (Vector Laboratories, UK); biotinylated horse anti-mouse (rat adsorbed) IgG (dilution 1:100) (Vector Laboratories, UK) for 1 hour. The tissue sections were washed three times for 10 minutes in PBS and incubated with ABC reagent from the Vectastain® Kit (Vector Laboratories, UK) for 30 minutes at room temperature before undergoing three further washes in PBS. Diaminobenzidine tetra hydrochloride (DAB) substrate (Vector Laboratories, Peterborough, UK) was prepared following the manufacturer's instructions before being applied to tissue sections for 2-10 minutes until a suitable brown colour developed. The sections were then counterstained with haematoxylin and mounted with DPX.

#### 4.2.4.3 *Glycosaminoglycan Assay*

Proteoglycan content of the tissue engineered constructs was assessed by measuring the amount of glycosaminoglycans (GAG) in the ECM. The constructs were weighed after and freeze dried overnight before being re-weighed in order to assess the water concentration within the construct. Freeze dried constructs were then digested overnight in a papain digestion buffer (0.05 % (w/v) papain (from papaya latex) and 6 mM n-acetyl cysteine in 200 mM phosphate buffer containing 1 mM EDTA, pH 6.8) at 60 °C.

The GAG concentration was then analysed using diethylmethylene blue (DMB) following the protocol described by (Farndale et al., 1986). DMB (10 mM in ethanol (Fisher Scientific, UK) was further dissolved into 500 mL distilled water containing 40 mM glycine and 40 mM sodium chloride, with pH adjusted to 3 using hydrochloric acid). 50 µL of sample was then mixed with 250 µL of DMB and the optical density was measured at 525 nm (530-10 absorbance filter) using the spectrophotometer. This reading was then compared to a chondroitin sulphate standard curve to give a GAG concentration present in the sample. Total percentage matrix was then calculated using the following formula:

$$\% \text{ of GAG in construct ECM} = \frac{\text{mass of GAG}}{\text{construct dry weight}} \times 100$$

#### 4.2.5 *Gene Expression*

The gene expression of the chondrocytes was assessed at various time points, as shown in the schematic (Figure 4-3) The gene expression was then either normalised to chondrocytes at passage 2 on tissue culture plastic or after 3 days on the scaffold materials in expansion media.

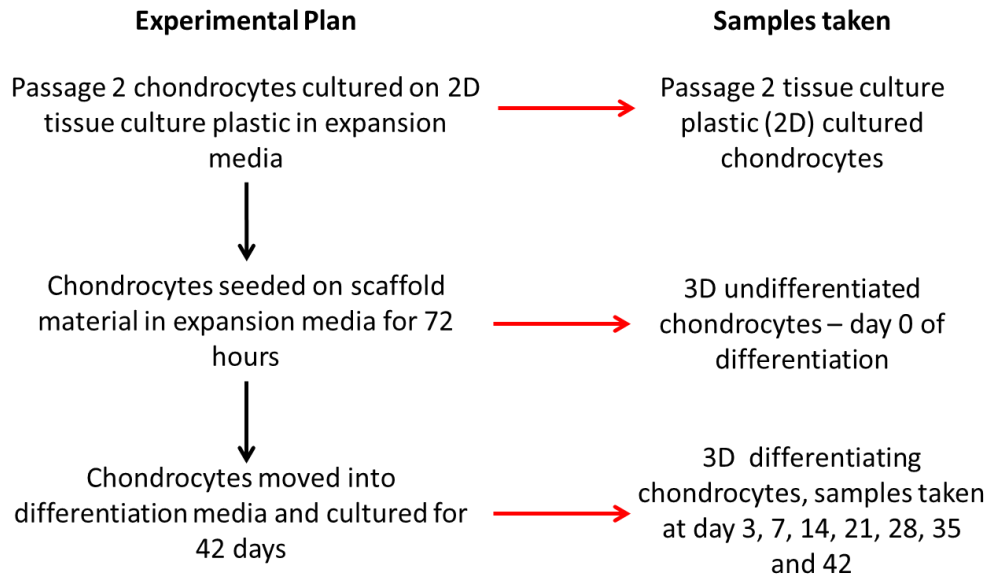


**Figure 4-3:** Schematic diagram showing the experimental plan and the time points at which the gene expression of the chondrocytes will be assessed

#### **4.2.5.1 RNA Extraction**

After culture the tissue engineered constructs were washed in PBS and flash frozen in liquid nitrogen for 30 seconds. A tissue pulveriser was then used for 1 minute in order to homogenise the sample in PBS. The homogenised sample was then centrifuged at 11,000 rpm for 2 minutes in order to gain a tissue pellet. RNA was extracted immediately from this tissue pellet using the Bioline Isolate II RNA Mini Kit (Bioline Reagents Ltd, UK) and the RNA concentration determined using a NanoDrop 2000. Isolated RNA was diluted to a concentration of  $10 \text{ ng} \cdot \mu\text{L}^{-1}$  using Rnase free water and stored at  $-80 \text{ }^\circ\text{C}$  until it was required for cDNA synthesis.

#### **4.2.5.2 Reverse Transcription Polymerase Chain Reaction**

cDNA was synthesised using a high capacity RNA to cDNA master mix (Life Technologies, UK) and 100 ng of RNA in total per reaction.



Table 4-1 gives the composition of a cDNA synthesis reaction, these reactions were run in a thermal cycler using a cycle of 10 minutes at 25 °C, 2 hours at 37 °C, 5 minutes at 85 °C and then 10 minutes at 4 °C. cDNA was then stored at -20 °C until real time PCR was performed.

**Table 4-1:** Composition of reagents per cDNA synthesis reaction

	Reagent	Volume per reaction (μL)
<b>Master Mix</b>	Reverse transcription buffer	2
	Random primers	2
	Deoxyribonucleotide triphosphate (dNTPS)	0.8
	Multiscribe Reverse Transcriptase	1
	Nuclease free water	4.2
<b>Sample</b>	RNA (10ng/μL)	10

#### 4.2.5.3 Real Time Polymerase Chain Reaction

Real time PCR was performed using a 7900Fast Real Time PCR machine in a 96 well plate with an experimental volume of 10 μL. Table 4-2 shows the reagents (Life Technologies, UK) required per real time PCR reaction. Three technical repeats were performed per reaction.

Table 4-2: **Composition of reagents per real time PCR reaction**

Reagent	Volume per reaction ( $\mu\text{L}$ )
Taqman mastermix	5
Nuclease free water	3.5
Target primer/probe	0.5
Endogenous control primer/probe (GAPDH)	0.5
cDNA sample (5 ng/ $\mu\text{L}$ )	0.5

Taqman probes and primers were used for the detection of the expression of collagen type II, collagen type X, alkaline phosphatase, *Ihh*, *sox9* and *runx2* (Life Technologies, UK). Non template and reverse transcriptase negative controls were used to check for cDNA contamination. Table 4-3 shows the assay identification numbers for the primers and probes used for q-PCR.

Results were analysed using the  $\Delta\Delta\text{ct}$  method in relation to the housekeeping gene, glyceraldehyde 3-phosphate dehydrogenase (GAPDH) expression. The  $\Delta\Delta\text{ct}$  value was then normalised to either a). gene expression of undifferentiated chondrocytes on 2D culture plastic, for comparison between the scaffolds, or b). undifferentiated 3D culture chondrocytes, to assess the differentiation on the scaffolds.

**Table 4-3:** Taqman primer and probe identification numbers of assays used during q-PCR.

Gene	Taqman primer and probe assay number
Collagen type II, alpha 1	Rn01637087_m1
Collagen type X, alpha 1	Rn01408030_m1
Alkaline phosphatase	Rn00575319_g1
Ihh	Rn03810376_m1
Sox9	Rn01751069_mH
Runx2	Rn01512298_m1
GAPDH	4352338E

#### 4.2.6 Construct Decellularisation

This protocol was adapted from a protocol for the decellularisation of articular cartilage published by Kheir *et al* (Kheir et al., 2011).

The tissue constructs were removed from culture and washed with PBS before undergoing three, freeze-thaw cycles. The constructs were frozen at -20 °C for 2 hours before being thawed at room temperature for 2 hours. The freeze thaw cycles were then repeated with the grafts submerged in hypotonic buffer (10 mM Tris- HCl, pH 8.0, filter sterilised, with the addition of protease inhibitors). The constructs were then placed in an ionic buffer (0.1 % (w/v) sodium dodecyl sulphate (SDS), 0.1 % (w/v) EDTA in distilled water, filter sterilised, with the addition of protease inhibitors) and left for 1 hour gently shaking at room temperature on an orbital shaker (at 100 rpm), before being transferred to hypertonic buffer for 1 hour on an orbital shaker (at 100 rpm) at room temperature. The tissue constructs were cycled through ionic and hypotonic buffers three times in order to lyse the chondrocytes in the construct. The constructs were then decontaminated using a 0.1 % (v/v) peracetic acid solution for 1 hour on an

orbital shaker at 100 rpm. The constructs were then washed 3 times with sterile PBS. The degree of decellularisation was assessed by DNA quantification (Section 4.2.6.1) and 4',6-diamidino-2-phenylindole (DAPI) staining (Section 4.2.6.2) and its effect on the extracellular matrix content was assessed using the glycosaminoglycan assay (Section 4.2.4.3).

#### **4.2.6.1 DNA Quantification**

DNA was isolated from the tissue constructs both pre and post decellularisation to assess the efficacy of the decellularisation process. Constructs were weighed before extraction with Trizol<sup>®</sup> reagent (Life Technologies, UK). Trizol<sup>®</sup> (0.5 mL) was added to each construct and the construct, homogenised and incubated for 5 minutes at room temperature. Chloroform was added (0.1 mL), shaken vigorously, incubated for 2 minutes and centrifuged at 12,000 g for 15 minutes at -4 °C. The aqueous phase was removed and ethanol (0.15 mL/sample) was added and the samples incubated for 2 minutes and then centrifuged at 2,000 g for 5 minutes at 4 °C. The supernatant fraction was removed and the pellets were incubated with 0.1 M sodium citrate in 10 % (v/v) ethanol solution (0.5mL) for 30 minutes and before being re-centrifuged at 2,000 g for 5 minutes at 4 °C. The supernatants were removed and 75 % (v/v) ethanol added to the pellets (1 mL/pellet) incubated for 15 minutes and centrifuged at 2,000 g for 5 minutes. The pellets were air dried before being re-suspended in 8 mM sodium hydroxide (0.3 mL/pellet). The DNA was then quantified using the NanoDrop 2000.

#### **4.2.6.2 4',6-diamidino-2-phenylindole Staining**

8 µm cryosections were cut from OCT mounted constructs and transferred to APES coated slides and fixed in 4 % (w/v) PFA for 10 minutes. The tissue sections were washed with PBS three times for 5 minutes. The chondrocytes were permeabilised in 0.1 % (v/v) Triton-X-100 for 10 minutes and PBS washes were repeated. The chondrocytes were stained with DAPI for 15 minutes in the dark. The tissue sections were then washed in PBS and imaged with a fluorescence microscope. When bound to

double-stranded DNA DAPI has an absorption maximum at a wavelength of 358 nm (ultraviolet) and its emission maximum is at 461 nm (blue). Therefore, for fluorescence microscopy DAPI is excited with ultraviolet light and is detected through a blue/cyan filter.

#### **4.2.7 *In Vivo Experiments***

*In vivo* experiments were carried out using tissue engineered constructs formed from rat nasal chondrocytes grown on PGA. The constructs were placed in 4 mm full thickness healing defect in the cranium of 8 week old Wistar rats (Figure 4-4). All *in vivo* work was carried out by Christine Freeman under the appropriate animal license (license number: 40/3311).

Rats were placed under anaesthetic using IsoFlo (Isoflurane) (Abbott Laboratories, UK) and given antibiotics, Synulox (Pfizer, UK), and a painkiller, Metacam (Boehringer-Ingelheim, Germany). Once under anaesthetic, the rats were weighed. A midline incision was made in the skin covering the skull and both the skin and periosteum were retracted to reveal the cranium. Two 4 mm full thickness defects were drilled into the skull using a 3.5 mm diamond burr with saline irrigation. Grafts were cut to 4 mm diameter using a sterile biopsy punch and placed into one of the defects with the other being left empty. The periosteum was closed over the defects and secured with 2 vicryl stitches, before the wound was closed using 4-5 stitches. Anaesthetic was turned off and the animal given oxygen for 3 minutes.

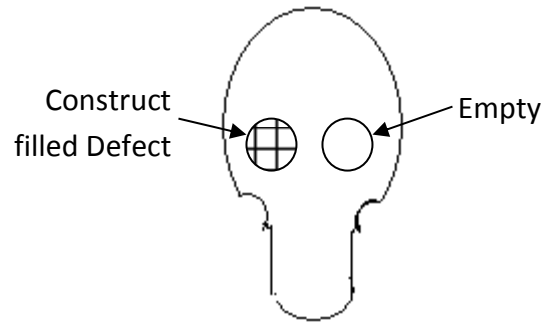


**Figure 4-4:** Schematic of operation showing the positioning of the two 4 mm defects in the skull and the filling of one defect with a construct.

Constructs were allowed to heal the defect for 4, 8 and 12 weeks, before the animals were culled. Rats were anaesthetised using IsoFlo and their vertebrae separated, the heads were then removed from the animal and placed in 10 % (w/v) neutral buffered formalin and stored at room temperature. The rat heads were then examined by microCT and histology to assess the degree of new bone formation in the defect area.

#### **4.2.7.1 'Living' Grafts**

Constructs were removed from the culture after 35 days and washed in PBS twice before implantation in to the bone defects.

#### **4.2.7.2 Decellularised Grafts**

Constructs were removed from culture after 35 days and decellularised using the protocol described in section 4.2.6 before being implanted into the bone defects.

#### **4.2.7.3 Recellularised Grafts**

Constructs were removed from culture after 35 days and decellularised using the protocol described in section 4.2.6. The decellularised constructs were then recellularised with BM-MSCs using the following methodology. BM-MSCs were harvested from femurs of a different rat to those undergoing the *in vivo* testing, as

described previously (Section 4.2.2.2) and cultured until passage 2 (Section 4.2.2.3). 48 hours before implantation, the cultures of BM-MSCs were trypsinised using the protocol described in section 4.2.2.3 and a cell count was performed using a haemocytometer. Decellularised constructs (4 mm diameter) were placed in culture dishes and  $1 \times 10^5$  cells in basic media with 5 % (v/v) FCS,  $1 \text{ mg}\cdot\text{mL}^{-1}$  BSA and 10 nM dexamethasone added per construct. The culture dishes were incubated on an orbital shaker set to 35 rpm at 37 °C humidified atmosphere of 5 % CO<sub>2</sub>/95 % air for 48 hours to enable cell seeding to occur. The BM-MSC-seeded constructs were then implanted into the bone defects.

#### **4.2.7.4 *Microcomputed Tomography Analysis***

Rat heads were fixed in 10 % (w/v) neutral buffered formalin and analysed using a desktop high resolution microcomputed tomography (microCT) system (Skyscan 1172, Skyscan, Belgium). The heads were placed horizontally into a polyethylene tube in the system and rotated, while the x-rays originated from a point source. Scans were performed at 100 kVp, with a 1 mm aluminium filter and a pixel size of 12.1 µm. Images were taken throughout 360 ° with 2 images being averaged at each point.

#### **4.2.7.5 *Decalcification of Rat Skulls***

After microCT analysis the rat heads were skinned and all the soft tissue was removed. The skulls were then placed in a neutral aqueous solution of 0.5 M EDTA and 0.4 M sodium hydroxide in distilled water pH 7.0 for 14 days changing the EDTA solution every 7 days as the EDTA becomes saturated with calcium. Skulls were then X-rayed to check that the calcium had been removed from the bone.

#### **4.2.7.6 *Paraffin Wax Embedding and Sectioning***

The skulls were washed in running water for 20 minutes before being dehydrated through alcohols and embedded in molten paraffin wax. The wax blocks were cooled for 30 minutes on ice and 5 µm sections were then cut using a microtome. Sections

were then stained using heamatoxylin and eosin (Section 4.2.4.2) and alcian blue (Section 4.2.4.2).

#### **4.2.8 Statistical Analysis**

All statistical analysis was performed using Graphpad software. Initially a D'Agostino-Pearson "omnibus K2" test was performed to check the normality of the data. Significance between two groups of data was then analysed using the student t-test. For comparison between three or more groups of data a one way ANOVA, followed by Tukey's test was used to assess the significant changes in the data. Significance was observed with data exhibiting a p value less than 0.05.



## **5 Results**

### **5.1 Scaffold Fabrication**

Scaffolds were fabricated by electrospinning PLLA to create randomly aligned fibre mats (Figure 5-2). These scaffolds were also modified using an alternate soaking protocol (Section 4.2.1.2) to create a composite PLLA/calcium phosphate scaffold material.

After treatment with the alternative soaking protocol the dry weight of the electrospun PLLA scaffold material significantly increased (Figure 5-1), suggesting that mineral material had been deposited in between or on the scaffold fibres. Imaging the composite scaffolds with SEM showed that a precipitate was present both in between, and on the scaffold fibres after treatment with the alternate soaking protocol (Figure 5-2). When comparing the SEM images of the electrospun PLLA and the PGA (Figure 5-2 and Figure 5-3 respectively), it can be seen that the fibre diameter and the pore size of the commercial PGA is larger. The precipitate was analysed using XRD and was found to consist of 2 phases of calcium phosphate, hydroxyapatite and brushite (Figure 5-4).

Contact angle determination was also performed on both the experimental PLLA and commercial PGA scaffold materials. The addition of calcium phosphate led to a decrease in the contact angle of distilled water with the scaffold material (Table 5-1), when compared to the PLLA alone and the commercial PGA.

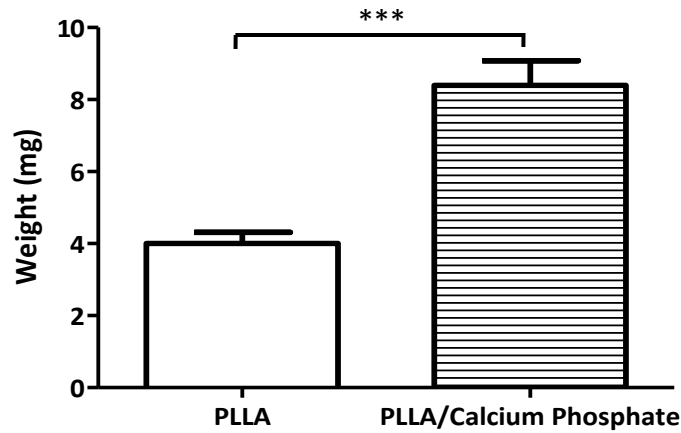


**Figure 5-1:** Weight of the PLLA scaffolds both pre-treatment and post-treatment by the alternative soaking technique to form a PLLA/calcium phosphate composite scaffold. (\*\*\*) =  $p < 0.001$ .  $n = 6$ ).

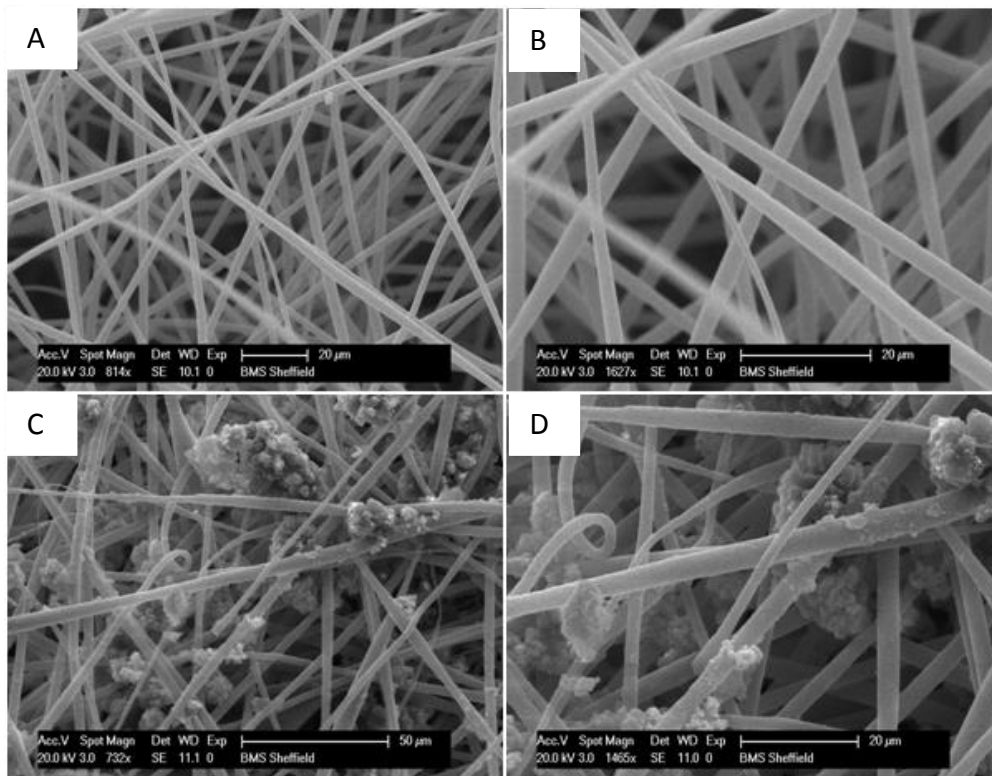


**Figure 5-2:** Randomly oriented electrospun PLLA polymer fibres, (A, B) before alternative soaking; (C, D) after alternative soaking. The scale bars in images A, B and D = 20 µm and in image C = 50 µm.

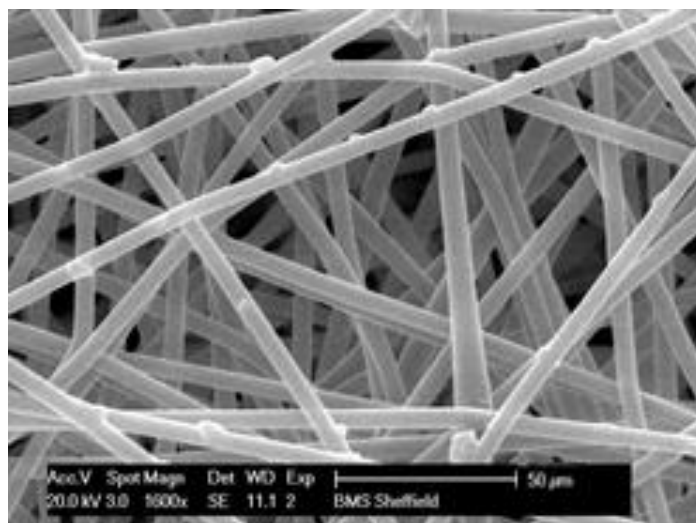


**Figure 5-3:** Scanning electron microscopy image of the non-woven needle punched PGA scaffold purchased from Cellon. (scale bar = 50  $\mu\text{m}$ )

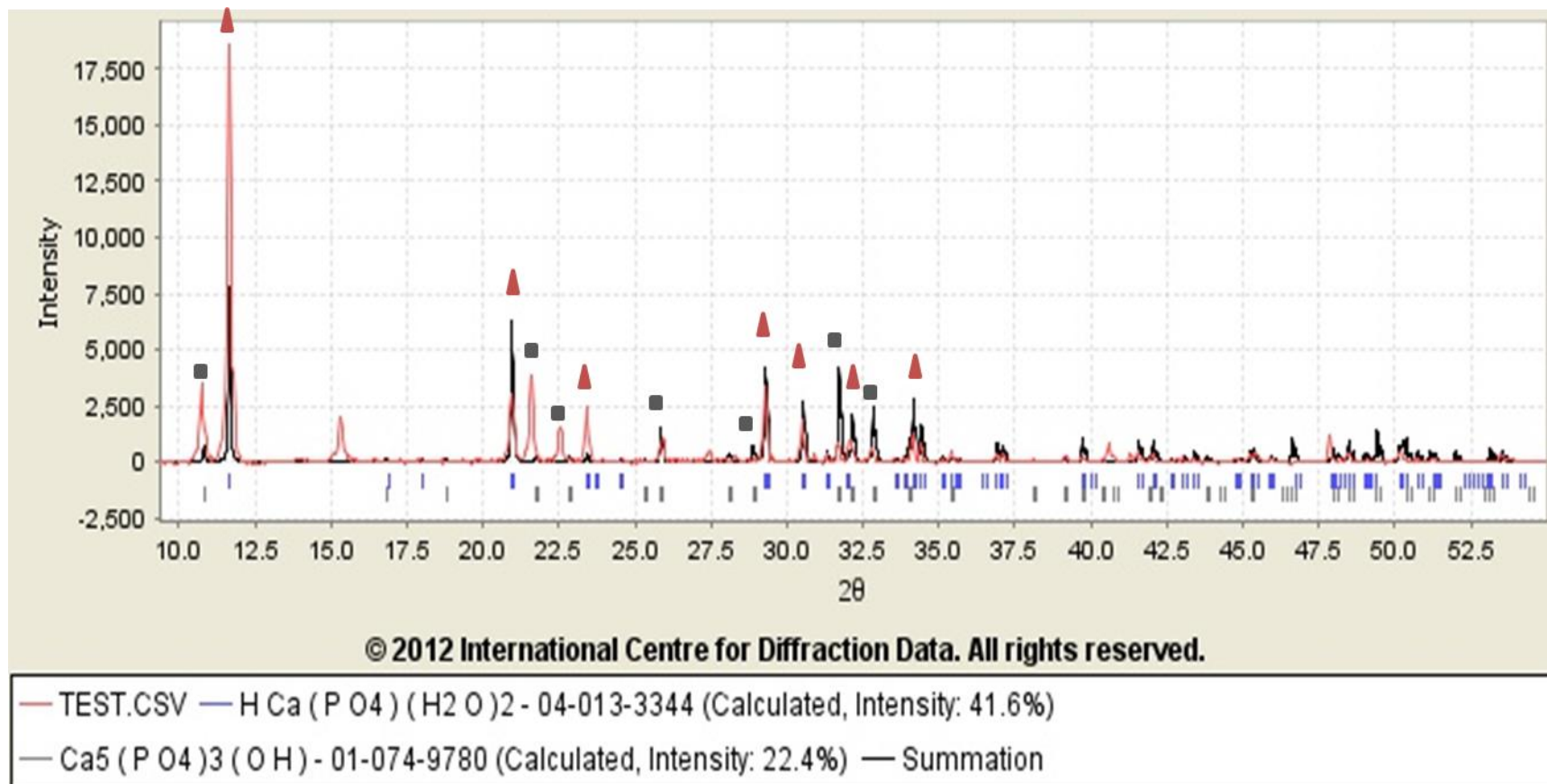


**Figure 5-4:** Representative XRD analysis of the precipitate on and within the PLLA fibres. This shows the presence of two phases of calcium phosphate, hydroxyapatite (■ grey) and brushite (▲ red) in the precipitate ( $n=3$ ).

**Table 5-1:** Measurement of the contact angle of water on the surface of the scaffold material. Analysis was performed on 3 individual specimens per scaffold group, the results are expressed as the means +/- standard deviations

Scaffold Material	Contact Angle
Electrospun PLLA	70 ± 3 °
PLLA/Calcium phosphate	15 ± 1 °
PGA	60 ± 4 °

## 5.2 The Effect of Serum on Chondrocyte Hypertrophy

Initial experiments of rat nasal chondrocytes cultures on PGA did not result in complete hypertrophic differentiation of the grafts after 42 days of culture. The constructs were observed to be heterogeneous in cell composition, with small pockets of morphologically large hypertrophic cells expressing collagen type X and alkaline phosphatase surrounded by large areas of smaller undifferentiated cells (Figure 5-4).

FCS batch testing was therefore undertaken to find a FCS which promoted the growth and proliferation of the chondrocytes without inhibiting the hypertrophic differentiation pathway. Table 5-2 shows the information on the 5 batches of FCS that were tested. For batch testing, pellet cultures of nasal chondrocytes were used to investigate the chondrogenic capacity of the sera (Section 4.2.3.1) and nasal chondrocyte/PGA constructs were used to investigate the effect of the sera on the ability of the chondrocytes to undergo hypertrophy (Section 4.2.3.3). The chondrogenic capacity of the sera was investigated by measurement of the amount of GAG in the pellet cultures. Hypertrophy of the chondrocyte constructs was monitored by histology to examine cell morphology and immunolocalisation of collagen type X.

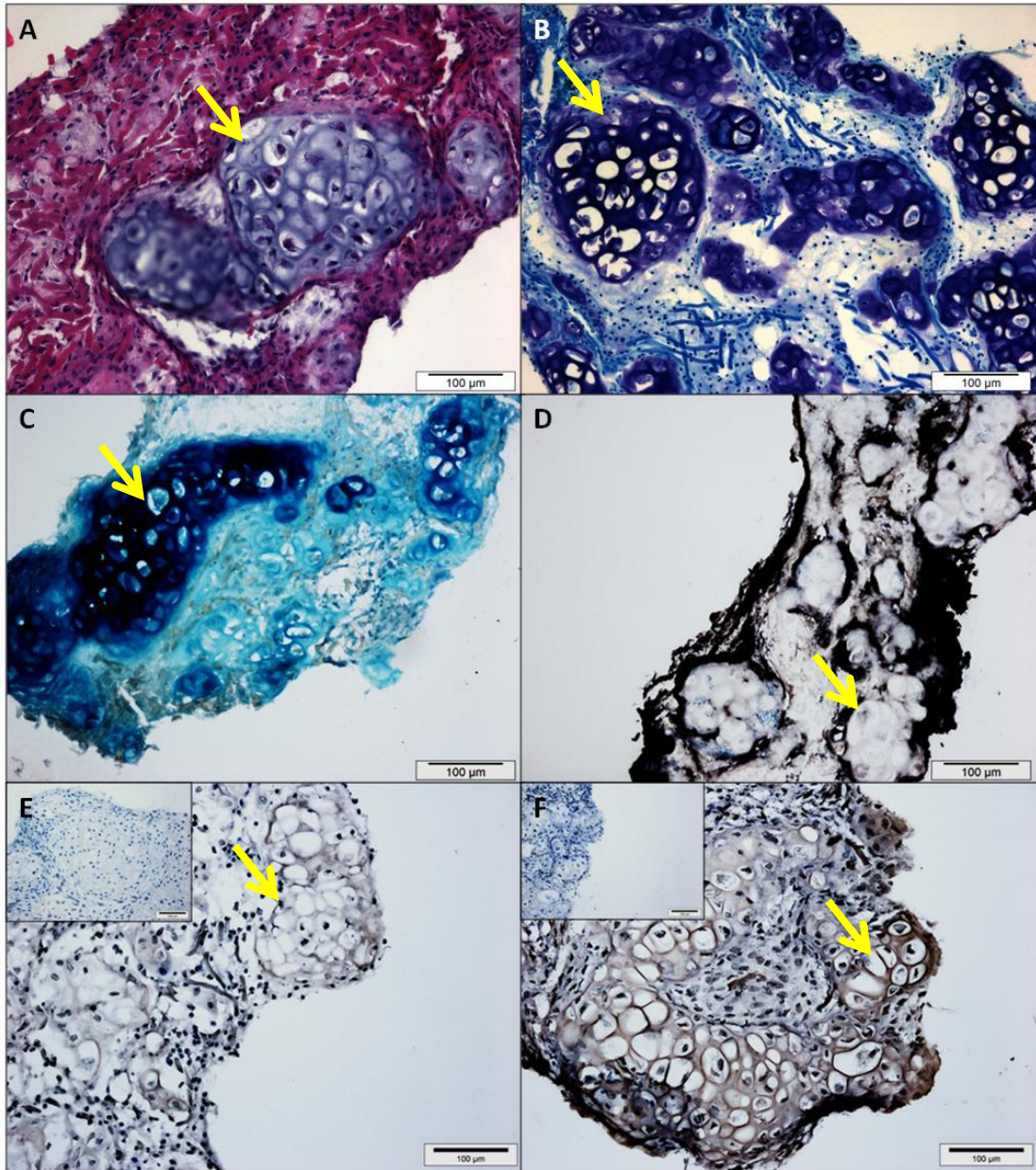


**Figure 5-5:** Immunohistochemical analysis of rat nasal chondrocyte constructs after 42 days culture. (A) haematoxylin and eosin stain; (B) toluidine blue; (C) alcian blue; (D) alkaline phosphatase; (E) collagen type II; (F) collagen type X. (Insert micrographs show non-specific staining). Arrows indicate areas of hypertrophy as shown by chondrocytes exhibiting a large morphology co located with high GAG concentrations and collagen type X expression.

**Table 5-2:** *Manufacturer and batch number of the five FCS batches tested for chondrocyte growth and hypertrophic differentiation*

FCS Number	Manufacturer	Batch Number
1	Biosera	S1900.050
2	Biosera	S10830.050
3	Sigma	F9665
4	Sigma	F7524
5	Biosera	-

As shown in Figure 5-6, the concentration of GAG within the constructs, which is indicative of the proteoglycan content of the extracellular matrix varied greatly depending on the FCS used during the pellet differentiation experiments. FCS 3 and 4 were shown to produce chondrocyte pellets with significantly lower GAG concentrations than FCS 1. However the changes in GAG were not significantly different when compared to FCS 5, which been used in previous experiments for the differentiation of rat nasal chondrocytes.

Figure 5-7 illustrates that the hypertrophic differentiation of chondrocyte cultures on PGA after 3 weeks of differentiation is highly variable depending on the batch of FCS used. Whilst FCS 1 had the highest % GAG in the pellet culture (Figure 5-6) it is own to inhibit the differentiation of chondrocytes down the hypertrophic pathway. Full hypertrophy of the construct was not expected after a 3 week culture period; however, hypertrophic chondrocytes should have been present after this period of culture. Constructs cultured using FCS 2, 4 and 5 have evidence of hypertrophic chondrocyte differentiation, which was demonstrated by not only the morphological increase in

chondrocyte cellular size (Figure 5-7) but also by the expression of hypertrophic marker collagen type X (Figure 5-7). FCS batch 4 was chosen for all further experiments as although the percentage GAG within the constructs is shown to be the lowest it did allow for the most extensive hypertrophy within the constructs, with comparable levels to that seen using FCS batch 5. FCS batch 4 was therefore used throughout the following experiments to ensure and that the degree of hypertrophy obtained between different experiments (using serum-containing media) was reproducible.

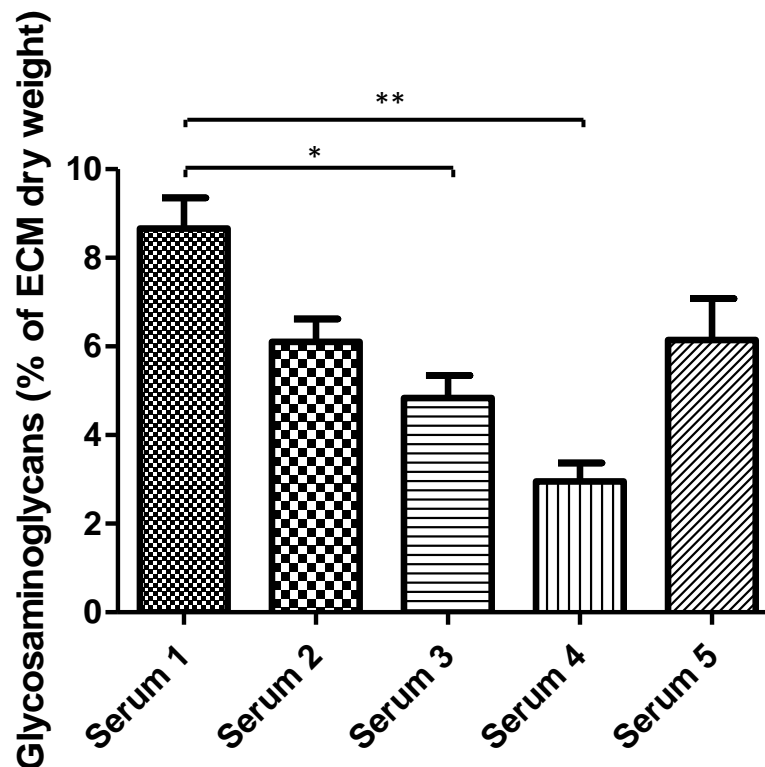


**Figure 5-6:** DMB assay showing the GAG concentration present in the PGA pellets 21 days after culture in the 5 different sera (\*  $p < 0.05$ , \*\* $p < 0.01$ ,  $n=5$ ).



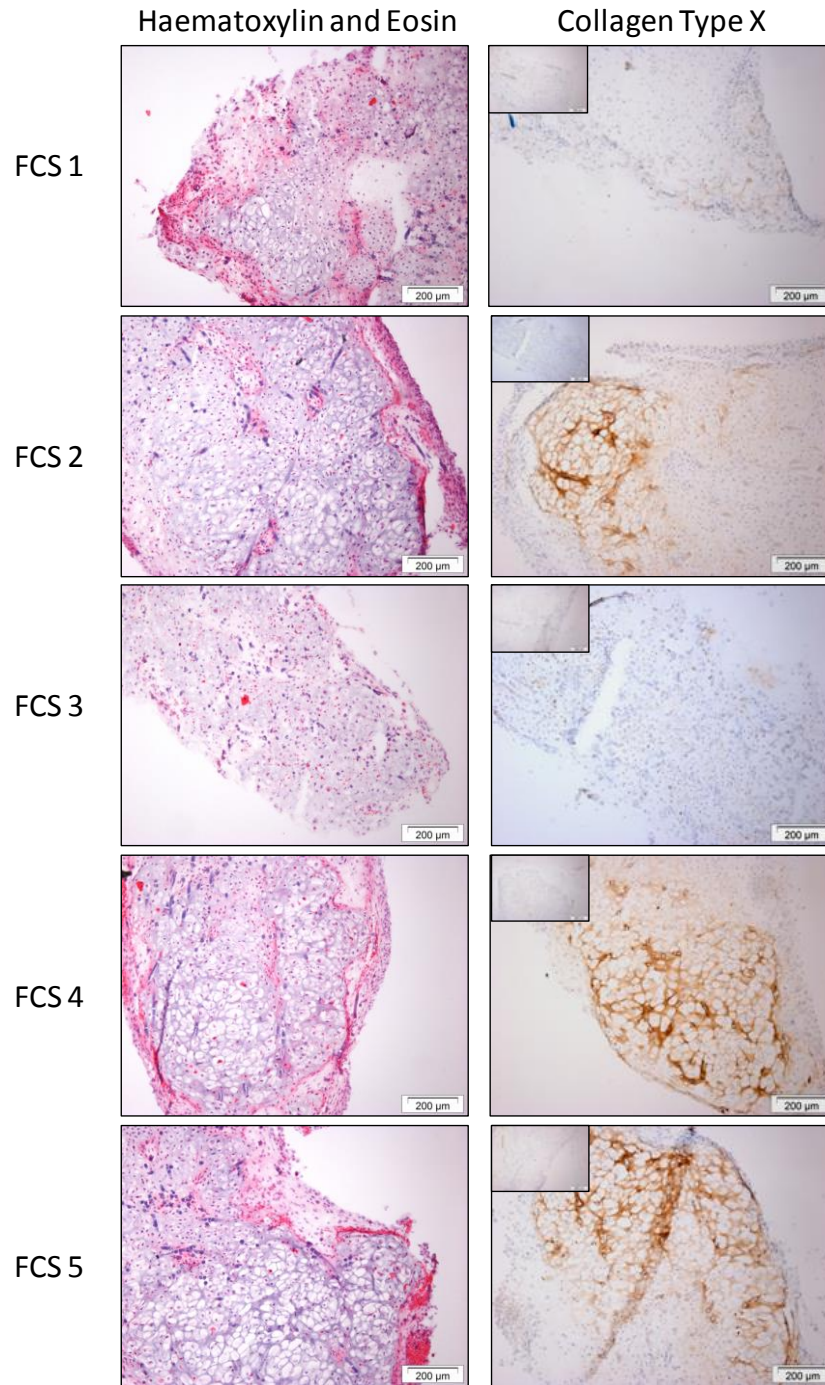


**Figure 5-7:** Representative analysis of constructs cultured in FCS 1-5, showing the degree of hypertrophic differentiation seen after three weeks of culture. Haematoxylin and eosin staining showed the increase in cellular volume co-located with expression of the hypertrophic marker collagen type X (magnification x10, scale bars = 200  $\mu$ m, insert micrographs show negative controls, n=5)

### 5.3 Hypertrophic Differentiation of Rat Nasal Chondrocytes

Both the experimental (electrospun PLLA and electrospun PLLA/calcium phosphate) and commercial (PGA) scaffold materials were assessed for their ability to support chondrocyte attachment, proliferation and hypertrophic differentiation after 42 days of culture in differentiation media.

Initial chondrocyte attachment studies showed that the PGA and PLLA/calcium phosphate scaffold allowed for comparable levels of attachment after 72 hours (84.75 % and 87 % respectively) (Figure 5-8). The PLLA, however, resulted in a significantly lower chondrocyte attachment of 68.92 % (Figure 5-8).

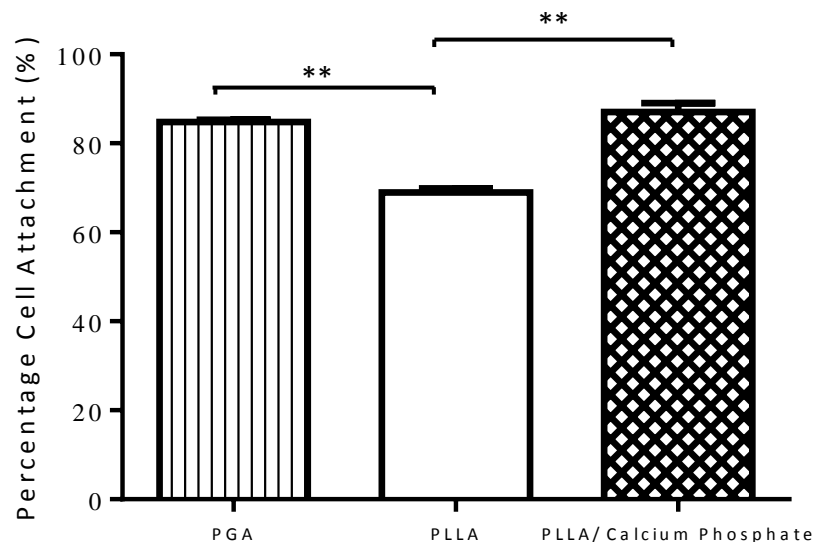


**Figure 5-8:** Chondrocyte attachment to PGA, PLLA and PLLA/calcium phosphate scaffold materials after 72 hours on a shaker plate. (\*\*  $p < 0.001$ ,  $n=6$ )

After a 42 day culture period on the scaffold materials, the chondrocytes exhibited hypertrophic differentiation on the PGA and PLLA/calcium phosphate scaffolds. Hypertrophy was shown by the chondrocytes exhibiting an increase in cellular volume with co-localisation of hypertrophic markers collagen type X and alkaline phosphatase (Figure 5-10) in the ECM. The constructs formed from either PGA or PLLA/calcium

phosphate composite scaffolds were also positive for collagen type II expression and stained strongly with toluidine blue and alcian blue showing GAG present in the ECM. The electrospun PLLA scaffold material, however, was unable to produce a homogenous construct, with small clusters of hypertrophic cells being formed on the scaffold surface. These chondrocyte clusters while expressing collagen type X, did not express alkaline phosphatase. The PLLA constructs also stained weakly with alcian blue or toluidine blue suggesting that there was low GAG accumulation within the ECM. Due to the poor performance of the PLLA scaffold material no further investigations using this scaffold material were performed.

The presence of GAG in the constructs was confirmed by the quantification of GAG within the construct ECM after 42 days of culture. The percentage of GAG accumulated within the ECM by PGA and PLLA/calcium phosphate-based constructs was comparable, with an average of 12.91 % and 14.10 % respectively of the dry weight of the ECM being constituted of GAG. When culturing on the PLLA scaffold material only 0.28 % of the ECM was found to be composed of GAG (Figure 5-11).

GAG production using the PLLA/calcium phosphate scaffold was also compared to that achieved using the PGA scaffold material throughout the culture period (Figure 5-12). The PLLA/calcium phosphate scaffold material allowed a higher GAG accumulation earlier on in the culture, with significantly higher percentage GAG being seen at day 14 and 28 compared to the PGA scaffold (Figure 5-12). However by day 42 the percentage of GAG while still higher is not significantly increased when using the new PLLA/calcium phosphate composite scaffold material (Figure 5-12).

No mineralisation of construct ECM was observed using the PGA scaffold material, while some alizarin red staining was observed in the PLLA/calcium phosphate constructs where staining was within or along the surface of the scaffold material with little staining seen within the tissue itself (Figure 5-13). Due to the intense loss in alizarin red staining in the PLLA/calcium phosphate this alizarin red staining may well

be due to the release of calcium ions from the scaffold which are entrapped within the tissue

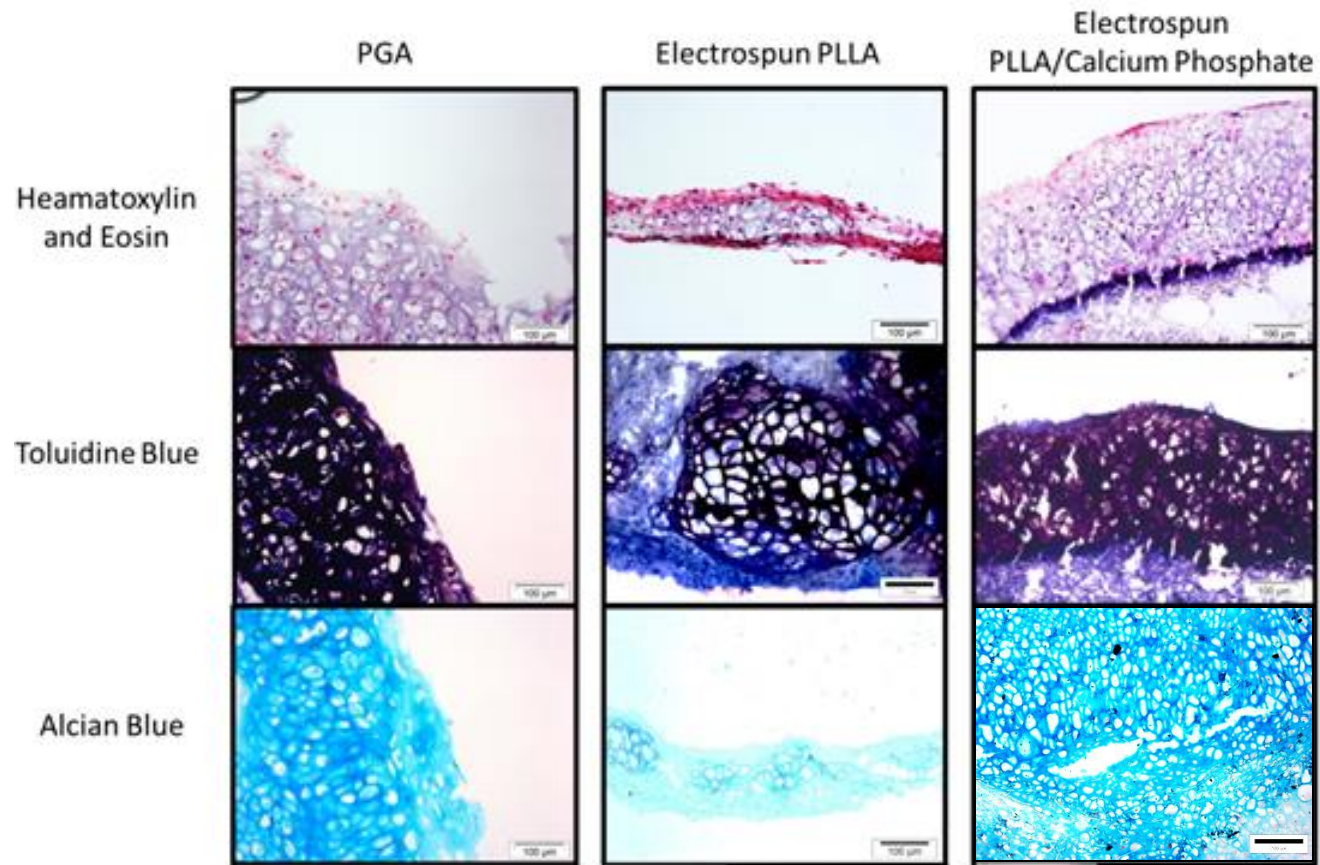


**Figure 5-9:** Histological and immunohistochemical analysis of constructs formed by culturing chondrocytes on PGA, PLLA and PLLA/calcium phosphate scaffold materials for 42 days. The images show haematoxylin and eosin; toluidine blue and alcian blue staining. (n=10). Scale bars = 100  $\mu\text{m}$ .

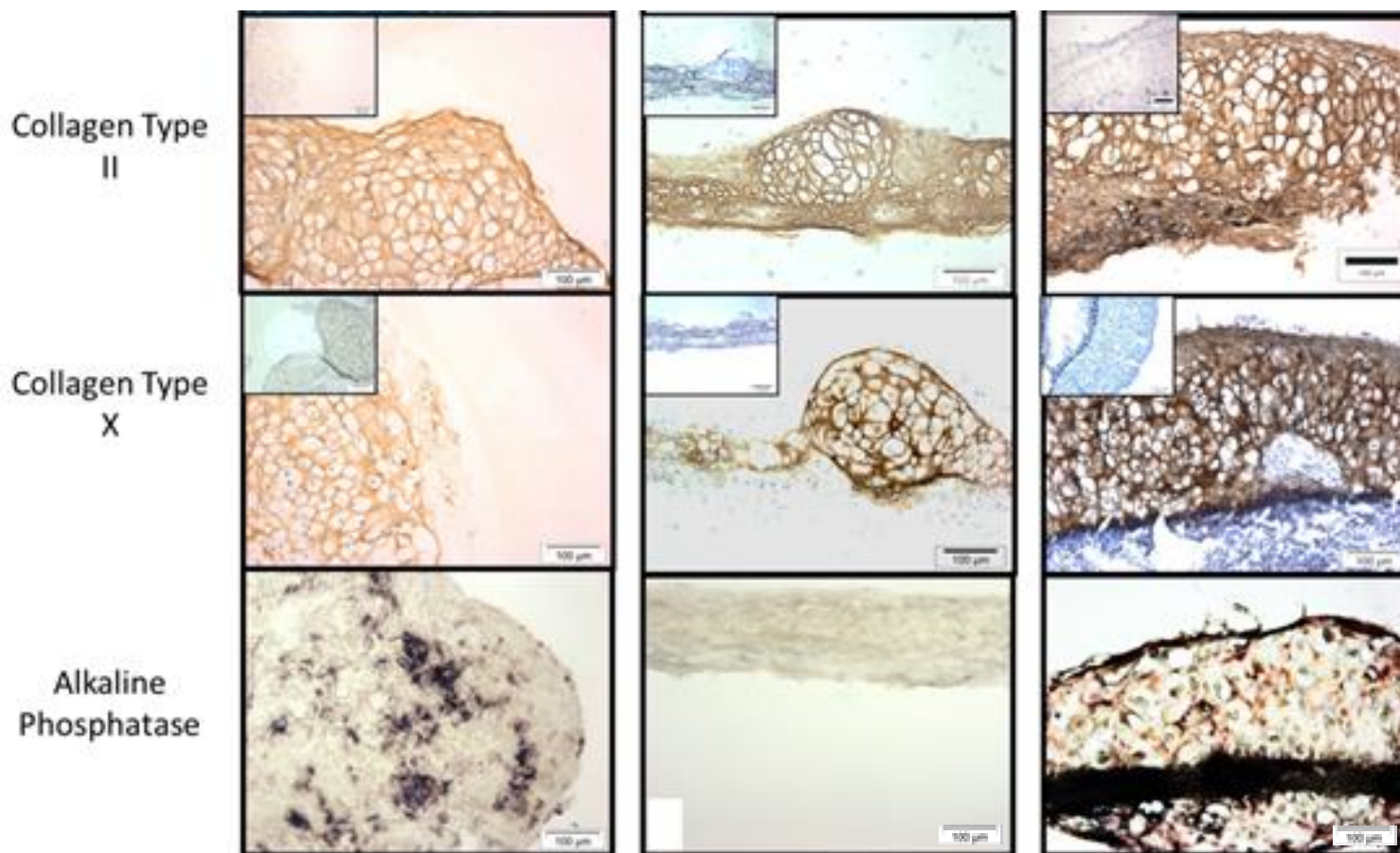


**Figure 5-10:** *Histological and immunohistochemical analysis of constructs formed by culturing chondrocytes on PGA, PLLA and PLLA/calcium phosphate scaffold materials for 42 days. The images show collagen type II; collagen type X and alkaline phosphatase staining. Insert micrographs show non-specific staining (n=10). Scale bars = 100 µm.*

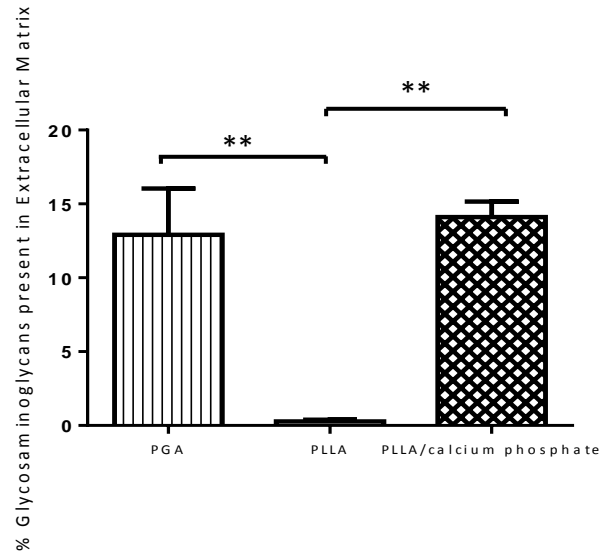


**Figure 5-11:** GAG content of chondrocyte constructs (expressed as a percentage of the dry weight of the ECM) after 42 days of culture on PGA, PLLA and PLLA/calcium phosphate scaffolds. (\*\* $p < 0.01$ ,  $n = 6$ )

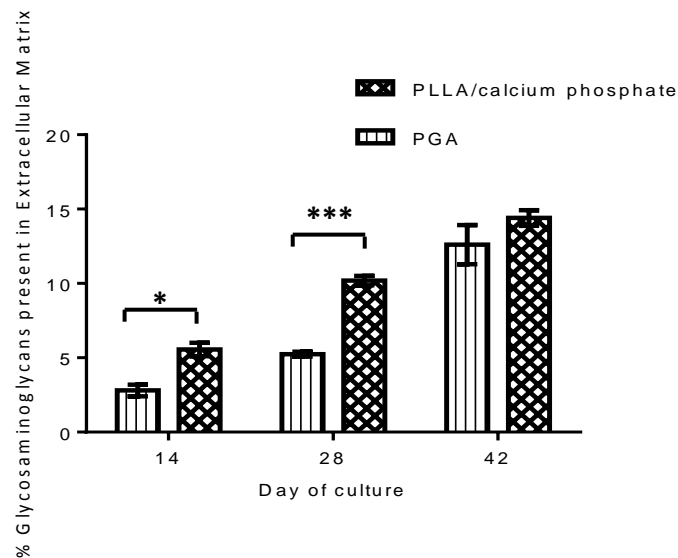


**Figure 5-12:** A comparison of the GAG content in the extracellular matrix of constructs produced by chondrocytes cultured on PGA and PLLA/calcium phosphate scaffold materials after 14, 28 and 42 days of culture. (\*  $p < 0.05$ , \*\*\*  $p < 0.001$ ,  $n = 6$ )

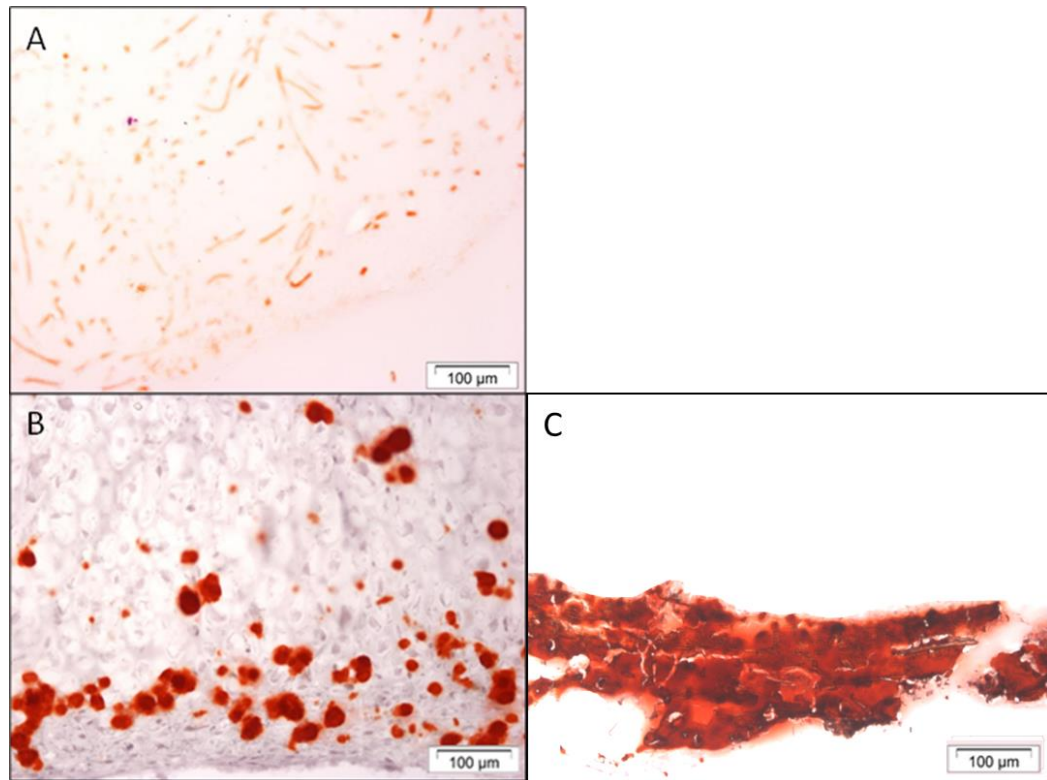


**Figure 5-13:** Mineralisation present within the constructs after 42 days of culture under semi-static conditions. Images show staining for calcium using alizarin red on the PGA scaffold material (A) and the PLLA/calcium phosphate composite scaffold material (B). (C) Shows alizarin red staining of the PLLA/calcium phosphate scaffold at day 0 of culture. Scale bars = 100 µm.



#### ***5.4 Protein and Gene Expression during Chondrocyte Hypertrophic Differentiation on PGA and PLLA/Calcium Phosphate Scaffold Materials***

In order to further understand the process of hypertrophic differentiation of the nasal chondrocytes, the ECM gene and protein expression was investigated as well as key signalling molecules, *Ihh*, and the transcription factors, *sox9* and *runx2*. The two scaffold materials, PGA and PLLA/calcium phosphate composite were investigated for their effect on the expression of these key genes and proteins.

##### ***5.4.1 The Effect of 3D Culture on Gene Expression***

Transferring chondrocytes from a monolayer (2D) culture to a 3D culture on the scaffolds was shown to have a significant impact on the gene expression of the chondrocytes after 24 hours. When using the PGA scaffold material, collagen type II, *Ihh* and *sox9* expression by the chondrocytes in the construct was increased. However, the genes associated with hypertrophic differentiation, collagen type X and alkaline phosphatase, were decreased (Figure 5-14). However, transferring the chondrocytes from 2D culture to culture on the PLLA/calcium phosphate composite scaffold, however, had a different effect to culture on PGA. While the expression of hypertrophic associated genes (collagen type X, alkaline phosphatase and *runx2*) was reduced and the expression of *Ihh* remained increased, the expression of *sox9* and collagen type II was reduced (Figure 5-15).

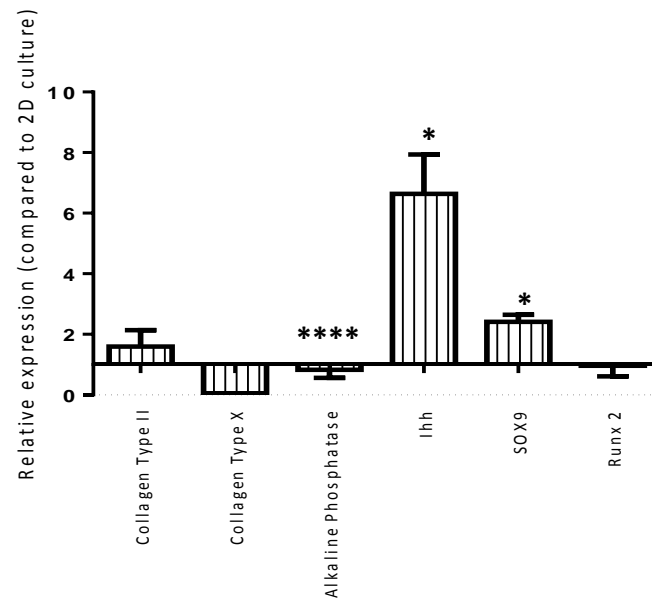


**Figure 5-14:** The effect of 3D culture of chondrocytes on the PGA scaffold material after 72 hours in expansion culture media on gene expression. The data is normalised to the gene expression observed at passage 2 on tissue culture plastic (2D culture) (\*  $p < 0.05$ , \*\*\*\*  $p < 0.0001$ ,  $n = 6$ )

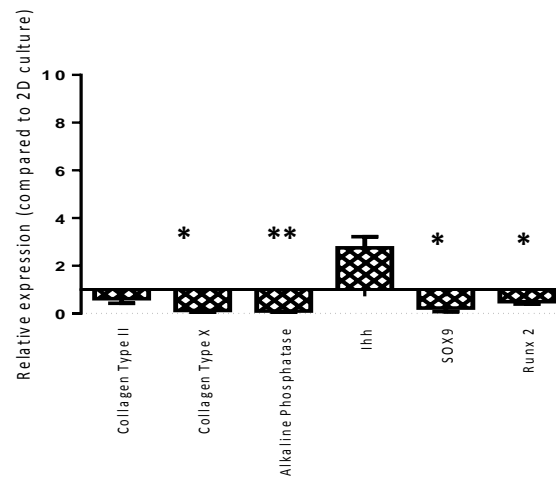


**Figure 5-15:** The effect of 3D culture of chondrocytes on PLLA/calcium phosphate scaffold material on cell gene expression after 72 hours in expansion media. The data is normalised to the gene expression observed at passage 2 on tissue culture plastic (2D culture). (\*  $p < 0.05$ , \*\*  $p < 0.01$ ,  $n = 6$ )

### ***5.4.2 Extracellular Matrix Gene and Protein Expression on PGA and PLLA/calcium phosphate composite scaffolds***

When comparing gene expression on the PGA scaffolds to that of the PLLA/calcium phosphate scaffolds it was necessary to normalise the values to those of the 3D undifferentiated construct values so that the effect of the scaffold material on chondrocyte gene expression can truly be assessed.

#### ***5.4.2.1 Collagen type II***

Collagen type II gene expression on both the PGA and PLLA/calcium phosphate scaffold material constructs also showed a significant increase in collagen type II expression between day 3 and day 7 and was found to peak at day 7 of the culture with 4.97 and 6.44 fold increases in expression observed respectively (Figure 5-16 and Figure 5-17 respectively). The PGA scaffold, however, caused a significant downregulation of collagen type II gene expression by day 14, with lower levels than the collagen type gene expression observed in the undifferentiated 3D PGA scaffold culture, (Figure 5-16). Both scaffold materials downregulated collagen type II expression throughout the culture with the lowest levels of expression being observed on day 42 of the culture (Figure 5-16 and Figure 5-17). Collagen type II was also deposited in the ECM of the constructs and was present throughout the culture period in both the PGA and PLLA/calcium phosphate scaffold constructs (Figure 5-26 and Figure 5-28 respectively).

Collagen type II expression of the PLLA/calcium phosphate constructs was downregulated throughout the culture period when compared to collagen type II gene expression on the PGA scaffold material (Figure 5-18). At day 28 and day 42 the collagen type II gene expression was observed to be significantly downregulated in the PLLA/calcium phosphate scaffold constructs (Figure 5-18).

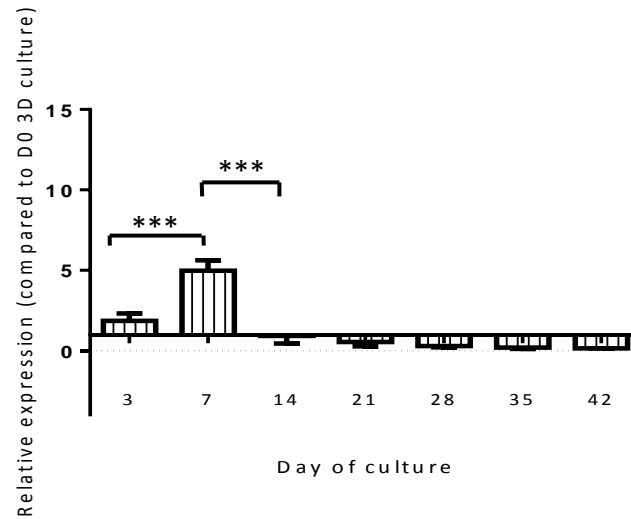


**Figure 5-16:** Collagen type II mRNA expression during hypertrophic differentiation on PGA scaffold material relative to its expression level seen after 72 hours of culture in expansion media (day 0 of 3D chondrocyte differentiation). (\*\*\*)  $p < 0.001$ .  $n = 8$ )

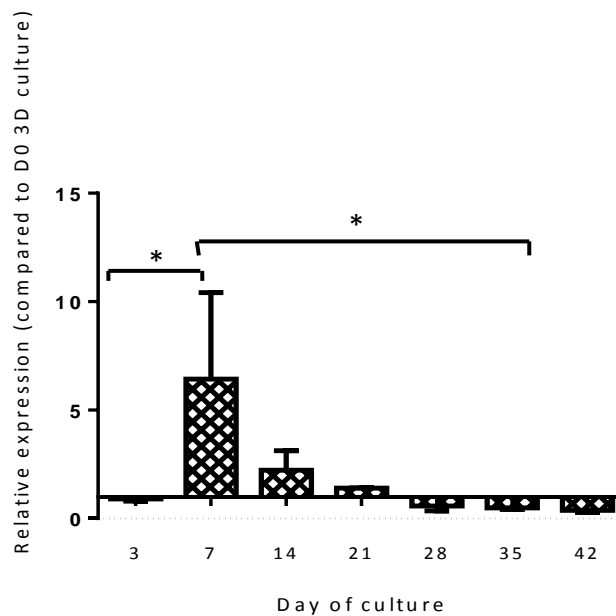


**Figure 5-17:** Collagen type II mRNA expression during hypertrophic differentiation on PLLA/calcium phosphate scaffold material relative to the mRNA expression levels seen after 72 hours of culture in expansion media (day 0 of 3D chondrocyte differentiation). (\*  $p < 0.05$ .  $n = 8$ ).

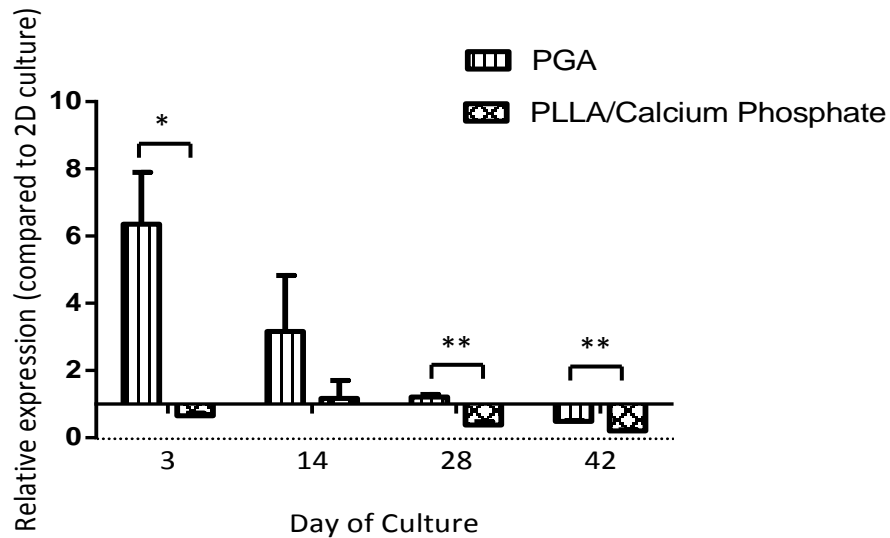


**Figure 5-18:** Collagen type II mRNA expression in the chondrocytes during hypertrophic differentiation culture on PLLA/calcium phosphate scaffold material compared to expression seen on the PGA scaffold material. The data is normalised to the gene expression observed at passage 2 on tissue culture plastic (2D culture). (\*\*  $p < 0.01$  and \* $p < 0.05$ .  $n = 8$ )

#### 5.4.2.2 Collagen type X

Collagen type X mRNA expression significantly increased throughout the hypertrophic differentiation of the chondrocytes on both the PGA and PLLA/calcium phosphate scaffold materials between day 3 and day 35 (Figure 5-19 and Figure 5-20 respectively). The gene expression peaked at day 35 with an 85.69 and 77.49 fold increase compared to day 0 of culture on the scaffold material. However, there was a trend for the collagen type X gene expression, to decrease day 42 on both scaffold materials (Figure 5-19 and Figure 5-20), although this trend did not reach significance. Collagen type X deposition within the matrix of both PGA and PLLA/calcium phosphate grafts by was detectable by immunohistochemical localisation by day 28, although its gene expression was upregulated by day 14. However, collagen type X protein was not detectable in the ECM at day 14 by immunohistochemical localisation (Figure 5-28 and Figure 5-26).

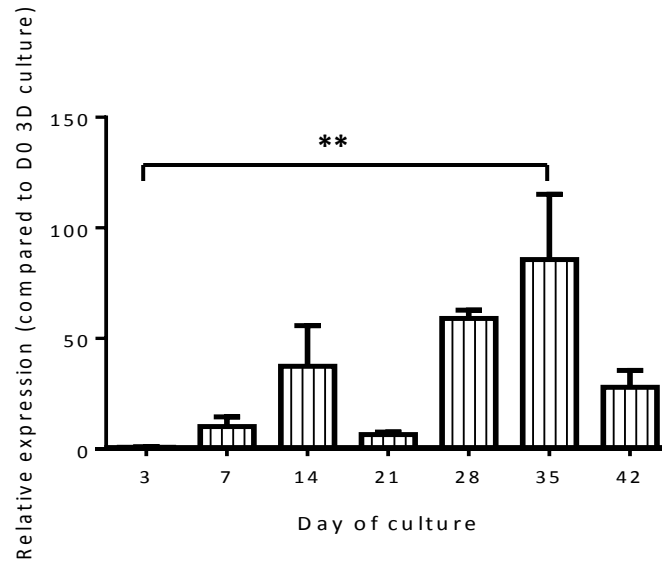


**Figure 5-19:** Collagen type X mRNA expression during hypertrophic differentiation on PGA scaffold material relative to mRNA expression levels seen after 72 hours of culture in expansion media (day 0 of 3D chondrocyte differentiation). (\*\*  $p < 0.01$ .  $n = 8$ )

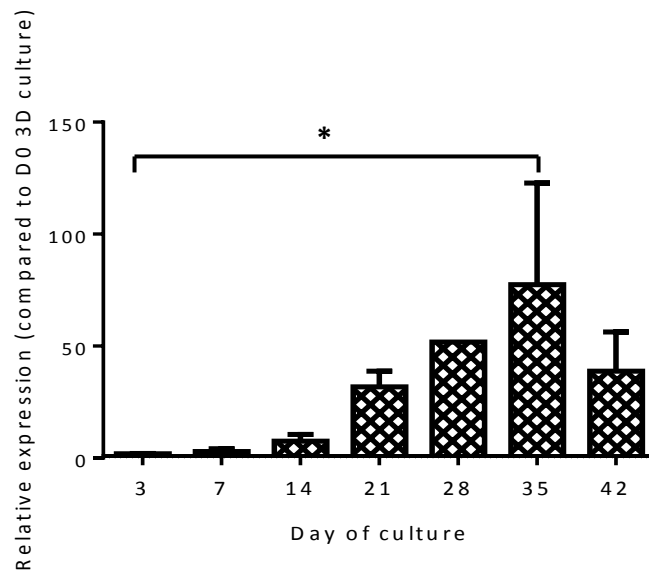


**Figure 5-20** Collagen type X mRNA expression during hypertrophic differentiation on PLLA/calcium phosphate scaffold material relative to mRNA expression levels seen after 72 hours of culture in expansion media (day 0 of 3D chondrocyte differentiation). (\*  $p < 0.05$ .  $n = 8$ )

When compared to the constructs formed on the PGA scaffold material, constructs on the PLLA/calcium phosphate scaffold showed an upregulation of collagen type X throughout the culture period, with significant increases seen on days 14 and day 42 (Figure 5-21).

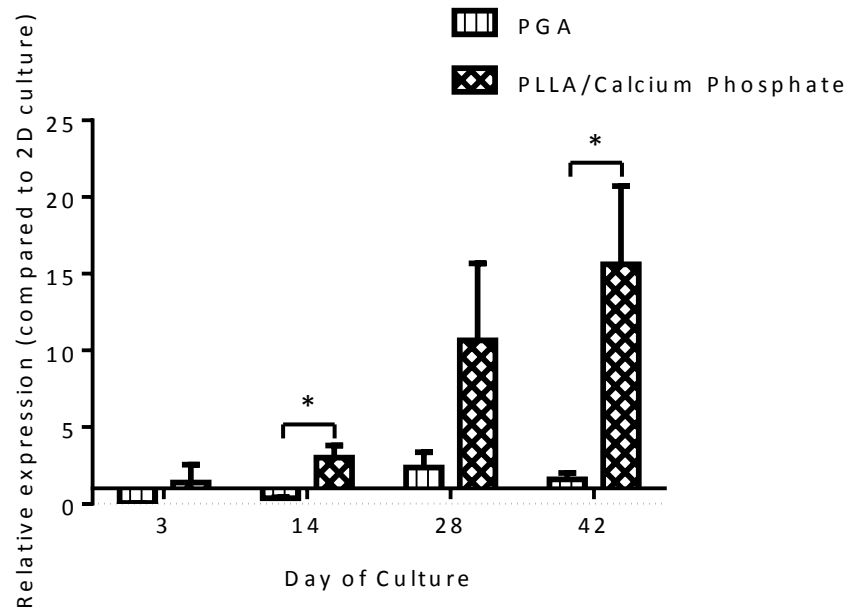


**Figure 5-21:** Collagen type X mRNA expression during hypertrophic differentiation of chondrocytes cultured on PLLA/calcium phosphate scaffolds compared to the expression observed on the PGA. The data is normalised to the gene expression observed at passage 2 on tissue culture plastic (2D culture). (\* $p < 0.05$ .  $n = 8$ )

#### 5.4.2.3 Alkaline Phosphatase

Alkaline phosphatase mRNA expression of PGA constructs (Figure 5-22) followed a similar pattern to that shown by collagen type X (refer Figure 5-19 and Figure 5-21) with a significant increase in expression between day 3 and day 35, followed by a non-significant decrease in expression at day 42. The PLLA/calcium phosphate constructs, however, give a continued increase of alkaline phosphatase throughout the culture

period up to day 42 (Figure 5-23). Unlike collagen type X, alkaline phosphatase activity was seen at the periphery of all the constructs at day 14 and was observed to increase throughout the culture period until day 42 where it was expressed throughout both the constructs made using both PGA and PLLA/calcium phosphate (Figure 5-26 and Figure 5-28)

Alkaline phosphatase expression was upregulated in the PLLA/calcium phosphate scaffold constructs when compared to the PGA constructs, with a significant increase in expression observed at day 14 in the PLLA/calcium phosphate constructs (Figure 5-24).

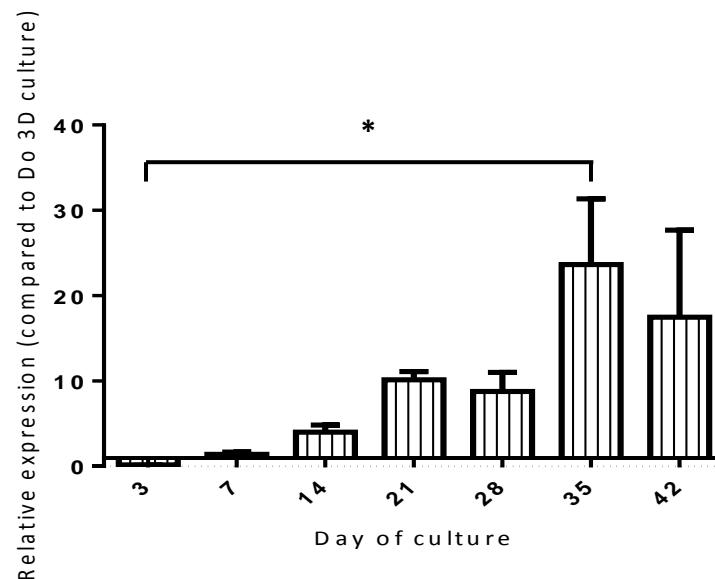


**Figure 5-22:** Alkaline phosphatase mRNA expression during hypertrophic differentiation of PGA constructs relative to mRNA expression levels seen after 72 hours of culture in expansion media (day 0 of 3D chondrocyte differentiation). (\* $p < 0.05$ .  $n = 8$ ).



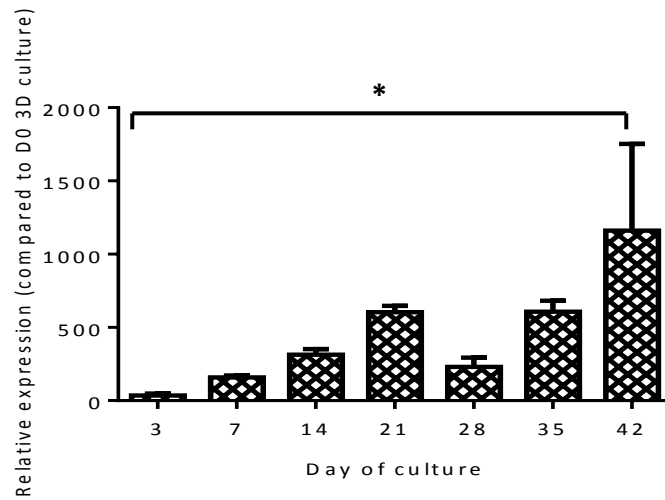


**Figure 5-23:** Alkaline phosphatase mRNA expression during hypertrophic differentiation of PLLA/calcium phosphate constructs relative to mRNA expression levels seen after 72 hours of culture in expansion media (day 0 of 3D chondrocyte differentiation). (\* $p < 0.05$ .  $n = 8$ ).

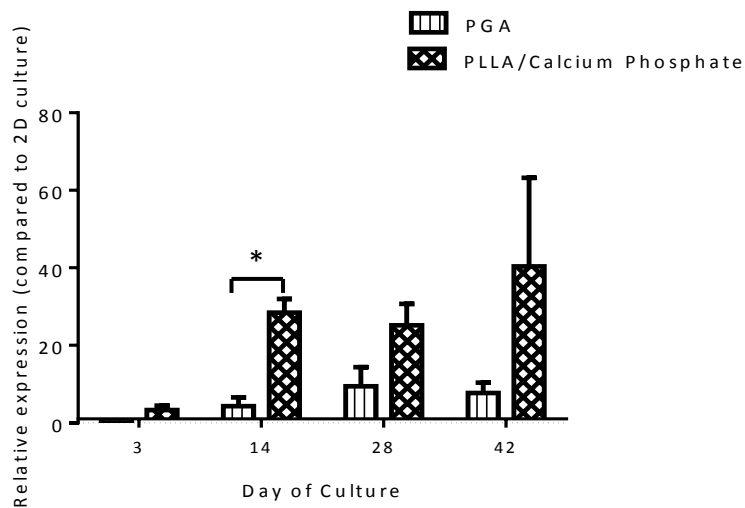


**Figure 5-24:** Alkaline phosphatase mRNA expression of chondrocytes during hypertrophic differentiation of PLLA/calcium phosphate constructs compared to the alkaline phosphatase expression seen in the PGA constructs. The data is normalised to the gene expression observed at passage 2 on tissue culture plastic (2D culture). (\* $p < 0.05$ .  $n = 8$ )

Analysis of the gene expression and protein localisation of alkaline phosphatase in constructs at day 14, 28 and 42 of culture, showed the progression of the hypertrophic differentiation. At day 14, staining with alcian blue and toluidine blue was pale illustrating the low amount of ECM present. At this early stage of differentiation, the ECM present in the constructs consisted of mainly collagen type II and no collagen type X expression was seen (Figure 5-26 and Figure 5-28). However, alkaline phosphatase was expressed on the periphery of the constructs. By day 28 collagen type X and alkaline phosphatase were present within the ECM and were associated with chondrocytes with large cell morphology (Figure 5-26 and Figure 5-28). By day 42 all the constructs reproducibly displayed hypertrophic features with chondrocytes with a large cellular volume and the ECM containing dense staining for collagen type X and alkaline phosphatase (Figure 5-26 and Figure 5-28).

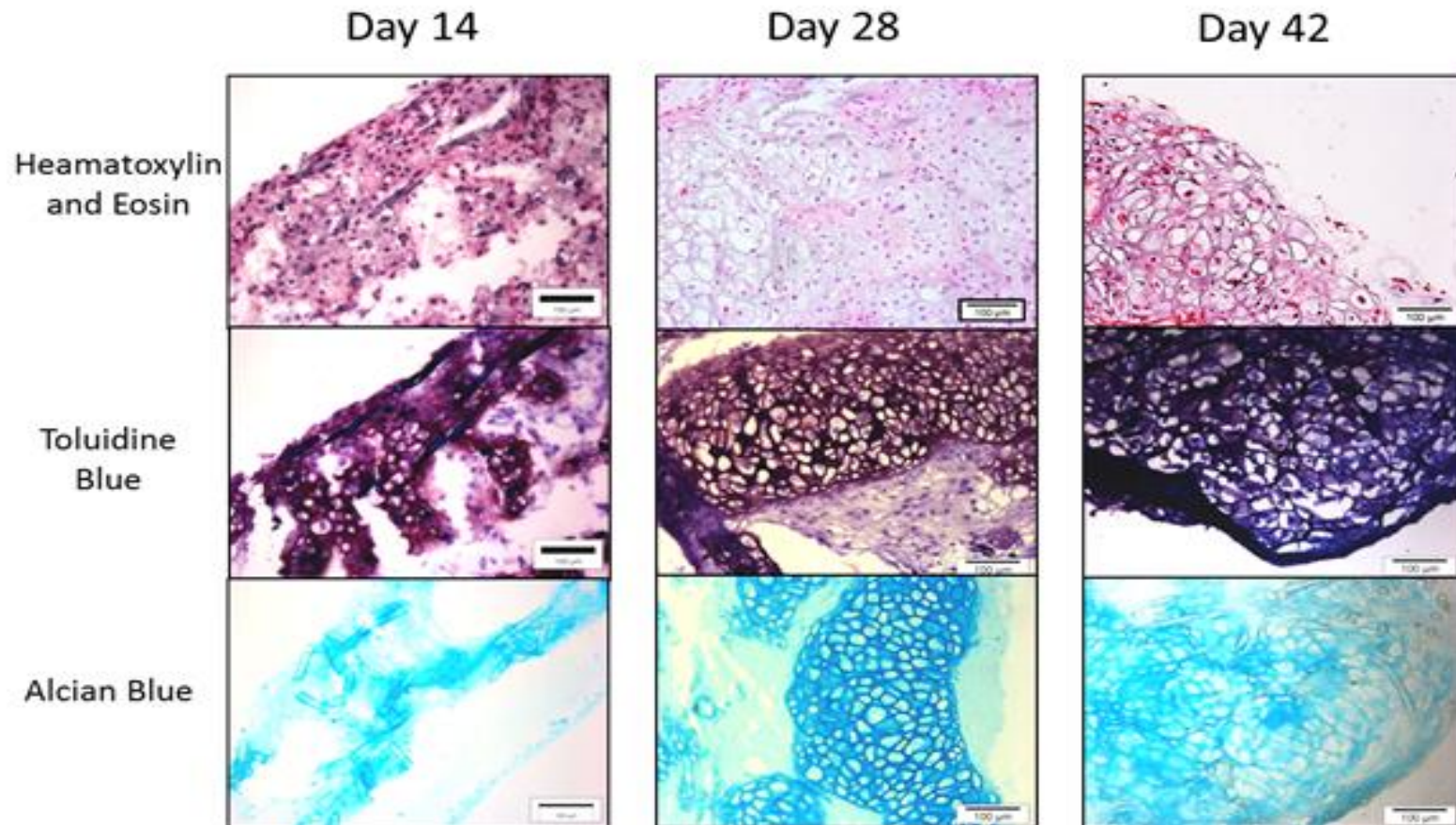


**Figure 5-25:** Representative histological analysis of chondrocytes grown on PGA scaffolds after 14, 28 and 42 days of culture, showing the localisation of extracellular proteins and within the ECM of the construct. Inset micrographs show negative controls, scale bars=100 μm (n=3 separate experiments).

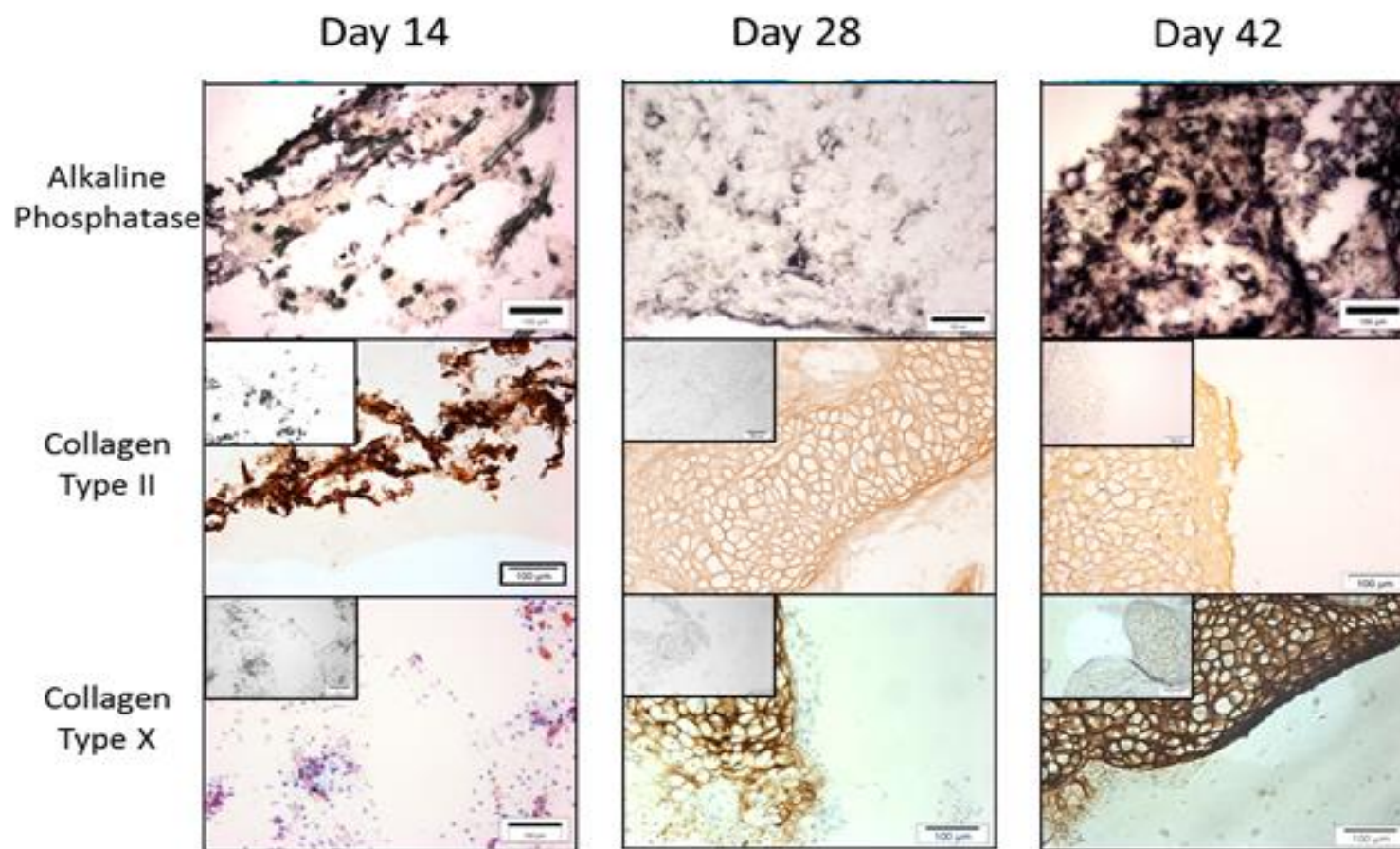


**Figure 5-26:** Representative immunohistological analysis of chondrocytes grown on PGA scaffolds after 14, 28 and 42 days of culture, showing the localisation of extracellular proteins and within the ECM of the construct. Inset micrographs show negative controls, scale bars=100 μm (n=3 separate experiments).

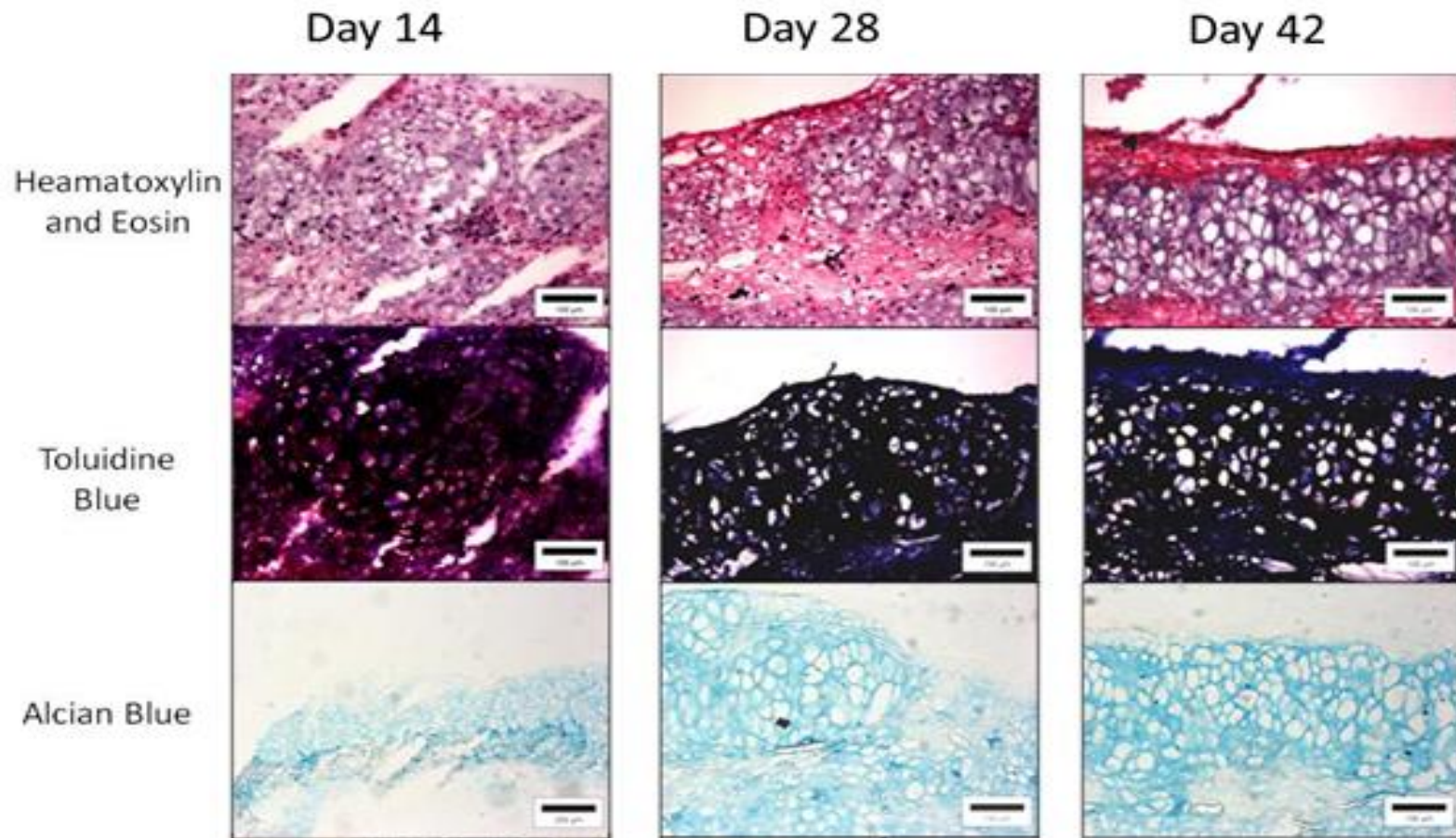


**Figure 5-27:** Representative histological analysis of chondrocytes grown on PLLA/calcium phosphate scaffolds after 14, 28 and 42 days of culture, showing the localisation of extracellular proteins within the ECM of the constructs. Inset micrographs show negative controls, scale bars=100  $\mu\text{m}$  ( $n=3$  separate experiments).

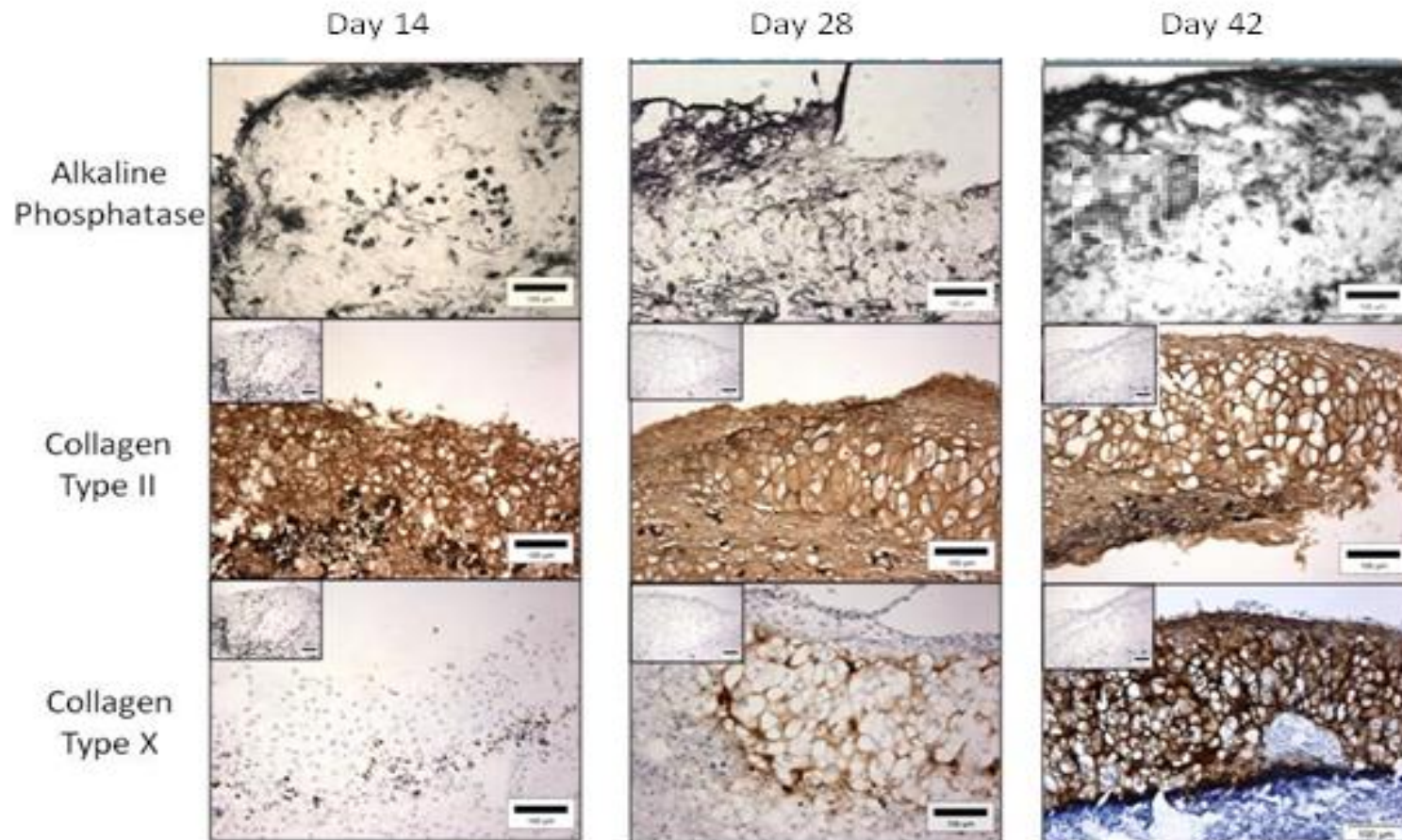


**Figure 5-28:** Representative immunohistological analysis of chondrocytes grown on PLLA/calcium phosphate scaffolds after 14, 28 and 42 days of culture, showing the localisation of extracellular proteins within the ECM of the constructs. Inset micrographs show negative controls, scale bars=100  $\mu\text{m}$  ( $n=3$  separate experiments).

### **5.4.3 Transcription Factor and Signalling Molecule Gene Expression**

#### **5.4.3.1 Sox9**

The expression levels of sox9 were different between constructs formed from the different scaffold materials. After an initial increase in sox9 expression as chondrocytes were moved from 2D to 3D culture on PGA scaffolds, (Figure 5-14) the expression of sox9 was significantly reduced at day 3 of culture. After this initial inhibition, the expression of sox9 was not significantly altered (Figure 5-29). A trend for an increase in sox9 expression peak was seen at day 35 which corresponded to the time period when peaks in collagen type X expression and alkaline phosphatase expression were observed (Figure 5-19 and Figure 5-22). In the PLLA/calcium phosphate constructs, the expression of sox9 was initially downregulated as the chondrocytes were transferred from a 2D to the 3D culture environment. The expression of sox9 was then significantly upregulated between day 3 and day 14 (with a 99.93 fold increase). However a second peak in expression was seen at day 35 was observed during chondrocyte culture on both the PGA and the PLLA/calcium phosphate scaffolds.

When sox9 mRNA expression on both scaffold materials was compared to the 2D culture hyaline chondrocytes sox9 is significantly upregulated in the PLLA/calcium phosphate constructs on day 14 of the culture. No such increase in sox9 gene expression was observed at day 14 in the PGA constructs. However, expression levels of sox9 were comparable on day 28 and day 42 (Figure 5-31).

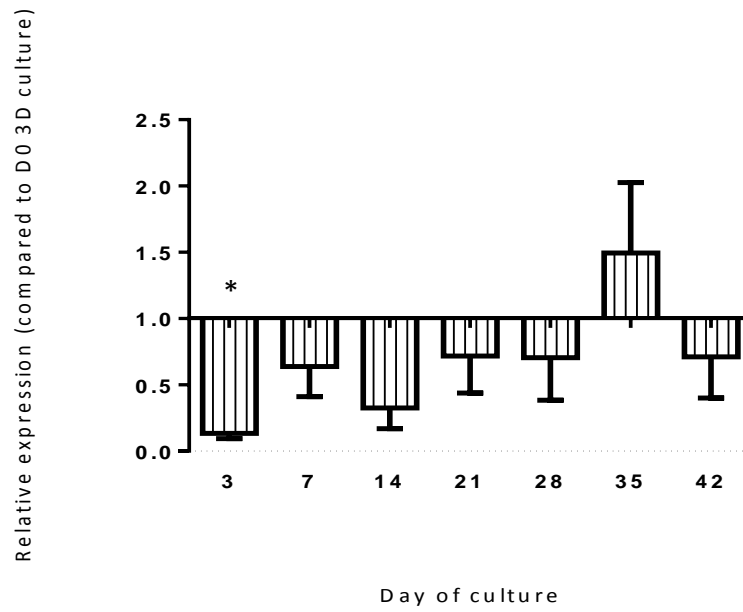


**Figure 5-29:** Sox9 mRNA expression during hypertrophic differentiation of chondrocytes on PGA scaffolds relative to mRNA expression levels seen after 72 hours of culture in expansion media (day 0 of 3D chondrocyte differentiation). (\* $p < 0.05$ .  $n = 8$ ).



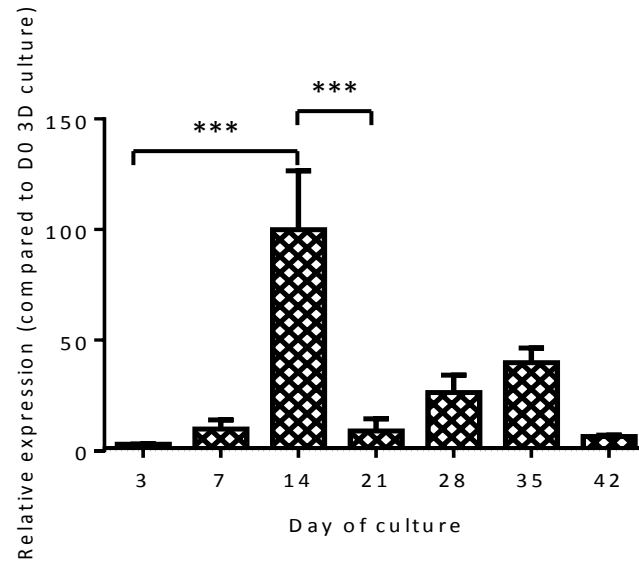


**Figure 5-30:** Sox9 mRNA expression during hypertrophic differentiation of chondrocytes on PLLA/calcium phosphate scaffolds relative to mRNA expression levels seen after 72 hours of culture in expansion media (day 0 of 3D chondrocyte differentiation). (\*\*\*) $p < 0.001$ .  $n = 8$ ).

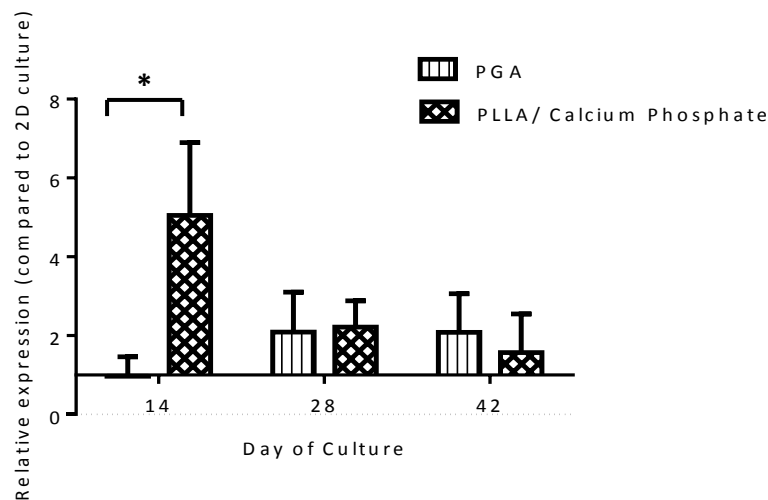


**Figure 5-31:** Sox9 mRNA expression in chondrocytes during hypertrophic differentiation on PLLA/calcium phosphate scaffolds relative to sox9 expression seen in chondrocytes cultured on the PGA scaffold. The data is normalised to the gene expression observed at passage 2 on tissue culture plastic (2D culture). (\* $p < 0.05$ .  $n = 8$ )

### 5.4.3.2 Indian Hedgehog

The expression profile of *Ihh* of both the PGA and PLLA/calcium phosphate constructs were shown to follow a similar temporal pattern, with a peak in *Ihh* expression observed at day 21 (Figure 5-32 and Figure 5-33 respectively), which was then significantly decreased by day 28. The relative fold expression was significantly higher for the PLLA/calcium phosphate constructs, peaking with a 62.40 fold increase, compared to a 20.32 fold increase in the PGA constructs. However, this can be partly attributed to the lower increase in expression as the chondrocytes were moved on to the PLLA/calcium phosphate scaffold (Section 5.4.1).

When comparing the two scaffold materials on the differentiation from 2D culture *Ihh* expression is seen to be significantly upregulated at day 14 and day 42 on the PLLA/calcium phosphate scaffold material when compared to the PGA scaffold material (Figure 5-34).

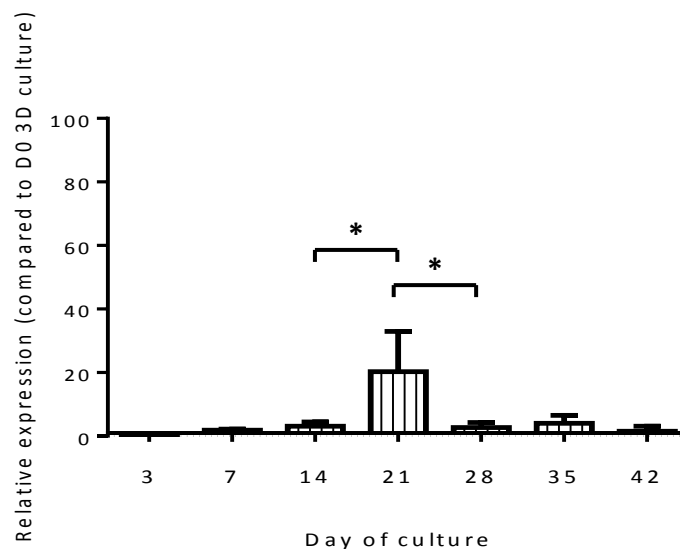


**Figure 5-32:** *Ihh* mRNA expression in the chondrocytes during hypertrophic differentiation culture on PGA relative to mRNA expression levels seen after 72 hours of culture in expansion media (day 0 of 3D chondrocyte differentiation). (\*  $p < 0.05$ .  $n = 8$ ).

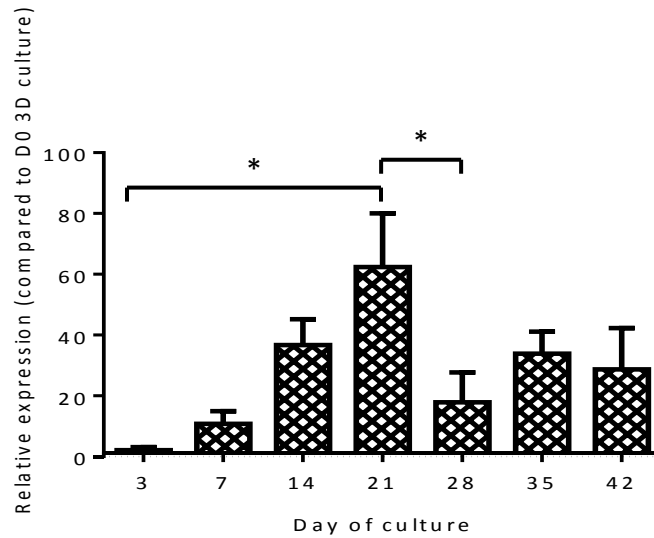


**Figure 5-33:** *Ihh* mRNA expression during chondrocyte hypertrophic differentiation on PLLA/calcium phosphate scaffolds relative to mRNA expression levels seen after 72 hours of culture in expansion media (day 0 of 3D chondrocyte differentiation). (\* $p < 0.05$ .  $n = 8$ ).

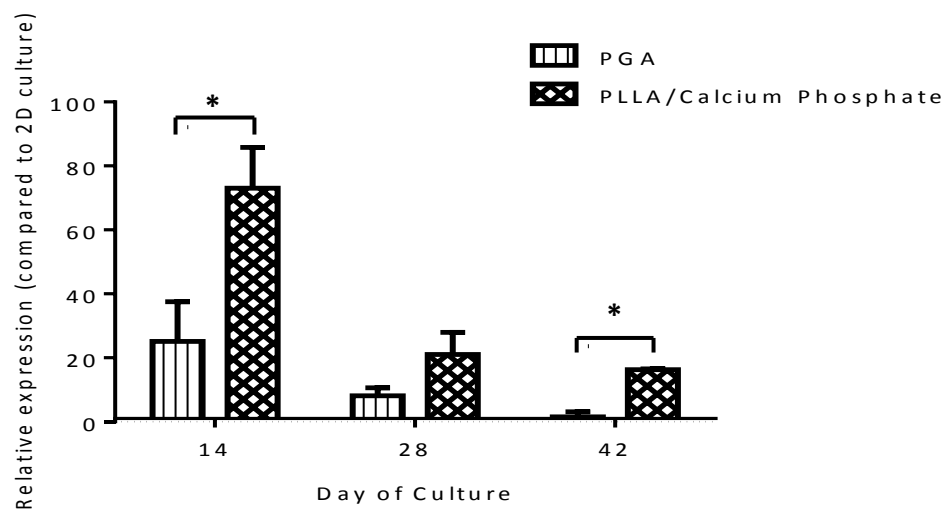


**Figure 5-34:** *Ihh* mRNA expression in the chondrocytes during hypertrophic differentiation culture on PLLA/calcium phosphate scaffolds material compared to *Ihh* expression seen in the PGA constructs. The data is normalised to the gene expression observed at passage 2 on tissue culture plastic (2D culture). (\* $p < 0.05$ .  $n = 8$ )

### 5.4.3.3 Runx2

Runx2 was initially downregulated when the chondrocytes were transferred from 2D monolayer culture to culture on either the PGA scaffolds or PLLA/calcium phosphate scaffolds (Figure 5-14 and Figure 5-15). However, the expression profile was found to differ once the chondrocytes were cultured on the two scaffold materials. PGA constructs showed a gradual increase in runx2 expression over time in culture with a significant peak of runx2 expression at day 28 (Figure 5-35). Whereas, in PLLA/calcium phosphate constructs, a significant increase in runx2 expression was seen on day 3 of culture, after which the expression levels did not significantly alter throughout the differentiation period (Figure 5-36).

When runx2 mRNA expression on both scaffold materials was compared to the runx2 expression level in 2D cultured hyaline chondrocytes, the expression of runx2 was seen to be comparable throughout the culture period (Figure 5-37).

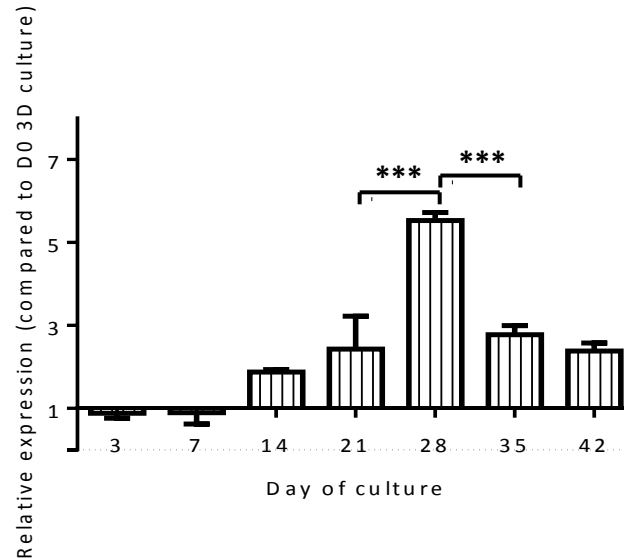


**Figure 5-35:** Runx2 mRNA expression during chondrocyte hypertrophic differentiation on PGA scaffolds relative to mRNA expression levels seen after 72 hours of culture in expansion media (day 0 of 3D chondrocyte differentiation). (\*\*\*) $p < 0.001$ .  $n = 8$ ).

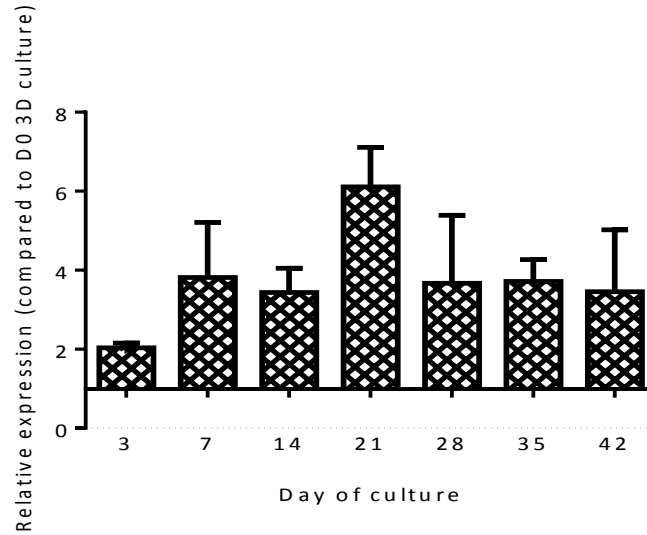


**Figure 5-36:** Runx2 mRNA expression during chondrocyte hypertrophic differentiation on PLLA/calcium phosphate scaffolds, relative to the runx2 mRNA expression level seen after 72 hours of culture in expansion media (day 0 of 3D chondrocyte differentiation). (\* $p < 0.05$ .  $n = 8$ ).

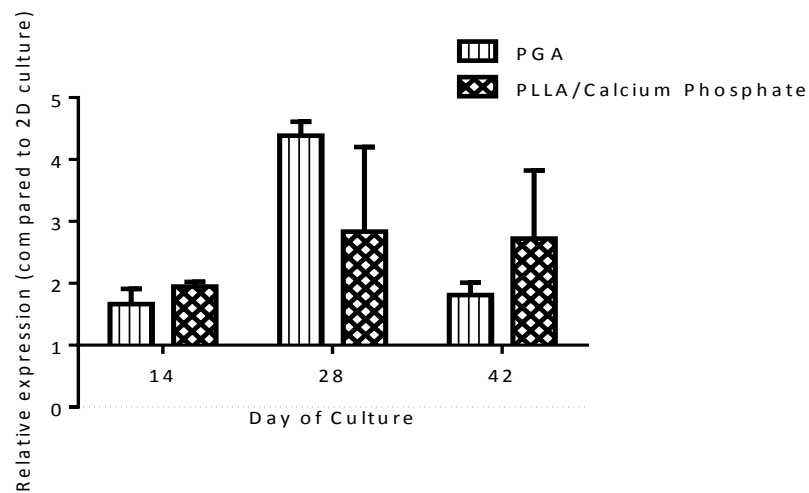


**Figure 5-37:** Runx2 mRNA expression in the chondrocytes during hypertrophic differentiation culture on PLLA/calcium phosphate scaffolds compared to expression seen on the PGA scaffold material. The data is normalised to the gene expression observed at passage 2 on tissue culture plastic (2D culture). ( $n = 8$ )

## 5.5 Cranial Implantation of Hypertrophic Constructs Cultured on PGA

### 5.5.1 Construct Decellularisation

PGA constructs were decellularised by washing the constructs with varying numbers of hypertonic and ionic buffer cycles (Section 4.2.6). After 2 cycles a significant decrease in genetic material was seen with an average of 79.68% DNA removal obtained. The removal of DNA was not significantly increased by the addition of another a cycle of washing with hypertonic and ionic buffers (Figure 5-38). The removal of genetic material is also confirmed by DAPI staining (Figure 5-38) Two cycles of washing with hypertonic and ionic buffers also did not have a significant effect on the percentage of GAG removed from the ECM of the constructs when compared to 1 cycle, whereas 3 cycles was shown to significantly increase the amount of GAG removed from the constructs (Figure 5-40).

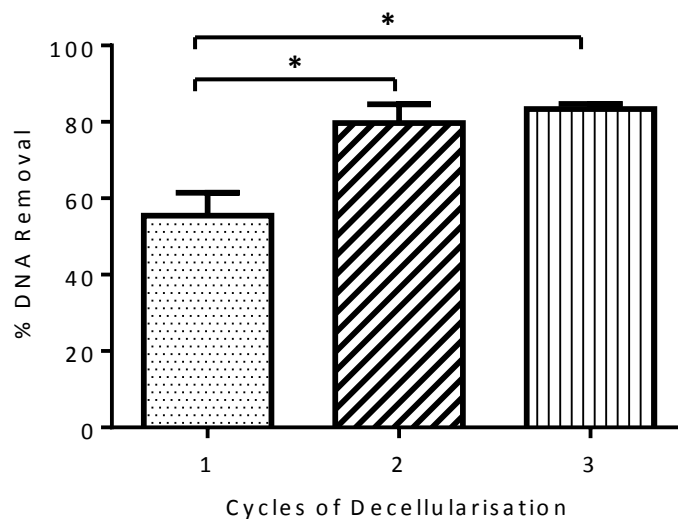


**Figure 5-38:** The percentage DNA removal after cycles of washing the constructs cultured on PGA with SDS and ionic buffers (\*  $p < 0.05$ ,  $n = 3$ )

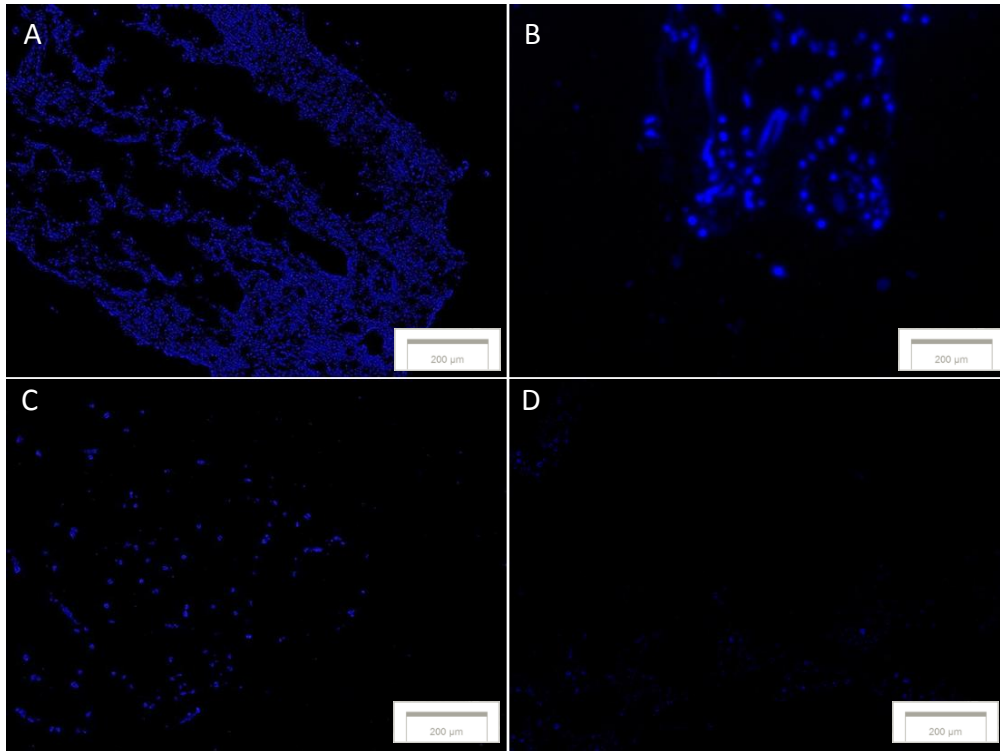


**Figure 5-39:** DAPI staining illustrating the removal of genetic material from hypertrophic constructs cultured on PGA after (B) 1 cycle, (C) 2 cycles and (D) 3 cycles of the decellularisation protocol compared (A) cellularised grafts (magnification x5).

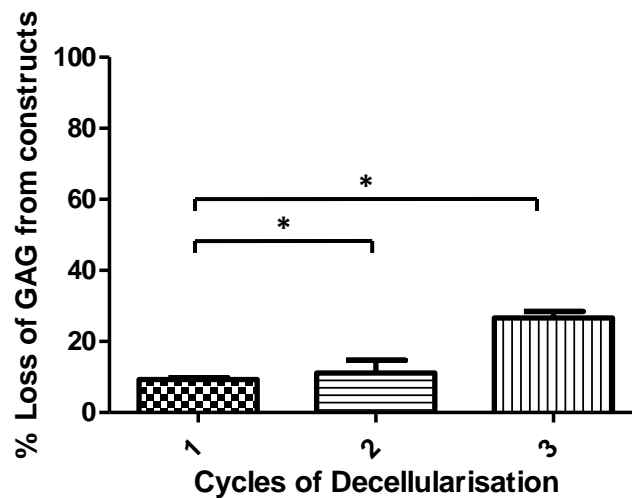


**Figure 5-40:** The percentage loss of GAG from the constructs cultured on PGA after cycles of washing the constructs with SDS and ionic buffers (\*  $p < 0.05$ ,  $n = 3$ ).

## 5.5.2 Constructs Pre-Implantation

### 5.5.2.1 'Living' Constructs

Before implantation, constructs were shown to stain positively for the markers of hypertrophy, collagen type X (Figure 5-41(E)) and alkaline phosphatase (Figure 5-41(D)). They were also shown to contain chondrocytes with a large cellular morphology (Figure 5-41(A)) and had a high GAG content (Figure 5-41 (B, C)). The constructs were also shown to be negative for alizarin red staining and therefore there was no mineralisation of the constructs before implantation into the defect.

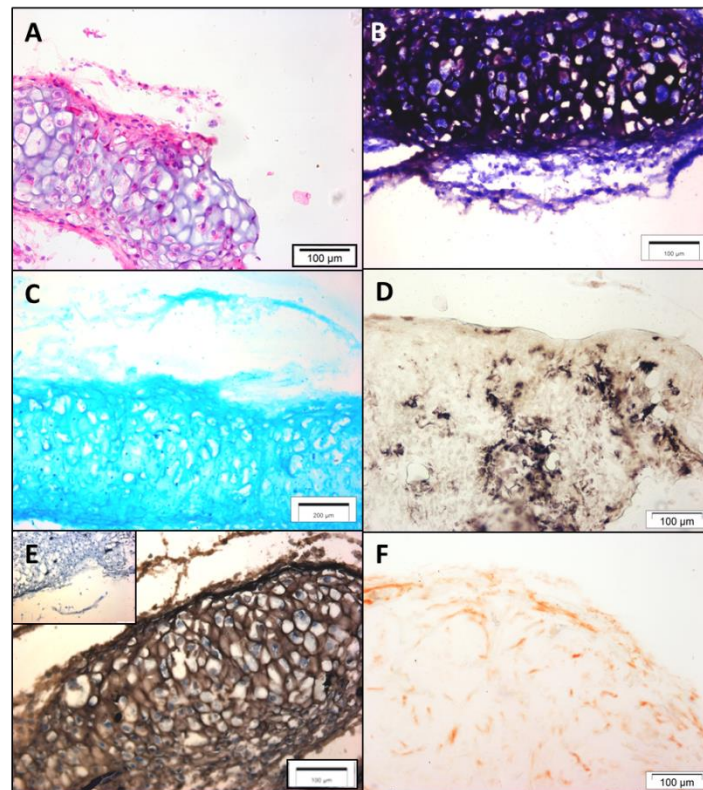


**Figure 5-41:** Immunohistochemical and histological staining of the PGA constructs before implantation into the cranial defect model. (A) haematoxylin and eosin stain; (B) toluidine blue; (C) alcian blue; (D) alkaline phosphatase; (E) collagen type X; (F) alizarin red. Insert micrographs show non-specific staining. Scale bars = 100µm.



### 5.5.2.2 Decellularised Constructs

An average of 79.68 % DNA removal was achieved during the decellularisation process (Figure 5-38), this removal of genetic material could be visualised by the decrease in DAPI staining shown in Figure 5-42 after the grafts underwent the decellularisation protocol.

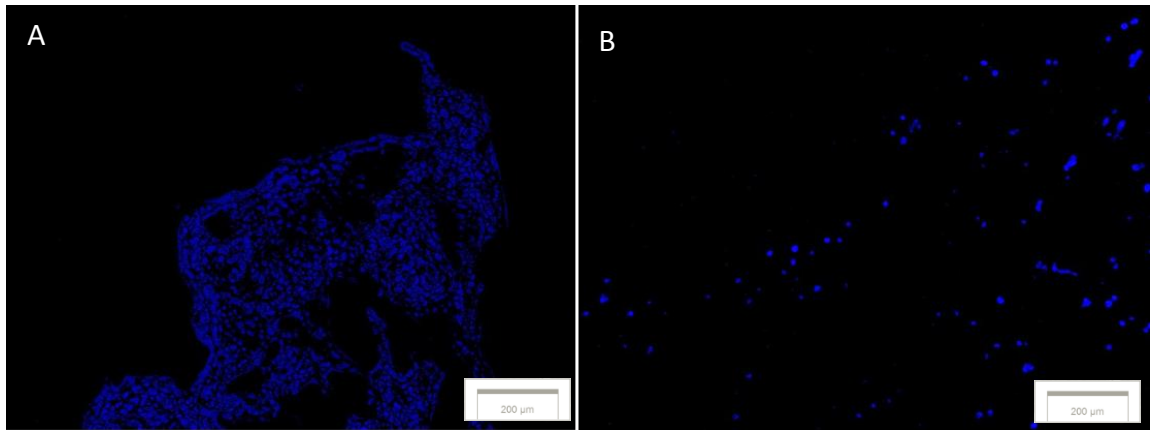


**Figure 5-42:** DAPI staining illustrating the decellularisation of the PGA constructs before implantation into the cranial defect. (A) Construct before decellularisation; (B) construct post decellularisation (magnification x5).

The decellularisation protocol led to a 10.18 % decrease in GAG content in the ECM and this can be seen in the lower intensity of both toluidine blue (Figure 5-43(B)) and alcian blue (Figure 5-43(C)) staining in the decellularised construct a when compared to the ‘living’ constructs (Figure 5.37). Staining for collagen type X was also decreased in the decellularised constructs (Figure 5-43(E)) compared to the ‘living’ constructs. The lack of staining by Alizarin red again showed that there was no mineralisation of the construct before implantation into the cranial defect (Figure 5-43(F)).

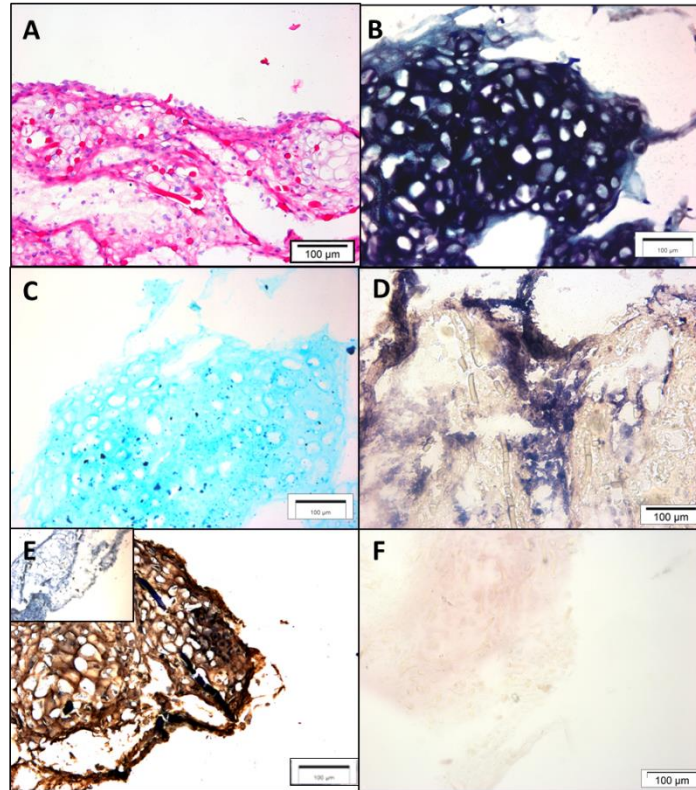


**Figure 5-43:** Immunohistochemical and histological staining of decellularised PGA constructs before implantation into the cranial defect. (A) haematoxylin and eosin stain; (B) toluidine blue; (C) alcian blue; (D) alkaline phosphatase; (E) collagen type X; (F) alizarin red. Insert micrographs show non-specific staining. Scale bars = 100 µm.

### 5.5.2.3 BM-MSC Recellularised Constructs

BM-MSCs were characterised to assess their differentiation multipotentiality before being used for construct recellularisation. Chondrogenic, osteogenic and adipogenic differentiation was achieved from the BM-MSCs derived from rat femurs (Figure 5-44) using well-described, classical differentiation protocols. Once characterised and seeded on to the decellularised constructs, DAPI staining showed that the BM-MSCs were able to attach and penetrate into the decellularised constructs (Figure 5-45).

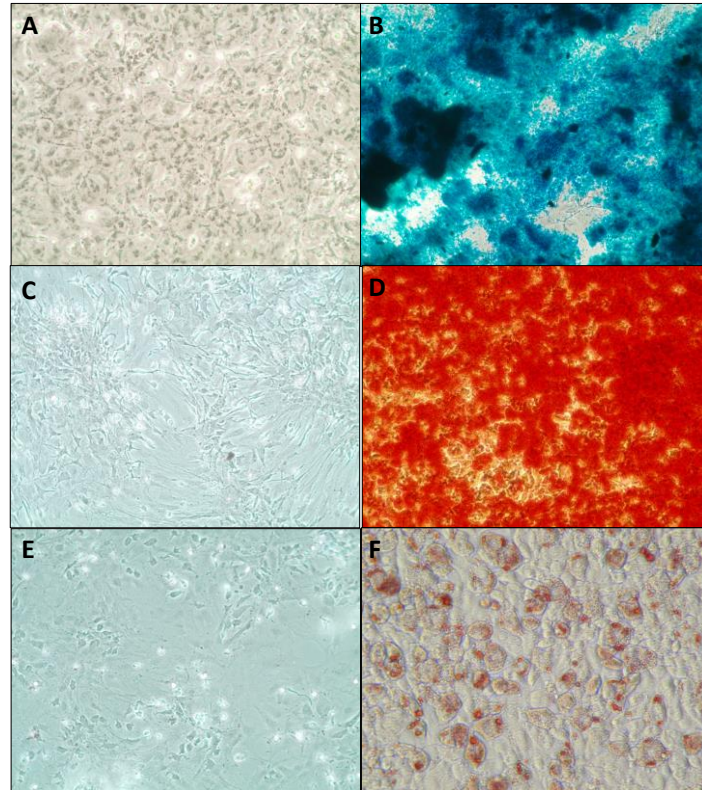


**Figure 5-44:** Staining to show the differentiation capacities of rat BM-MSCs. (B) Alcian blue staining to show proteoglycan-rich extracellular matrix of micromass cultures of MSCs cultured under conditions to induce chondrogenic differentiation (control (A)); (D) Alizarin red staining to show mineralisation in MSCs cultured under conditions to induce osteogenesis (control (C)); (F) oil red O staining of lipid vesicles in MSCs cultured under conditions to induce adipogenic differentiation (control (E)).

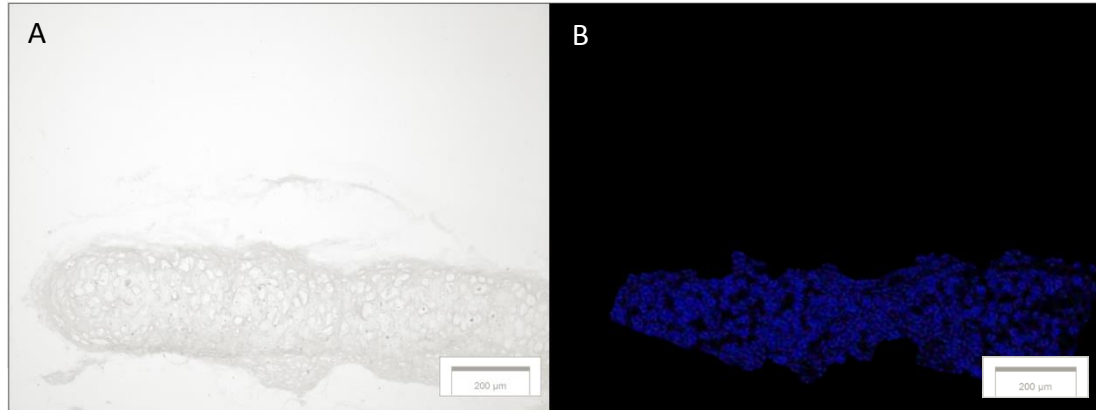


**Figure 5-45:** DAPI staining showing the attachment and penetration of BM-MSCs into the decellularised PGA constructs. (A) brightfield image of the decellularised construct, (B) DAPI image showing the penetration of the BM-MSCs into the

### **5.5.3 Repair of Cranial Defects 4 Weeks after Implantation**

After 4 weeks of implantation, a small amount of bone formation, indicative of defect healing was observed using microCT. Some mineralisation was evident in all defects implanted with constructs with little apparent bone formation in the empty defects (Figure 5-46). Further analysis showed that the average percentage bone volume in the defect treated with the ‘living’ graft, decellularised graft and MSC recellularised graft was 15.15 %, 19.91 % and 14.10 % therefore all grafts showed an increased healing compared to the empty defects where percentage bone volume in these defects was 7.60 % (Figure 5-47). While these increases were not significant it suggested that the grafts may have enhanced better healing (i.e. bone formation) at later time periods.

Histological analysis of the defects showed that vascularisation of both the ‘living’ and decellularised grafts had occurred by week 4. The decellularised graft also shows some bone formation within the defect as highlighted by the arrow (Figure 5-48). The alcian blue staining shows a decrease in ECM, highlighted by a decrease in GAG, around the invading blood vessels (Figure 5-49)

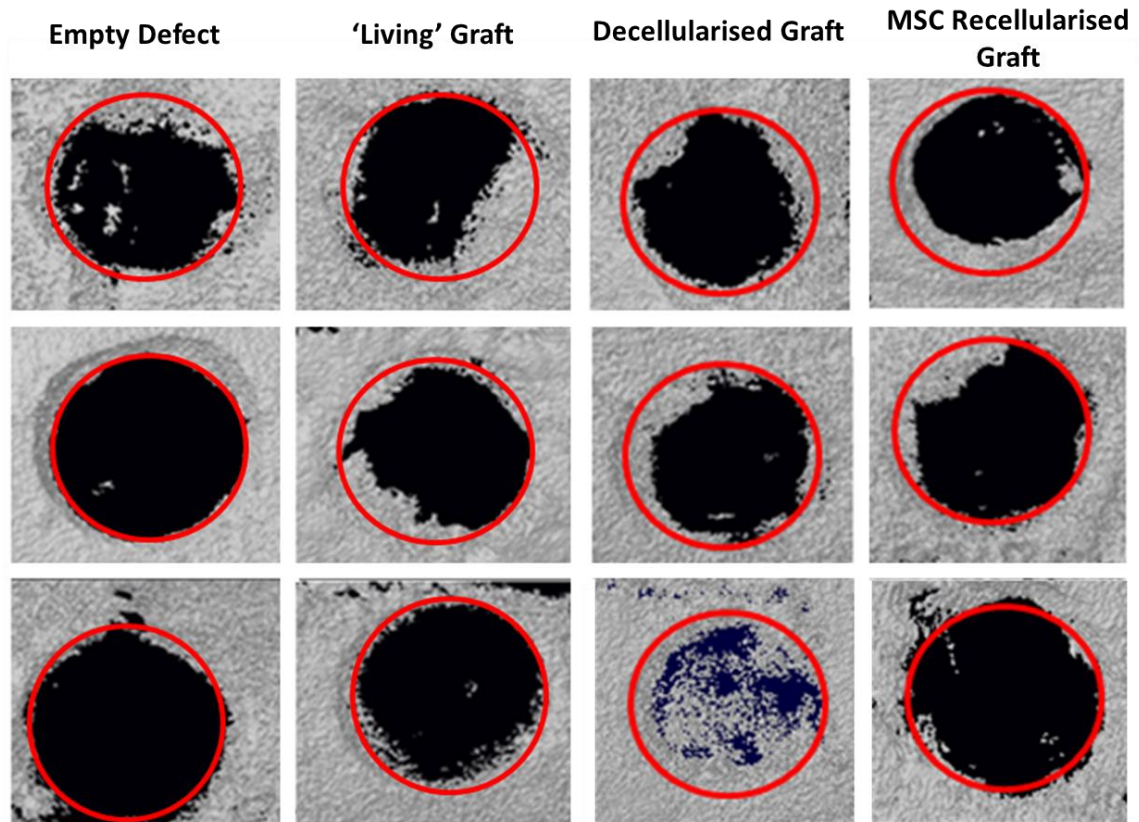


**Figure 5-46:** MicroCT analysis of the cranial bone defects 4 weeks after implantation of either 'living', decellularised and BM-MSC recellularised PGA constructs compared to the control 'empty' defects. (n=3 animals/construct group)

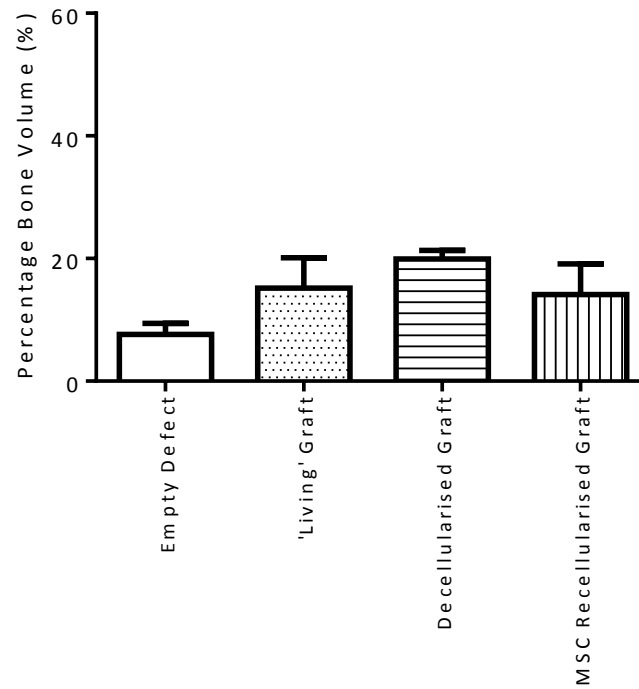


**Figure 5-47:** Percentage bone volume in the empty defect compared to the repair seen using 'living', decellularised and MSC recellularised PGA constructs 4 weeks after implantation ( $n=3$  animals/construct group).

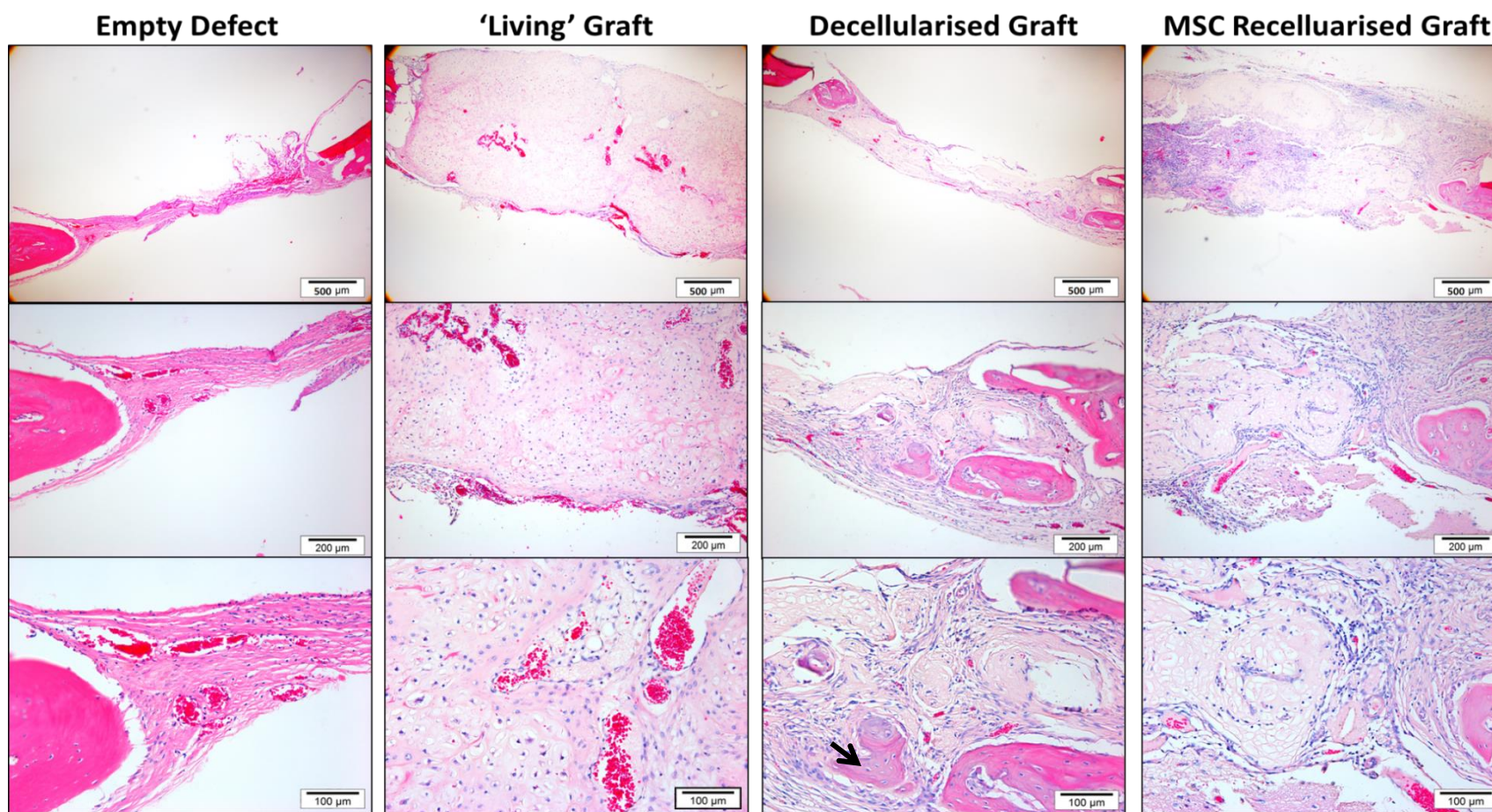


**Figure 5-48:** Haematoxylin and eosin staining of cranial defects 4 weeks after implantation with either a 'living' PGA construct, decellularised PGA construct, decellularised PGA construct re-seeded with BM-MSCs or left unfilled. The arrow highlights the initial bone formation in the decellularised PGA construct. Magnifications are x4 (upper 4 images), x10 (middle 4 images) and x20 (bottom 4 images). Scale bars = 500  $\mu\text{m}$  (upper 4 images), 200  $\mu\text{m}$  (middle 4 images) and 100  $\mu\text{m}$  (bottom 4 images). ( $n=3$  animals/construct group)

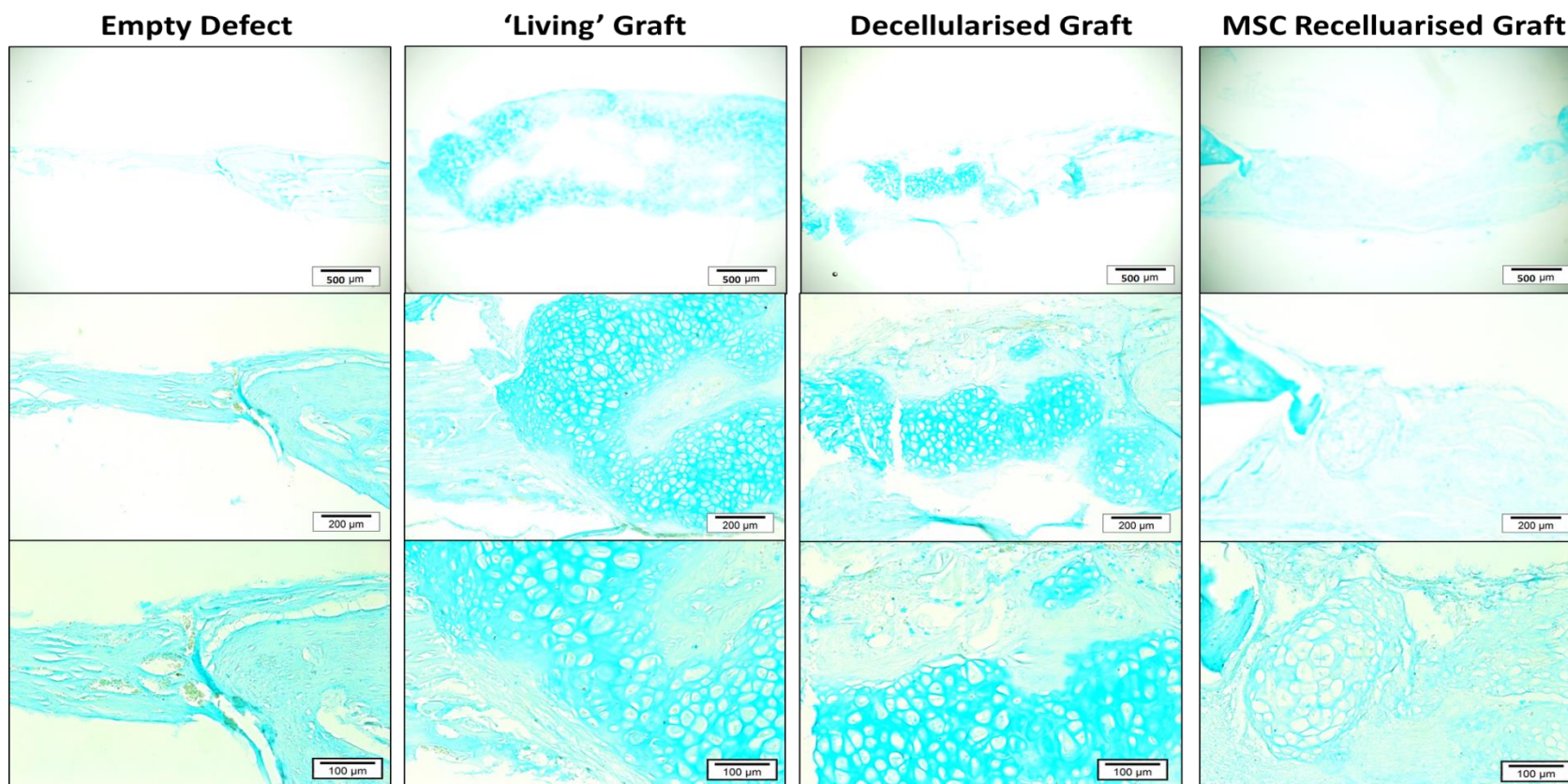


**Figure 5-49:** Alcian blue staining of cranial defects to show localisation of the glycosaminoglycans in the defects. 4 weeks after implantation with either a 'living' PGA construct, decellularised PGA construct, decellularised PGA construct re-seeded with BM-MSCs or left unfilled. Magnifications are x4 (upper 4 images), x10 (middle 4 images) and x20 (bottom 4 images). Scale bars = 500  $\mu\text{m}$  (upper 4 images), 200  $\mu\text{m}$  (middle 4 images) and 100  $\mu\text{m}$  (bottom 4 images). ( $n=3$  animals/construct group)



#### **5.5.4 Repair of Cranial Defects 8 Weeks after Implantation**

After 8 weeks of implantation, two of the 'living' constructs visibly showed the ability to significantly heal the defects (i.e. stimulate bone formation) when compared to the empty defects (Figure 5-50). The average percentage bone volume was significantly higher when a 'living' construct (22.94 %) was implanted compared to an average healing in the empty defect (7.07 %) (Figure 5-55). The decellularised constructs also gave a significant increase in bone healing both visually by microCT (Figure 5-50) and through percentage bone volume analysis (Figure 5-51) where a 30.73 % bone healing was observed. Bone regeneration using the decellularised constructs was greater than that of the 'living' constructs. However, this increase was not significant. A smaller increase in bone formation was observed with the BM-MSc recellularised constructs (Figure 5-50). However, the average percentage increase in bone volume of 18.29 % was not found to be significantly different when compared to that of the empty defect (Figure 5-51).

Histological analysis of the defects showed that bone regeneration was occurring throughout both the 'living' and decellularised grafts. The BM-MSc recellularised construct, however, did not show signs of being remodelled into bone (Figure 5-52). Alcian blue staining of the defects showed a decrease in ECM in both the 'living' and BM-MSc recellularised constructs as the Hypertrophic cartilage ECM is degraded, as represented by low intensity staining indicating a decrease in GAG (Figure 5-53).

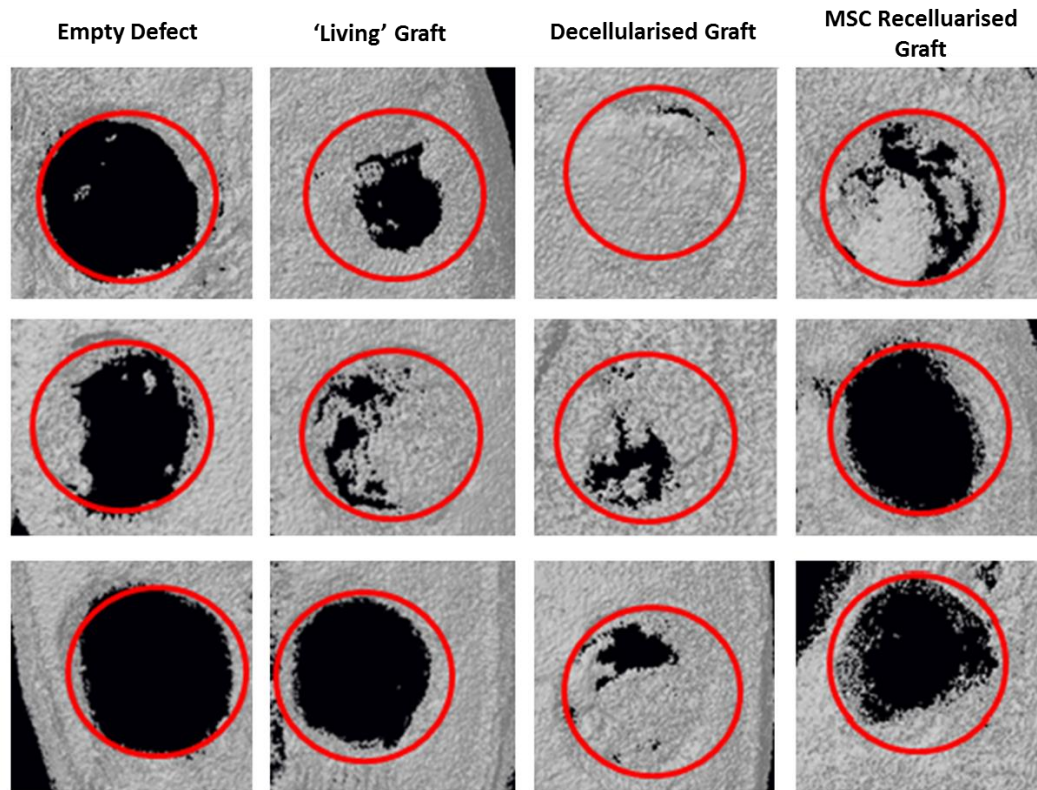


**Figure 5-50:** MicroCT analysis of cranial defects after 8 weeks of implantation of either 'living', decellularised or BM-MSC recellularised hypertrophic constructs cultured on PGA compared to the empty (control) defects. (n=3 animals/construct group)

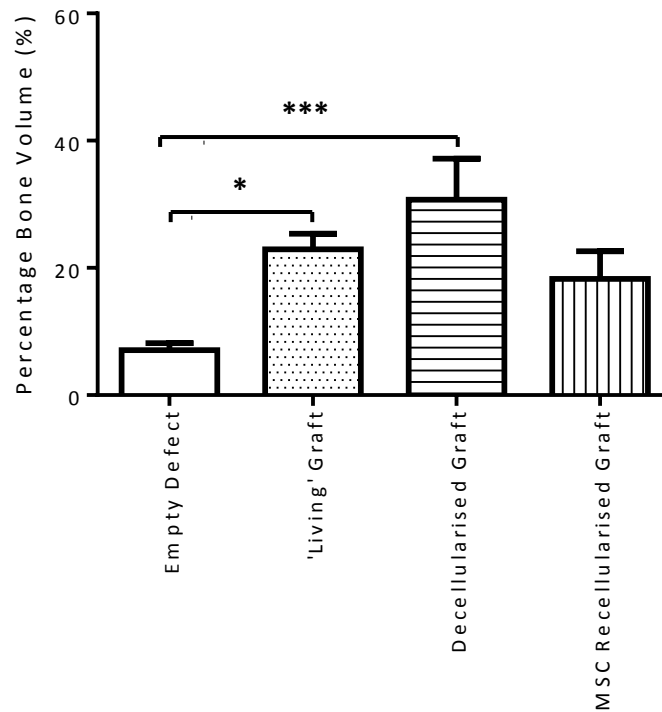


**Figure 5-51:** Percentage bone volume in the empty defect compared to the repair seen using 'living', decellularised and BM-MSC recellularised hypertrophic constructs cultured on PGA 8 weeks after implantation. (\*  $p < 0.05$ , \*\*  $p < 0.01$ .  $n = 3$  animals/construct group)

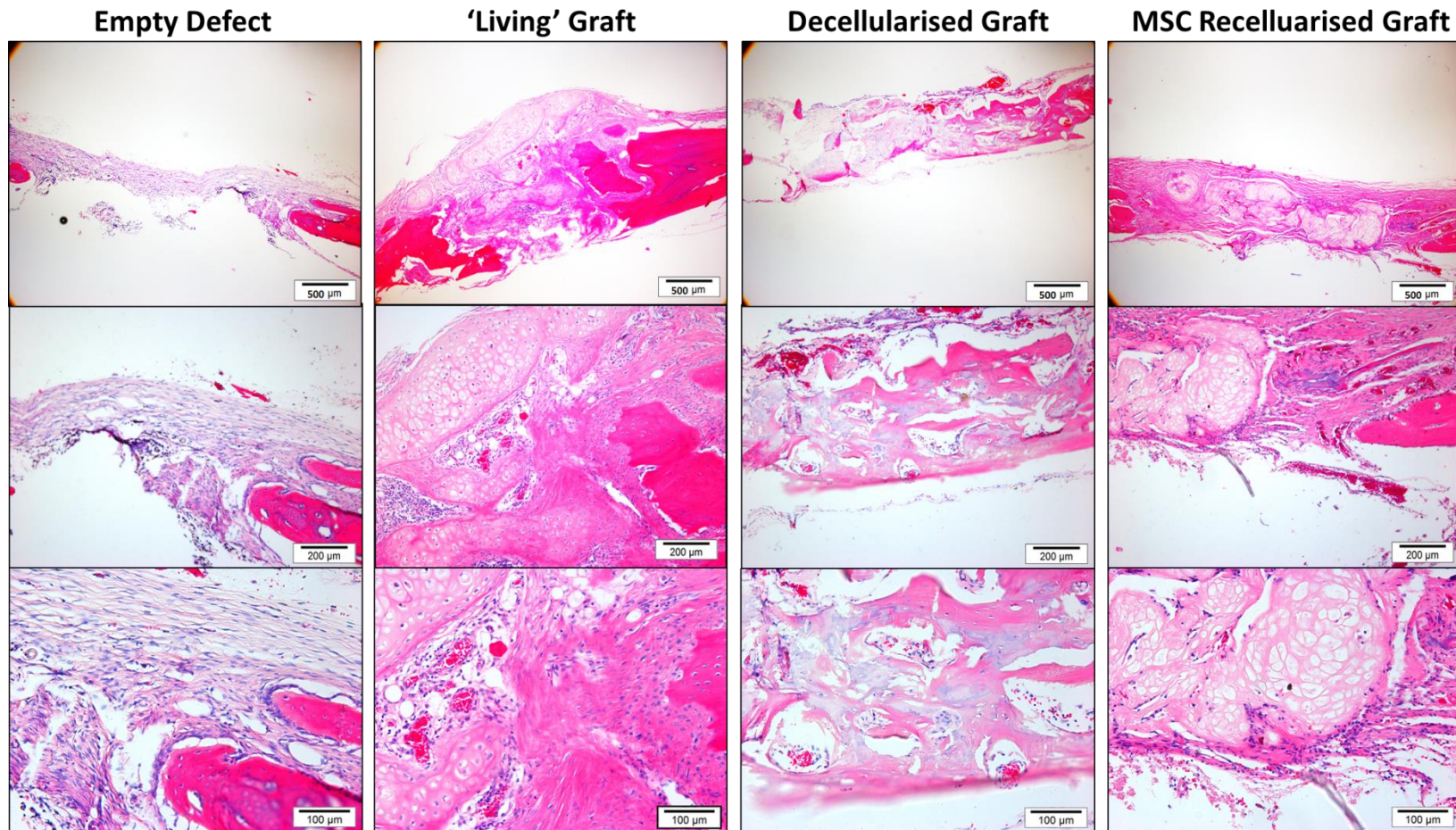


**Figure 5-52:** Haematoxylin and eosin staining of defects 8 weeks after implantation with either a 'living' PGA construct, decellularised PGA construct, decellularised PGA construct re-seeded with BM-MSCs or left unfilled. Magnifications are x4 (upper 4 images), x10 (middle 4 images) and x20 (bottom 4 images). Scale bars = 500 µm (upper 4 images), 200 µm (middle 4 images) and 100 µm (bottom 4 images). (*n=3 animals/construct group*)

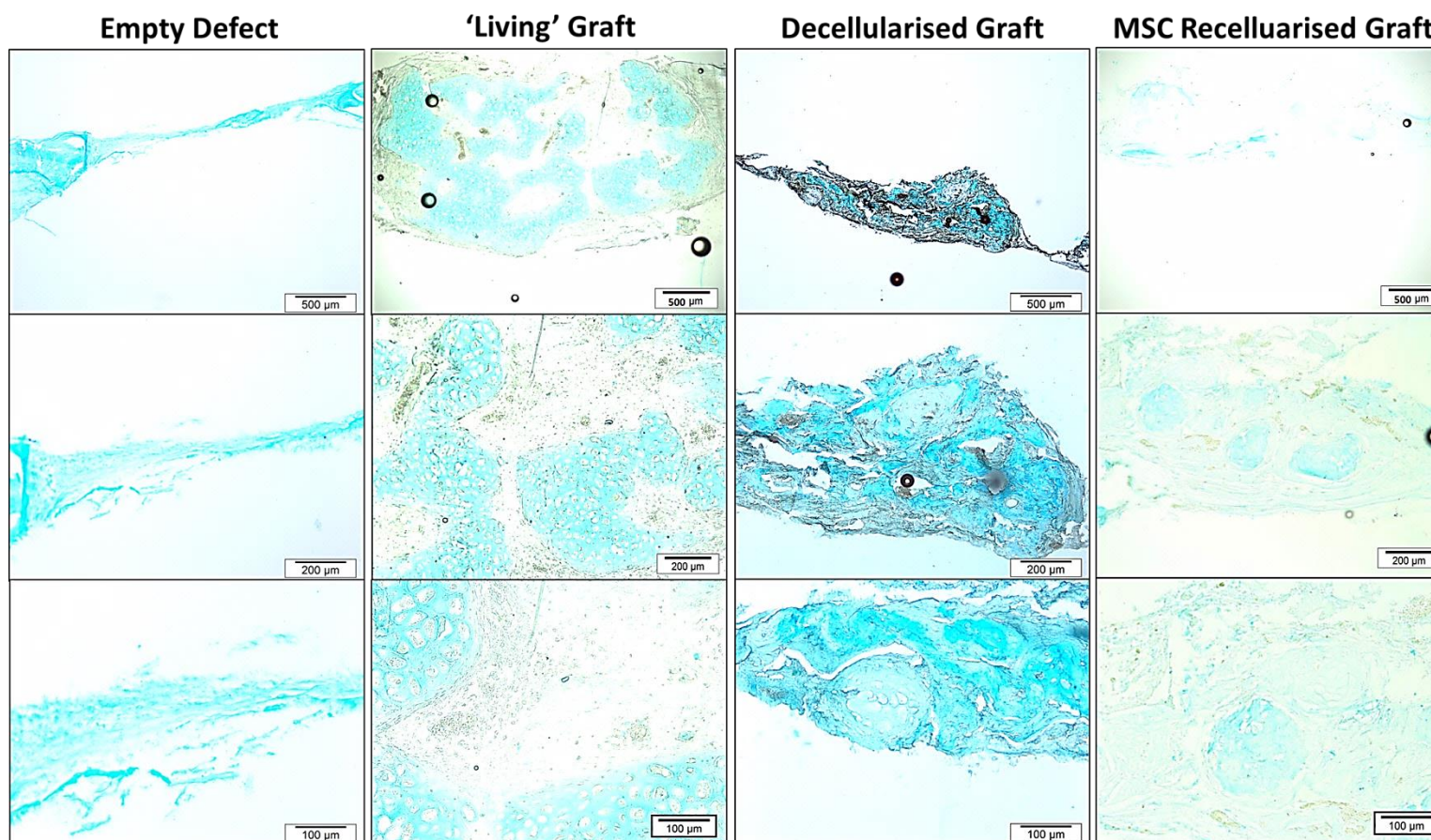
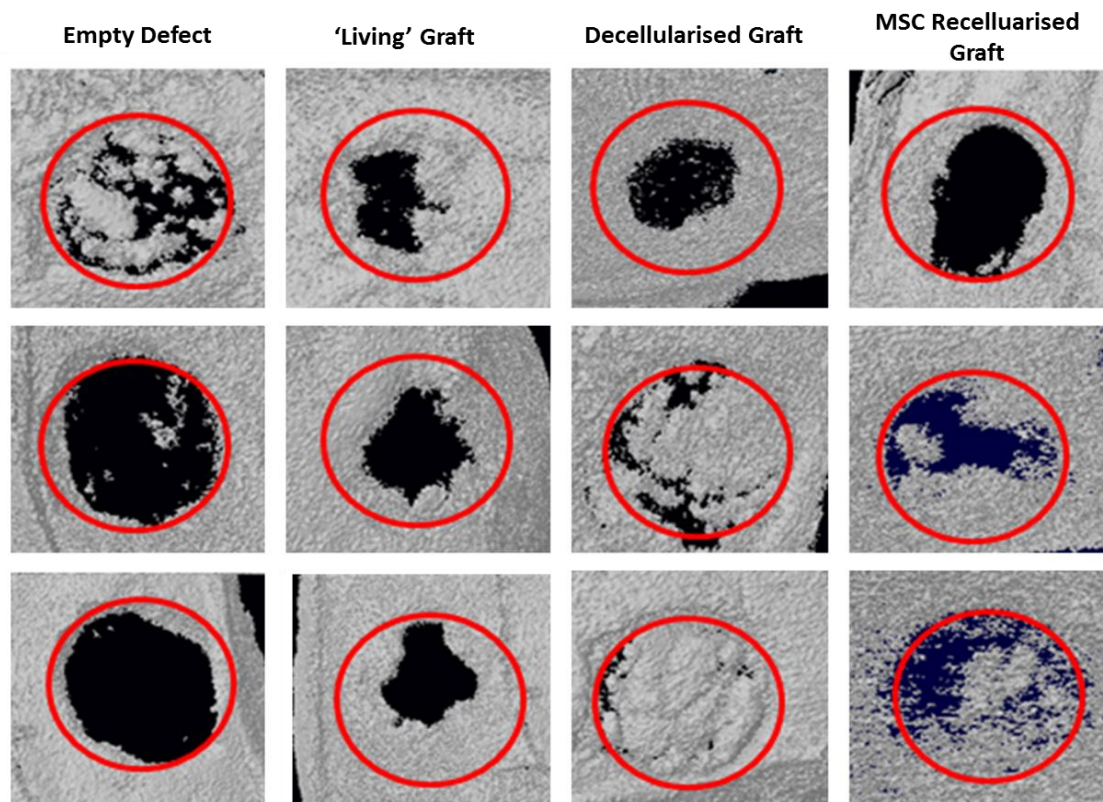


Figure 5-53: : Alcian blue staining of cranial defects to show localisation of the glycosaminoglycans 8 weeks after implantation with either a 'living' PGA construct, decellularised PGA construct, decellularised PGA construct re-seeded with BM-MSCs or left unfilled. Magnifications are x4 (upper 4 images), x10 (middle 4 images) and x20 (bottom 4 images). Scale bars = 500 µm (upper 4 images), 200 µm (middle 4 images) and 100 µm (bottom 4 images). ( $n=3$  animals/construct group)

### 5.5.5 Repair of Cranial Defects 12 Weeks after Implantation

Visual assessment of microCT images showed a higher degree of bone healing with all construct types compared to that of the empty defect (Figure 5-54). Significant increases in percentage bone volume were observed when using both 'living' grafts (38.48 %) and decellularised grafts (38.59 %) when compared to the empty graft (7.56 %) (Figure 5-55). There was no significant difference in bone formation between the 'living' and decellularised constructs. BM- MSC recellularised constructs showed a percentage bone volume of 21.22 % which was not significant when compared to the empty defects (Figure 5-55).



**Figure 5-54:** MicroCT images of the cranial defects after 12 weeks of implantation of either 'living', decellularised or BM-MSC recellularised hypertrophic constructs cultured on PGA compared to the empty (control) defects. (n=3 animals/construct group)

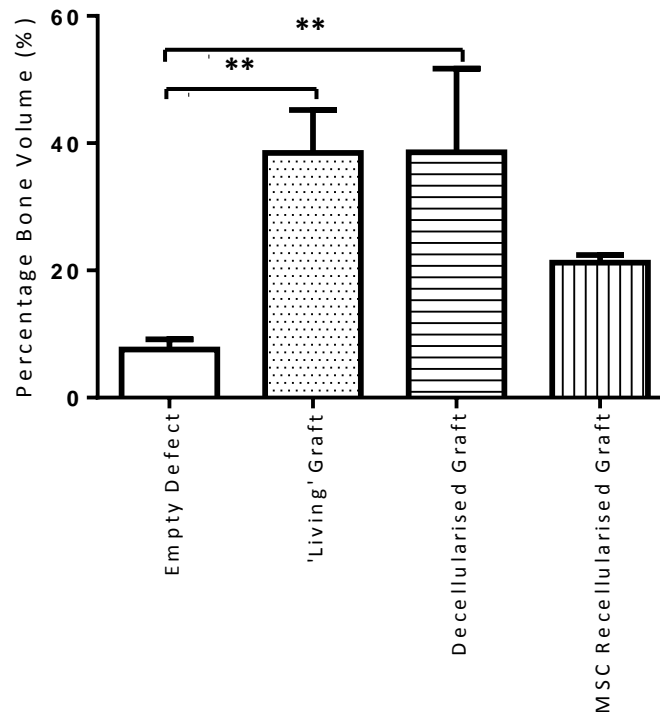


**Figure 5-55:** Percentage bone volume in the empty defect compared to the repair seen using 'living', decellularised and MSC recellularised hypertrophic constructs cultured on PGA after 12 weeks after implantation. (\*\*  $p < 0.01$ .  $n = 3$  animals/construct group).

Histological analysis of the defects showed continued bone regeneration in the 'living' and decellularised grafts, however, at week 12 there is also some evidence of bone regeneration in the BM-MSC recellularised graft (Figure 5-56). More intense alcian blue staining is observed in the areas of new bone regeneration (Figure 5-57).

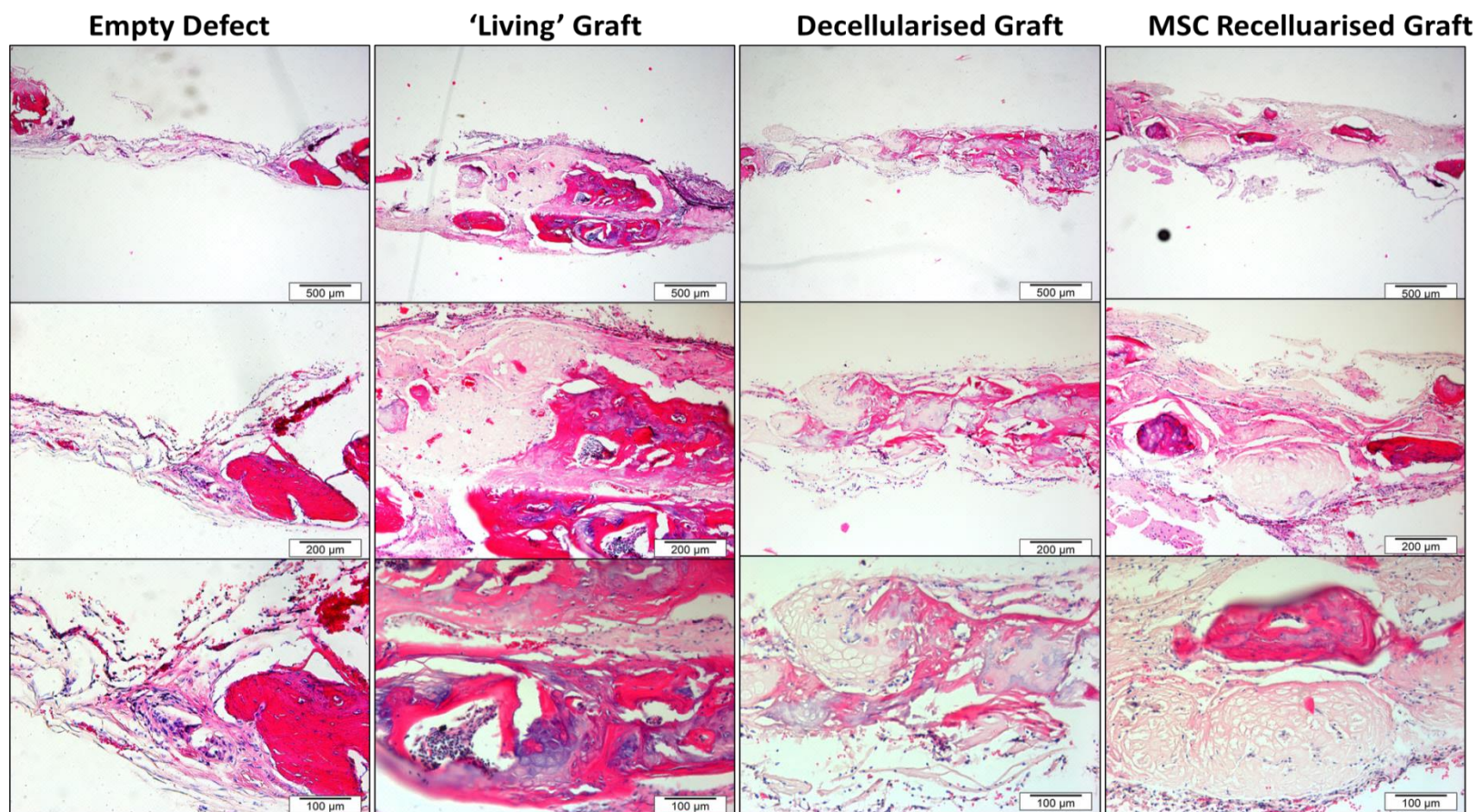


**Figure 5-56:** Haematoxylin and eosin staining of cranial defects 12 weeks after implantation with either a 'living' PGA construct, decellularised PGA construct, decellularised PGA construct re-seeded with BM-MSCs or left unfilled. Magnifications are x4 (upper 4 images), x10 (middle 4 images) and x20 (bottom 4 images). Scale bars = 500 µm (upper 4 images), 200 µm (middle 4 images) and 100 µm (bottom 4 images). (*n=3 animals/construct group*)



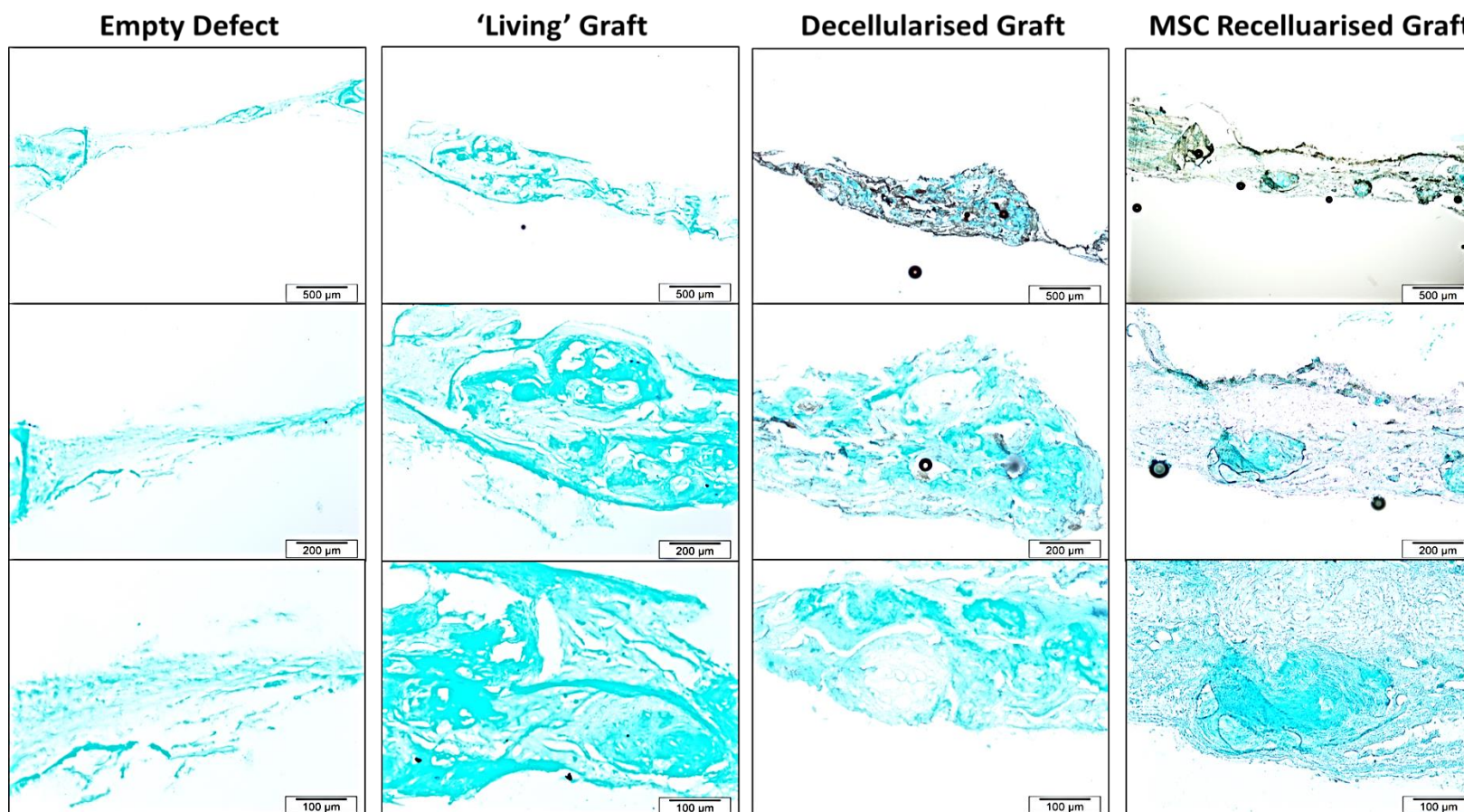


**Figure 5-57:** Alcian blue staining of cranial defects 12 weeks after implantation to show localisation of the glycosaminoglycans 12 weeks after implantation with either a 'living' PGA construct, decellularised PGA construct, decellularised PGA construct re-seeded with BM-MSCs or left unfilled. Magnifications are x4 (upper 4 images), x10 (middle 4 images) and x20 (bottom 4 images). Scale bars = 500 µm (upper 4 images), 200 µm (middle 4 images) and 100 µm (bottom 4 images). (*n=3 animals/construct group*)

### 5.5.6 Healing Over a 12 Week Period

'Living' and decellularised constructs were shown to significantly increase the percentage bone volume within the cranial defect over the 12 week implantation (Figure 5-58 and Figure 5-59 respectively). While an increase in percentage bone volume was observed when using a BM-MSC recellularised construct this increase was not significant over the 12 week implantation period (Figure 5-60).

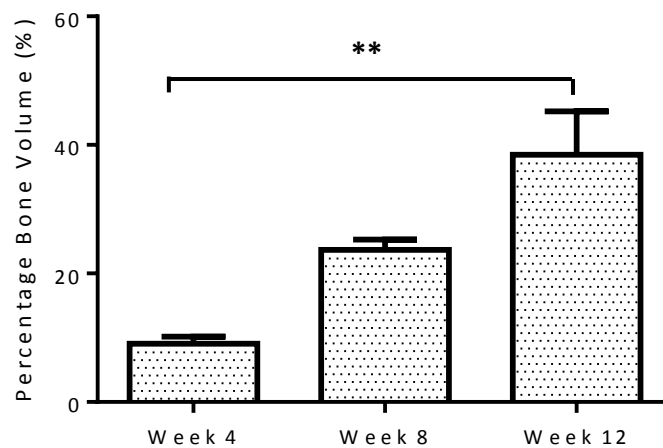


**Figure 5-58:** Increase in the percentage bone volume in cranial defects implanted with a 'living' hypertrophic construct cultured on PGA over a 12 week period following implantation ( $p^{**}<0.01$ .  $n=3$  animals/time point)

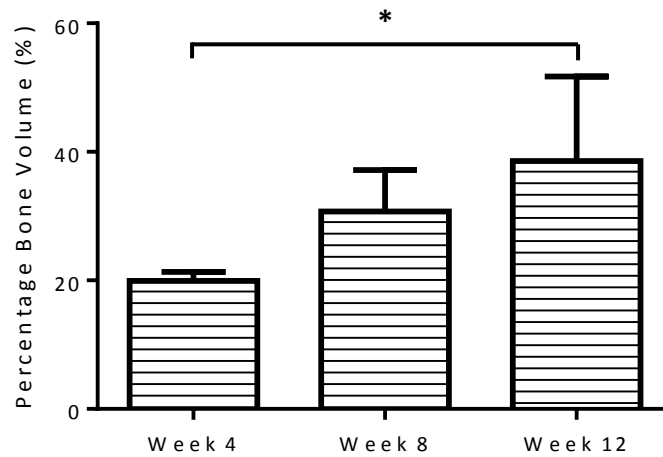


**Figure 5-59:** Increase in the percentage bone volume in cranial defects implanted with a decellularised hypertrophic construct cultured on PGA over a 12 week period following implantation ( $p < 0.05$ ,  $n=3$  animals/time point).

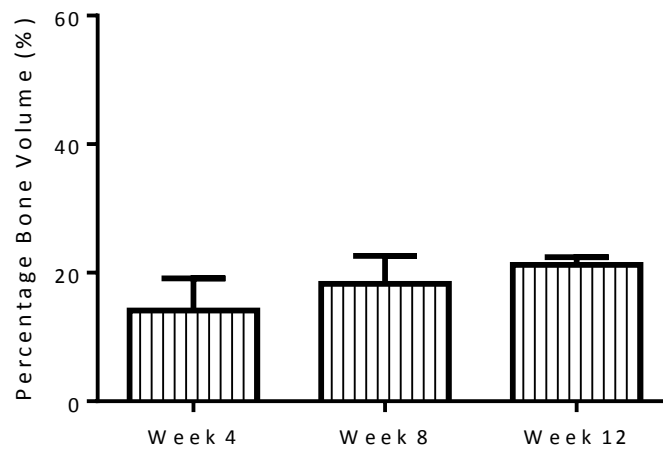


**Figure 5-60:** Increase in the percentage bone volume increase in cranial defects implanted with BM-MSc recellularised hypertrophic construct cultured on PGA over a 12 week period following implantation ( $n=3$  animals/time point).

## **5.6 The Effect of Bioreactor Culture on Hypertrophic Differentiation**

The amount of GAG accumulation by the PLLA/calcium phosphate constructs varied significantly depending on the culture conditions utilised (Figure 5-61). A significant increase in the GAG accumulation in the ECM was observed by day 28 when the constructs were cultured utilising semi-static culture conditions compared to constructs cultured under static conditions. The accumulation of GAG into the ECM was the greatest at all time points when the constructs were cultured in the perfusion bioreactor compared to the semi-static or static conditions (Figure 5-61). The constructs incubated in the bioreactor contained 49.81 % GAG within their ECM compared to GAG levels of 14.10 % in the ECM of constructs cultured under semi-static conditions and 1.54 % in the ECM of constructs cultured under static conditions.

Histological and immunohistochemical analysis illustrated a lack of hypertrophic differentiation in constructs cultured under static conditions. This was indicated by the absence of collagen type X and alkaline phosphatase expression in the constructs. Alcian blue and toluidine blue staining (indicative of proteoglycan formation) was present but at a low intensity. Collagen type II expression was also conserved under static conditions (Figure 5-62). However, both the semi-static and bioreactor conditions enabled full hypertrophic differentiation of the chondrocytes after 42 days of culture. This was confirmed by the chondrocytes developing a larger cell morphology, typical of hypertrophic chondrocytes, and expressing collagen type X and alkaline phosphatase (Figure 5-62).

Analysing the constructs for mRNA expression showed that all of the culture conditions resulted in downregulation of collagen type II and by day 42 there was no significant difference in the collagen type II gene expression between the culture conditions (Figure 5-64). Collagen type X and alkaline phosphatase gene expression was not significantly upregulated during static culture and the expression of these proteins remained at a low level (Figure 5-65 and Figure 5-66 respectively). The low level of

collagen type X and alkaline phosphatase gene expression corresponded to the low levels of hypertrophic differentiation seen in the constructs incubated under static conditions (Figure 5-62). The semi-static conditions and the bioreactor gave constructs similar levels of collagen type X upregulation throughout the 42 day culture period (Figure 5-65). However the use of the semi-static conditions resulted in higher gene expression for alkaline phosphatase and denser staining for the enzyme in the constructs compared to constructs incubated in the bioreactor (Figure 5-66 and Figure 5-62 respectively).

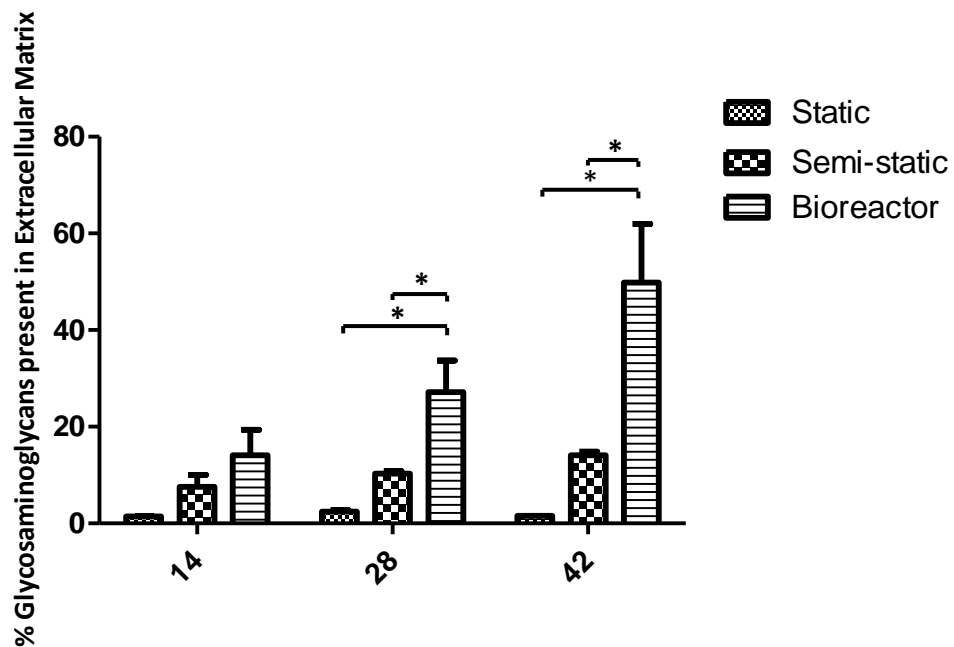


**Figure 5-61:** Percentage GAG accumulation within the ECM of hypertrophic constructs cultured on the PLLA/calcium phosphate scaffold material at day 14, 28 and 42 under static, semi-static and bioreactor culture conditions. (\*  $p < 0.05$ .  $n = 6$ )

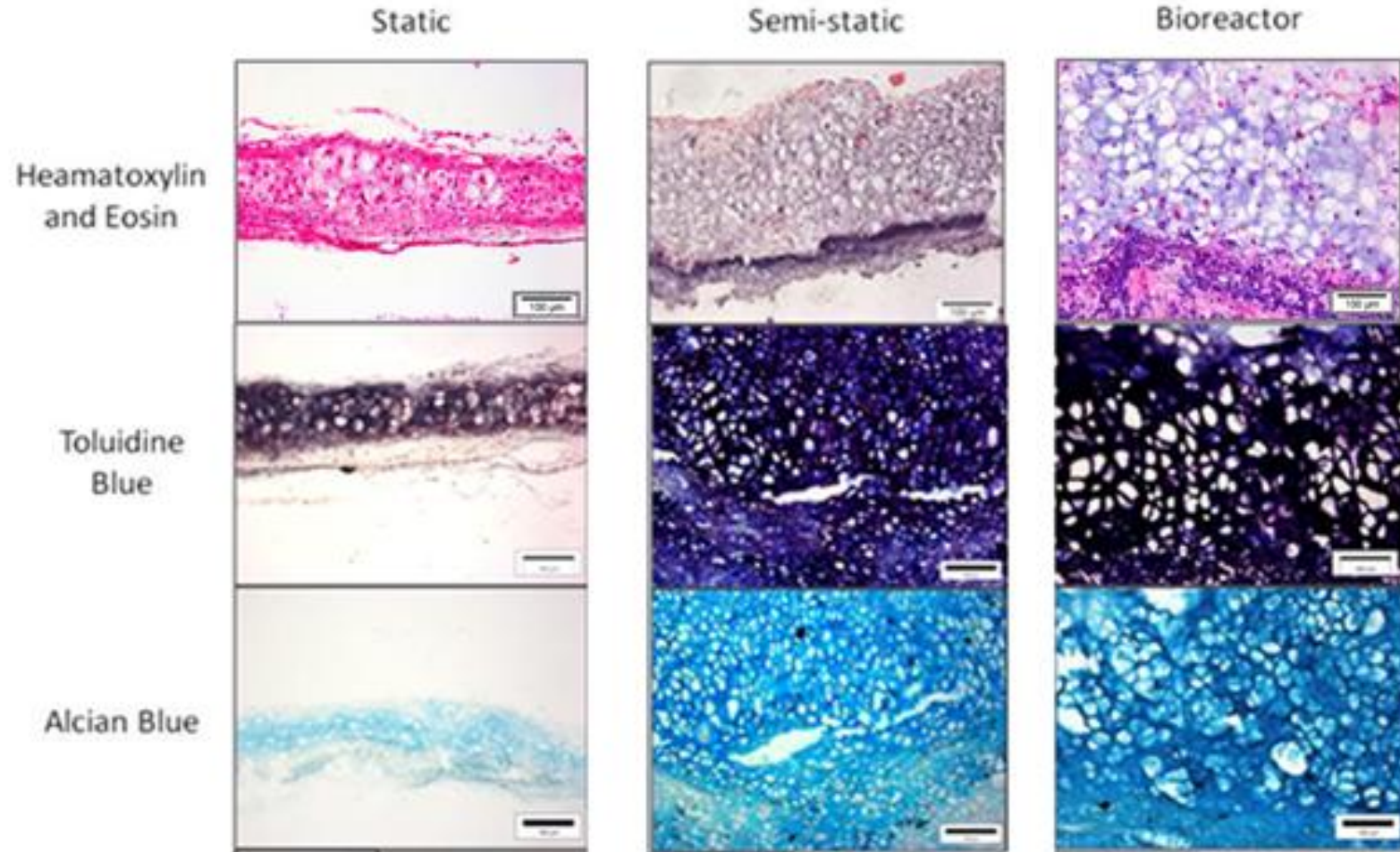


**Figure 5-62:** Histological analysis of PLLA/calcium phosphate constructs cultured under static, semi-static and bioreactor culture conditions. Insert micrographs show non-specific staining. Scale bars = 100 μm. (representative images n=6)

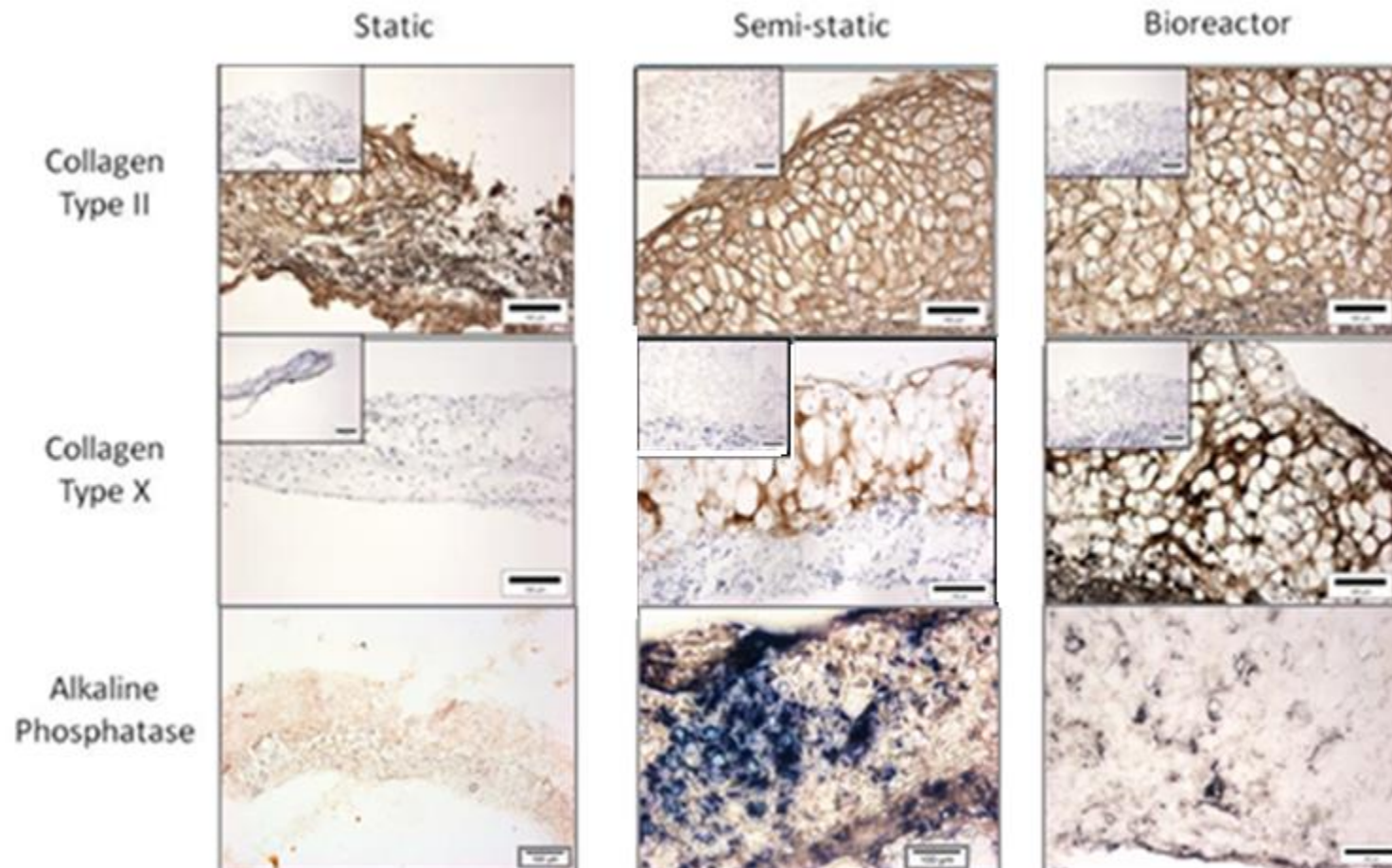


**Figure 5-63:** Immunohistochemical analysis of PLLA/calcium phosphate constructs cultured under static, semi-static and bioreactor culture conditions. Insert micrographs show non-specific staining. Scale bars = 100 $\mu$ m. (representative images n=6)

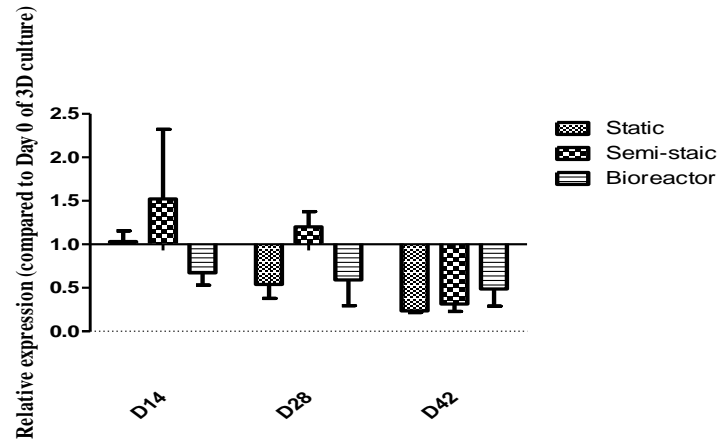


**Figure 5-64:** Comparison of the effect of static, semi-static and bioreactor culture conditions on collagen type II mRNA expression during a 42 day incubation period. The data is normalised to the gene expression observed after 72 hours on culture in expansion media on the PLLA/calcium phosphate scaffold materials (D0 of 3D chondrocyte differentiation). (n=6).

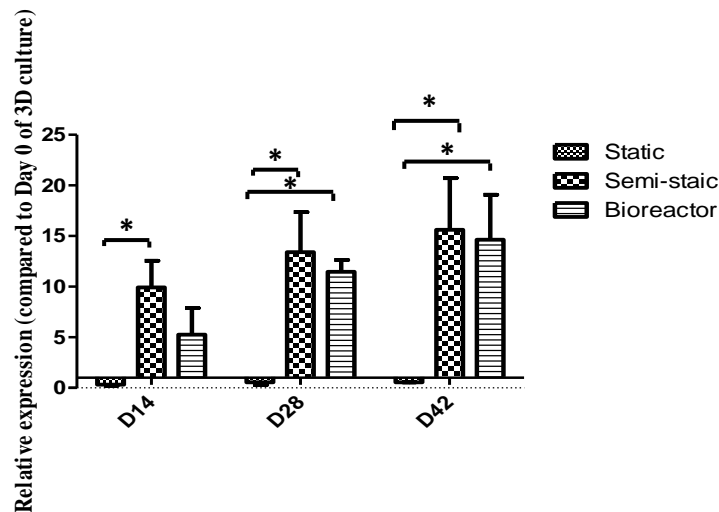


**Figure 5-65:** Comparison of the effect of static, semi-static and bioreactor culture conditions on collagen type X mRNA expression during a 42 day incubation. The data is normalised to the gene expression observed after 72 hours on culture in expansion media on the PLLA/calcium phosphate scaffold materials (D0 of 3D chondrocyte differentiation). (\* p < 0.05. n = 6)



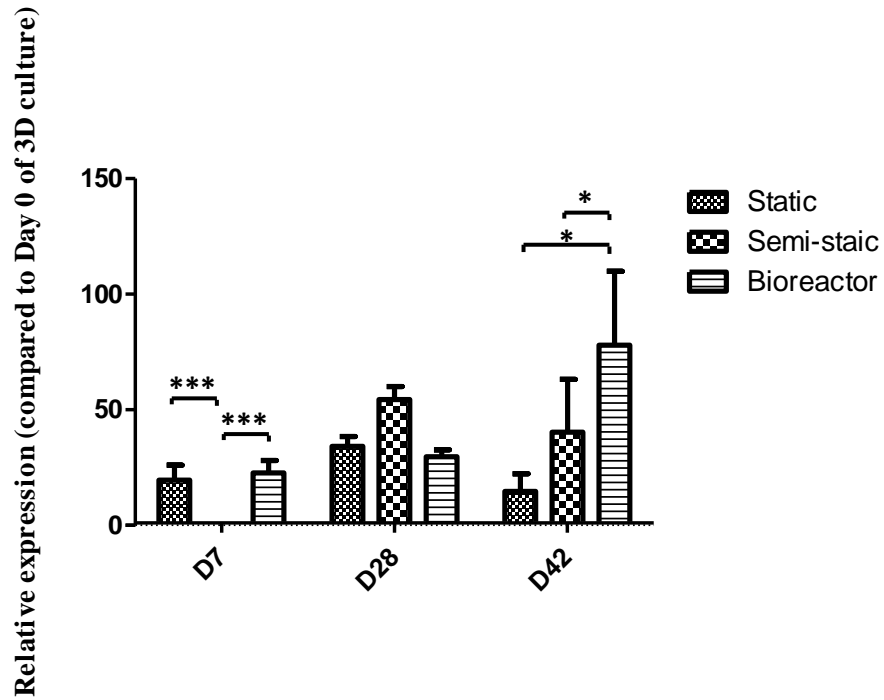


**Figure 5-66:** Comparison of the effect of static, semi-static and bioreactor culture conditions on alkaline phosphatase mRNA expression during a 42 day differentiation period. The data is normalised to the gene expression observed after 72 hours on culture in expansion media on the PLLA/calcium phosphate scaffold materials (D0 of 3D chondrocyte differentiation. (\*  $p < 0.05$ , \*\*\*  $p < 0.005$ .  $n=6$ ).

## 5.7 Serum-Free media

Three serum-free media (Table 5-3) were assessed for their ability to not only support chondrocyte growth and survival but also to support hypertrophic differentiation.

**Table 5-3:** Composition of the three serum-free media and serum-containing media tested for chondrocyte survival, growth and hypertrophic differentiation.

	Media composition
Media 1	Basic media with 1 mg.mL <sup>-1</sup> BSA, 1 µg.mL <sup>-1</sup> insulin and 50 µg.mL <sup>-1</sup> ascorbic acid
Media 2	Basic media with 1 mg.mL <sup>-1</sup> BSA, 100 µL.mL <sup>-1</sup> 10X ITS (1.0 mg.mL <sup>-1</sup> recombinant human insulin, 0.55 mg.mL <sup>-1</sup> human transferrin (substantially iron-free), 0.5 µg.mL <sup>-1</sup> sodium selenite, 470 µg.mL <sup>-1</sup> linoleic acid, 470 µg.mL oleic acid and 50 mg.mL <sup>-1</sup> bovine FCS albumin) and 50 µg.mL <sup>-1</sup> ascorbic acid
Media 3	Basic media with 1 mg.mL <sup>-1</sup> BSA, 100 µL.mL <sup>-1</sup> 10X ITS (1.0 mg.mL <sup>-1</sup> recombinant human insulin, 0.55 mg.mL <sup>-1</sup> human transferrin (substantially iron-free), 0.5 µg.mL <sup>-1</sup> sodium selenite, 470 µg.mL <sup>-1</sup> linoleic acid, 470 µg.mL <sup>-1</sup> oleic acid and 50 mg.mL <sup>-1</sup> bovine FCS albumin), 50 µg.mL <sup>-1</sup> ascorbic acid and 1 nM thyroxine
Serum-containing media	Basic media with 10% FCS, 1 µg.mL <sup>-1</sup> insulin and 50 µg.mL <sup>-1</sup> ascorbic acid

Serum-free media 1 was shown to produce constructs with a significantly lower GAG content (1.94 % of ECM dry weight) than constructs cultured in serum-free media 2 (15.94 % of ECM dry weight), serum-free media 3 (19.44 % of ECM dry weight) and serum-containing media used in previous experiments (12.91 % of ECM dry weight)

(Section 5.3) (Figure 5-67). No significant difference was seen between serum-free media 2 and 3 and the serum-containing media (Figure 5-67).

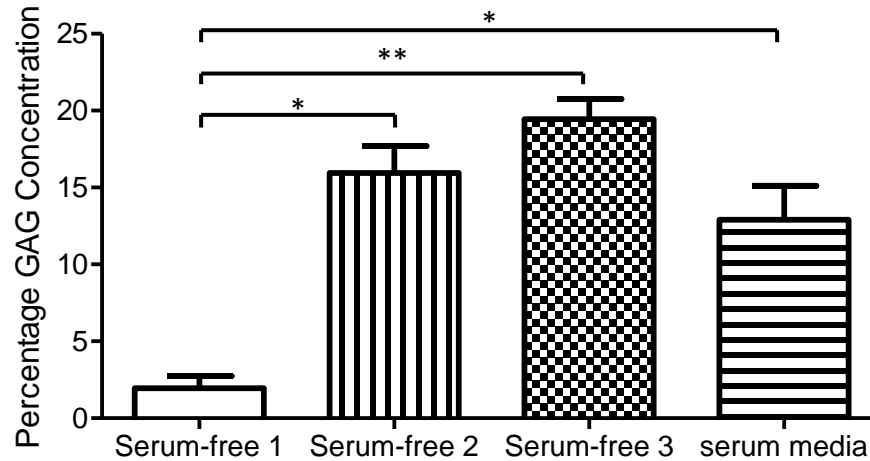


**Figure 5-67:** The percentage GAG concentration present in the PGA constructs cultured in three serum-free media compared to the serum-containing media. (\*  $p < 0.05$ , \*\*  $p < 0.01$ .  $n = 9$ )

Serum-free media 1 produced grafts with a low level toluidine blue (Figure 5-68(B)) and alcian blue (Figure 5-68(C)) confirming that the quality of the ECM was poor with a low GAG concentration. Chondrocytes with a large cellular morphology can be seen in within the constructs (Figure 5-68(A)). However, chondrocytes in these constructs did not produce alkaline phosphatase (Figure 5-68(D)) or collagen type X (Figure 5-68(F)).

Serum-free media 2 was shown to produce chondrocytes with a large cellular morphology (Figure 5-69(A)) and good quality ECM with dense staining for toluidine blue (Figure 5-69(B)) and alcian blue (Figure 5-69(C)). The grafts were also shown to express collagen type X (Figure 5-69(F)) and alkaline phosphatase (Figure 5-69(D)) showing that cell proliferation and hypertrophic differentiation were supported by serum-free media 2.

This level of hypertrophic differentiation and chondrocyte proliferation was also supported by serum-free media 3 (Figure 5-70). However staining for alkaline

phosphatase was more intense when using this media 3 compared to serum-free media 2 (Figure 5-70(D)).

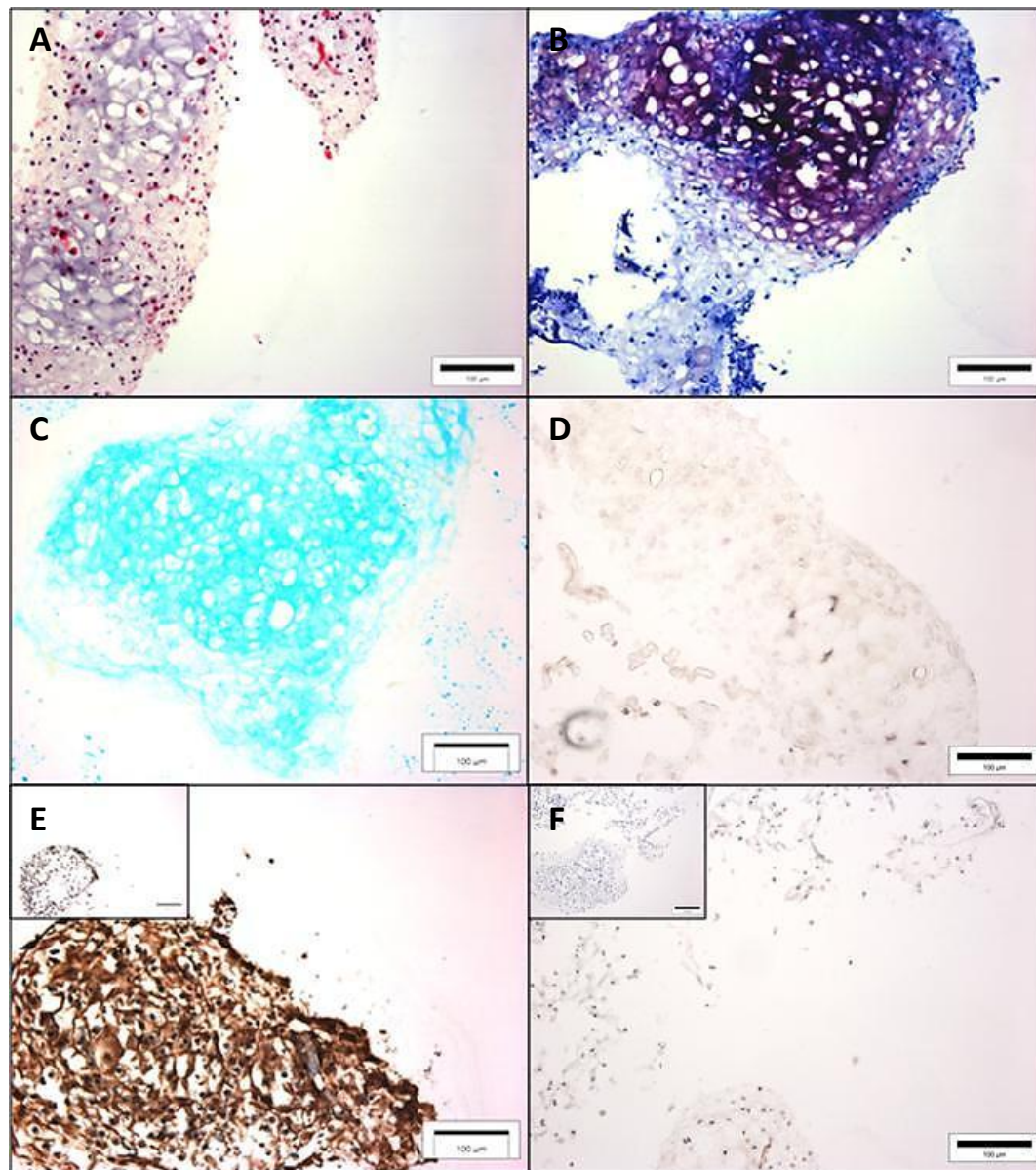


**Figure 5-68:** Representative histological and immunohistochemical analysis of rat nasal chondrocyte constructs after 42 days culture on PGA in serum-free media 1. (A) Haematoxylin and Eosin Stain; (B) Toluidine Blue; (C) Alcian Blue; (D) Alkaline Phosphatase; (E) Collagen II; (F) Collagen X. Insert micrographs show non-specific staining. Scale bars =100 µm. (Representative images n=9)

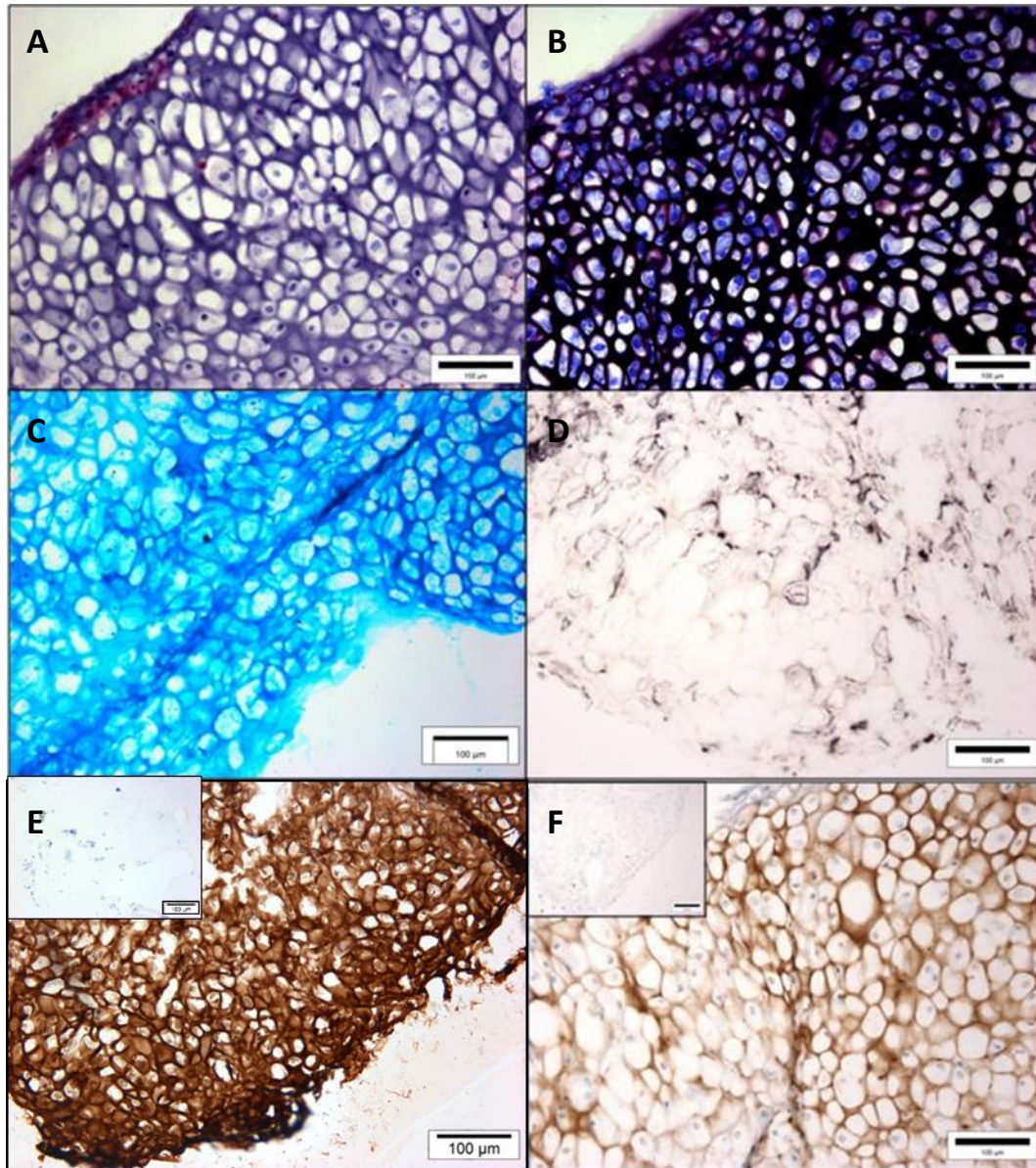


**Figure 5-69:** Representative histological and immunohistochemical analysis of rat nasal chondrocyte constructs after 42 days culture on PGA in serum-free media 2. (A) Haematoxylin and Eosin Stain; (B) Toluidine Blue; (C) Alcian Blue; (D) Alkaline Phosphatase; (E) Collagen II; (F) Collagen X. Insert micrographs show non-specific staining. Scale bars =100  $\mu\text{m}$ . (representative images n=9)

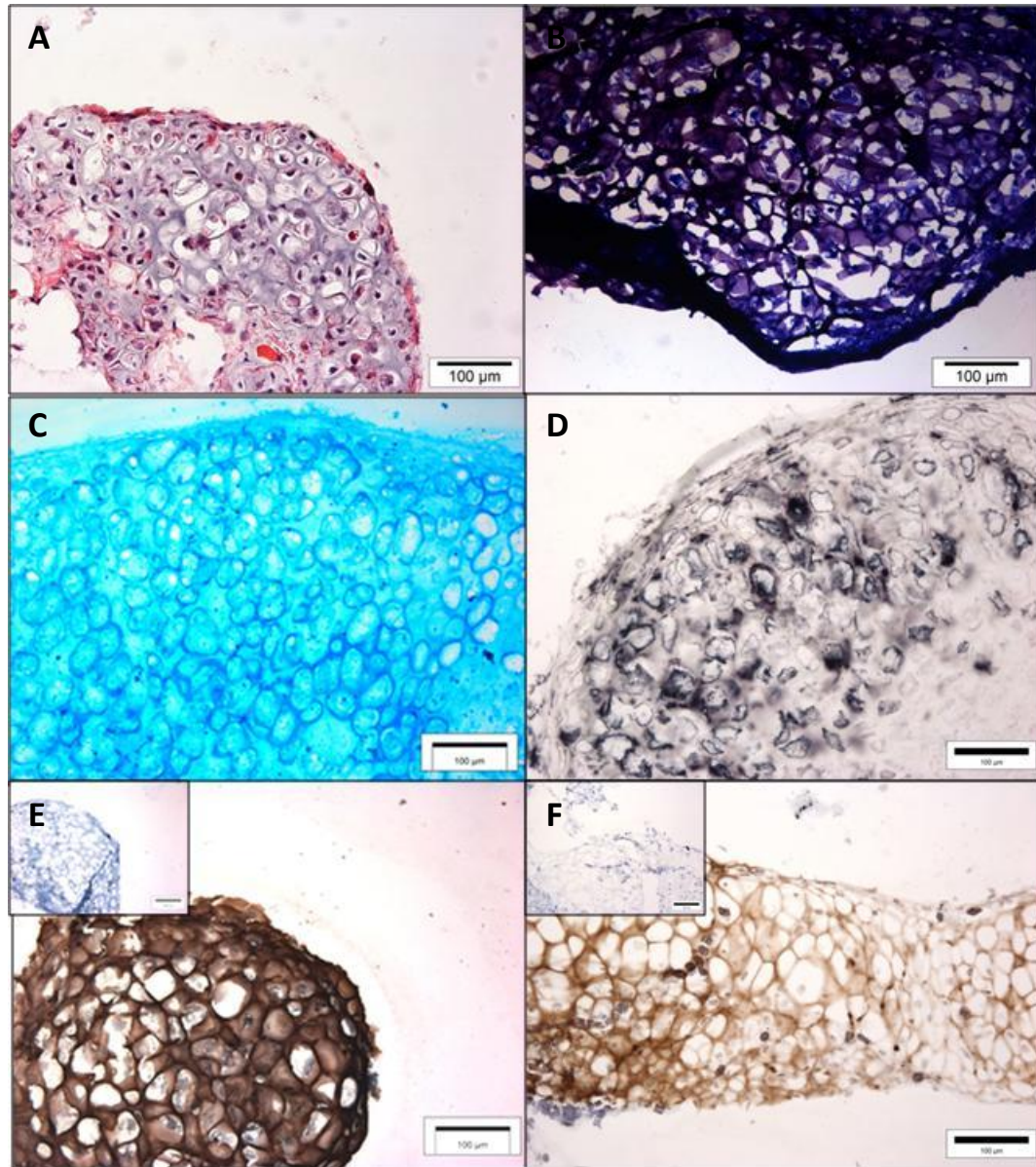


**Figure 5-70:** Representative histological and immunohistochemical analysis of rat nasal chondrocyte constructs after 42 days culture on PGA in serum-free media 3. (A) Haematoxylin and Eosin Stain; (B) Toluidine Blue; (C) Alcian Blue; (D) Alkaline Phosphatase; (E) Collagen II; (F) Collagen X. Insert micrographs show non-specific staining. Scale bars =100 µm. (Representative images n=9)

Gene expression analysis illustrated that serum-free media 2 caused the downregulation of collagen type II however that serum media allows for a significantly higher decrease in expression at day 42. Collagen type X expression was significantly increased at day 42 however this increase occurred at a later stage of culture. Alkaline phosphatase levels were comparable to those seen when using the serum media.

Media 3 also allowed for the downregulation of collagen type II although once again at a significantly lower level than the serum media. Collagen type X significantly higher at d 28 but comparable at day 42. Alkaline phosphatase expression was significantly higher at day 42, which is in agreement with the more intense alkaline phosphatase staining seen within the construct.

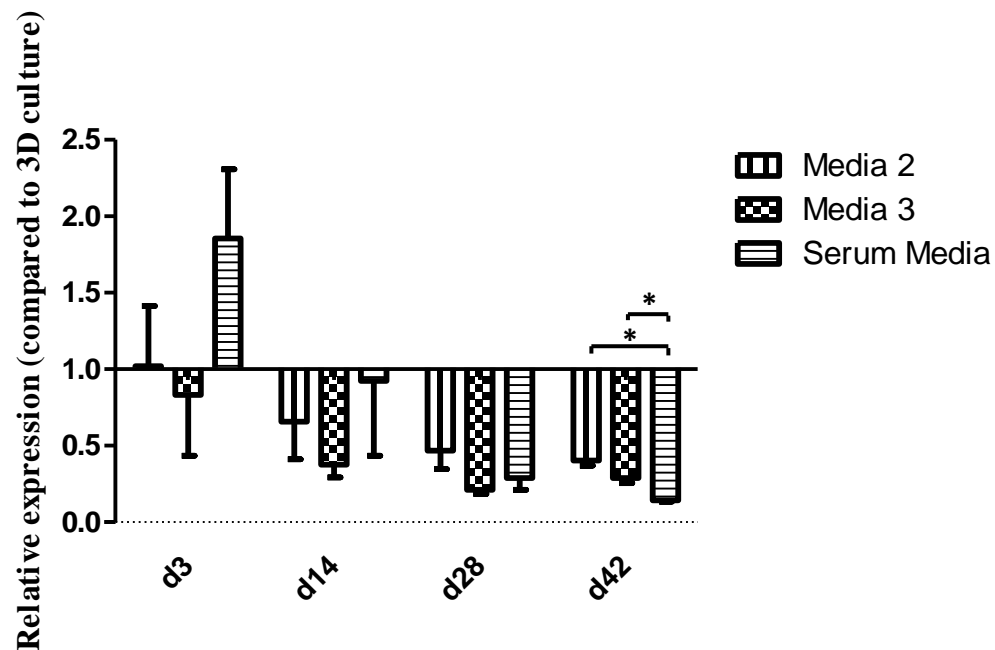


**Figure 5-71:** Collagen type II mRNA expression of the chondrocytes throughout the 42 day culture period on PGA. Showing the effect of serum-free media 2 and serum-free media 3 compared to serum media on the expression of collagen type II within the grafts. The data is normalised to the gene expression observed after 72 hours on culture in expansion media on the PLLA/calcium phosphate scaffold materials (D0 of 3D chondrocyte differentiation). (\*  $p < 0.05$ ,  $n = 6$ )

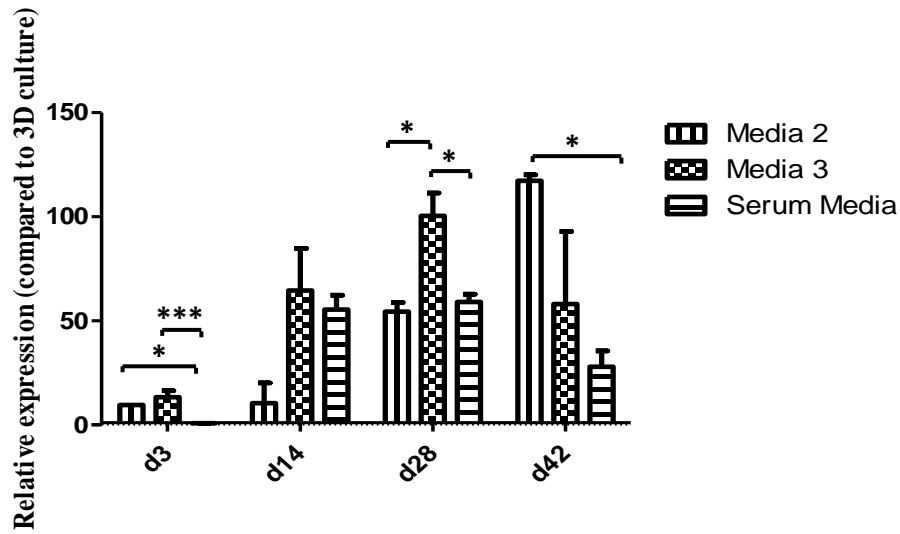


**Figure 5-72 :** *Collagen type X mRNA expression of chondrocytes throughout the 42 day culture period on PGA. Showing the effect of serum-free media 2 and serum-free media 3 compared to serum media on the expression of collagen type II within the grafts. The data is normalised to the gene expression observed after 72 hours on culture in expansion media on the PLLA/calcium phosphate scaffold materials (D0 of 3D chondrocyte differentiation. (\*  $p < 0.05$  and \*\*  $p < 0.01$ ,  $n=6$ )*



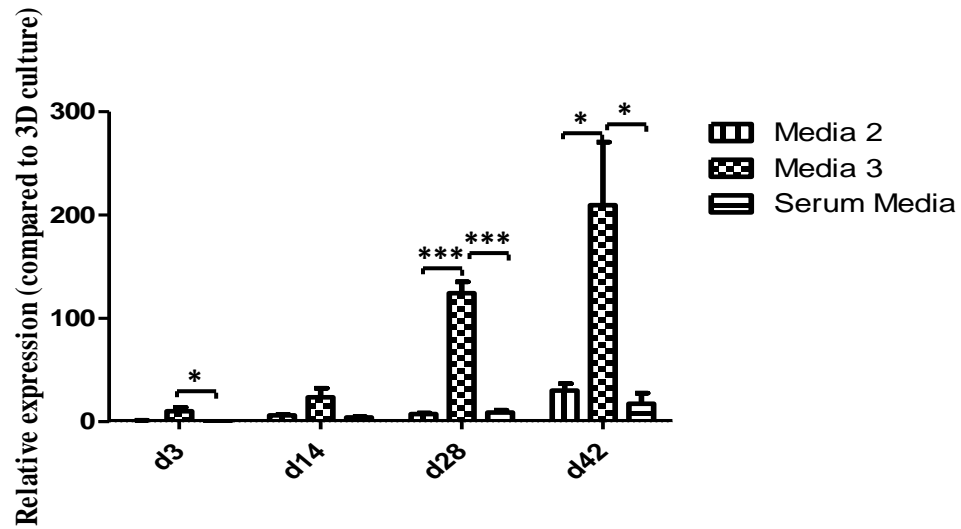


**Figure 5-73:** Alkaline phosphatase mRNA expression of chondrocytes throughout the 42 day culture period on PGA. Showing the effect of serum-free media 2 and serum-free media 3 compared to serum-containing media on the expression of collagen type II within the grafts. The data is normalised to the gene expression observed after 72 hours on culture in expansion media on the PLLA/calcium phosphate scaffold materials (D0 of 3D chondrocyte differentiation). (\*  $p < 0.05$  and \*\*\*  $p < 0.005$ ,  $n=6$ )

## 6 Discussion

The repair of large bone defects is still a major challenge for surgeons, and the current 'gold standard' (autologous bone transplant) while effective has complications such as the possibility of donor site pain and infection, and a low limited volume of bone available for transplant. Therefore tissue-engineering has been investigated for the production of bone grafts that are capable of promoting tissue regeneration.

The majority of bone tissue-engineering research, as discussed in the literature review, has been directed towards the differentiation of stem cells into osteoblasts to produce bone tissue, therefore mimicking the intramembranous ossification pathway. This differentiation technique, however, has several drawbacks for clinical applications. Osteoblasts and the resulting bone tissue require high nutrient exchange rates and oxygen levels within the tissue and because of these requirements, cannot withstand the hypoxic conditions usually found in a wound bed. The use of the endochondral pathway for producing bone grafts may have significant potential as the hypertrophic chondrocytes can survive the lower oxygen and nutrient environments present at the site graft site and provide growth factors which will promote vascularisation, graft integration and bone regeneration.

To date there has been little research directed at the potential of tissue engineering hypertrophic cartilage as bone graft substitute. Research published by Scotti et al investigating this tissue-engineering approach used BM-MSCs (Scotti et al., 2010). However, the use of BM-MSCs as a cell source for tissue-engineering has disadvantages. As with bone grafting, bone marrow biopsies may result in long-term post-operative pain and older patients have less proliferative and viable BM-MSCs which may fail to differentiate. Therefore, in this study, chondrocytes were isolated from the nasal septum. The nasal septum was used as it represents a potential clinically relevant biopsy site which should have less morbidity than bone grafts or bone marrow biopsies. Nasal chondrocytes were relatively easy to isolate and proliferated well *in*

*vitro*. Previous work by Kwarciak in this laboratory has showed that nasal chondrocytes were able to differentiate into hypertrophic chondrocytes *in vitro* and formed mineralised cartilage matrix once implanted subcutaneously *in vivo* (Kwarciak, 2009). The research presented in this thesis has investigated different scaffold materials in order to produce larger constructs, as well as investigating the hypertrophic differentiation of nasal chondrocytes through exploration of gene expression and extracellular matrix protein deposition. The potential of these hypertrophic cartilage constructs to regenerate bone tissue in a cranial defect *in vivo* has also been investigated. Preliminary studies into the use of bioreactor culture and serum-free media have also been performed in order to make translation of this research to the clinic more likely.

### **6.1 Scaffold Fabrication**

As discussed in section 2.5.2, poly(hydroxyorthoesters) such as PGA and PLLA have been used as scaffolds in tissue-engineering due to the availability, biocompatibility and processibility of these materials (Moran et al., 2003). These materials have also gained regulatory approval, which makes them advantageous for investigation. PLLA does have the advantage of a lower degradation rate (Tsai et al., 2006) which will allow for the formation of a more robust construct which will retain both size and shape, this may become important when looking at the production of customised grafts for facial reconstruction. Therefore, electrospun random-fibre PLLA scaffold was compared to a commercial non-woven PGA scaffold material for their ability to drive hypertrophic chondrocyte differentiation.

Calcium phosphates are also regularly used in bone tissue-engineering (Section 2.5.2) as it is an osteoconductive material, which is biocompatible with minimal immunological, toxicity or foreign body effects (Burg et al., 2000). Calcium phosphates also have the ability to bind directly to the bone and therefore enable continuous tissue healing (LeGeros, 2002). A modified PLLA/calcium phosphate composite scaffold

material was therefore also fabricated for this study to investigate its potential as a scaffold material for hypertrophic cartilage tissue-engineering.

A composite scaffold was produced which XRD showed contained two phases of calcium phosphate, brushite and hydroxyapatite, both of which are currently used in bone cements (Grover et al., 2003). Hydroxyapatite is the main calcium phosphate seen within bone itself, making up around 90% of bone mineral (Lichte et al., 2011). During endochondral ossification, hydroxyapatite is the mineral initially laid down in the calcifying cartilage matrix (Mackie et al., 2008). Brushite has also been shown to be present within the calcifying cartilage matrix, although less abundant than hydroxyapatite (Rey et al., 1991). Brushite also has the ability to be converted into hydroxyapatite *in vivo* over time, through dissolution in low pH and re-precipitation as hydroxyapatite (Grover et al., 2003). The PLLA/calcium phosphate scaffold material fabricated for this study should therefore, mimic the natural environment of hypertrophic chondrocytes within the growth plate as well as being more osteogenic than the plain PLLA and PGA scaffolds.

Differences in hydrophilicity of the scaffolds were observed through contact angle measurements with the PLLA scaffold material being hydrophobic and the PLLA/calcium phosphate scaffold being more hydrophilic (*Table 5-1*). Chen *et al* discovered that apatite coated PLLA surfaces were more hydrophilic than non-coated PLLA, allowing for a flatter attached chondrocyte morphology and therefore, a better adhesion to the polymer/ceramic composite (Chen et al., 2008). The commercial PGA scaffold material was also observed to be more hydrophilic than the PLLA scaffold material. The differences seen in hydrophilicity will have an effect on protein adsorption and therefore the ability of the chondrocytes to adhere to the biomaterials. Both PGA and PLLA have been shown to adsorb proteins, however the increased rate of hydrolysis of PGA has been shown to increase the rate of protein adsorption to the polymer surface (Atthoff and Hilborn, 2007). The addition of the calcium phosphate dramatically alters the contact angle making the scaffold highly hydrophilic. Highly

hydrophilic biomaterials have been shown to expel proteins and inhibit protein adsorption. The calcium phosphate, however, is known to be bioactive and is able to adsorb proteins, this bioactivity may be able to overcome the inhibition seen by hydrophilic surface (Wang et al., 2012).

## **6.2 The Effect of FCS on Chondrocyte Hypertrophy**

It is a well-known fact that the FCS used during *in vitro* cell culture has a significant effect on cell proliferation; however, in this study it was important to investigate the effect of various batches FCS on the hypertrophic differentiation of chondrocytes to see if the sera influenced this process.

The FCS batches tested for cell culture had a significant effect on the production of GAG within the ECM (Figure 5-6) as well as the hypertrophic differentiation of the chondrocytes (Figure 5-7). Different batches of FCS therefore supported different aspects of chondrocyte survival and development. This was highlighted by FCS 1 which gave a comparatively high level of GAG in the extracellular matrix while the hypertrophic differentiation of the chondrocytes was either not promoted or inhibited. In contrast, use of FCS 4 produced constructs with a lower GAG incorporation but enabled/promoted hypertrophic differentiation. The differences shown in the effects of the FCS batches on the extracellular matrix composition of the constructs was due to the variability of protein and growth factor composition of each batch of FCS (Honn et al., 1975).

FCS contains a cocktail of serum proteins and bioactive agents, including growth factors, hormones, enzymes, vitamins and trace elements, which are essential for cell attachment and survival (Brunner et al., 2010), making FCS a vital addition to *in vitro* cell culture media. FCS batches, however, contain different concentrations of these proteins which can make the culture of cells variable (Brunner et al., 2010).

Proteins present in FCS, which affect the proliferation and differentiation of chondrocytes include growth factors, such as fibroblast growth factor (FGF), insulin-like

growth factor 1 (IGF-1), endothelial growth factor (EGF) and transforming growth factor- $\beta$  (TGF $\beta$ ) (Olney et al., 2004), and hormones, such as insulin and thyroid hormones.

The FGF family of growth factors is important in chondrocyte growth and differentiation with FGF-1,-2,-18 all have been shown to stimulate chondrocyte proliferation (Olney et al., 2004). FGF-2 (bFGF) in particular can inhibit the hypertrophic differentiation of chondrocytes in a dose dependent manner (Kato and Iwamoto, 1990). Therefore, FCS with a high concentration of FGF-2 will cause the chondrocytes to maintain a hyaline phenotype, producing collagen type II.

TGF- $\beta$ 1 has been shown to stabilise pre-hypertrophic chondrocyte morphology enabling the expression of collagen type II (Ballock et al., 1993). TGF- $\beta$ 1 inhibited chondrocyte hypertrophy in a dose dependent manner through activation of the PTHrP/Ihh pathway (Pateder et al., 2000). This activation results in an increase in PTHrP expression which maintains the proliferative, hyaline chondrocyte phenotype, inhibiting terminal differentiation and decreasing collagen type X expression (Pateder et al., 2000, Ferguson et al., 2000).

IGF-1 is an important stimulator of chondrocyte proliferation (Olney et al., 2004) and has been shown to initiate a morphological increase in cellular volume of the chondrocytes (Bohme et al., 1992a). EGF, also present in the FCS, reduced the synthesis of IGF-1 and therefore, the proliferation and differentiation of the chondrocytes (Chan and Wong, 2000). Insulin can be used as an alternative to IGF as it has the ability to bind to both insulin receptor and IGF-I receptor (Ballock and Reddi, 1994) and promotes the morphological increase in the cellular volume of the chondrocytes as well as being mitogenic (Bohme et al., 1992a). Insulin was added to the differentiation media and therefore, IGF and insulin concentrations within the FCS were unlikely to dramatically affect chondrocyte proliferation or differentiation.

Thyroid hormones, triiodothyronine and thyroxine, are components of the of the growth hormone-insulin axis and increase cellular metabolism (Mello and Tuan, 2006). Thyroid hormones have been shown to be strong initiators of chondrocyte hypertrophy when present at a concentration similar to that found in plasma and can create linearly organised chondrocytes while increasing the production of collagen type X and alkaline phosphatase in serum-free conditions (Bohme et al., 1992b, Ballock and Reddi, 1994, Robson et al., 2000, Okubo and Reddi, 2003, Bohme et al., 1992a). It is therefore suggested that thyroxine may be an important factor in FCS responsible for the terminal differentiation of chondrocytes *in vitro* (Ballock and Reddi, 1994).

As discussed in Section 2.1.4 endochondral ossification is a tightly regulated process with requires the correct expression of growth and transcription factors in order for the correct hypertrophic differentiation to occur. Therefore, it was essential that batch tests of FCS are performed before any differentiation studies are performed. In order to overcome this issue of FCS variability, the development of a defined serum-free media would be advantageous (sections 0 and 6).

### **6.3 Hypertrophic Differentiation of Chondrocytes**

Once a suitable FCS batch had been found, a comparison of the experimental electrospun PLLA and modified PLLA/calcium phosphate scaffolds fabricated in section 5.1 and a commercial PGA scaffold obtained from Cellon was undertaken.

Initial studies showed that attachment on the more hydrophilic surfaces, PGA and PLLA/calcium phosphate scaffolds was significantly increased when compared to the more hydrophobic electrospun PLLA. Moran *et al* showed that chondrocytes attached to hydrophilic surfaces, such as PGA, had a flat morphology with several projections attached to the polymer fibres, whereas chondrocytes seeded on PLLA had a spherical morphology (Moran et al., 2003). The flat morphology of chondrocytes on the scaffold allowed both increased cell attachment and also, retention of cells on the scaffold during semi-static culture due to the high surface area cell contact to the polymer and

the high number of projections securing the cells to the polymer fibres (Papadaki et al., 2001).

The use of the electrospun PLLA scaffold not only decreased initial cell attachment but the construct produced after 42 days was poor in quality, with significantly lower GAG incorporation within the ECM (0.28 % of the dry weight of the ECM ) compared to both the PGA and PLLA/calcium phosphate scaffold materials (Figure 5-11). Areas of hypertrophic differentiation, containing chondrocytes with a large cellular volume, with co-localised expression of collagen type X, were observed within these constructs. Alkaline phosphatase, however, was not expressed in chondrocytes differentiated on the PLLA scaffold material. This significant decrease in PLLA construct quality can be attributed to the hydrophobic nature of the PLLA, as it was observed that the chondrocytes will attach with a rounded morphology. This morphology will not only affect the retention of the chondrocytes during semi-static culture, but has also been shown to decrease cellular proliferation on the scaffold material (Singhvi et al., 1994, Moran et al., 2003).

Both the PGA and PLLA/calcium phosphate scaffold materials enabled chondrocyte attachment) and proliferation and also hypertrophic differentiation of nasal chondrocytes after 42 days in differentiation media in a semi-static environment. Constructs expressed both collagen type X and alkaline phosphatase which are characteristic markers of hypertrophy and are co-located with hypertrophic chondrocytes in the growth plate during endochondral ossification. Chondrocytes in the constructs also exhibited an increase in cell volume, adopting the large cellular morphology which is typical of hypertrophic chondrocytes. Culture on the PGA and PLLA/calcium phosphate scaffold materials also enabled the accumulation of GAG in the ECM (indicative of the level of proteoglycan content). By day 42 the constructs had accumulated GAG levels (as a percentage of ECM dry weight) of 12.91 % (PGA) and 14.10 % (PLLA/calcium phosphate) (Figure 5-11). A significantly quicker production and incorporation of GAG in the ECM occurred on the PLLA/calcium phosphate constructs



when compared to the PGA constructs in the initial stages of culture. However, by day 42 the percentage GAG in the ECM of the PLLA/calcium phosphate constructs were not significantly higher than that seen in the PGA scaffold material (Figure 5-12).

While the production of an engineered tissue with all characteristics of hypertrophic cartilage was successful *in vitro* on both the PGA and PLLA/calcium phosphate scaffold materials these constructs failed to mineralise *in vitro*. There are several hypotheses as to why this occurred; either the culture conditions used in the culture were not conducive to further differentiation, apoptosis or mineralisation of the hypertrophic chondrocytes or that the addition of another cell type, endothelial cells or osteoblasts, was required in order to kick start mineralisation. If this graft material is to be potentially clinically effective, it needs to be shown to mineralise *in vivo* and be remodelled into bone. It was also hoped that this *in vivo* implantation may indicate on the reasons the constructs failed to mineralise *in vitro* (Section 5.5 and 6.5).

There was also some evidence of an alignment of the hypertrophic chondrocytes within the constructs produced on the PLLA/calcium phosphate scaffold material. This alignment of hypertrophic chondrocytes is naturally found within the growth plate of the long bones. Therefore, the engineered constructs were mimicking to some degree, the natural hypertrophic differentiation and cellular organisation of the growth plate hypertrophic chondrocytes. While it is not known whether this cellular organisation contributed to the increased expression of hypertrophic markers, it is important that the engineered tissue mimics the hypertrophic tissue found within the body. This cellular organisation may also effect the mineralisation and formation of bone when the grafts are placed in an *in vivo* environment.

#### **6.4 Protein and Gene Expression**

While it was shown that both the PGA and PLLA/calcium phosphate scaffold materials were both able to support hypertrophic differentiation, it was necessary to further examine the differentiation through gene and protein expression for any differences

between the scaffold materials. During the literature review several key ECM proteins, growth factors and signalling molecules were discussed for their importance in the endochondral ossification pathway (Section 2.1.4). It was therefore decided to investigate the expression of these key proteins and factors throughout chondrocyte differentiation on both scaffold materials.

The differentiation of chondrocytes from a hyaline to a hypertrophic phenotype can be followed throughout the differentiation period and is characterised in particular, by a change in ECM components. During the initial differentiation period, the gene expression of the hyaline ECM component, collagen type II was increased. Collagen type II is incorporated into the ECM before giving way to the expression of hypertrophic ECM proteins, collagen type X and alkaline phosphatase. The signalling molecule, *Ihh*, and transcription factors, *sox9* and *runx2* are also vital for the regulation of hypertrophic differentiation during embryogenesis and long bone growth, with disruptions in the expression of these proteins causing dwarfism and other growth defects (Kronenberg, 2003).

#### ***6.4.1 The Effect of Three Dimensional Culture on Gene Expression***

As the chondrocytes were transferred from a 2D to 3D culture system, significant alterations in the gene expression profile of the chondrocytes were observed (Figure 5-14 and Figure 5-15). A decrease in expression of hypertrophic lineage genes, collagen type X, alkaline phosphatase and *runx2* was observed on both PGA and PLLA/calcium phosphate scaffold materials as the chondrocytes regained their hyaline phenotype. Use of 3D environments for the culture of chondrocytes is important. In a 2D environment chondrocytes dedifferentiate; displaying a fibroblastic-like phenotype and expressing low levels of ECM proteins such as collagen type I. Dedifferentiation was reversed when the chondrocytes were placed into a 3D environment, leading to an increase in ECM production and an upregulation of collagen type II as the chondrocytes regained their hyaline phenotype.

An initial upregulation of collagen type II mRNA expression was observed as the cells were transferred a 2D environment to the PGA scaffold material (Figure 5-14), suggesting that the chondrocytes may have initially regained a hyaline phenotype. However, collagen type II mRNA expression was decreased in chondrocytes cultured on the PLLA/calcium phosphate scaffold (Figure 5-15). Changes in the morphology of the scaffold material may account for this difference in gene expression. The PGA scaffold material was a highly porous material (>97%) with a large pore size which allowed for the infiltration of chondrocytes into the scaffold, whereas electrospun scaffolds typically have a smaller pore size and therefore do not allow for cellular penetration (Lannutti et al., 2007). Therefore, it could be assumed that the PLLA/calcium phosphate scaffold material will act like a mat on which the chondrocytes will proliferate. This may contribute to the initial decreases in collagen type II expression seen when the chondrocytes are seeded on to the PLLA/calcium phosphate scaffold material., Alternatively, the lowered collagen type II expression may have resulted as the PLLA/calcium phosphate scaffolds inhibited the chondrocytes assuming an initial hyaline phenotype.

The gene expression of the signalling molecule, *Ihh*, was increased in chondrocytes cultured on both scaffold materials. The gene expression of *sox9* was increased on the PGA scaffold. Both of these agents are known to act through the PTHrP pathway to keep the chondrocytes in a proliferative state and inhibit hypertrophy. This chondrocyte proliferation is important as it is essential for the chondrocytes to multiply to inhabit the large surface area provided by the scaffold materials.

This significant change in gene expression showed the importance of a 3D culture system for the differentiation of chondrocytes. It also suggests that the two scaffold materials may act differently on the hyaline and hypertrophic differentiation of the chondrocytes by either delaying or accelerating the different stages of differentiation.

#### **6.4.2 Extracellular Matrix Gene Expression**

The collagen type II mRNA expression profile is similar on both the PGA and PLLA/calcium phosphate scaffold materials (Figure 5-16 and Figure 5-17 respectively). Collagen type II expression increases until day 7 as the cells continue to re-differentiate in the 3D system. It is well known that in the growth plate, the highest expression of collagen II is observed in resting and proliferating chondrocytes (Okeefe et al., 1994). Therefore, the peak of collagen II observed at day 7 can be attributed to the chondrocytes being in a proliferative, hyaline state. Between day 7 and day 14 there is a significant decrease in collagen II gene expression suggesting that the chondrocytes were beginning to further differentiate changing their gene expression profile from that of hyaline chondrocytes. Okeefe *et al* observed that collagen type II expression in the growth plate was also inhibited by high levels of collagen type X expression seen in the hypertrophic zone (Okeefe et al., 1994), this may explain the continued decrease in collagen type II expression throughout the culture until day 42. While the mRNA expression is strongly inhibited by day 14 immunohistochemical staining shows that collagen type II protein is present within the ECM throughout the culture until day 42 (Figure 5-26 and Figure 5-28) on both scaffold materials. When looking at the growth plate in Figure 2-2 collagen type II is seen throughout the hypertrophic region. Collagen type II is degraded and removed from the ECM by collagenases, such as matrix metalloproteinase 13 (MMP-13) (collagenase-3) (Inada et al., 2004). MMP-13 is a downstream target of runx2 (Komori, 2005), which was not significantly upregulated until day 28 of culture (Figure 5-35) and therefore, may account for the abundance of collagen type II within the ECM of the constructs at day 42.

Collagen type X is an important ECM protein for endochondral ossification expressed by hypertrophic chondrocytes within the growth plate (Shen, 2005). During *in vitro* culture, collagen type X gene expression was shown to significantly increase between day 3 and day 35 of culture on both the PGA and PLLA/calcium phosphate scaffold material (Figure 5-19 and Figure 5-20 respectively). Although collagen type X was

expressed by day 14 the protein was not incorporated within the ECM. However, by day 28, collagen type X protein can be detected immunochemically in the ECM of the construct co-located with chondrocytes with a large cellular morphology (*Figure 5-26*). This accumulation of collagen type X within the ECM is important during endochondral ossification as collagen type X has several essential functions while mineralisation occurs as well as regulating the mineralisation of ECM itself (Shen, 2005). Kirsch *et al* stated that collagen type X is essential for the binding and entrapment of matrix vesicles within the ECM and also allows for the influx of calcium ions into those vesicles (Kirsch and Wuthier, 1994). Collagen type X knockout mice were shown to have abnormal trabecular architectural development and produced under developed bones (Kwan et al., 1997, Chung et al., 1997). Expression of collagen type X peaked at day 35 with a slight decrease seen at day 42. It is hypothesised that this decrease at day 35 could be due to two possible mechanisms which depend on the fate of the chondrocytes once they have reached terminal differentiation. As discussed in Section 2.1.4, it is generally considered that terminally differentiated chondrocytes either apoptose or further differentiate into chondroclasts, both of these chondrocyte fates will alter the gene expression profile of the chondrocytes and may possibly explain the decrease in collagen type X expression observed at day 42.

Alkaline phosphatase expression was significantly upregulated during the hypertrophic differentiation of the nasal chondrocytes cultured on either PGA or PLLA/calcium phosphate scaffold materials (*Figure 5-22* and *Figure 5-23* respectively). Tissue-nonspecific alkaline phosphatase has been shown to be expressed on the membranes of hypertrophic chondrocytes within the growth plate, with alkaline phosphatase knockout mice exhibiting hypomineralisation of bones (Anderson et al., 2004). There is a lot of debate about the role of alkaline phosphatase in the mineralisation of the growth plate. It was first suggested by Robison *et al* that alkaline phosphatase hydrolyses organic phosphate esters, such as inorganic pyrophosphate (PPi), to produce orthophosphate for incorporation into the calcium phosphate mineral (Robison, 1926). Another hypothesis is that it PPi inhibits mineral formation at the site

of mineral crystal production (Fleisch et al., 1966) and alkaline phosphatase activity is required at the site of mineralisation to breakdown PPI and enable matrix mineralisation. It is therefore essential that alkaline phosphatase is present within the ECM in order for mineralisation to occur within the construct after *in vivo* implantation. It has been shown that alkaline phosphatase is present on the periphery of grafts from day 14 and by day 42 it is present throughout the construct (Figure 5-26).

Gene expression of chondrocytes cultured on the PLLA/calcium phosphate scaffolds suggested that this scaffold maybe advantageous in supporting the hypertrophic differentiation of the chondrocytes, through a significant decrease in the expression of collagen type II and a significant upregulation of collagen type X, when compared to the PGA scaffold material (Figure 5-18 and Figure 5-21 respectively). An upregulation of alkaline phosphatase expression was also observed when using the PLLA/calcium phosphate scaffold material although this increase was not significant by day 42 of the differentiation (Figure 5-24). This change in gene expression is possibly due to the release of both phosphate (Pi) and calcium (Ca) ions from the calcium phosphates into the culture media, either due to pH associated or cellular degradation (Legeros, 1993). Ca ions have been shown to have an important effect on cell division and DNA synthesis of chondrocytes (Legeros, 1993), while Pi ions have been reported to up-regulate the expression of genes associated with the terminal differentiation of chondrocytes, such as collagen type X (Coe et al., 1992, Fujita et al., 2001, Magne et al., 2003). Ca and Pi ions have also been shown to have an effect on the apoptosis of the chondrocytes once they have reached a stage of terminal differentiation and leads to extra-cellular matrix mineralisation (Magne et al., 2003), through the upregulation of genes, such as osteopontin, that are present within mineralising cell types (Magne et al., 2003, Beck et al., 2000).

### **6.4.3 Transcription Factor and Signalling Molecule Gene Expression**

Sox9 is one of the key fate determining transcription factors in endochondral ossification, with a heterozygous deletion resulted in campomelic dysplasia, a severe form of dwarfism affecting all cartilage and endochondral structures. Sox9 is highly expressed by proliferating columnar chondrocytes and acts through the PTHrP signalling pathway to keep the chondrocytes in a proliferative state (Hattori et al., 2010). The expression profile of sox9 varied greatly between the two scaffold materials, with chondrocytes cultured on PGA downregulating sox9 expression after an initial increase in sox9 expression as the chondrocytes were transferred from culture to the scaffolds (Figure 5-29), until day 35 when a non-significant increase was observed. On the PLLA/calcium phosphate scaffold material, however, the chondrocytes initially, downregulated sox9 gene expression as they were transferred to the scaffold from monolayer culture before significantly upregulating expression peaking at day 14. There was also a secondary non-significant peak of sox9 at day 35. These results suggested the chondrocytes cultured on the PLLA/calcium phosphate scaffold required longer to re-differentiate into a hyaline phenotype, this is also shown the initial decreases in collagen type II expression observed on the PLLA/calcium phosphate scaffold.

This work also highlights the possibility of a secondary role for sox9 in hypertrophic differentiation and is illustrated by an upregulation of expression on both scaffold materials at day 35 of differentiation, correlating to the highest expression of both collagen type X and alkaline phosphatase (Figure 5-19 and 5-18 and Figure 5-22 and 5-21 respectively). Recent work by Dy *et al* has shown that sox9 is also an important transcription factor for hypertrophic differentiation (Dy et al., 2012), where it is located to the nuclei of chondrocytes where it acts upon the collagen type X promoter both independently and through cooperation with mef2c. Sox9 also has the ability to inhibit the mineralisation of the hypertrophic matrix by inhibiting  $\beta$ -catenin signalling.

Therefore, the increase in *sox9* gene expression seen at day 35 may hinder the mineralisation of the constructs *in vitro*.

In the growth plate, *Ihh* expression is localised to the area of post-mitotic, pre-hypertrophic chondrocytes which is adjacent to the proliferating columnar cells (Mak et al., 2008). It has been reported that *Ihh* acts through both the activation of the PTHrP signalling pathway (Lai and Mitchell, 2005, Kronenberg, 2003) and Ptc-1 receptor (St-Jacques et al., 1999) which keep the chondrocytes in a proliferative state. (Pateder et al., 2000). However Mak *et al* has also suggested that *Ihh* also works independently of PTHrP to promote hypertrophic differentiation through the activation of the Wnt/BMP signalling pathway (Mak et al., 2008). It is therefore essential that the expression of *Ihh* occurs at the correct time within the differentiation process and is downregulated in the later stages of differentiation in order to allow for full hypertrophy to be observed. In both PGA and PLLA/calcium phosphate constructs a significant peak of *Ihh* gene expression was observed on day 21 of culture suggesting that the chondrocytes had undertaken a pre-hypertrophic phenotype (Figure 5-32 and Figure 5-33). This day 21 peak of *Ihh* gene expression also correlated to the decrease in collagen type X expression observed at day 21 in the PGA constructs (Figure 5-19). Therefore, *Ihh* may have inhibited collagen type X expression in an attempt to keep the chondrocytes in a proliferative state and delay the differentiation of the chondrocytes.

*Runx2* is expressed by hypertrophic chondrocytes within the endochondral growth plate and is essential for both promoting hypertrophic differentiation as well as regulating the expression of other genes associated with mineralisation and angiogenesis (Kim et al., 1999). The increase in expression seen during the differentiation of the chondrocytes is important as a heterozygous mutation leads to a lack of endochondral ossification in mice (Inada et al., 1999).

*Runx2* has been shown to regulate the expression of osteopontin (Sato et al., 1998), which is one of the main non-collagenous bone matrix proteins and is believed to allow the attachment of osteoclasts to the mineralised matrix and therefore, enables the



remodelling of the cartilage matrix (Reinholt et al., 1990). MMP-13 is also up-regulated by the expression of runx2 (Komori, 2005). As discussed previously, MMP-13 is vital for the degradation of the helical collagen type II and is highly expressed at the centres of ossification. (Inada et al., 2004), runx2 null mice also lacked vascularisation in mature hypertrophic cartilage (Inada et al., 1999, Zelzer et al., 2001), due to the repression of VEGF. This suggested that VEGF expression is regulated by the expression of runx2 (Zelzer et al., 2001, Provot and Schipani, 2005). VEGF and its receptors are important in the regulation of angiogenesis during endochondral bone formation as well as inducing the migration and alkaline phosphatase activity of osteoblasts (Midy and Plouet, 1994) and being a chemo-attractant for osteoclasts (Engsig et al., 2000).

Therefore, runx2 expression within the constructs suggested that the ECM of the constructs cultured on both the PGA and PLLA/calcium phosphate scaffold materials expressed all the growth factors and proteins required for mineralisation and vascularisation when implanted *in vivo*.

Monitoring the hypertrophic differentiation of chondrocytes is important for the development of a tissue-engineered graft material, as it is essential to ensure that the cells follow the same differentiation pathway and that that pathway mimics that seen during the natural differentiation in the endochondral ossification growth plate. It also highlights the stages at which the chondrocytes are in the differentiation with the high expression of collagen type II suggesting a hyaline phenotype, Ihh a pre-hypertrophic phenotype and the expression of collagen type X, alkaline phosphatase and runx2 for hypertrophic chondrocytes.

Due to the increase in hypertrophic marker expression and the high percentage GAG seen using the PLLA/calcium phosphate scaffold, it may be interesting to assess these scaffolds *in vivo*. As it has also been shown that both Ca and Pi ions effect the apoptosis of the chondrocytes once they have reached a stage of terminal differentiation and leads to extra-cellular matrix mineralisation (Magne et al., 2003). PLLA/calcium phosphate scaffolds may therefore be able to increase bone healing and mineralisation

when compared to grafts grown on the PGA scaffold material. However longer degradation rates of PLLA, may mean that there may be an inflammatory response due to the acid produced during the degradation, which is not seen when using the PGA scaffold material as this was already degraded before implantation.

## **6.5 *In Vivo Experiments***

In Section 5.3 it can be seen that the hypertrophic constructs did not mineralise during *in vitro* culture (Figure 5-13), however, the potential of these constructs to mineralise and be remodelled into bone *in vivo* needed to be assessed. It was decided to use the PGA scaffold material during these *in vivo* experiments as we were interested in the ability of hypertrophic chondrocyte construct to promote bone formation in a healing bone defect compared to an empty defect and therefore did not want any scaffold material remaining which may either aid in defect healing or cause an inflammatory response.

At week 4 significantly increased bone regeneration within the cranial defect was observed using both the 'living' and decellularised constructs. However, the BM-MS-C re-seeded constructs failed to significantly increase regeneration within the defect at week 4 (Figure 5-46 and Figure 5-47). The histological analysis of the defects highlights the importance of vascularisation in the regeneration of bone, since a vascular network was present within the implanted constructs (Figure 5-48). This need for initial vascularisation before mineralisation can proceed throughout the construct may explain the lack of mineralisation observed during the *in vitro* culture. Alcian blue staining of construct sections illustrated the degradation of the hypertrophic cartilage matrix around the areas of vascularisation (Figure 5-49).

Previous research has highlighted the importance of endothelial progenitors and haematopoietic stem cells which express CD34+ for the neovascularisation of fractures and subsequent fracture healing (Matsumoto et al., 2008). Interestingly, Olmsted-Davis *et al* observed that CD34+ cells are able to generate osteogenic cells, which express

both osteocalcin and alkaline phosphatase (Olmsted-Davis et al., 2003). The decrease in ECM observed around the vascularisation of the graft can be attributed to the activity of MMPs expressed by and around areas of vascularisation. As discussed in Section 6.4.3 MMP-13 is expressed by hypertrophic chondrocytes and degrades the collagen type II present in the ECM. MMP-9 (gelatinase B) has been shown to be particularly important in its degradation of collagens within the ECM of hypertrophic cartilage (Vu et al., 1998). This highlights the importance of the expression of growth factors, such as VEGF, within the grafts in order to recruit the CD34+ cells from the bone marrow, to the peripheral blood and finally to areas of neovascularisation (Gerber et al., 1999).

By week 8, significantly increased bone regeneration is once again observed by both the 'living' and decellularised constructs, with 22.94 % and 30.73 % bone volume seen within the defects respectively. At week 8 the repair of the living defects is seen to be less, than that of the decellularised construct although this decrease did not reach statistical significance (Figure 5-50 and Figure 5-51). Histological analysis of the defects showed the formation of bone within the defects treated with both 'living' and decellularised constructs (Figure 5-52).

Bone formation originates from the periphery of the all the defects including the untreated defects. Previous research has shown that bone regeneration in cranial defects mainly occurs at the periphery of the defect, due to the increased mechanical stability at these locations (Hammerle et al., 1995). The larger the cranial defect the more this bone regeneration is marginalised and pushed towards the periphery of defects. The implantation of the graft materials in to the defect will increase the mechanical stability of the injury site. This increase in stability alone will allow for an increase in bone healing across the site of injury. In some of the defects bony islands are observed within the grafts materials throughout the defects and are established around the blood vessels and bone is formed out from these locations. This may be due to the influx of osteoblasts and monocyte-derived osteoclasts to regulate bone

formation through the blood vessels (Gerber and Ferrara, 2000). The formation of bony islands within the grafts increases the mechanical stability of the defect, which should in turn accelerate the rate of bone regeneration within the defect (Hammerle et al., 1995). The decellularised grafts exhibit early vascularisation and bony islands form within the defect, this increase in bony island formation will increase the mechanical stability of the injury site and should therefore increase bone formation.

There are a couple of possible hypotheses for the increase in bone regeneration observed using the decellularised graft. It has been reported that hypertrophic chondrocytes within the growth plate apoptose before mineralisation can proceed. The apoptosis of chondrocytes before implantation through the decellularisation of the graft may therefore increase the rate at which mineralisation can occur. There are also possible immunogenic reasons for the decrease in regeneration seen within the 'living' graft. The rats used in the *in vivo* experiments are relatives of the rats used for *in vitro* graft production it is possible that there is an inflammatory or a graft vs. host response to the graft, which will impair the repair of the defect. Toben *et al* observed that the expression of pro-inflammatory cytokines, such as tumour necrosis factor- alpha (TNF- $\alpha$ ), produced by lymphocytes in the adaptive immune system impairs bone regeneration in fractures.

By week 12, both the 'living' and decellularised constructs had comparable bone regeneration (38.48 % and 38.59 % respectively), which was significantly greater than that seen in the untreated defect (7.56 %) (Figure 5-55). Therefore, by week 12 of *in vivo* implantation both 'living' and decellularised constructs had equivalent potential for bone regeneration. The MSC re-seeded constructs, however, while initiating some bone regeneration (21.22 %) did not reach statistical significance.

As discussed in the literature review the use of BM-MSCs for bone regeneration has been well documented (Section 2.4 and 2.5.1). The bone regeneration by the BM-MSCs re-seeded decellularised construct, while increased compared to the empty defect, was slower than when using other types of constructs. Previously, it was hypothesised that

healing could be impaired by an inflammatory response however; BM-MSCs have an immature immune system which decreases the risk of an allogeneic immune reaction. The decrease in bone regeneration, therefore, cannot be attributed to an inflammatory response caused by the BM-MSCs re-seeded on the decellularised constructs. Little research has been performed on the differentiation of BM-MSCs on decellularised hypertrophic cartilage and therefore, the mechanisms which delay the regeneration of bone. It can be hypothesised that as the BM-MSCs differentiate down a chondrogenic lineage, they progress through a hyaline phenotype, which produce factors which can inhibit vascularisation of cartilage and this may account for the delay in bone regeneration as vascularisation of the graft is essential for bone regeneration. The multi-lineage potential of BM-MSCs may also contribute to the delay in bone regeneration, as once implanted it is not known which lineage the BM-MSC will differentiate down. The BM-MSCs may also not be able to survive within the hypoxic conditions found within the wound bed. More research is therefore required to decipher the fate of the BM-MSCs after implantation and whether further *in vitro* differentiation on the graft would be advantageous for bone regeneration.

The potential of a decellularised hypertrophic cartilage to regenerate bone could provide an interesting new clinical approach to bone repair. The removal of both cellular and genetic material from the construct enables the formation of an allogeneic graft, leading to a potential 'off the shelf' therapy. It may also mean that these constructs could be made xenogenically and therefore, human donor tissue, would not be required. The use of a xenogeneic graft, however, would require more a stringent decellularisation protocol, in order to ensure further removal of genetic material and fully remove the immune response to the graft. However it is essential that the ECM and the growth factors which are present are not disrupted as this will impair the grafts ability to regenerate bone.

## 6.6 *Bioreactor Culture*

As discussed in the literature review (Section 2.5.4) the flow regime within the culture system of hypertrophic cartilage grafts is important and the use of bioreactors for the production of tissue *in vitro* and for tissue-engineering may become essential. Bioreactors have the ability to standardise cultures and limit the amount of operator variability during *in vitro* culture periods giving rise to the reproducible tissue production. This will be essential when looking for regulatory approval for future tissue-engineered therapies.

Due to the flow of media within the bioreactor the PLLA/calcium phosphate scaffold material was used as it has slower rate of degradation when compared to the PGA scaffold material which loses its' tensile strength within two weeks of semi-static culture. It was therefore decided that under bioreactor culture conditions the PGA scaffold material may lose strength before sufficient ECM could be formed, decreasing the size and quality of the constructs produced.

The use of fluid flow has been shown to have a positive effect on the accumulation of GAG and collagen within the ECM of cartilage grafts (Davisson et al., 2002). This effect was highlighted by the decrease in percentage GAG incorporated into the ECM of constructs formed using static conditions, compared to both the semi-static culture systems (Figure 5-61). The lack of ECM production in static conditions explains why all 3D culture was performed on a gently oscillating, shaker plate set at 30 rpm. It is believed that this change in ECM production is modulated by the mobilisation of intracellular calcium signalling, caused by fluid flow, which results in an increase in cell proliferation and ECM production (Yellowley et al., 1997). The use of the bioreactor gave comparable GAG accumulation within the ECM of constructs, when compared to the semi-static culture system. Bioreactors must be able to support the proliferation and differentiation of the chondrocytes by providing efficient nutrient exchange as well as provide the fluid flow required for increased ECM accumulation. It is important, however, that this fluid flow does not produce high levels of shear stress which is

detrimental to the cells and would inhibit ECM accumulation. A flow rate of  $110 \mu\text{l minute}^{-1}$  led to an increased chondrocyte proliferation without shear detachment of cells or a change in morphology in a 2D culture system (unpublished data).

Bioreactor culture was shown to produce fully hypertrophic grafts, with expression of collagen type X and alkaline phosphate with the ECM of the grafts, co-localised with chondrocytes with a large morphology (Figure 5-62). Accumulation of GAG within the ECM was observed to be significantly higher when compared to the semi-static conditions used previously in section 5.3 (Figure 5-62). Use of the bioreactor also produced chondrocytes expressing slightly higher levels of collagen type X and significantly higher levels of alkaline phosphatase when compared to semi-static culture conditions (Figure 5-65 and Figure 5-66 respectively). The use of the bioreactor was also shown to significantly downregulate the expression of collagen type II (Figure 5-64).

The changes observed may be due to the type of flow present within bioreactor when compared to that seen on the shaker plate and the shear forces associated with it. Mild cyclic shear stress has been shown to accelerate endochondral ossification and lead to an increase in collagen type X and runx2 expression (Gawlitta et al., 2010, Wong et al., 2003) during hypertrophic differentiation. The shear in the bioreactor is linear and occurs across the top surface of the constructs, so the majority of the chondrocytes exist in a low shear environment, whereas the shear experienced by the graft in the semi-static conditions is more turbulent and occurs all over the surface of the graft. The higher area and the more turbulent nature of shear stress experienced by the chondrocytes may be detrimental to the production of GAG in the graft. The shear stresses experienced by the chondrocytes within the scaffold material will alter throughout the differentiation culture as the chondrocytes differentiate. Initially the chondrocytes will attach to the microfibers with a flattened morphology, however as they increase in volume they will expand and bridge between the scaffold fibers making them more susceptible to shear stress. Therefore the laminar, low wall shear

stresses observed within the bioreactor maybe more suited to the larger morphology of hypertrophic chondrocytes in the later stages of the culture when compared to the more turbulent flow in the semi-static conditions. Turbulent flow conditions have been shown to be more shear damaging to cells than laminar flow shear. Although the turbulent flow within the semi static environment is low, the laminar flow bioreactor seems to support better chondrocyte differentiation and GAG accumulation.

Use of this fluid flow bioreactor produced a high quality hypertrophic construct which could potentially be implanted *in vivo*. Therefore, bioreactors may become essential when looking at the clinical development of an engineered tissue *in vitro*, as the products will need to be reproducible, safe and economically competitive (Chen and Hu, 2006).

## **6.7 Serum-Free Media**

Serum, is an important method of delivering growth factors for both cell maintenance and proliferation during *in vitro* culture (Brunner et al., 2010). As discussed in Section 6.2, serum is a highly variable additive for culture media as its composition is dependent on the species (e.g. animal or human) and source of the donor(s); which in terms of FCS, from the bovine herd from which the serum is obtained. Every batch of FCS will have slightly different concentrations of growth factors, hormones, proteins, enzymes, fatty acids and lipids, vitamins and trace elements (Brunner et al., 2010). This variance can affect both the ability of cells to proliferate and differentiate. During the batch testing of FCS (Section 5.2), the sera had differing significant effects not only the amount of ECM produced during pellet culture, but also the ability for the chondrocytes to differentiate and mature into hypertrophic chondrocytes on a PGA scaffold material. Some of the sera completely inhibited or failed promote the hypertrophic differentiation of the chondrocytes (Figure 5-7), highlighting the problems associated with serum variability during tissue-engineering.



The variability of FCS and its impact on the differentiation of chondrocytes was the primary reason for looking into developing a serum-free media (Section 5.2 and 6.2). However, there was also a secondary reason; that of a regulatory requirement for a defined medium in developing an advanced tissue engineering medicinal product. The ideal end point of this research is to produce a clinically applicable treatment for large bone defects; therefore it is important to remove serum from the culture of tissue constructs as this will be a large step towards making the culture process highly reproducible.

All serum-free media investigated contained BSA, which is adsorbed to the polymer surface of the PGA and allows for cell adhesion and the spreading of the cells on the scaffold fibres. While BSA only gives a 5% of cell spreading compared to fibronectin (lemons et al, 2012), it does aid cellular adhesion to the PGA in a serum-free environment where the plethora of proteins present in serum, which usually allow to cell attachment, are removed.

Serum-free media 1 illustrated that the addition of FCS components was essential for the development of ECM in the constructs. The removal of FCS from the media, without making any growth factor substitutions to support cell survival and proliferation, resulted in the formation of a small construct with a significantly lower GAG content (1.94 % of ECM dry weight) within the ECM of the constructs, when compared to those seen when using serum-containing media (12.91 % ECM dry weight)(Figure 5-67). Limited hypertrophic differentiation was also observed with serum-free medium-1, the chondrocytes showed an increase in cell volume, but lacked expression of hypertrophic markers, collagen type X and alkaline phosphatase (Figure 5-68). Therefore, additions of growth factors and/or hormones to the culture media were vital to replace the role of FCS in order to provide support for cell survival, proliferation and subsequent hypertrophic differentiation of the chondrocytes.

ITS has previously been used as a basic cell culture addition when creating a serum-free cell culture media (van der Valk et al., 2010, Chua et al., 2005). Therefore ITS was

added to the serum-free media to give serum-free medium-2. This medium enabled attachment, proliferation and hypertrophic differentiation of the chondrocytes within the constructs (Figure 5-69). Serum-free media 2 resulted in constructs with significantly higher percentage of GAG in the ECM when compared to serum-free media 1 and comparable to those seen when using normal FCS media (Figure 5-67). The removal of FCS and its replacement with ITS also caused a significant upregulation of collagen type X gene expression by the chondrocytes within the construct at day 42. In these experiments, the commercial ITS preparation used was composed of recombinant human insulin, human transferrin (substantially iron-free), sodium selenite, linoleic acid, oleic acid and bovine serum albumin (Section 4.2.3.5), which have all been shown to influence cells during *in vitro* culture. At the dilution used the final concentrations of these agents in the culture media were: insulin ( $10 \mu\text{g.mL}^{-1}$ ), transferrin ( $5.5 \mu\text{g.mL}^{-1}$ ), selenium ( $5 \text{ ng.mL}^{-1}$ ), and linoleic ( $4.7 \mu\text{g.mL}^{-1}$ ) and oleic ( $4.7 \mu\text{g.mL}^{-1}$ ) acids.

The addition of transferrin is important for the maintenance of mammalian cells during *in vitro* culture. Transferrin is a homologous iron-binding glycoprotein that enables free iron to be sequestered and transported into cells, regulating the bioavailability of iron to the cells (Brandsma et al., 2010). Iron is important in cell culture as it supports several metabolic processes, such as DNA synthesis and oxygen transport (Richardson and Ponka, 1997), as well as being closely linked with cell proliferation (Laskey et al., 1988). Also non bound iron can cause free radical formation, which in turn causes tissue damage (Conrad et al., 1999). Selenium is an essential trace metal in cell culture for normal cell development and growth. It is required to be incorporated into essential seleno-enzymes which protect cells against oxidative damage (Saito et al., 2003, Helmy et al., 2000). Linoleic acid is an unsaturated fatty acid which cannot be produced by cells and therefore these fatty acids along with others, such as oleic acid, are a necessary media addition. Not only are these acids important elements in the formation of cellular structures but are required as precursors to other molecules such as phospholipids and vitamins as well as allowing for long term energy storage within

the cells through the formation of triglycerides (Hewlett, 1991). Insulin whilst being important for the differentiation of the chondrocytes down a hypertrophic lineage (Bohme et al., 1992a) and also has an important role in cell survival as it regulates the uptake, utilization and storage of glucose, amino acids and fatty acids while inhibiting the breakdown of glycogen, protein and fat (Hewlett, 1991). ITS is therefore essential for the serum-free differentiation of the chondrocytes as it not only supports cell attachment, survival and proliferation but it also provides the insulin required to initiate the increase in cellular volume and hypertrophic differentiation.

Thyroxine was added to the media as thyroid hormones have been shown to have an important effect on chondrocyte hypertrophic differentiation as discussed in Section 6.2. Thyroxine was shown by Robson *et al* to induce hypertrophic differentiation chondrocytes in a serum-free media (Robson et al., 2000). Thyroxine was incorporated into serum-free media 3 (Section 0). Use of serum-free medium 3 did not cause in a significant increase in the amount of GAG present within the ECM when compared to serum-free media 2 (Figure 5-67). However, both the staining and the mRNA expression for alkaline phosphatase were significantly increased (Figure 5-70 and Figure 5-73). Interestingly, collagen type X gene expression (Figure 5-72) was decreased although not significantly when compared to serum-free media 2 although this effect did not reach statistical significance.

Current hypotheses suggested that the thyroid hormones act through the Wnt/ $\beta$ -Catenin signalling pathway to induce the terminal differentiation of the chondrocytes (Figure 6-1) (Wang et al., 2007). Wang *et al* demonstrated that after addition of thyroid hormone to chondrocytes cultured as cell pellets, induced an increased accumulation of  $\beta$ -Catenin and up-regulation of Wnt-4 and runx2 mRNA expression after 4 or 5 days (Wang et al., 2007). Bohme *et al* observed that the addition of thyroxine had a positive effect on the expression of collagen type X and alkaline phosphatase (Bohme et al., 1992a). In the study reported in this thesis, collagen type X gene expression was not

increased when constructs were cultured with thyroxine; however, the alkaline phosphate expression was increased.

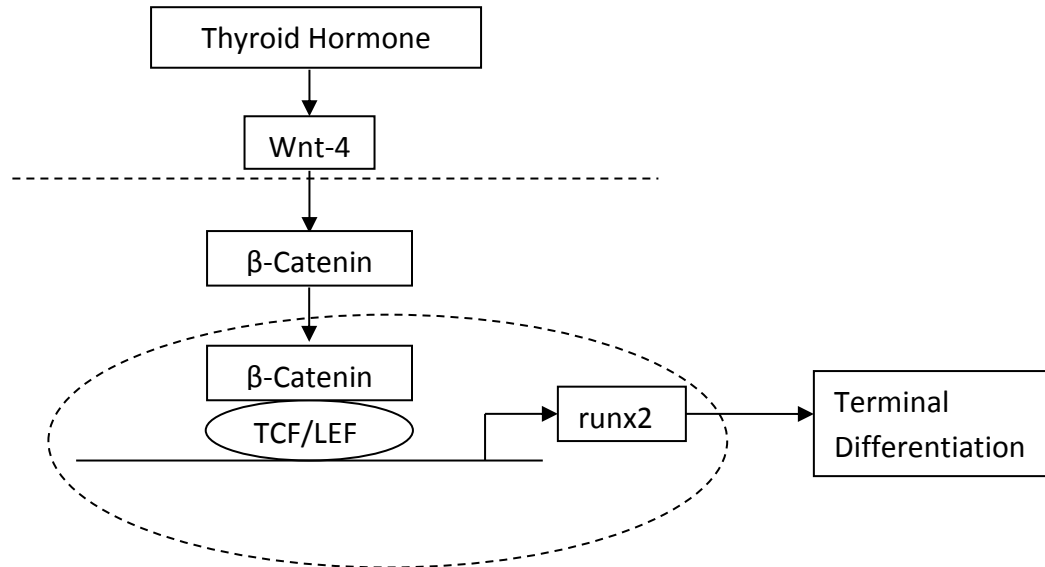


**Figure 6-1:** Thyroid hormone activation of the Wnt signalling pathway leading to the production of runx2 and the terminal differentiation of chondrocytes.

Addition of thyroxine to the serum-free media enabled a higher gene expression of alkaline phosphatase, when compared to other media (Figure 5-73). As discussed previously, alkaline phosphatase is essential for the degradation of PPI within the mineralising tissue, therefore it can be hypothesised that the use of serum-free media 3 would enable an increased rate of mineralisation *in vivo*.

## 7 Conclusions

Tissue-engineering a new graft material using the endochondral ossification pathway has been shown to have potential for the regeneration of bone tissue in challenging defects (Section 0). This research has advanced this tissue-engineering approach by investigating the effect of serum, scaffolds and culture conditions on the hypertrophic differentiation *in vitro*, as well as examining the potential of these hypertrophic tissue-engineering grafts to regenerate bone defects *in vivo*. After careful analysis and discussion of results, the following conclusions were reached:

- An electrospun PLLA scaffold was produced and was successfully modified to incorporate both hydroxyapatite and brushite on and in between the scaffold fibres. The addition of a calcium phosphate increased the hydrophilicity of the electrospun PLLA scaffold material.
- FCS had a significant effect on construct quality, not only on the amount of GAG accumulated within the grafts but also on the terminal differentiation of the chondrocytes. While it is well-known that FCS has a significant effect of cells during *in vitro* culture, it was essential that this work was carried out to ensure that hypertrophic differentiation of the nasal chondrocytes could be repeated successfully.
- The electrospun PLLA did not support the formation of a hypertrophic chondrocyte graft under the conditions used. The electrospun PLLA/calcium phosphate and PGA scaffold materials, however, did reproducibly support the formation of a high quality hypertrophic chondrocyte graft with the expression of hypertrophic markers co-located with chondrocytes with a large cellular morphology.
- Measurement of gene and protein expression demonstrated the different stages of differentiation throughout the 42 day culture period, with collagen type II and sox9 being downregulated as the chondrocytes differentiate toward

an *Ihh* expressing pre-hypertrophic phenotype at day 21, before becoming fully hypertrophic with peaks in *runx2* at day 28 and collagen type X and alkaline phosphatase expression at day 35.

- Hypertrophic cartilage constructs were able to promote bone regeneration *in vivo*, over the control (construct and scaffold-free defect) in a healing cranial bone defect model. Vascularisation of the constructs was required for subsequent bone formation within the defect.
- Decellularised hypertrophic cartilage constructs were also able to promote bone regeneration *in vivo*. This potential for a decellularised hypertrophic cartilage graft has exciting clinical promise for an allogeneic, off the shelf therapy for bone regeneration.
- Bioreactor culture increased the GAG content within the ECM of the constructs when compared to semi-static culture; there was also an increase in alkaline phosphatase expression at day 42. Therefore, the use of the flow bioreactor may be advantageous not only for culture standardisation and regulatory approval but also for the production of a high quality hypertrophic cartilage tissue graft.
- Addition of ITS and thyroxine to the serum-free culture enabled the chondrocytes to reproducibly undergo hypertrophic differentiation. Removal of FCS is an important step forward in making this research more clinically applicable as in order to gain regulatory approval it will be necessary to use a defined culture media.

To summarise, this work has substantially added to knowledge of hypertrophic differentiation of nasal chondrocytes and the ability of hypertrophic tissue engineered hypertrophic grafts to be used to regenerate bone tissue within complex or large defects.

## 8 *Future Work*

The research presented in this thesis demonstrated the ability of rat nasal chondrocytes to produce a tissue-engineered hypertrophic chondrocyte graft which can regenerate bone tissue *in vivo*. More research, however, is required in order to make this a clinically applicable therapy for the treatment of non-union fractures or large defects.

- The gene and protein expression of the chondrocytes during *in vitro* culture of tissue engineered constructs has provided insights into hypertrophic differentiation pathway of the cells. Further investigation, however, into gene expression both at the initial stages to examine PTHrP expression and at the final stages to investigate the expression of VEGF, osteocalcin and osteopontin, would be helpful. Research in this area, especially towards the end of the culture period may be able to explain the failure of the hypertrophic grafts to mineralise *in vitro*.
- While the hypertrophic constructs were shown to remodel into bone tissue *in vivo*, cartilage mineralisation *in vitro* did not occur in this study. The histological data from the *in vivo* experiments suggested that vascularisation and the recruitment of endothelial cells into the graft, was essential for the bone formation observed. A co-culture of endothelial cells with the chondrocytes may therefore enable cartilage mineralisation *in vitro*.
- The PLLA/calcium phosphate scaffold material was able to support the hypertrophic differentiation of chondrocytes *in vitro*. The ability of these grafts to heal defects *in vivo* was not assessed. Therefore, investigation of the ability of a hypertrophic cartilage graft grown on the PLLA/calcium phosphate scaffold material to increase bone regeneration *in vivo*, is therefore required. The ability for the PLLA/calcium phosphate scaffold material on its own to regenerate defects should also be investigated due to its increased osteogenic potential.

- The decellularised hypertrophic cartilage graft enabled bone regeneration at a slightly increased rate over that of the 'living' graft; while this is an exciting new development in bone tissue-engineering, further work needs to be performed in order further develop this method. Optimisation of the decellularisation technique is required to further increase DNA removal without adversely affecting the ECM composition or ultra-structure. Further reduction of DNA from the graft would further decrease the chance of viral transmission or an inflammatory response. It would also be interesting to investigate a developing a porcine or bovine decellularised graft, which could be utilised as a cell-free xenogeneic graft material for clinical applications in bone regeneration.
- The use of a decellularised graft reseeded with MSCs induced bone regeneration, however, this was at a slower rate than the other grafts used. Therefore, it would be interesting to investigate the fate of the MSC on the decellularised hypertrophic cartilage both *in vitro* and *in vivo*, to help explain the delay in bone regeneration observed. Other cell types could also be used to reseed the decellularised graft, such as chondrocytes and endothelial cells.
- A serum-free media was developed in this research which resulted in production of hypertrophic cartilage grafts. While this is a step forward in producing a defined media which is not reliant on the use of highly variable FCS, to produce a clinically applicable cellularised graft it is necessary to use a defined, serum-free, animal-free media. Therefore, future work on the removal of animal products from the media is essential to reduce a risk of viral transmission.
- The preliminary studies using the Quasi-vivo® flow bioreactor produced hypertrophic cartilage grafts with higher percentages of GAG within the ECM and a higher expression of alkaline phosphatase. Further work needs to be performed to ensure that these results are reproducible under the defined flow conditions used in section 5.6. Further work using the bioreactor under different flow conditions would also be interesting as it has been suggested that



cyclic shear may increase both collagen type X and alkaline phosphatase expression in hypertrophic chondrocytes.

## 9 References

- ALBEE, F. H. 1920. Studies in bone growth - Triple calcium phosphate as a stimulus osteogenesis. *Annals of Surgery*, 71, 32-39.
- ALBREKTSSON, T. & JOHANSSON, C. 2001. Osteoinduction, osteoconduction and osseointegration. *European Spine Journal*, 10, S96-S101.
- ANDERSON, H. C., SIPE, J. B., HESSLE, L., DHAMYAMRAJU, R., ATTI, E., CAMACHO, N. P. & MILLAN, J. L. 2004. Impaired calcification around matrix vesicles of growth plate and bone in alkaline phosphatase-deficient mice. *American Journal of Pathology*, 164, 841-847.
- ATTHOFF, B. & HILBORN, J. 2007. Protein adsorption onto polyester surfaces: Is there a need for surface activation? *Journal of Biomedical Materials Research Part B-Applied Biomaterials*, 80B, 121-130.
- BADYLAK, S. E. 2002. The extracellular matrix as a scaffold for tissue reconstruction. *Seminars in Cell & Developmental Biology*, 13, 377-383.
- BADYLAK, S. F., FREYTES, D. O. & GILBERT, T. W. 2009. Extracellular matrix as a biological scaffold material: Structure and function. *Acta Biomaterialia*, 5, 1-13.
- BALLOCK, R. T., HEYDEMANN, A., WAKEFIELD, L. M., FLANDERS, K. C., ROBERTS, A. B. & SPORN, M. B. 1993. TGF-beta-1 prevents hypertrophy of epiphyseal chondrocytes- regulation of gene-expression for cartilage matrix proteins and metalloproteases. *Developmental Biology*, 158.
- BALLOCK, R. T. & REDDI, A. H. 1994. Thyroxine is the serum factor that regulates morphogenesis of columnar cartilage from isolated chondrocytes in chemically defined medium. *Journal of Cell Biology*, 126, 1311-1318.
- BARNES, G. L., KOSTENUK, P. J., GERSTENFELD, L. C. & EINHORN, T. A. 1999. Growth factor regulation of fracture repair. *Journal of Bone and Mineral Research*, 14, 1805-1815.
- BECK, G. R., ZERLER, B. & MORAN, E. 2000. Phosphate is a specific signal for induction of osteopontin gene expression. *Proceedings of the National Academy of Sciences of the United States of America*, 97, 8352-8357.
- BENDERS, K. E. M., VAN WEEREN, P. R., BADYLAK, S. F., SARIS, D. B. F., DHERT, W. J. A. & MALDA, J. 2013. Extracellular matrix scaffolds for cartilage and bone regeneration. *Trends in Biotechnology*, 31, 169-176.
- BOHME, K., CONSCIENCEGLI, M., TSCHAN, T., WINTERHALTER, K. H. & BRUCKNER, P. 1992a. Induction of proliferation or hypertrophy of chondrocytes in serum-free culture - the role of insulin-like growth factor-1, insulin, or thyroxine. *Journal of Cell Biology*, 116, 1035-1042.
- BOHME, K., CONSCIENCEGLI, M., TSCHAN, T., WINTERHALTER, K. H. & BRUCKNER, P. 1992b. Induction of proliferation or hypertrophy of chondrocytes in serum-free culture - the role of insulin-like growth factor-1, insulin or thyroxine. *Journal of Cell Biology*, 116, 1035-1042.
- BOLANDER, M. E. 1992. REGULATION OF FRACTURE REPAIR BY GROWTH-FACTORS. *Proceedings of the Society for Experimental Biology and Medicine*, 200, 165-170.

- BONEWALD, L. F. 1999. Establishment and characterization of an osteocyte-like cell line, MLO-Y4. *Journal of Bone and Mineral Metabolism*, 17, 61-65.
- BORSCHEL, G. H., DENNIS, R. G. & KUZON, W. M. 2004. Contractile skeletal muscle tissue-engineered on an acellular scaffold. *Plastic and Reconstructive Surgery*, 113, 595-602.
- BOYLE, W. J., SIMONET, W. S. & LACEY, D. L. 2003. Osteoclast differentiation and activation. *Nature*, 423, 337-342.
- BRANDSMA, M. E., DIAO, H., WANG, X., KOHALMI, S. E., JEVIKAR, A. M. & MA, S. 2010. Plant-derived recombinant human serum transferrin demonstrates multiple functions. *Plant Biotechnology Journal*, 8.
- BRUDER, S. P., KRAUS, K. H., GOLDBERG, V. M. & KADIYALA, S. 1998. The effect of implants loaded with autologous mesenchymal stem cells on the healing of canine segmental bone defects. *Journal of Bone and Joint Surgery-American Volume*, 80A, 985-996.
- BRUNNER, D., FRANK, J., APPL, H., SCHOEFFL, H., PFALLER, W. & GSTRUNTHALER, G. 2010. Serum-free Cell Culture: The Serum-free Media Interactive Online Database. *Altex-Alternatives to Animal Experimentation*, 27.
- BRYDONE, A. S., MEEK, D. & MACLAINE, S. 2010. Bone grafting, orthopaedic biomaterials, and the clinical need for bone engineering. *Proceedings of the Institution of Mechanical Engineers Part H-Journal of Engineering in Medicine*, 224, 1329-1343.
- BUENO, E. M., BILGEN, B. & BARABINO, G. A. 2005. Wavy-walled bioreactor supports increased cell proliferation and matrix deposition in engineered cartilage constructs. *Tissue Engineering*, 11, 1699-1709.
- BURCH, W. M. & LEOVITZ, H. E. 1983. Parathyroid-hormone stimulates growth of embryonic chick pelvic cartilage in vitro. *Calcified Tissue International*, 35, 526-532.
- BURG, K. J. L., PORTER, S. & KELLAM, J. F. 2000. Biomaterial developments for bone tissue engineering. *Biomaterials*, 21, 2347-2359.
- CARANO, R. A. D. & FILVAROFF, E. H. 2003. Angiogenesis and bone repair. *Drug Discovery Today*, 8, 980-989.
- CARLEVARO, M. F., CERMELLI, S., CANCEDDA, R. & CANCEDDA, F. D. 2000. Vascular endothelial growth factor (VEGF) in cartilage neovascularization and chondrocyte differentiation: auto-paracrine role during endochondral bone formation. *Journal of Cell Science*, 113.
- CARRAGEE, E. J., HURWITZ, E. L. & WEINER, B. K. 2011. A critical review of recombinant human bone morphogenetic protein-2 trials in spinal surgery: emerging safety concerns and lessons learned. *Spine Journal*, 11, 471-491.
- CHAN, S. Y. & WONG, R. W. C. 2000. Expression of epidermal growth factor in transgenic mice causes growth retardation. *Journal of Biological Chemistry*, 275, 38693-38698.
- CHANG, S. C. N., TAI, C. L., CHUNG, H. Y., LIN, T. M. & JENG, L. B. 2009. Bone Marrow Mesenchymal Stem Cells Form Ectopic Woven Bone In Vivo Through Endochondral Bone Formation. *Artificial Organs*, 33, 301-308.

- CHATTERJEA, A., MEIJER, G., VAN BLITTERSWIJK, C. & DE BOER, J. 2010. Clinical Application of Human Mesenchymal Stromal Cells for Bone Tissue Engineering. *Stem Cells International*.
- CHEN, F., YOO, J. J. & ATALA, A. 1999. Acellular collagen matrix as a possible "off the shelf" biomaterial for urethral repair. *Urology*, 54, 407-410.
- CHEN, H.-C. & HU, Y.-C. 2006. Bioreactors for tissue engineering. *Biotechnology Letters*, 28, 1415-1423.
- CHEN, L. B., MURRAY, A., SEGAL, R. A., BUSHNELL, A. & WALSH, M. L. 1978. Studies on intracellular lets glycoprotein matrices. *Cell*, 14, 377-391.
- CHEN, Y., MAK, A. F. T., WANG, M., LI, J. S. & WONG, M. S. 2008. In vitro behavior of osteoblast-like cells on PLLA films with a biomimetic apatite or apatite/collagen composite coating. *Journal of Materials Science-Materials in Medicine*, 19, 2261-2268.
- CHUA, K. H., AMINUDDIN, B. S., FUZINA, N. H. & RUSZYMAH, B. H. I. 2005. Insulin-transferrin-selenium prevent human chondrocyte dedifferentiation and promote the formation of high quality tissue engineered human hyaline cartilage. *European cells & materials*, 9, 58-67.
- CHUNG, K. S., JACENKO, O., BOYLE, P., OLSEN, B. R. & NISHIMURA, I. 1997. Craniofacial abnormalities in mice carrying a dominant interference mutation in type X collagen. *Developmental Dynamics*, 208, 544-552.
- CLARKE, B. 2008. Normal Bone Anatomy and Physiology. *Clinical Journal of the American Society of Nephrology*, 3, S131-S139.
- COE, M. R., SUMMERS, T. A., PARSONS, S. J., BOSKEY, A. L. & BALIAN, G. 1992. Matrix mineralisation in hypertrophic chondrocyte cultures - Beta glycerophosphate increases type-X collagen messenger RNA anmd the specific activity of PP60(C-SRC) kinase. *Bone and Mineral*, 18, 91-106.
- CONRAD, M. E., UMBREIT, J. N. & MOORE, E. G. 1999. Iron absorption and transport. *American Journal of the Medical Sciences*, 318.
- DAMIEN, C. J. & PARSONS, J. R. 1991. Bone-graft and bone-graft substitutes - A review of current technology and applications. *Journal of Applied Biomaterials*, 2, 187-208.
- DAVISSON, T., SAH, R. L. & RATCLIFFE, A. 2002. Perfusion increases cell content and matrix synthesis in chondrocyte three-dimensional cultures. *Tissue Engineering*, 8, 807-816.
- DE UGARTE, D. A., MORIZONO, K., ELBARBARY, A., ALFONSO, Z., ZUK, P. A., ZHU, M., DRAGOO, J. L., ASHJIAN, P., THOMAS, B., BENHAIM, P., CHEN, I., FRASER, J. & HEDRICK, M. H. 2003. Comparison of multi-lineage cells from human adipose tissue and bone marrow. *Cells Tissues Organs*, 174, 101-109.
- DENG, X.-L., SUI, G., ZHAO, M.-L., CHEN, G.-Q. & YANG, X.-P. 2007. Poly(L-lactic acid)/hydroxyapatite hybrid nanofibrous scaffolds prepared by electrospinning. *Journal of Biomaterials Science-Polymer Edition*, 18, 117-130.
- DESCHASEAUX, F., SENSEBE, L. & HEYMANN, D. 2009. Mechanisms of bone repair and regeneration. *Trends in Molecular Medicine*, 15, 417-429.

- DIMITRIOU, R., TSIRIDIS, E. & GIANNOUDIS, P. V. 2005. Current concepts of molecular aspects of bone healing. *Injury-International Journal of the Care of the Injured*, 36, 1392-1404.
- DROSSE, I., VOLKMER, E., CAPANNA, R., DE BIASE, P., MUTSCHLER, W. & SCHIEKER, M. 2008. Tissue engineering for bone defect healing: An update on a multi-component approach. *Injury-International Journal of the Care of the Injured*, 39, S9-S20.
- DY, P., WANG, W., BHATTARAM, P., WANG, Q., WANG, L., BALLOCK, R. T. & LEFEBVRE, V. 2012. Sox9 Directs Hypertrophic Maturation and Blocks Osteoblast Differentiation of Growth Plate Chondrocytes. *Developmental Cell*, 22, 597-609.
- EL-AMIN, S. F., ATTAWIA, M., LU, H. H., SHAH, A. K., CHANG, R., HICKOK, N. J., TUAN, R. S. & LAURENCIN, C. T. 2002. Integrin expression by human osteoblasts cultured on degradable polymeric materials applicable for tissue engineered bone. *Journal of Orthopaedic Research*, 20, 20-28.
- ENGSIG, M. T., CHEN, Q. J., VU, T. H., PEDERSEN, A. C., THERKIDSEN, B., LUND, L. R., HENRIKSEN, K., LENHARD, T., FOGED, N. T., WERB, Z. & DELAISSE, J. M. 2000. Matrix metalloproteinase 9 and vascular endothelial growth factor are essential for osteoclast recruitment into developing long bones. *Journal of Cell Biology*, 151.
- FARNDALE, R. W., BUTTLE, D. J. & BARRETT, A. J. 1986. Improved quantitation and discrimination of sulphated glycosaminoglycans by use of dimethylmethylene blue. *Biochimica Et Biophysica Acta*, 883, 173-177.
- FERGUSON, C. M., SCHWARZ, E. M., REYNOLDS, P. R., PUZAS, J. E., ROSIER, R. N. & O'KEEFE, R. J. 2000. Smad2 and 3 mediate transforming growth factor-beta 1-induced inhibition of chondrocyte maturation. *Endocrinology*, 141.
- FLEISCH, H., STRAUMAN, F., SCHENK, R., BISAZ, S. & ALLGOWER, M. 1966. Effect of condensed phosphates on calcification of chick embryo femurs in tissue culture. *American Journal of Physiology*, 211, 821-&.
- FRIESS, W., ULUDAG, H., FOSKETT, S., BIRON, R. & SARGEANT, C. 1999. Characterization of absorbable collagen sponges as rhBMP-2 carriers. *International Journal of Pharmaceutics*, 187, 91-99.
- FROHLICH, M., GRAYSON, W. L., WAN, L. Q., MAROLT, D., DROBNIC, M. & VUNJAK-NOVAKOVIC, G. 2008. Tissue engineered bone grafts: biological requirements, tissue culture and clinical relevance. *Curr Stem Cell Res Ther*, 3, 254-64.
- FUJITA, T., MEGURO, T., IZUMO, N., YASUTOMI, C., FUKUYAMA, R., NAKAMUTA, H. & KOIDA, M. 2001. Phosphate stimulates differentiation and mineralization of the chondroprogenitor clone ATDC5. *Japanese Journal of Pharmacology*, 85, 278-281.
- GAWLITTA, D., FARRELL, E., MALDA, J., CREEMERS, L. B., ALBLAS, J. & DHERT, W. J. A. 2010. Modulating endochondral ossification of multipotent stromal cells for bone regeneration. *Tissue Eng Part B Rev*, 16, 385-95.
- GERBER, H. P. & FERRARA, N. 2000. Angiogenesis and bone growth. *Trends in Cardiovascular Medicine*, 10, 223-228.

- GERBER, H. P., VU, T. H., RYAN, A. M., KOWALSKI, J., WERB, Z. & FERRARA, N. 1999. VEGF couples hypertrophic cartilage remodeling, ossification and angiogenesis during endochondral bone formation. *Nature Medicine*, 5.
- GILBERT, S. F. 2000. *Developmental biology*, Sunderland, Mass., Sinauer Associates.
- GILBERT, T. W., SELLARO, T. L. & BADYLAK, S. F. 2006. Decellularization of tissues and organs. *Biomaterials*, 27, 3675-3683.
- GLOWACKI, J. 1998. Angiogenesis in fracture repair. *Clinical Orthopaedics and Related Research*, S82-S89.
- GORNA, K. & GOGOLEWSKI, S. 2006. Biodegradable porous polyurethane scaffolds for tissue repair and regeneration. *Journal of Biomedical Materials Research Part A*, 79A, 128-138.
- GOULET, J. A., SENUNAS, L. E., DESILVA, G. L. & GREENFIELD, M. 1997. Autogenous iliac crest bone graft - Complications and functional assessment. *Clinical Orthopaedics and Related Research*, 76-81.
- GROVER, L. M., KNOWLES, J. C., FLEMING, G. J. P. & BARRALET, J. E. 2003. In vitro ageing of brushite calcium phosphate cement. *Biomaterials*, 24, 4133-4141.
- GUGALA, Z., LINDSEY, R. W. & GOGOLEWSKI, S. 2007. New approaches in the treatment of critical-size segmental defects in long bones. *Macromolecular Symposia*, 253, 147-161.
- HAMMERLE, C. H. F., SCHMID, J., LANG, N. P. & OLAH, A. J. 1995. Temporal dynamics of healing in rabbit cranial defects using guided bone regeneration. *Journal of Oral and Maxillofacial Surgery*, 53, 167-174.
- HATTORI, H., SATO, M., MASUOKA, K., ISHIHARA, M., KIKUCHI, T., MATSUI, T., TAKASE, B., ISHIZUKA, T., KIKUCHI, M. & FUJIKAWA, K. 2004. Osteogenic potential of human adipose tissue-derived stromal cells as an alternative stem cell source. *Cells Tissues Organs*, 178, 2-12.
- HATTORI, T., MULLER, C., GEBHARD, S., BAUER, E., PAUSCH, F., SCHLUND, B., BOSL, M. R., HESS, A., SURMANN-SCHMITT, C., VON DER MARK, H., DE CROMBRUGGHE, B. & VON DER MARK, K. 2010. SOX9 is a major negative regulator of cartilage vascularization, bone marrow formation and endochondral ossification. *Development*, 137, 901-911.
- HEDMAN, K., KURKINEN, M., ALITALO, K., VAHERI, A., JOHANSSON, S. & HOOK, M. 1979. Isolation of the pericellular matrix of human fibroblast cultures. *Journal of Cell Biology*, 81, 83-91.
- HELMY, M. H., ISMAIL, S. S., FAYED, H. & EL-BASSIOUNI, E. A. 2000. Effect of selenium supplementation on the activities of glutathione metabolizing enzymes in human hepatoma Hep G2 cell line. *Toxicology*, 144.
- HEWLETT, G. 1991. Strategies for optimising serum-free media. *Cytotechnology*, 5.
- HING, K. A. 2004. Bone repair in the twenty-first century: biology, chemistry or engineering? *Philosophical Transactions of the Royal Society of London Series a-Mathematical Physical and Engineering Sciences*, 362, 2821-2850.
- HIRAO, M., TAMAI, N., TSUMAKI, N., YOSHIKAWA, H. & MYOUI, A. 2006. Oxygen tension regulates chondrocyte differentiation and function during endochondral ossification. *Journal of Biological Chemistry*, 281, 31079-31092.

- HONN, K. V., SINGLEY, J. A. & CHAVIN, W. 1975. Fetal bovine serum - multivariate standard. *Proceedings of the Society for Experimental Biology and Medicine*, 149, 344-347.
- HOSHIBA, T., LU, H., KAWAZOE, N. & CHEN, G. 2010. Decellularized matrices for tissue engineering. *Expert Opinion on Biological Therapy*, 10, 1717-1728.
- HOWARD, D., BUTTERY, L. D., SHAKESHEFF, K. M. & ROBERTS, S. J. 2008. Tissue engineering: strategies, stem cells and scaffolds. *Journal of Anatomy*, 213, 66-72.
- HUTMACHER, D. W., SCHANTZ, J. T., LAM, C. X. F., TAN, K. C. & LIM, T. C. 2007. State of the art and future directions of scaffold-based bone engineering from a biomaterials perspective. *Journal of Tissue Engineering and Regenerative Medicine*, 1, 245-260.
- IM, G. I., SHIN, Y. W. & LEE, K. B. 2005. Do adipose tissue-derived mesenchymal stem cells have the same osteogenic and chondrogenic potential as bone marrow-derived cells? *Osteoarthritis and Cartilage*, 13, 845-853.
- INADA, M., WANG, Y. M., BYRNE, M. H., RAHMAN, M. U., MIYAURA, C., LOPEZ-OTIN, C. & KRANE, S. M. 2004. Critical roles for collagenase-3 (Mmp13) in development of growth and in endochondral plate cartilage ossification. *Proceedings of the National Academy of Sciences of the United States of America*, 101.
- INADA, M., YASUI, T., NOMURA, S., MIYAKE, S., DEGUCHI, K., HIMENO, M., SATO, M., YAMAGIWA, H., KIMURA, T., YASUI, N., OCHI, T., ENDO, N., KITAMURA, Y., KISHIMOTO, T. & KOMORI, T. 1999. Maturation disturbance of chondrocytes in Cbfa1-deficient mice. *Developmental Dynamics*, 214, 279-290.
- JANSEN, J. A., VEHOFF, J. W. M., RUHE, P. Q., KROEZE-DEUTMAN, H., KUBOKI, Y., TAKITA, H., HEDBERG, E. L. & MIKOS, A. G. 2005. Growth factor-loaded scaffolds for bone engineering. *Journal of Controlled Release*, 101, 127-136.
- JONES, J. R. 2013. Review of bioactive glass: From Hench to hybrids. *Acta Biomaterialia*, 9, 4457-4486.
- KANCZLER, J. A., GINTY, P. J., BARRY, J. J. A., CLARKE, N. M. P., HOWDLE, S. M., SHAKESHEFF, K. M. & OREFFO, R. O. C. 2008. The effect of mesenchymal populations and vascular endothelial growth factor delivered from biodegradable polymer scaffolds on bone formation. *Biomaterials*, 29, 1892-1900.
- KASIMIR, M. T., RIEDER, E., SEEBACHER, G., SILBERHUMER, G., WOLNER, E., WEIGEL, G. & SIMON, P. 2003. Comparison of different decellularization procedures of porcine heart valves. *International Journal of Artificial Organs*, 26, 421-427.
- KATO, Y. & IWAMOTO, M. 1990. Fibroblast growth-factor is an inhibitor of chondrocyte terminal differentiation. *Journal of Biological Chemistry*, 265, 5903-5909.

- KHEIR, E., STAPLETON, T., SHAW, D., JIN, Z., FISHER, J. & INGHAM, E. 2011. Development and characterization of an acellular porcine cartilage bone matrix for use in tissue engineering. *Journal of Biomedical Materials Research Part A*, 99A, 283-294.
- KIM, H.-W., LEE, H.-H. & KNOWLES, J. C. 2006. Electrospinning biomedical nanocomposite fibers of hydroxyapatite/poly(lactic acid) for bone regeneration. *Journal of Biomedical Materials Research Part A*, 79A, 643-649.
- KIM, I. S., OTTO, F., ZABEL, B. & MUNDLOS, S. 1999. Regulation of chondrocyte differentiation by Cbfa1. *Mechanisms of Development*, 80, 159-170.
- KIM, S., KIM, S. S., LEE, S. H., AHN, S. E., GWAK, S. J., SONG, J. H., KIM, B. S. & CHUNG, H. M. 2008. In vivo bone formation from human embryonic stem cell-derived osteogenic cells in poly(D,L-lactic-co-glycolic acid)/hydroxyapatite composite scaffolds. *Biomaterials*, 29, 1043-1053.
- KIPP, D. E., MCELVAIN, M., KIMMEL, D. B., AKHTER, M. P., ROBINSON, R. G. & LUKERT, B. P. 1996. Scurvy results in decreased collagen synthesis and bone density in the guinea pig animal model. *Bone*, 18, 281-288.
- KIRSCH, T. & WUTHIER, R. E. 1994. Stimulation of calcification of growth plate cartilage matrix vesicles by binding to type-II and type-X collagens. *Journal of Biological Chemistry*, 269, 11462-11469.
- KOMORI, T. 2005. Regulation of skeletal development by the Runx family of transcription factors. *Journal of Cellular Biochemistry*, 95, 445-453.
- KRONENBERG, H. M. 2003. Developmental regulation of the growth plate. *Nature*, 423, 332-336.
- KUHNE, J. H., BARTL, R., FRISCH, B., HAMMER, C., JANSSON, V. & ZIMMER, M. 1994. Bone-formation in coralline hydroxyapatite - Effects of pore-size studied in rabbits. *Acta Orthopaedica Scandinavica*, 65, 246-252.
- KWAN, K. M., PANG, M. K. M., ZHOU, S., COWAN, S. K., KONG, R. Y. C., PFORDTE, T., OLSEN, B. R., SILLENCE, D. O., TAM, P. P. L. & CHEAH, K. S. E. 1997. Abnormal compartmentalization of cartilage matrix components in mice lacking collagen X: Implications for function. *Journal of Cell Biology*, 136, 459-471.
- KWARCIAK, A. 2009. *Tissue Engineering of Hypertrophic Cartilage for Bone Repair*. PhD, The University of Sheffield.
- LAI, L. P. & MITCHELL, J. 2005. Indian hedgehog: Its roles and regulation in endochondral bone development. *Journal of Cellular Biochemistry*, 96, 1163-1173.
- LANGER, R. & VACANTI, J. P. 1993. Tissue engineering. *Science*, 260, 920-926.
- LANNUTTI, J., RENEKER, D., MA, T., TOMASKO, D. & FARSON, D. F. 2007. Electrospinning for tissue engineering scaffolds. *Materials Science & Engineering C-Biomimetic and Supramolecular Systems*, 27, 504-509.
- LASKEY, J., WEBB, I., SCHULMAN, H. M. & PONKA, P. 1988. Evidence that transferrin supports cell-proliferation by supplying iron for DNA-synthesis. *Experimental Cell Research*, 176.
- LAWSON, A. C. & CZERNUSZKA, J. T. 1998. Collagen-calcium phosphate composites. *Proceedings of the Institution of Mechanical Engineers Part H-Journal of Engineering in Medicine*, 212, 413-425.



- LEBOY, P. S., SULLIVAN, T. A., NOOREYAZDAN, M. & VENEZIAN, R. A. 1997. Rapid chondrocyte maturation by serum-free culture with BMP-2 and ascorbic acid. *Journal of Cellular Biochemistry*, 66, 394-403.
- LEBOY, P. S., VAIAS, L., USCHMANN, B., GOLUB, E., ADAMS, S. L. & PACIFICI, M. 1989. Ascorbic acid induces alkaline-phosphatase, type-X collagen and calcium deposition in cultured chick chondrocytes. *Journal of Biological Chemistry*, 264, 17281-17286.
- LEGEROS, R. Z. 1993. Biodegradation and bioresorption of calcium phosphate ceramics. *Clinical Materials*, 14, 65-88.
- LEGEROS, R. Z. 2002. Properties of osteoconductive biomaterials: Calcium phosphates. *Clinical Orthopaedics and Related Research*, 81-98.
- LEVI, B., JAMES, A. W., NELSON, E. R., VISTNES, D., WU, B., LEE, M., GUPTA, A. & LONGAKER, M. T. 2010. Human Adipose Derived Stromal Cells Heal Critical Size Mouse Calvarial Defects. *Plos One*, 5.
- LICHTE, P., PAPE, H. C., PUFE, T., KOBBE, P. & FISCHER, H. 2011. Scaffolds for bone healing: Concepts, materials and evidence. *Injury-International Journal of the Care of the Injured*, 42, 569-573.
- LICKORISH, D., GUAN, L. & DAVIES, J. E. 2007. A three-phase, fully resorbable, polyester/calcium phosphate scaffold for bone tissue engineering: Evolution of scaffold design. *Biomaterials*, 28, 1495-1502.
- LIU, X. H. & MA, P. X. 2004. Polymeric scaffolds for bone tissue engineering. *Annals of Biomedical Engineering*, 32, 477-486.
- LYONS, F. G., AL-MUNAJJED, A. A., KIERAN, S. M., TONER, M. E., MURPHY, C. M., DUFFY, G. P. & O'BRIEN, F. J. 2010. The healing of bony defects by cell-free collagen-based scaffolds compared to stem cell-seeded tissue engineered constructs. *Biomaterials*, 31, 9232-9243.
- MACKIE, E. J., AHMED, Y. A., TATARCZUCH, L., CHEN, K. S. & MIRAMS, M. 2008. Endochondral ossification: How cartilage is converted into bone in the developing skeleton. *International Journal of Biochemistry & Cell Biology*, 40, 46-62.
- MAGNE, D., BLUTEAU, G., FAUCHEUX, C., PALMER, G., VIGNES-COLOMBEIX, C., PILET, P., ROUILLON, T., CAVERZASIO, J., WEISS, P., DACULSI, G. & GUICHEUX, J. 2003. Phosphate is a specific signal for ATDC5 chondrocyte maturation and apoptosis-associated mineralization: Possible implication of apoptosis in the regulation of endochondral ossification. *Journal of Bone and Mineral Research*, 18, 1430-1442.
- MAK, K. K., KRONENBERG, H. M., CHUANG, P. T., MACKEM, S. & YANG, Y. Z. 2008. Indian hedgehog signals independently of PTHrP to promote chondrocyte hypertrophy. *Development*, 135, 1947-1956.
- MALDA, J., MARTENS, D. E., TRAMPER, J., VAN BLITTERSWIJK, C. A. & RIESLE, J. 2003. Cartilage tissue engineering: Controversy in the effect of oxygen. *Critical Reviews in Biotechnology*, 23, 175-194.
- MANKIN, H. J., SPRINGFIELD, D. S., GEBHARDT, M. C. & TOMFORD, W. W. 1992. Current status of allografting for bone-tumors. *Orthopedics*, 15, 1147-1154.

- MARTIN, I., MIOT, S., BARBERO, A., JAKOB, M. & WENDT, D. 2007. Osteochondral tissue engineering. *Journal of Biomechanics*, 40, 750-765.
- MARTIN, I., OBRADOVIC, B., FREED, L. E. & VUNJAK-NOVAKOVIC, G. 1999. Method for quantitative analysis of glycosaminoglycan distribution in cultured natural and engineered cartilage. *Annals of Biomedical Engineering*, 27, 656-662.
- MASON, C. & DUNNILL, P. 2008. A brief definition of regenerative medicine. *Regenerative Medicine*, 3, 1-5.
- MATSUMOTO, T., KURODA, R., MIFUNE, Y., KAWAMOTO, A., SHOJI, T., MIWA, M., ASAHARA, T. & KUROSAKA, M. 2008. Circulating endothelial/skeletal progenitor cells for bone regeneration and healing. *Bone*, 43, 434-439.
- MEHLHORN, A. T., NIEMEYER, P., KAISER, S., FINKENZELLER, G., STARK, G. B., SUDKAMP, N. P. & SCHMAL, H. 2006. Differential expression pattern of extracellular matrix molecules during chondrogenesis of mesenchymal stem cells from bone marrow and adipose tissue. *Tissue Engineering*, 12, 2853-2862.
- MEIJER, G. J., DE BRUIJN, J. D., KOOLE, R. & VAN BLITTERSWIJK, C. A. 2007. Cell-based bone tissue engineering. *Plos Medicine*, 4, 260-264.
- MEIJER, G. J., DE BRUIJN, J. D., KOOLE, R. & VAN BLITTERSWIJK, C. A. 2008. Cell based bone tissue engineering in jaw defects. *Biomaterials*, 29, 3053-3061.
- MELLO, M. A. & TUAN, R. S. 2006. Effects of TGF-beta 1 and triiodothyronine on cartilage maturation: In vitro analysis using long-term high-density micromass cultures of chick embryonic limb mesenchymal cells. *Journal of Orthopaedic Research*, 24, 2095-2105.
- MESIMAKI, K., LINDROOS, B., TORNWALL, J., MAUNO, J., LINDQVIST, C., KONTIO, R., MIETTINEN, S. & SUURONEN, R. 2009. Novel maxillary reconstruction with ectopic bone formation by GMP adipose stem cells. *International Journal of Oral and Maxillofacial Surgery*, 38, 201-209.
- MIDY, V. & PLOUET, J. 1994. Vasculotropin vascular endothelial growth factor induces differentiation in cultured. *Biochemical and Biophysical Research Communications*, 199.
- MORAN, J. M., PAZZANO, D. & BONASSAR, L. J. 2003. Characterization of polylactic acid polyglycolic acid composites for cartilage tissue engineering. *Tissue Engineering*, 9, 63-70.
- NAIR, M. B., BABU, S. S., VARNIA, H. K. & JOHN, A. 2008. A triphasic ceramic-coated porous hydroxyapatite for tissue engineering application. *Acta Biomaterialia*, 4, 173-181.
- OGOSE, A., HOTTA, T., KAWASHIMA, H., KONDO, N., GU, W. G., KAMURA, T. & ENDO, N. 2005. Comparison of hydroxyapatite and beta tricalcium phosphate as bone substitutes after excision of bone tumors. *Journal of Biomedical Materials Research Part B-Applied Biomaterials*, 72B, 94-101.
- OKEEFE, R. J., PUZAS, J. E., BRAND, J. S. & ROSIER, R. N. 1988. Effects of transforming growth factor-beta on matrix synthesis by chick growth plate chondrocytes. *Endocrinology*, 122, 2953-2961.

- OKEEFE, R. J., PUZAS, J. E., LOVEYS, L., HICKS, D. G. & ROSIER, R. N. 1994. An analysis of type-II and type-X collagen synthesis in cultured growth plate chondrocytes by in-situ hybridisation - rapid induction of type-X collagen in culture. *Journal of Bone and Mineral Research*, 9, 1713-1722.
- OKUBO, Y. & REDDI, A. H. 2003. Thyroxine downregulates Sox9 and promotes chondrocyte hypertrophy. *Biochemical and Biophysical Research Communications*, 306, 186-190.
- OLMSTED-DAVIS, E. A., GUGALA, Z., CAMARGO, F., GANNON, F. H., JACKSON, K., KIENSTRA, K. A., SHINE, H. D., LINDSEY, R. W., HIRSCHI, K. K., GOODELL, M. A., BRENNER, M. K. & DAVIS, A. R. 2003. Primitive adult hematopoietic stem cells can function as osteoblast precursors. *Proceedings of the National Academy of Sciences of the United States of America*, 100, 15877-15882.
- OLNEY, R. C., WANG, J. W., SYLVESTER, J. E. & MOUGEY, E. B. 2004. Growth factor regulation of human growth plate chondrocyte proliferation in vitro. *Biochemical and Biophysical Research Communications*, 317, 1171-1182.
- OONISHI, H., HENCH, L. L., WILSON, J., SUGIHARA, F., TSUJI, E., MATSUURA, M., KIN, S., YAMAMOTO, T. & MIZOKAWA, S. 2000. Quantitative comparison of bone growth behavior in granules of Bioglass (R), A-W glass-ceramic, and hydroxyapatite. *Journal of Biomedical Materials Research*, 51, 37-46.
- OONISHI, H., KUSHITANI, S., YASUKAWA, E., IWAKI, H., HENCH, L. L., WILSON, J., TSUJI, E. I. & SUGIHARA, T. 1997. Particulate bioglass compared with hydroxyapatite as a bone graft substitute. *Clinical Orthopaedics and Related Research*, 316-325.
- ORNITZ, D. M. & MARIE, P. J. 2002. FGF signaling pathways in endochondral and intramembranous bone development and human genetic disease. *Genes & Development*, 16, 1446-1465.
- OYAJOBI, B. O., FRAZER, A., HOLLANDER, A. P., GRAVELEY, R. M., XU, C., HOUGHTON, A., HATTON, P. V., RUSSELL, R. G. G. & STRINGER, B. M. J. 1998. Expression of type X collagen and matrix calcification in three-dimensional cultures of immortalized temperature sensitive chondrocytes derived from adult human articular cartilage. *Journal of Bone and Mineral Research*, 13, 432-442.
- PAPADAKI, M., MAHMOOD, T., GUPTA, P., CLAASE, M. B., GRIJPMAN, D. W., RIESLE, J., VAN BLITERSWIJK, C. A. & LANGER, R. 2001. The different behaviors of skeletal muscle cells and chondrocytes on PEGT/PBT block copolymers are related to the surface properties of the substrate. *Journal of Biomedical Materials Research*, 54, 47-58.
- PARIKH, S. N. 2002. Bone graft substitutes: past, present, future. *Journal of postgraduate medicine*, 48, 142-8.
- PATEDER, D. B., ROSIER, R. N., SCHWARZ, E. M., REYNOLDS, P. R., PUZAS, J. E., D'SOUZA, M. & O'KEEFE, R. J. 2000. PTHrP expression in chondrocytes, regulation by TGF-beta, and interactions between epiphyseal and growth plate chondrocytes. *Experimental Cell Research*, 256.

- PETITE, H., VIATEAU, V., BENSAID, W., MEUNIER, A., DE POLLAK, C., BOURGUIGNON, M., OUDINA, K., SEDEL, L. & GUILLEMIN, G. 2000. Tissue-engineered bone regeneration. *Nature Biotechnology*, 18, 959-963.
- PROVOT, S. & SCHIPANI, E. 2005. Molecular mechanisms of endochondral bone development. *Biochemical and Biophysical Research Communications*, 328, 658-665.
- QUARTO, R., MASTROGIACOMO, M., CANCEDDA, R., KUTEPOV, S. M., MUKHACHEV, V., LAVROUKOV, A., KON, E. & MARCACCI, M. 2001. Repair of large bone defects with the use of autologous bone marrow stromal cells. *New England Journal of Medicine*, 344, 385-386.
- RAHAMAN, M. N., DAY, D. E., BAL, B. S., FU, Q., JUNG, S. B., BONEWALD, L. F. & TOMSIA, A. P. 2011. Bioactive glass in tissue engineering. *Acta Biomaterialia*, 7, 2355-2373.
- REICHERT, J. C., SAIFZADEH, S., WULLSCHLEGER, M. E., EPARI, D. R., SCHUETZ, M. A., DUDA, G. N., SCHELL, H., VAN GRIENSVEN, M., REDL, H. & HUTMACHER, D. W. 2009. The challenge of establishing preclinical models for segmental bone defect research. *Biomaterials*, 30, 2149-2163.
- REINHOLT, F. P., HULTENBY, K., OLDBERG, A. & HEINEGARD, D. 1990. Osteopontin - A possible anchor of osteoclasts to bone. *Proceedings of the National Academy of Sciences of the United States of America*, 87, 4473-4475.
- REMLINGER, N. T., CZAJKA, C. A., JUHAS, M. E., VORP, D. A., STOLZ, D. B., BADYLAK, S. F., GILBERT, S. & GILBERT, T. W. 2010. Hydrated xenogeneic decellularized tracheal matrix as a scaffold for tracheal reconstruction. *Biomaterials*, 31, 3520-3526.
- REN, T. B., REN, J., JIA, X. Z. & PAN, K. F. 2005. The bone formation in vitro and mandibular defect repair using PLGA porous scaffolds. *Journal of Biomedical Materials Research Part A*, 74A, 562-569.
- REY, C., BESHAK, K., GRIFFIN, R. & GLIMCHER, M. J. 1991. Structural studies of the mineral phase of calcifying cartilage. *Journal of Bone and Mineral Research*, 6, 515-525.
- RHO, J. Y., KUHN-SPEARING, L. & ZIOUPOS, P. 1998. Mechanical properties and the hierarchical structure of bone. *Medical Engineering & Physics*, 20, 92-102.
- RICHARDSON, D. R. & PONKA, P. 1997. The molecular mechanisms of the metabolism and transport of iron in normal and neoplastic cells. *Biochimica Et Biophysica Acta-Reviews on Biomembranes*, 1331.
- RIEDER, E., KASIMIR, M. T., SILBERHUMER, G., SEEBACHER, G., WOLNER, E., SIMON, P. & WEIGEL, G. 2004. Decellularization protocols of porcine heart valves differ importantly in efficiency of cell removal and susceptibility of the matrix to recellularization with human vascular cells. *Journal of Thoracic and Cardiovascular Surgery*, 127, 399-405.
- ROBISON, R. 1926. The possible significance of hexosephosphoric esters in ossification. A reply to Shipley, Kramer and Howland. *Biochemical Journal*, 20, 388-391.

- ROBSON, H., SIEBLER, T., STEVENS, D. A., SHALET, S. M. & WILLIAMS, G. R. 2000. Thyroid hormone acts directly on growth plate chondrocytes to promote hypertrophic differentiation and inhibit clonal expansion and cell proliferation. *Endocrinology*, 141, 3887-3897.
- SAITO, Y., YOSHIDA, Y., AKAZAWA, T., TAKAHASHI, K. & NIKI, E. 2003. Cell death caused by selenium deficiency and protective effect of antioxidants. *Journal of Biological Chemistry*, 278.
- SATO, M., MORII, E., KOMORI, T., KAWAHATA, H., SUGIMOTO, M., TERAJ, K., SHIMIZU, H., YASUI, T., OGIHARA, H., YASUI, N., OCHI, T., KITAMURA, Y., ITO, Y. & NOMURA, S. 1998. Transcriptional regulation of osteopontin gene in vivo by PEBP2 alpha A/CBFA1 and ETS1 in the skeletal tissues. *Oncogene*, 17, 1517-1525.
- SCOTTI, C., TONNARELLI, B., PAPADIMITROPOULOS, A., SCHERBERICH, A., SCHAEREN, S., SCHAUERTE, A., LOPEZ-RIOS, J., ZELLER, R., BARBERO, A. & MARTIN, I. 2010. Recapitulation of endochondral bone formation using human adult mesenchymal stem cells as a paradigm for developmental engineering. *Proceedings of the National Academy of Sciences of the United States of America*, 107, 7251-7256.
- SHAPIRO, I. M., ADAMS, C. S., FREEMAN, T. & SRINIVAS, V. 2005. Fate of the hypertrophic chondrocyte: Microenvironmental perspectives on apoptosis and survival in the epiphyseal growth plate. *Birth Defects Research*, 75, 330-339.
- SHEN, G. 2005. The role of type X collagen in facilitating and regulating endochondral ossification of articular cartilage. *Orthodontics & craniofacial research*, 8, 11-7.
- SHOICHET, M. S. 2010. Polymer Scaffolds for Biomaterials Applications. *Macromolecules*, 43, 581-591.
- SILVA, R. V., CAMILLI, J. A., BERTRAN, C. A. & MOREIRA, N. H. 2005. The use of hydroxyapatite and autoenous cancellous bone grafts to repair bone defects in rats. *International Journal of Oral and Maxillofacial Surgery*, 34, 178-184.
- SINGHVI, R., KUMAR, A., LOPEZ, G. P., STEPHANOPOULOS, G. N., WANG, D. I. C., WHITESIDES, G. M. & INGBER, D. E. 1994. Engineering cell shape and function. *Science*, 264, 696-698.
- ST-JACQUES, B., HAMMERSCHMIDT, M. & MCMAHON, A. P. 1999. Indian hedgehog signaling regulates proliferation and differentiation of chondrocytes and is essential for bone formation. *Genes & Development*, 13, 2072-2086.
- STEVENS, M. M. 2008. Biomaterials for bone tissue engineering. *Materials Today*, 11, 18-25.
- STEVENS, M. M. & GEORGE, J. H. 2005. Exploring and engineering the cell surface interface. *Science*, 310, 1135-1138.
- STRINGER, B., WADDINGTON, R., SLOAN, A., PHILLIPS, I., TELFORD, G., HUGHES, D., CRAIG, G., GANGEMI, L., BROOK, I., FREEMAN, C., CAO, X., GOSAL, M., SMITH, S., RUSSELL, G. & FOSTER, G. 2007. Bespoke human hypertrophic chondrocytic cell lines provide the osteoinductive signals required for vascularized bone formation. *Tissue Engineering*, 13, 133-145.
- SUTHERLAND, R. M., SORDAT, B., BAMAT, J., GABBERT, H., BOURRAT, B. & MUELLERKLIESER, W. 1986. Oxygenation and differentiation in multicellular spheroids of huma-colon carcinoma. *Cancer Research*, 46, 5320-5329.

- TAGUCHI, T., KISHIDA, A. & AKASHI, M. 1999. Apatite formation on/in hydrogel matrices using an alternate soaking process: II. Effect of swelling ratios of poly(vinyl alcohol) hydrogel matrices on apatite formation. *Journal of Biomaterials Science-Polymer Edition*, 10, 331-339.
- TAICHMAN, R. S. 2005. Blood and bone: two tissues whose fates are intertwined to create the hematopoietic stem-cell niche. *Blood*, 105, 2631-2639.
- TRUETA, J. 1963. THE ROLE OF THE VESSELS IN OSTEOGENESIS. *Journal of Bone and Joint Surgery-British Volume*, 45, 402-418.
- TSAI, W. B., CHEN, C. H., CHEN, J. F. & CHANG, K. Y. 2006. The effects of types of degradable polymers on porcine chondrocyte adhesion, proliferation and gene expression. *Journal of Materials Science-Materials in Medicine*, 17, 337-343.
- TUAN, R. S., BOLAND, G. & TULI, R. 2003. Adult mesenchymal stem cells and cell-based tissue engineering. *Arthritis Research & Therapy*, 5, 32-45.
- UEDA, H. & TABATA, Y. 2003. Polyhydroxyalkanoate derivatives in current clinical applications and trials. *Advanced Drug Delivery Reviews*, 55, 501-518.
- VAN DER VALK, J., BRUNNER, D., DE SMET, K., SVENNINGSEN, A. F., HONEGGER, P., KNUDSEN, L. E., LINDL, T., NORABERG, J., PRICE, A., SCARINO, M. L. & GSTRATHALER, G. 2010. Optimization of chemically defined cell culture media - Replacing fetal bovine serum in mammalian in vitro methods. *Toxicology in Vitro*, 24.
- VU, T. H., SHIPLEY, J. M., BERGERS, G., BERGER, J. E., HELMS, J. A., HANAHAN, D., SHAPIRO, S. D., SENIOR, R. M. & WERB, Z. 1998. MMP-9/gelatinase B is a key regulator of growth plate angiogenesis and apoptosis of hypertrophic chondrocytes. *Cell*, 93, 411-422.
- VUNJAK-NOVAKOVIC, G., MARTIN, I., OBRADOVIC, B., TREPPO, S., GRODZINSKY, A. J., LANGER, R. & FREED, L. E. 1999. Bioreactor cultivation conditions modulate the composition and mechanical properties of tissue-engineered cartilage. *Journal of Orthopaedic Research*, 17, 130-138.
- WANG, K., ZHOU, C., HONG, Y. & ZHANG, X. 2012. A review of protein adsorption on bioceramics. *Interface Focus*, 2, 259-277.
- WANG, L., SHAO, Y. Y. & BALLOCK, R. T. 2007. Thyroid hormone interacts with the Wnt/beta-catenin signaling pathway in the terminal differentiation of growth plate chondrocytes. *Journal of Bone and Mineral Research*, 22, 1988-1995.
- WEIR, E. C., PHILBRICK, W. M., AMLING, M., NEFF, L. A., BARON, R. & BROADUS, A. E. 1996. Targeted overexpression of parathyroid hormone-related peptide in chondrocytes causes chondrodysplasia and delayed endochondral bone formation. *Proceedings of the National Academy of Sciences of the United States of America*, 93, 10240-10245.
- WILSON, C. J., CLEGG, R. E., LEAVESLEY, D. I. & PEARCY, M. J. 2005. Mediation of biomaterial-cell interactions by adsorbed proteins: A review. *Tissue Engineering*, 11, 1-18.
- WONG, M., SIEGRIST, M. & GOODWIN, K. 2003. Cyclic tensile strain and cyclic hydrostatic pressure differentially regulate expression of hypertrophic markers in primary chondrocytes. *Bone*, 33, 685-693.

- WUELLING, M. & VORTKAMP, A. 2010. Transcriptional networks controlling chondrocyte proliferation and differentiation during endochondral ossification. *Pediatric Nephrology*, 25, 625-631.
- XYNOS, I. D., EDGAR, A. J., BUTTERY, L. D. K., HENCH, L. L. & POLAK, J. M. 2000. Ionic products of bioactive glass dissolution increase proliferation of human osteoblasts and induce insulin-like growth factor II mRNA expression and protein synthesis. *Biochemical and Biophysical Research Communications*, 276, 461-465.
- YELLOWLEY, C. E., JACOBS, C. R., LI, Z. Y., ZHOU, Z. Y. & DONAHUE, H. J. 1997. Effects of fluid flow on intracellular calcium in bovine articular chondrocytes. *American Journal of Physiology-Cell Physiology*, 273, C30-C36.
- ZELZER, E., GLOTZER, D. J., HARTMANN, C., THOMAS, D., FUKAI, N., SOKER, S. & OLSEN, B. R. 2001. Tissue specific regulation of VEGF expression during bone development requires Cbfa1/Runx2. *Mechanisms of Development*, 106, 97-106.
- ZENMYO, M., KOMIYA, S., KAWABATA, R., SASAGURI, Y., INOUE, A. & MORIMATSU, M. 1996. Morphological and biochemical evidence for apoptosis in the terminal hypertrophic chondrocytes of the growth plate. *Journal of Pathology*, 180, 430-433.
- ZHANG, W., ZHU, C., WU, Y., YE, D., WANG, S., ZOU, D., ZHANG, X., KAPLAN, D. L. & JIANG, X. 2014. VEGF and BMP-2 promote bone regeneration by facilitating bone marrow stem cell homing and differentiation. *European Cells & Materials*, 27, 1-12.
- ZUK, P. A., ZHU, M., ASHJIAN, P., DE UGARTE, D. A., HUANG, J. I., MIZUNO, H., ALFONSO, Z. C., FRASER, J. K., BENHAIM, P. & HEDRICK, M. H. 2002. Human adipose tissue is a source of multipotent stem cells. *Molecular Biology of the Cell*, 13, 4279-4295.